AD/A-006 682

SHOCK TUNNEL TESTS OF ARCHED WALL PANELS

Bernard Gabrielsen, et al

URS Research Company

Prepared for:

Defense Civil Preparedness Agency

July 1974

Unclassified

SECURITY CLASSIFICATION OF THIS PAGE (When Data Entered)

REPORT DOCUMENTATION PAGE		READ INSTRUCTIONS BEFORE COMPLETING FORM
1 REPORT NUMBER	2 GOVT ACCESSION NO.	3 RECIPIENT'S CATALOG NUMBER AD/A-006 682
4 TITLE (and Subtitle) SHOCK TUNNEL TESTS OF ARCHED PANEL WALLS		5 TYPE OF REPORT & PERIOD COVERED Final Report Nov. 1972-Oct. 1973
		6 PERFORMING ORG. REPORT NUMBER URS 7030-19
7 AUTHOR(s) Bernard Gabrielsen and C. Wilton, Scientific Services, Inc.		8 CONTRACT OR GRANT NUMBER(s) DAHC20-71-C-0223
9 PERFORMING ORGANIZATION NAME AND ADDRESS URS Research Company 155 Bovet Road San Mateo, California 94402		10 PROGRAM ELEMENT, PROJECT, TASK AREA & WORK UNIT NUMBERS Work Unit 1123G
11 CONTROLLING OFFICE NAME AND ADDRESS Defense Civil Preparedness Agency Washington, D.C. 20301		12 REPORT DATE July, 1974
		13 NUMBER OF PAGES 231
14 MONITORING AGENCY NAME & ADDRESS (if different from Controlling Office)		15 SECURITY CLASS (of this report) UNCL
		15a DECLASSIFICATION DOWNGRADING SCHEDULE

16 DISTRIBUTION STATEMENT (of this Report)

"Approved for Public Release; Distribution Unlimited"

17 DISTRIBUTION STATEMENT (of the abstract entered in Block 20, if different from Report)

18 SUPPLEMENTARY NOTES

19 KEY WORDS (Continue on reverse side if necessary and identify by block number)

Shock Tests, Nuclear Weapons, Nuclear Effects, Walls, Structural Properties, Performance (Engineering), Civil Defense

20 ABSTRACT (Continue on reverse side if necessary and identify by block number)

The objectives of this program were to determine the failure strengths of wall panels typical of those found in existing buildings, and in particular wall panels found in those buildings which contain designated fallout shelter spaces. Brittle materials, such as brick and concrete block, were the primary materials investigated. Fullscale walls (8½ ft by 12 ft), with and without

DD FORM 1 JAN 73 1473 EDITION OF 1 NOV 65 IS OBSOLETE

Unclassified

SECURITY CLASSIFICATION OF THIS PAGE (When Data Entered)

window or door openings, were exposed to air-blast waves in the URS Shock Tunnel. Concurrently, an analytical study of the mechanical properties of these construction materials was undertaken to link test results with prediction theory.

It was found that walls which were fitted very snugly into a frame (rigid arching) were considerably stronger than non-arched (i.e., gapped) walls (with failure overpressure four-to-five times those from non-arched walls), but not as strong as previous theory would suggest. Walls with a small gap, however, were only slightly stronger than non-arched walls.

URS 7030-19

FINAL REPORT

SHOCK TUNNEL TESTS OF ARCHED WALL PANELS

by

Bernard Gabrielsen, Ph.D.
C. Wilton

December 1974

for the

DEFENSE CIVIL PREPAREDNESS AGENCY
Washington, D.C. 20301

Contract No. DAHC20-71-C-0223
DCPA Work Unit 1123G

Approved for public release;
distribution unlimited.

This report has been reviewed in the Defense Civil Preparedness Agency and approved for publication. Approval does not signify that the contents necessarily reflect the views and policies of the Defense Civil Preparedness Agency.

URS RESEARCH COMPANY
A URS Company
155 BOVET ROAD · SAN MATEO, CA. 94402 · (415) 574-5000

URS 7030-19

FINAL REPORT

SHOCK TUNNEL TESTS OF ARCHED WALL PANELS

by

Bernard Gabrielsen, Ph.D.
C. Wilton

December 1974

for the

DEFENSE CIVIL PREPAREDNESS AGENCY
Washington, D.C. 20301

Contract No. DAHC20-71-C-0223
DCPA Work Unit 1123G

Approved for public release;
distribution unlimited.

This report has been reviewed in the Defense Civil Preparedness Agency and approved for publication. Approval does not signify that the contents necessarily reflect the views and policies of the Defense Civil Preparedness Agency.

URS
A URS Company
RESEARCH COMPANY
155 BOVET ROAD · SAN MATEO, CA. 94402 · (415) 574-5000

ib

Summary Report

SHOCK TUNNEL TESTS OF ARCHED WALL PANELS

TYPE OF STUDY

This is a combined analytical and experimental study of the behavior of full-scale structural wall panels under blast loading. Emphasis in this report is on arched* wall panels.

OBJECTIVE

The major objective of this program has been to determine the failure strengths of wall panels typical of those found in existing buildings, and in particular wall panels found in those buildings which contain designated fallout shelter spaces. Since a large majority of designated buildings have walls constructed of brittle materials, such as brick and concrete block, these have been the primary materials investigated.

PROCEDURE

Full-scale walls (approximately 8-1/2 ft high by 12 ft wide) of these materials with and without window door openings have been constructed and exposed to air-blast waves in the URS Shock Tunnel. Along with these shock tunnel tests, an analytical study and a study of the mechanical properties of the construction materials were undertaken in order to insure that the shock tunnel test results could be extrapolated

---

* Arching of a wall panel loaded by a shock wave normal to its face takes place when the panel supports permit essentially no motion in the direction of the plane of the panel. This can occur when a wall is tightly supported in a rigid frame.

ic

to conditions, wall panel strength characteristics, and wall panel types other than those tested in the Shock Tunnel. Using this approach (which tends to minimize the number of tests that must be conducted), techniques for predicting when and how walls fail are being generated. The basic requirement for this information is for use in updating estimates of building damage and casualties from both nuclear and natural disasters.

This report has been organized to serve two functions: first to present the results of the research effort conducted during the reporting period (November 1, 1972 to October 30, 1973); and second, by combining these results with others previously reported, to present a summary of program results to date. As before, the primary emphasis during the reporting period was on shock tunnel tests of walls made of brittle material (brick and concrete block) and supporting analytical effort. However, these walls were all tested in the so-called arched support condition; that is, as if they were in-fill walls fitted into a rigid frame structure. Two types of arching were investigated: "rigid" arching in which the wall is fitted very snugly into the frame; and "gapped" arching in which a small gap is left at the top of the wall.

FINDINGS

The work done on arched walls during this reporting period included static tests, which were recorded to acquire information on the material properties and were also used to aid in the understanding of certain elements of the arching phenomena. Analytical work using the MACE finite element computer program was expanded, and shock tunnel tests on both solid panels and panels with a window opening were conducted. As anticipated, walls which were fitted very snugly into a frame were considerably stronger than non-arched walls (with failure overpressure four-to-five times those from nonarched walls), but not as strong as previous theory would suggest. Walls with a gap, however, were only slightly stronger than non-arched walls.

ABSTRACT

The objectives of this program were to determine the failure strengths of wall panels typical of those found in particular wall panels found in those buildings which contain designated fallout shelter spaces. Brittle matrials, such as brick and concrete block, were the primary materials investigated.

Full-scale walls (8-1/2 by 12 feet) with and without window or door openings were exposed to air blast waves in the URS Shock Tunnel. Concurrently, an analytical study of the mechanical properties of these construction materials was undertaken to link test results with prediction theory.

It was found that walls which were fitted very snugly into a frame (rigid arching) were considerably stronger than non-arched (i.e., gapped) walls (with failure overpressure four to five times those from non-arched walls), but not as strong as previous theory would suggest. Walls with a small gap, however, were only slightly stronger than non-arched walls.

FOREWORD

This volume reports work accomplished by URS Research Company at its Fort Cronkhite Shock Tunnel under the sponsorship of the Defense Civil Preparedness Agency. Messrs. Joseph Boyes and Paul Kennedy of URS Research Company were responsible for the planning and execution of all test efforts including instrumentation, photography, and preliminary data evaluation. Messrs. Bernard Gabrielsen and C. Wilton of Scientific Services, Inc., under subcontract 7030-74-100 to URS Research Company, analyzed the test data and prepared this report. In this effort they were assisted by Mr. K. Kaplan, Mr. R. Lindskog, Mrs. L.T. White, and Miss T. Wilton.

CONTENTS

Section		Page
1	INTRODUCTION	
	General Discussion	1-1
	Report Organization	1-2
2	ARCHED WALLS	
	Practical Considerations	2-1
	Rigid Arching	2-9
	Arching With a Gap	2-18
	Resistance Predictions - Gapped Walls	2-31
	Arched Walls With Doorways	2-33
	Two-Way Arched Walls	2-34
3	LOADING STUDIES	
	Open Tunnel Tests	3-1
	Closed Tunnel Tests	3-5
4	WALL PROGRAM SUMMARY, CONCLUSIONS AND RECOMMENDATIONS	
	General	4-1
	Program Description	4-2
	Summary of Important Results	4-4
5	REFERENCES	5-1
	APPENDIX	
	A TEST DATA	
	Arched Solid Wall Tests	A-1
	B SUMMARY OF THE COMPUTER EFFORT	B-1
	Introduction	B-1
	Description of SAMIS	B-2

CONTENTS

Section		Page
APPENDIX		
B	SUMMARY OF THE COMPUTER EFFORT (Cont'd)	
	Input Data	B-4
	Solid Wall Solution	B-8
	Wall With a Doorway	B-31
	Wall With a Window	B-47
C	STATIC TEST PROGRAM	
	Introduction	C-1

ILLUSTRATIONS

Figure		Page
2-1	Wall to Frame Anchorage Detail	2-4
2-2	Continuation of Fig. 2-1, Wall to Frame Anchorage Details	2-5
2-3	Sketch Showing Resistance to Motion Along Line Contacts in One-Way Arching	2-10
2-4	Geometries for Exploratory Static Tests	2-10
2-5	Freebody of Half-Wall	2-13
2-6	Computer Model Submitted MACE	2-15
2-7	Arched Wall, Static Resistance	2-17
2-8	Phase I - Cantilever Wall	2-24
2-9	Phase I - Cantilever in Bending	2-25
2-10	Phase II - Gapped Wall "Arched"	2-26
2-11	Geometry for Determination of "Degenerate" Static Line Load	2-31
2-12	Arched Wall Static Resistance	2-35
2-13	Arched Wall, With Doorway Static Resistance	2-36
2-14	Posttest Photographs and Crack Patterns (first test) for Test 83	2-38
2-15	Posttest Photographs and Crack Pattern (second test) for Test 83	2-38
3-1	Sample Traces from Open Tunnel Calibration Test Series	3-3
3-2	Summary of Peak Incident Overpressure (psi) as a Function of Number of Parallel Strands of Primacord Detonated Simultaneously in the Compression Chamber	3-4
3-3	Gauge Locations for Closed Tunnel Tests	3-6
3-4	Average Peak Overpressure vs Time for One Strand Solid Wall Loading Study Test 10-19-72-07, 08 and 09, Gauges B-12, B-13, B-14 and B-15	3-7
3-5	Average Peak Overpressure vs Time for Two Strand Solid Wall Loading Study Tests 10-19-72-04 and 06; Gauges B-12, B-14 and B-15	3-8

ILLUSTRATIONS

Figure		Page
3-6	Average Peak Overpressure vs Time for Three Strand Solid Wall Loading Study Tests 10-19-72-01, 02 and 03; Gauges B-12, B-13, B-14 and B-15	3-9
3-7	Average Peak Overpressure vs time for Four Strand Solid Wall Loading Study Tests 10-17-72-03, 10-17-72-04 and 10-18-72-01	3-10
3-8	Average Peak Overpressure vs time for Five Strand Solid Wall Loading Study Tests 10-16-72-01, 10-17-72-01 and 02; Gauges B-12, B-13, B-14 and B-15	3-11
3-9	Peak Reflected Overpressure (psi) as a Function of the Number of Parallel Strands of Primacord Detonated Simultaneously in the Compression Chamber	3-12
4-1	Failure Strength Matrix - Solid Walls	4-5
4-2	Failure Strength Matrix - Windows	4-6
4-3	Failure Strength Matrix - Doorways	4-7
A-1	Top and Bottom Support Systems for Arching Walls Constructed and Cured Outside Shock Tunnel. Note: 1. Mortar installed when wall placed in Shock Tunnel. 2. Mortar installed when wall was constructed	A-2
A-2	Pretest Photographs of Wall No. 87	A-4
A-3	Posttest Photographs of Wall No. 84	A-5
A-4	Displacement as a Function of Time, Wall No. 87, Tests 1, 2 and 3	A-6
A-5	Posttest Photographs of Wall No. 88	A-8
A-9	Displacement as a Function of Time, Wall No. 88	A-9
A-7	Posttest Photographs of Wall No. 94	A-10
A-8	Displacement as a Function of Time, Wall No. 94	A-11
A-9	Posttest Photographs of Wall No. 96	A-13
A-10	Displacement as a Function of Time, Wall No. 96	A-14
A-11	Support Systems for Wall 92, 6 in. Concrete Block With 4 in. Brick Facing. Note: 1. Mortar Installed when wall placed in Shock Tunnel. 2. Mortar installed when wall was constructed.	A-15
A-12	Posttest Photographs of Wall No. 92.	A-17

ILLUSTRATIONS

Figure		Page
A-13	Displacement as a Function of Time, Wall No. 92, Tests 1, 2 and 3	A-18
A-14	Posttest Photographs of Wall No. 83	A-20
A-15	Displacement as a Function of Time, Wall No. 89	A-21
A-16	Posttest Photographs of Wall No. 89	A-22
A-17	Posttest Photograph of Wall No. 89	A-23
A-18	Posttest Photographs of Wall No. 90	A-24
A-19	Displacement as a Function of Time, Wall No. 90	A-25
A-20	Displacement as a Function of Time, Wall No. 86, Tests 1 and 2	A-27
A-21	Displacement as a Function of Time, Wall No. 95	A-28
A-22	Posttest Photographs of Wall No. 95	A-29
A-23	Posttest Photographs of Wall No. 84 Second Test	A-32
A-24	Displacement as a Function of Time, Wall No. 84, Tests 1 and 2	A-33
A-25	Pre and Posttest Photographs of Wall No. 85	A-35
A-26	Posttest Photographs of Wall No. 85	A-36
A-27	Posttest Photographs of Wall No. 91	A-37
A-28	Displacement as a Function of Time, Wall No. 91	A-38
A-29	Displacement as a Function of Time, Wall No. 93	A-39
B-1	Loading Input for SAMIS for Wall With a Doorway	B-6
B-2	Comparison of SAMIS Input Data in Fig. B-1 With Loading Study Data from Ref. 1.	B-7
B-3	Average Input Loading for Wall With a Window	B-9
B-4	Simple (Pinned) and Moment Resisting (Fixed) Supports Top and Bottom	B-10
B-5	Node and Element Locations for Solid Walls	B-11
B-6	Element Coordinate System and Relation with Principal Stresses	B-13
B-7	Displacement and Velocity vs Time for Node 360 on a Solid Wall Pinned Top and Bottom	B-14

ILLUSTRATIONS

Figure		Page
B-8	Displacement vs Time for Nodes 10, 160 and 310 on a Solid Wall Pinned Top and Bottom	B-15
B-9	Contour Display of Maximum Deflection of Wall Surface at t = 17 msec	B-16
B-10	Stress and θ vs Time for Element No. 9 on a Solid Wall Pinned Top and Bottom	B-17
B-11	Stress Contours for Solid Wall (+Z Face) Pinned Top and Bottom at 17 msec	B-18
B-12	Velocity and Deflection vs Time for Node 360 Fixed Support Top and Bottom of Wall	B-20
B-13	Deflection vs Time for Nodes 10, 160 and 310 With Fixed Supports Top and Bottom	B-21
B-14	Deflection Contours (in.) for Time = 0.008 seconds With Fixed Supports Top and Bottom	B-22
B-15	Stress and θ vs Time for Element No. 9 With Fixed Supports Top and Bottom	B-23
B-16	Stress Contours for Time = 0.008 Second for Downstream (+Z) Face With Fixed Supports Top and Bottom	B-24
B-17	Displacement and Velocity vs Time for Node 360 on a Solid Wall With Pinned Supports on All Sides	B-25
B-18	Deflection vs Time for Nodes 10, 160 and 310 With Pinned Supports All Sides	B-26
B-19	Deflection Contours (in.) for Time - 0.012 seconds With Pinned Supports on All Sides	B-27
B-20	Stress and θ vs Time for Element No. 9 With Pinned Suppports on All Sides	B-28
B-21	Shear Contours for Time = 0.012 seconds for Downstream (+Z) Face With Pinned Support	B-29
B-22A	Test Wall No. 24 Downstream Face Simply Supported All Sides	B-30
B-22B	Closeup of Cracking Toward Corners for Test Wall No. 24	B-30
B-23	Velocity and Deflection vs Time for Node 360 with Fixed Supports on All Sides	B-32

ILLUSTRATIONS

Figure		Page
B-24	Deflection vs Time for Nodes 10, 160 and 310 With Fixed Supports All Sides	B-33
B-25	Deflection Contours (in.) for Time - 0.007 Seconds With Fixed Supports on All Sides	B-34
B-26	Stress and θ vs Time for Element No. 9 With Fixed Supports on All Sides	B-35
B-27	Stress Contours for a Solid Wall Fixed on All Sides at 8 msec	B-36
B-28	Node and Element Grid for Wall With a Doorway	B-37
B-28	Deflection vs Time for Nodes 10, 210 and 410 with Pinned Supports Top and Bottom of Wall	B-39
B-29	Deflection vs Time for Nodes 10, 210 and 410 With Pinned Supports Top and Bottom of Wall	B-39
B-30	Wall With Doorway Deflection Contour (in.) at 1⅞ msec, Normalized to 1 psi Loading	B-40
B-31	Stress and θ vs Time for Element No. 9 With Pinned Supports Top and Bottom	B-41
B-32	Stress Contours for a Wall With Doorway Pinned Top and Bottom at Time =.017 seconds on the (+Z) Face	B-42
B-33	Deflection vs Time for Nodes 10, 210 and 410 With Fixed Supports Top and Bottom of Wall	B-43
B-34	Deflection Contours (in.) for Time - 0.007 Seconds With Fixed Supports Top and Bottom	B-44
B-35	Stress and θ vs Time for Element No. 9 With Fixed Supports Top and Bottom	B-45
B-36	Stress Contours for Time = 0.007 Seconds for Downstream (+Z) Face with Fixed Supports Top and Bottom	B-46
B-37	Deflection vs Time for Nodes 10, 210 and 410 With Pinned Supports on All Sides	B-48
B-38	Deflection Contours (in.) for Time = 0.012 Seconds With Pinned Supports on All Sides	B-49
B-39	Stress and θ vs Time for Element No. 9 With Pinned Supports on All Sides	B-50

ILLUSTRATIONS

Figure		Page
B-40	Stress Contours on (+Z) Face at Time - 0.13 Seconds for a Wall With Doorway Pinned on Three Sides	B-51
B-41	Deflection vs Time for Nodes 10, 210 and 410 With Fixed Supports All Sides	B-52
B-42	Deflection Contours (in.) for Time = 0.006 Seconds With Fixed Supports All Sides	B-53
B-43	Stress and θ vs Time for Element No. 9 With Fixed Supports All Sides	B-54
B-44	Stress Contours on the (+Z) Face at t = 0.006 Seconds For a Wall With Doorway Fixed on Three Sides	B-55
B-45	Node and Element Locations for Wall With Window	B-56
B-46	Velocity and Deflection vs Time for Node 60	B-58
B-47	Deflection vs Time for Nodes 220 and 550 With Pinned Supports Top and Bottom	B-59
B-48	Deflection Contours (in.) for Time - 0.015 Seconds With Pinned Supports Top and Bottom	B-60
B-49	Stress and θ vs Time for Element No. 22 With Pinned Supports Top and Bottom	B-61
B-50	Stress Contours for Time = 0.016 Seconds for Downstream (+Z) Face With Pinned Supports Top and Bottom	B-62
B-51	Deflection and Velocity vs Time for Node 60 With Fixed Supports Top and Bottom	B-63
B-52	Deflection vs Time for Nodes 220 and 500 With Fixed Supports Top and Bottom	B-64
B-53	Deflection Contours (in.) for Time = 0.006 Seconds With Fixed Supports Top and Bottom	B-65
B-54	Stress and θ vs Time for Element No. 22 With Fixed Supports Top and Bottom	B-67
B-55	Stress Contours for Time = 0.006 Seconds for Downstream (+Z) Face With Fixed Supports Top and Bottom	B-68
B-56	Deflection and Velocity vs Time for Node 60 With Pinned Supports All Sides	B-69
B-57	Deflection vs Time for Nodes 220 and 550 With Pinned Supports All Sides	B-70

ILLUSTRATIONS

Figure		Page
B-58	Deflection Contours (in.) for Time = 0.009 Seconds With Pinned Supports All Sides	B-71
B-59	Stress and θ vs Time for Element No. 22 With Pinned Supports All Sides	B-72
B-60	Stress Contours for Time = 0.008 (+Z) Face With Pinned Supports All Sides	B-73
B-61	Deflection and Velocity vs Time for Node 60 With Fixed Supports All Sides	B-74
B-62	Deflection vs Time for Nodes 220 and 500 With Fixed Supports All Sides	B-75
B-63	Deflection Contours (in.) for Time = 0.004 Seconds With Fixed Supports Top and Bottom	B-76
B-64	Stress and θ vs Time for Element No. 22 With Fixed Supports All Sides	B-77
B-65	Stress Contours on (+Z) Face at Time = 0.003 Seconds for a Wall With Window Fixed on All Four Sides	B-78
C-1	Brick Beam Flexural Test, Third-point Loading	C-3
C-2	Brick and Concrete Beam Patterns	C-4
C-3	Special Type Brick and Concrete Beam Pattern	C-7
C-4	Test Method for Brick and Concrete Block Arched Beams	C-8
C-5	Method of Loading and Test Results for Brick and Concrete Block Arched Beams	C-9
C-6	Typical Failure Crack Patterns Arched Brick Beams	C-10
C-7	Typical Failure Concrete Block Arched Beam	C-11
C-8	Method of Loading and Results from Composite Brick Concrete Block Beam Tests	C-12
C-9	Sketches of Masonry Assemblies	C-16
C-10	Brick Assemblies Tested in Compression	C-20
C-11	Vertical "Line Loading" of Brick Assemblies	C-23
C-12A	Concrete Block	C-27
C-12B	Concrete Block Composite	C-27

TABLES

Table		Page
2-1	Spacing of Wall Ties	2-7
2-2	MACE Displacements (E - 100,000 psi, p - 1.0 psi)	2-16
2-3	Summary of Arched Solid Wall Tests	2-19
"	" " " " " "	2-20
"	" " " " " "	2-21
2-4	Summary of Data For Table 2-3	2-22
4-1	Summary of Shock Tunnel Test Data	4-8
"	" " " " " "	4-9
"	" " " " " "	4-10
"	" " " " " "	4-11
"	" " " " " "	4-12
C-1	Summary of Static Test Data (Brick)	C-6
C-2	Summary of Static Test Data (Concrete Block)	C-13
C-3	Static Test Data for 8-1/2" x 3-7/8" x 8-1/2" Brick Assemblies in Compression - Standard Test	C-17
C-4	Static Test Data for 8-1/2" x 8-1/2" x 8-1/2" Brick Assemblies in Compression	C-18
C-5	Static Test Data for 8-1/2" x 3-7/8" x 8-1/2" Brick Assemblies in "Line Loading"	C-21
C-6	Static Test Data for 8-1/2" x 8-1/2" x 8-1/2" Brick Assemblies in "Line Loading"	C-22
C-7	Test Data for Vertical "Line Loading" of Brick/Mortar Specimens	C-24
C-8	Static Test Data For Brick Concrete Block Composite "Line Load" on Brick	C-25
C-9	Static Test Data for Brick Concrete Block Composite "Line Load" on Block	C-26
C-10	Static Test Data for Concrete Blocks in Compression	C-28
C-11	Static Test Data for Concrete Blocks in "Line Loading"	C-29

Section 1

INTRODUCTION

GENERAL DISCUSSION

URS Research Company has been conducting a combined analytical and experimental program to determine the loading, structural response, and debris characteristics of building wall panels. This program was sponsored by the Defense Civil Preparedness Agency, Hazard Evaluation and Vulnerability Reduction Division, under Contract No. DAHC-20-71-C-0223.

The primary emphasis in the program has been to determine the failure strengths of wall panels typical of those found in existing buildings, and in particular wall panels found in those buildings which contain designated fallout shelter spaces. Since a large majority of designated buildings have walls constructed of brittle materials, such as brick and concrete block, these have been the primary materials investigated.

Full-scale walls (approximately 8-1/2 ft high by 12 ft wide) of these materials with and without window or door openings have been constructed and exposed to air-blast waves in the URS Shock Tunnel. Along with these shock tunnel tests, an analytical study and a study of the mechanical properties of the construction materials were undertaken in order to insure that the shock tunnel test results could be extrapolated to conditions, wall panel strength characteristics, and wall panel types other than those tested in the Shock Tunnel. Using this approach (which tends to minimize the number of tests that must be conducted in the Shock Tunnel), techniques for predicting when and how walls fail are being generated. The basic requirement for this information is for use in updating estimates of building damage and casualties from both nuclear and natural disasters.

REPORT ORGANIZATION

This report has been organized to serve two functions: first, to present the results of the research effort conducted during the reporting period (November 1, 1972 to October 30, 1973); and second, by combining these results with others previously reported, to present a summary of program results to date.

As before, the primary emphasis during the reporting period was on shock tunnel tests of walls made of brittle material (brick and concrete block) and supporting analytical effort. However, these walls were all tested in the so-called arched support condition, that is, as if they were in-fill walls fitted very snugly into a rigid frame structure. The results of the analytical effort for these walls and a summary of the wall panel tests are presented in Section 2.

In addition to the wall panel failure tests, during the reporting period, some effort was placed on measuring blast loads both with and without a wall in place. The results of this limited loading study test series, which utilized both an open tunnel configuration and one with an instrumented nonfailing wall in place, are discussed in Section 3.

Section 4 is concerned with a brief summary of the analytical and experimental results of the entire program to date.

There are three Appendices with this report: Appendix A - Wall Panel Test Data, Appendix B - Summary of the Computer Effort, and Appendix C - Static Test Data.

Section 2

ARCHED WALLS

PRACTICAL CONSIDERATIONS

Considerable theoretical work on arched walls has been done (e.g., see Ref. 1) to provide insight into the phenomenon of arching. In this subsection the applicability of this theoretical base to real world structure has been examined by consideration of some of the pertinent actual construction and design practices, thus the title, "practical considerations."

Walls can be divided into two functional classes, structural and nonstructural. Structural walls, which perform some structural function other than carrying their own weight, are of two fundamental types, bearing walls and shear walls. Bearing walls, i.e., walls that support vertical loads in addition to their own weight, were treated to some extent earlier in this program (Ref. 1). Shear walls, which are walls designed to resist lateral structural loads parallel to the faces of the walls, have not as yet been investigated in this program.

In this report we are concerned with some of the walls in the second functional class, that is, nonstructural walls whose only functions are to protect the interior of a structure from the elements or to divide up interior space. More particularly our concern is limited to exterior, nonstructural walls which, because they are nonstructural, are also nonbearing, that is, they support no vertical loads in addition to their own weight. The principal masonry walls in this class are curtain walls and panel walls, defined below:

Curtain Wall - An exterior nonbearing wall built between columns or piers and not supported at each story. This definition (from Ref.2) is used the most often in building codes (but unfortunately, the

term is frequently considered to be synonymous with "panel wall"). We will also class as "curtain walls" those walls built entirely external to a frame, that is, external to columns as well as spandrels.

Panel Wall - A nonbearing wall built between columns in skeleton construction and wholly supported at each story. This corresponds to the usual building code definitions (but unfortunately, again, panel walls are frequently called "curtain walls"), also called enclosure walls. Note that a panel wall may be provided with a facing wythe or veneer of masonry which extends outside the frame. But, because such a wall is supported at each story, it still constitutes a panel wall.

During the remainder of this discussion we will remain within this framework of definitions to avoid confusion.

Both panel and curtain walls are intended to hold out weather and hold in comfort without performing any specific structural task (other than holding themselves up). Yet their inherent structural characteristics must be considered if one is interested in predicting building damage and injuries to people.

Textbooks and design manuals spend a great deal of effort in recommending that walls designed to be nonstructural, are made to be truly nonstructural. If, for example, a building is designed to have a "rigid frame structure" (skeleton frame, space frame, etc.), care should be taken to prevent the walls from interfering with the behavior of the frame. This is for two reasons: first, if the walls do interfere with the behavior of the frame, engineering calculation for design that assume frame behavior are wrong, and the structure will behave differently than predicted; second, if the walls (and especially masonry walls), which are much stiffer than the frame, interfere with the motions that frame structures undergo, they are likely to crack.

Despite these strong recommendations, however, especially in concrete frame structures with panel walls completely inset into the frame (which type of construction reduces the tendency of the walls to form shrinkage cracks), it appears to be common practice, especially with low rise structures, for the walls to be built snugly against the frame members (both spandrels beams and columns). Sometimes this type of wall is "released" at the floor and ceiling level and anchored only at the columns to resist wind load.

Good design practice, however, puts great emphasis on knowing what load the spandrel beam is to support and thus requires that a good deal of thought be put into the wall design to allow the frame to move freely and thus to keep a known load on the spandrel beam. A recommended detail for steel frames is shown in Fig. 2-1 (from Ref. 3).

As can be seen, common practice (see also Ref. 4) is to caulk between a spandrel beam and the wall below it; this allows each spandrel to carry only its share of load. The walls are then anchored with flexible anchors to the columns for structural resistance to the wind. If the facing wythe or veneer of masonry extends past the column it is very important to have a flexible tie to the column to prevent vertical cracks at the column in the facing material.

For similar reasons, i.e., to permit frame action without interference from the walls, and to prevent wall cracking, flexible ties to the columns are strongly recommended for curtain walls, both those built between columns, and those completely external to the frame. Some recommended details for such flexible connections to spandrel beams are shown in Fig. 2-1 and to columns in Fig. 2-2 (from Ref. 5).

The material in the next two and one-half text pages, drawn directly from Ref. 5, expands on the reasons for specifying flexible ties, and gives some common modern standards.

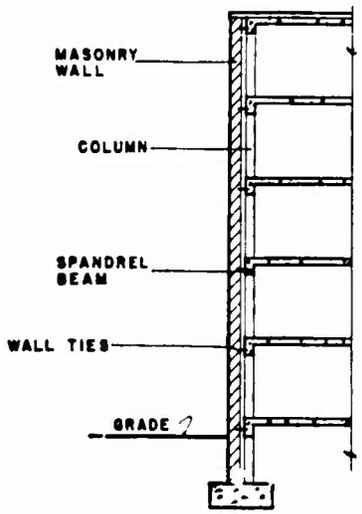

A. Masonry wall braced but not supported by building frame

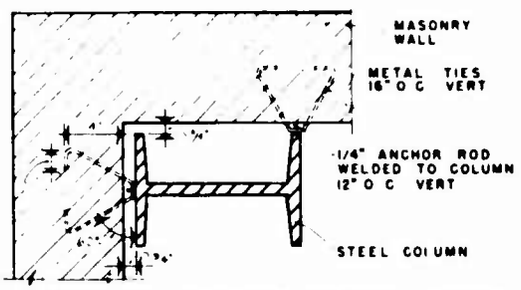

PLAN OF WALL ANCHORAGE TO STEEL COLUMN

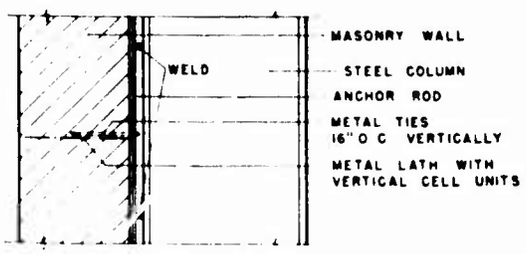

ELEVATION OF WALL ANCHORAGE TO STEEL COLUMN

B. Wall anchorage to steel column

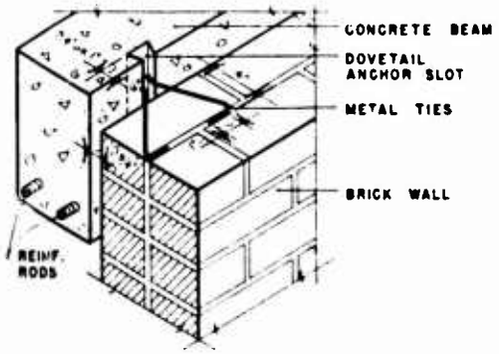

WALL ANCHORAGE TO CONCRETE BEAM

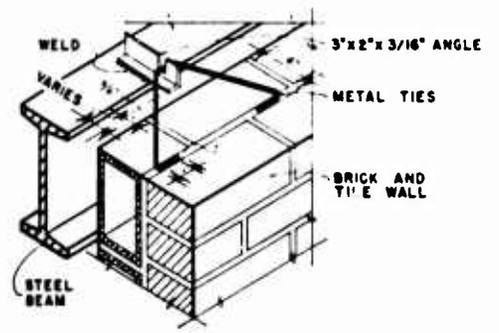

WALL ANCHORAGE TO STEEL BEAM

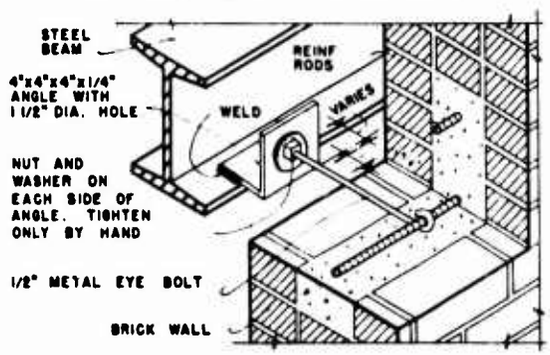

ALTERNATE WALL ANCHORAGE TO STEEL BEAM

C. Typical beam-wall anchorage

Fig. 2-1. Wall to Frame Anchorage Detail.

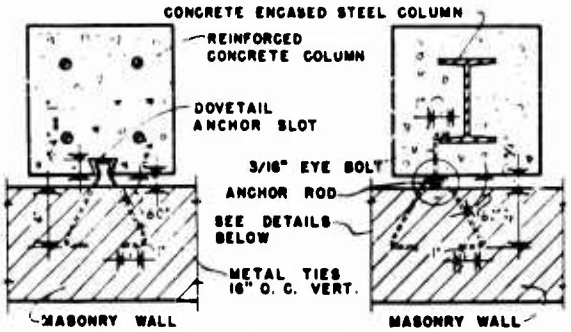

PLANS OF WALL ANCHORAGE TO REINFORCED CONCRETE COLUMNS

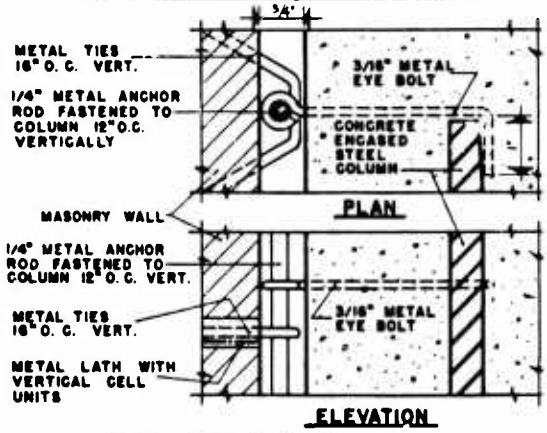

WALL ANCHORAGE DETAILS

A. Wall anchorage details

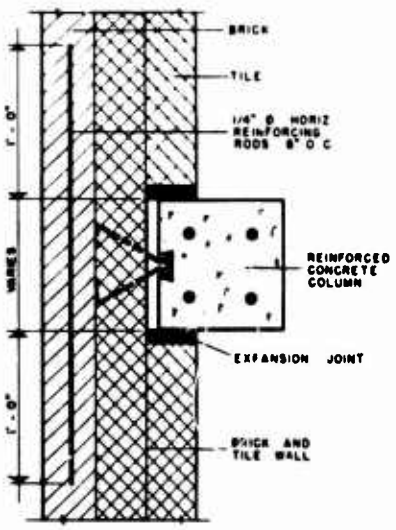

B. Column partially encased in masonry wall

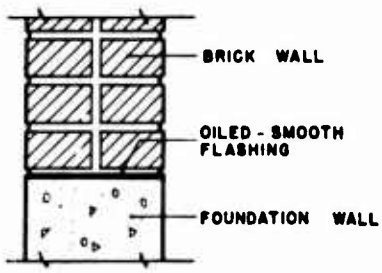

C. Prevention of bond at foundation

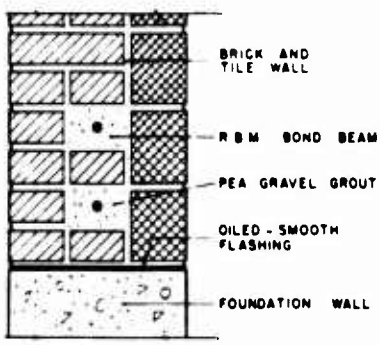

D. Reinforcement of wall at foundation

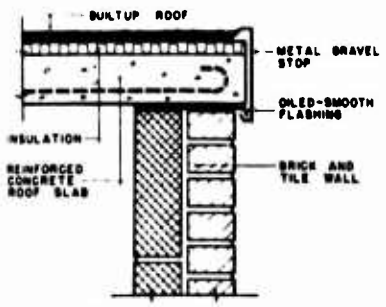

E. Prevention of bond between masonry wall and roof slab

Fig. 2-2. Continuation of Fig. 2-1, Wall to Frame Anchorage Details.

"Masonry walls in skeleton-frame construction are especially susceptible to cracking caused by thermal and other kinds of movement. In addition to thermal movement within the wall itself (discussed on the previous page), there may be differential movement between the wall and the building frame. Perhaps even more important is the fact that skeleton frames are more flexible than masonry walls and undergo greater deflection due to floor loads and to wind and other lateral forces.

"A solution to this problem is the use of flexible ties between the masonry walls and the columns and spandrel beams of the building frame. Recommended details of such flexible anchorages are shown in Fig. 2-1.

"If the building is not too high, the exterior walls can be erected completely independent of the columns and beams for vertical support. The walls then carry their own dead weight to the foundation, and thus reduce the size and cost of the frame. The skeleton frame provides the wall with lateral support and carries all other vertical loads. The wall is tied to the frame by flexible anchors that take tension and compression, but no shear, and thus permit differential longitudinal vertical movements between the frame and the wall (Fig. 2-1A, B, C and Fig. 2-2A). A schematic diagram for such a structural system is shown in Fig. 2-2A.

"Metal ties should be No. 6 gage galvanized steel or other noncorrosive metal of equal strength. To avoid buckling of the ties the distance between the inside face of the wall and the anchor seat should not exceed 3 in., and preferably not more than 3/4 in. The size and spacing of ties are based on tensile and compressive loads induced by wind suction on the wall (Table 2-1 shows the maximum spacing of No. 6 gage ties on spandrel beams for three wind pressure, based on the maximum distance between lateral supports for several wall types). If lateral support is provided only by columns, the spacing of ties should be the same as shown in Table 2-1.

Table 2-1

SPACING OF WALL TIES

Wall Type	Maximum Distance Between Lateral Supports for Walls	Maximum Spacing of No. 6 Gage Tie Anchors at Lateral Supports		
		40 psf	30 psf	20 psf
6" tile	10' 0"	1'-6"	2'-0"	2'-0"
6" brick or 8" tile	12' 0"	1' 3"	1'-8"	2'-0"
8" brick	13'-4"	1' 3"	1'-6"	2' 0"
12" tile	18'-0"	1'-0"	1'-6"	1'-8"
12" brick	20'-0"	0'-8"	1'-0"	1'-6"

"Steel or concrete columns, beams, and spandrels should not be surrounded with masonry unless absolutely necessary. It is especially important that masonry not be placed in contact with columns. Physical contact between the edges of decks or floor slabs and the inside face of masonry walls should be prevented. If steel columns are fire-protected by masonry or other material, the fireproofing should not be in contact with the masonry wall.

"If it is considered necessary to encase columns, the encasement should not exceed 4 in. in a 12 in. wall (Fig. 2-1C). Columns should not be encased in an 8 in. wall.

"To prevent cracks resulting from differential movement between the foundation and the wall, the oil smooth flashing shown in detail in Fig. 2-2C will prevent the bond between the two and permit each to move independently. This detail may be used in structures for which it is not necessary to anchor the walls to the foundation. In general, such anchorage is unnecessary for skeleton frame structures in which the enclosing walls may be anchored to the frame.

"Additional resistance to cracking resulting from any forces that may be transmitted to the wall by friction may be obtained by incorporating a reinforced "bond beam" in the base of the wall (Fig. 2-2D).

"A somewhat similar condition occurs where masonry bearing walls support a concrete floor or roof slab. Investigations have shown that such slabs as a rule not only shrink horizontally but also curl upward at the corners. If the walls are tied rigidly to the slab, cracking of the masonry is almost certain to result. This condition is most severe in roof slabs, and in such cases it is recommended that parapets be eliminated and that positive means be provided to break the bond between wall and slab. A suggested detail for this condition is shown in Fig. 2-2D. The natural struggle between the inside and outside portions of a wall becomes most intense at the juncture of roof and parapet wall. This struggle may continue until there is, literally, an explosion. Indeed, cracked or broken parapet walls, particularly at roof corners, are quite common."

The preceding discussion indicates that the relationship between nonbearing exterior walls and a structural frame can consist of walls that are snugly fitted into the frame all around, walls that are "released" at floor level, walls that are caulked to the spandrel beam above, and flexibly anchored to the columns (panel walls), and finally, walls that have flexible ties to both spandrels and columns (curtain walls).

This range of mounting details very strongly affects the capability of the walls to "arch" when they are loaded normal to their faces. Classical or rigid arching occurs when a wall is completely prevented from moving parallel to its face by rigid, unyielding frame members. When this occurs, a wall's collapse strength is greatly enhanced. The greatest enhancement occurs when motion in both the vertical and horizontal directions is prevented (two way arching), but very significant enhancement occurs of motion in either vertical or horizontal directions is prevented (one way arching).

But in many of the wall to frame descriptions, instead of the walls being snugly fitted in between frame members, they are separated from the members by a gap or by caulking (which can be considered a gap as far as arching is concerned). As will be shown later, the existence of such gaps changes the arching mechanisms, and it is therefore necessary to identify a second type of arching which will be termed "arching with a gap."

For completeness, two additional conditions should be discussed. First, those curtain walls flexibly held external to the frame will definitely not undergo any arching phenomena. (There's considerable doubt that even those curtain walls flexibly anchored between columns can arch.) Second, though it has not been discussed -- and is not yet analyzed -- there can exist a kind of arching termed flexible arching in which the frame enclosing a wall is not "infinitely" rigid, and will thus allow only partial restraint to motion parallel to the wall face.

Rigid arching and arching with a gap are discussed in some detail in the remainder of this section.

RIGID ARCHING

When this type of arching takes place, the wall acts as a fixed edge plate or slab until flexural cracking occurs. After flexural failure has occurred, the structure continues to exhibit resistance to out-of-plane motion and force. This post-fracture resistance is derived from the geometric fixity supplied by the "rigid" edge members. In the simple case of one-way arching (for example, a wall fixed only on the top and bottom with the sides free to move), the flexural cracking occurs at the top, bottom, and center, and the resistance to motion, induced by "wedging" or geometric fixity, occurs along line contacts as sketched in Fig. 2-3.

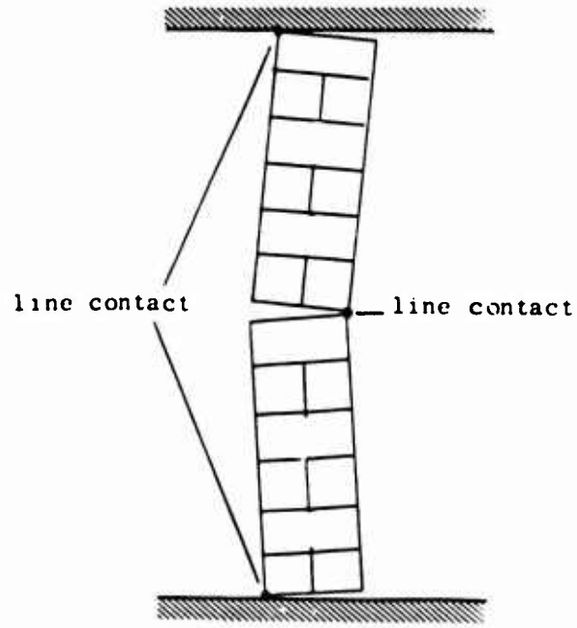

Fig. 2 3. Sketch Showing Resistance to Motion Along Line Contacts in One-Way Arching.

The notion of line contact has led to a series of exploratory static tests which have aided greatly in prediction of failure strengths of arched walls. These tests are sketched in Fig. 2-4.

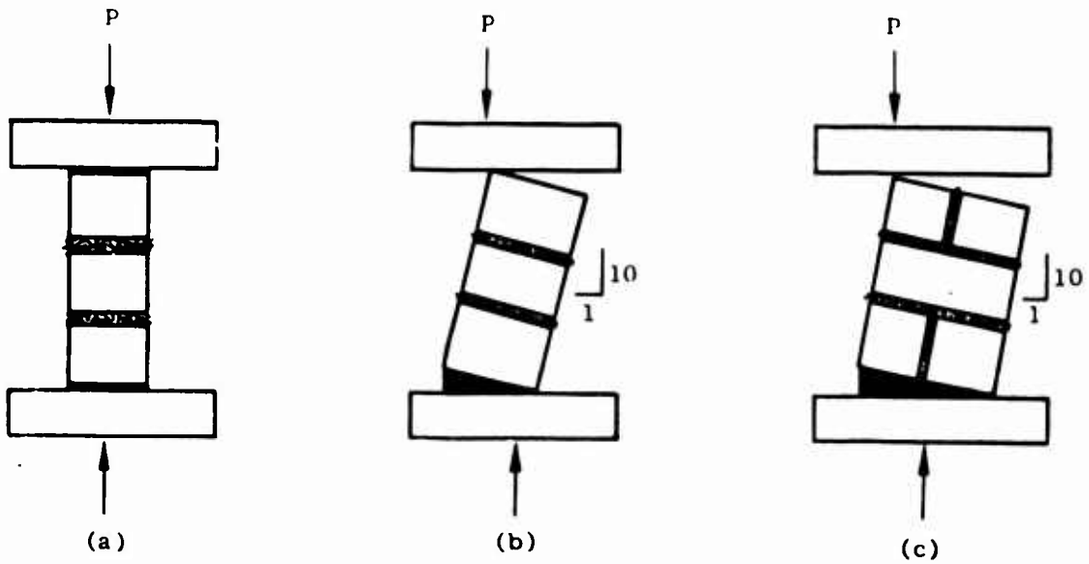

Fig. 2-4. Geometries for Exploratory Static Tests

Test geometry, or configuration, A is the standard ASTM "Composite" strength test geometry 4" x 8-1/2" x 8-1/2". The average results of a series of these tests are as follows:

p (lbs)	f_c' (psi)	E (psi
78,000	2 400	410,000

where p = loading force

f_c' = stress at failure

E = Young's modulus

Note: This is the average data from 15 tests; the individual test values are given in Appendix C, Table C-3.

From this series of tests it appears that a "composite" E of about 400,000 and an ultimate strain $\epsilon = (f_c'/E)$ of about 0.006 in./in. for collapse is accurate for prediction purposes.

The next series - test geometry B (4" x 8-1/2" x 8-1/2") - was conducted to model the first (4 in. thick) arched wall tested in the Shock Tunnel and provided insight into the strain behavior of 4 in. thick, line loaded samples, see Appendix C, Table 5.

P lbs	f_c' (psi)	f_ℓ (lb/in.)	E (psi)	E^* ($\frac{lb\ in./}{in.^2}$)
28,100†	860	3,100	77 700	282,000†

The load P and the average stress f_c' from configuration (B) were lower than those from configuration (A) as would be expected since the stress along a line contact is much larger (theoretically infinite) than stress imparted by an area contact. A more meaningful parameter than average stress f_c' (which is based on the loaded area of the composite) would be f_ℓ, i.e., the force per unit length of the line load on the composite material. The last term in the table, E^*, is thought to be a

† Remains linear until f_ℓ approximately 3,000 lbs/in.

better descriptor of these line load situations than E. It is defined as:

$$E^* = f_\ell / \epsilon \text{ (lb/in.)}$$

Test (C) was a series conducted to do two things: first, to aid in prediction of the behavior of 8 in. walls; and second, to check if the parameters f_ℓ and E^* were independent of thickness of the section, from Appendix A, Table A-5.

P	f_c'	f_ℓ	E	E^*
(lbs)	(psi)	(lb/in.)	(psi)	(lb in./in.^{2})
43,100†	600	1,500	51,000	384,800†

Comparison of Group (3) and Group (C) results show that the nominal E and f_c' decreased even though the load P increased, however, both f_ℓ and E^* increased. E^*, therefore, appears to be a more consistent measure of stifness.

As an additional source of information basic material properties were derived from testing 8-1/2" x 8-1/2" x 8-1/2" brick assemblies in compression (as in geometry A above) from Table C-4 in Appendix C.

P	f_c'	E
(lbs)	(psi)	(psi)
189,000	2,700	625,000

From the foregoing observations, static tests, and analysis, a model which could be used in the computer program MACE** was evolved. Inspection of a uniformly loaded three-hinged arch shows that only half the structure need be modeled, as the center hinge is an axis of symmetry; see freebody sketch in Fig. 2-5.

---

† Remains linear until f_ℓ approximately 4,000 lbs/in.

** A discussion of the computer output is presented in Appendix A.

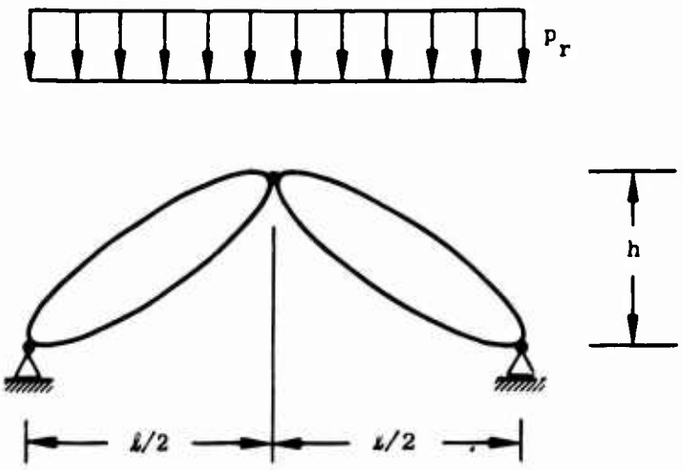

THREE-HINGED ARCH

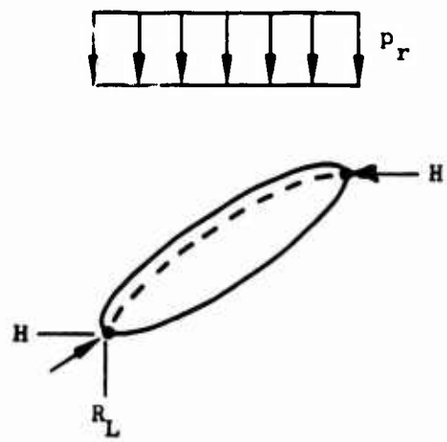

$$R_L = \frac{p_r \ell}{2}$$

$$H = \frac{p_r \ell^2}{8h}$$

$$\frac{R_L}{H} = \frac{4h}{\ell}$$

Fig. 2-5. Freebody of Half Wall

From Fig. 2-5 it can be seen that, in the case of an arching wall, the line loads differ in both magnitude and direction at different points on the arch. This explains the differences observed on full-scale tests in spalling behavior at the centerline and the top and bottom, namely, that more material is fractured at the top and bottom than at the centerline. The computer model used with MACE* is shown in Fig. 2-6. It represents half of a full scale, 8 in., one-way arched brick wall subjected to a one psi static load. The section is 1 in. thick, 8 in. high and 48 in. long. The assumed E = 1,000,000 psi. The supports (joints 8 and 17) are put 1 in. inboard, which appeared to be about the center of thrust (crushing) on static test specimens and full scale tests. With this geometry, ($\ell/2$ = 48, h = 6 in., t = 8 in.), the left hand thrust is found to be 192 lbs/in./psi horizontal.

The coarse grid of this model makes strain calculations less accurate than could be desired, but they do provide a reasonable approximation of the gross behavior of the wall. At 5 psi the center deflection (see Table 2-2, joint 17, y direction) is 0.6055 in., which is a large deformation, since it is about 10 percent of h. The center thrust is 960 lbs/in. and the support thrust is 988 lbs/in. for E_m = 100,000** psi. An assumption that each added increment of displacement provides a proportionately reduced thrust resistance, i.e., each increase in deflection reduces the resisting moment $[R.M. = H(h-\delta)]$, permits drawing the predicted static resistance function shown by the mean curve in Fig. 2-7. The E^* value is constant until f_ℓ = 4,000 lbs/in. (at about 2.4 in. displacement) whereupon the E^* value drops radically as f_ℓ goes to 5,000 lbs/in. ultimate resistance.

The mean value curve is constructed by a step-by-step reduction in resisting moment with each increase in displacement. Based on statistical work done earlier in the program (Ref. 7) a coefficient of variation of

---

* For description of this program see Appendix B.

** E_m, a Young's modulus that provides for gross deformation of the wall (including crushing) was shown in Ref. 1 to be about 100,000 psi.

γ = 0.833 lbs/in.^{3}

g = 386 in./sec^2

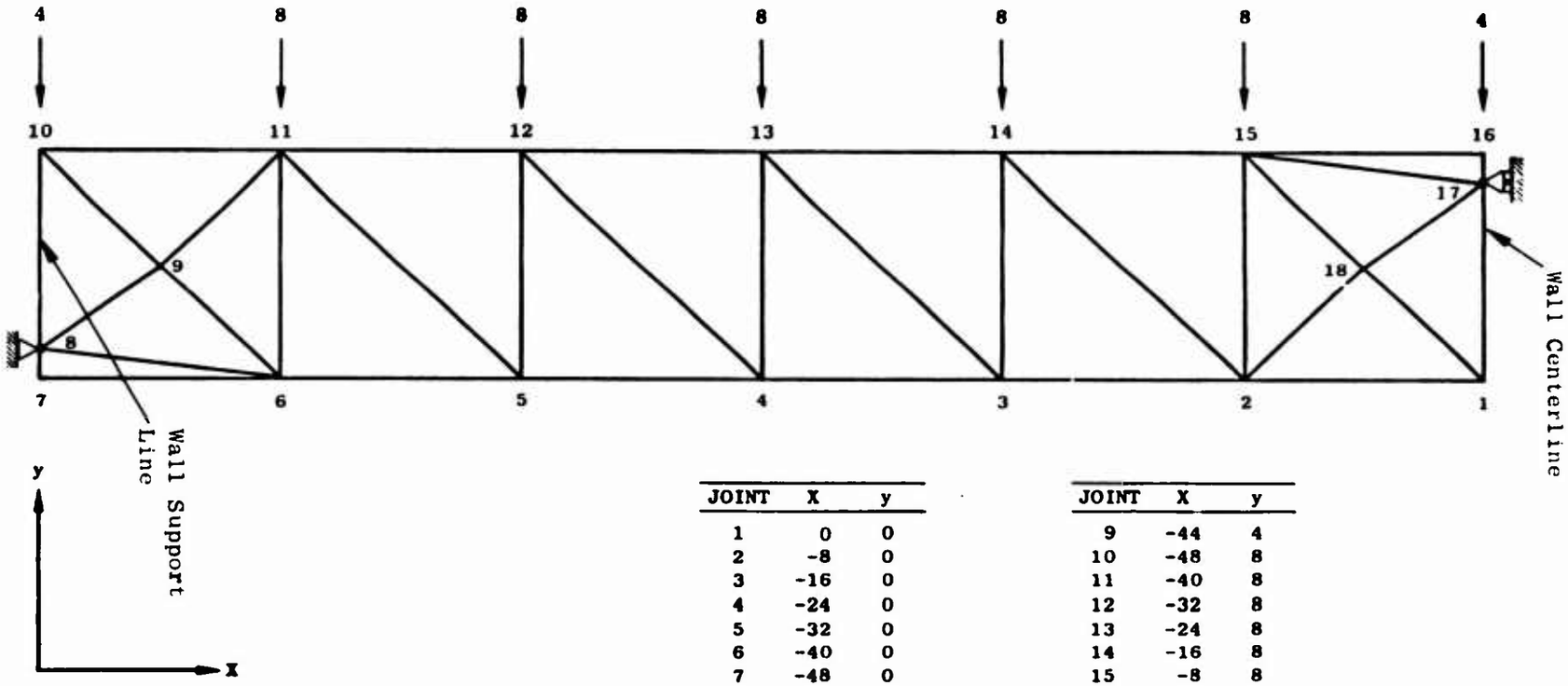

JOINT	X	y
1	0	0
2	-8	0
3	-16	0
4	-24	0
5	-32	0
6	-40	0
7	-48	0
8	-48	1

JOINT	X	y
9	-44	4
10	-48	8
11	-40	8
12	-32	8
13	-24	8
14	-16	8
15	-8	8
16	0	8
17	0	7
18	-4	4

Fig. 2-6. Computer Model Submitted to MACE.

Table 2-2

MACE DISPLACEMENTS (E = 100,000 psi, p = 1.0 psi)

NODE	x	y
1	-1.147×10^{-2}	-1.211×10^{-1}
2	-1.195×10^{-2}	-1.054×10^{-1}
3	-1.093×10^{-2}	-8.612×10^{-2}
4	-9.655×10^{-3}	-6.523×10^{-2}
5	-8.052×10^{-3}	-4.323×10^{-2}
6	-5.954×10^{-3}	-2.107×10^{-2}
7	-2.740×10^{-3}	-3.395×10^{-5}
8	-	-
9	5.742×10^{-3}	-1.026×10^{-2}
10	1.547×10^{-2}	-4.566×10^{-4}
11	1.536×10^{-2}	-2.079×10^{-2}
12	1.362×10^{-2}	-4.319×10^{-2}
13	1.141×10^{-2}	-6.516×10^{-2}
14	8.865×10^{-3}	-8.601×10^{-2}
15	6.029×10^{-3}	-1.050×10^{-1}
16	2.143×10^{-3}	-1.211×10^{-1}
17	-	-1.211×10^{-1}
18	3.983×10^{-3}	-1.136×10^{-1}

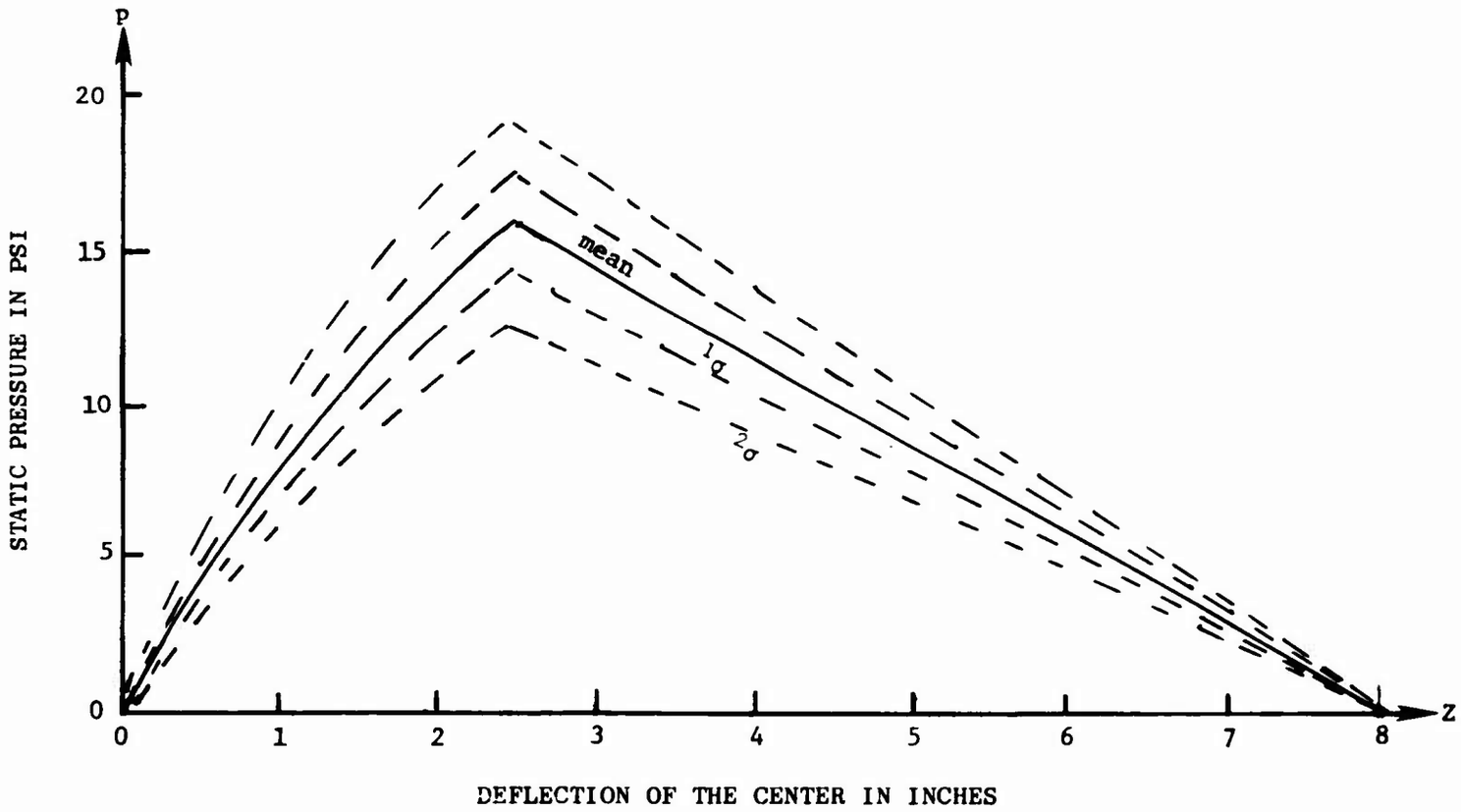

Fig. 2-7. Arched Wall, Static Resistance

10 percent was assumed for the f_ℓ values. Using the 10 percent coefficient of variation and assuming a normal distribution, the 68 percent ($\pm 1\sigma$) and 95 percent ($\pm 2\sigma$) lines were added to the prediction curve. This was done to make possible more realistic predictions and to improve corrciation with actual test data.

A summary of tests on "rigidly" arched walls conducted to date are presented in Table 2-3. Walls 71, 74, 75 and 76 from Test Series 1 (conducted in 1972) and Walls 87, 88, 94 and 96 from Test Series 2 (conducted in 1973) were all 8 in. brick one-way arched walls. The data from these tests are summarized in Table 2-4. From Table 2-3 we see that Walls 74, 75, and 76 failed at about 12 psi and Wall 71 which was loaded four times failed at 9 psi. From this one could deduce that Series 1 walls had a range of 9-12 psi or a resistance along the lower bound of the failure-prediction curve. Walls for Series 2, however, indicate a wall strength from below 14 psi to slightly over 17 psi which is toward the upper bound of wall strengths on the prediction curve.

It can be seen that the mean pressure is only about 10 percent below that predicted from the crude model and the scatter is less than predicted. Hence, it appear that the prediction model warrants further work and expansion. In addition, a closer study of all the static test data could improve predictability.

ARCHING WITH A GAP

As discussed under "practical considerations," some frames have a "gap" intentionally built-in to insure freedom of frame behavior. In other situations such a gap can result from shrinkage and workmanship flaws. Regardless of how the gap arises, it is of interest to treat the problem analytically, and since arching is a geometrically induced phenomenon, it is necessary to study the geometry.

Table 2-3

SUMMARY OF ARCHED SOLID WALL TESTS

Type of Test	Wall No.	Primacord Length	No. of Strands	p_r (psi)	Description of Tests
Series 1					
4 in. brick beam	68	60	1	1.5	wall cracked
	68	60	2	3.4	wall failed
8 in. brick beam	71	12	1	-	test for natural period
	71	60	2	3.8	wall cracked
	71	60	3	5.8	cracks enlarged
	71	60	4	8.6	wall failed
	74	60	2	~3.8	wall cracked
	74	60	4	11.0	wall failed
8 in. brick beam	75	60	5	11.9	wall failed
	76	60	5	11.1	wall failed
8 in. concrete block beam	77	60	3	6.5	wall cracked
	77	60	2	4.1	no additional damage
	77	60	3	6.8	wall failed
	78	60	4	9.1	wall failed
6 in. concrete block beam with 4 in. brick facing on side toward blast	79	60	5	11.2	wall failed
Series 2					
Arched Solid Walls					
8 in. brick (1 way)*	87	60	4	10.3	wall cracked
		60	5	12.7	cracks enlarged
		60	6	16.3	wall failed

* One-way arched-fixed top and bottom only.
Two-way arched-fixed on all four sides.

Table 2-3 (Cont'd)

Type of Test	Wall No.	Primacord Lengths	No. of Strands	p_r (psi)	Description of Tests
Series 2 (Cont'd)					
Arched Solid Walls					
8 in. brick (1 way)*	88	60	6	15.7	wall cracked
		60	3	7.2	cracks enlarged
8 in. brick (1 way)*	94	60	6	15.5	wall failed
8 in. brick (1 way)*	96	60	5	13.4	wall failed
10 in. concrete block with brick facing (1 way)*	92	60	3	6.9	wall cracked
		60	3	6.9	no additional damage
		60	4	9.9	cracks enlarged
4 in. brick (2 way)*	83	60	2	4.4	wall cracked
		60	2	4.2	wall failed
8 in. concrete block (2 way)*	89	60	4	10	wall failed
8 in. concrete block (2 way)*	90	60	3	8	wall failed
Arched Walls with a Doorway Opening					
8 in. brick (1 way)*	86	60	5	12.2	wall cracked
		60	6	16.8	cracks enlarged
8 in. brick (1 way)* with gap at top	95	60	6	17.2	wall failed
Arched Walls with a Window Opening					
8 in. brick (1 way)	84	60	5	12.8	wall cracked
			6	15.5	wall failed

Table 2-3 (Cont'd)

Type of Test	Wall	Primacord Length	Strands	(psi)	Description of Tests
Series 2					
Arched Walls with a Window Opening					
8 in. brick (1 way)	85	60	5	12.4	wall cracked
		60	5	11.7	cracks enlarged
		60	6	15.0	slight additional cracking
		60	7	~19	wall failed
8 in. concrete block (1 way)	91	60	3	6.8	wall failed
8 in. concrete block (1 way)	93	60	3	6.2	wall cracked

Table 2-4

SUMMARY OF DATA FOR TABLE 2-3

Wall	P_r (failure)	
71	8.6	(3 loadings)
74	11.0	
75	12.0	
76	11.1	
87	16.3	(3 loadings)
88	15.7	(2 loadings)
94	15.5	
96	13.4	(pre-split)

Mean $P_r \leq 13.8$

Figure 2-8, Phase I, illustrates the wall position prior to being loaded. The gap is at the top, and the base is fixed to the foundation. This configuration means that the wall, when subjected to a lateral load such as a blast, will act like a cantilever beam (see Fig. 2-9) until it fractures at the bottom and wedges in at A and B as shown in Fig. 2-10.

Fracture at the base occurs at very low pressure levels, i.e., let

$$\sigma_r = 100 \text{ psi}, \quad E = 400{,}000 \text{ psi}$$

$$t = 8 \text{ in.}$$

$$\ell = 96 \text{ in.}$$

$$M = \frac{p\ell^2}{2}$$

$$I = \frac{t^3}{12}$$

we find statically, for a unit width of wall,

$$p = \frac{\sigma_r}{3} \frac{t^2}{I}$$

$$p = 0.25 \text{ psi}$$

It follows, that, if motion is to take place at the top, the gap must be larger than any lengthening the wall might do while being loaded as a cantilever beam. Assuming that the neutral axis does not change length it then follows that:

$$S_\ell = \Psi \frac{t}{2} \quad \text{and} \quad \Psi = \frac{p\ell^3}{EI}$$

where

S_ℓ = Lengthening of tension side (see Fig. 2-9)

Ψ = Slope of beam at force end (see Fig. 2-9)

therefore

$$S_\ell = \frac{p\ell^3}{Et}$$

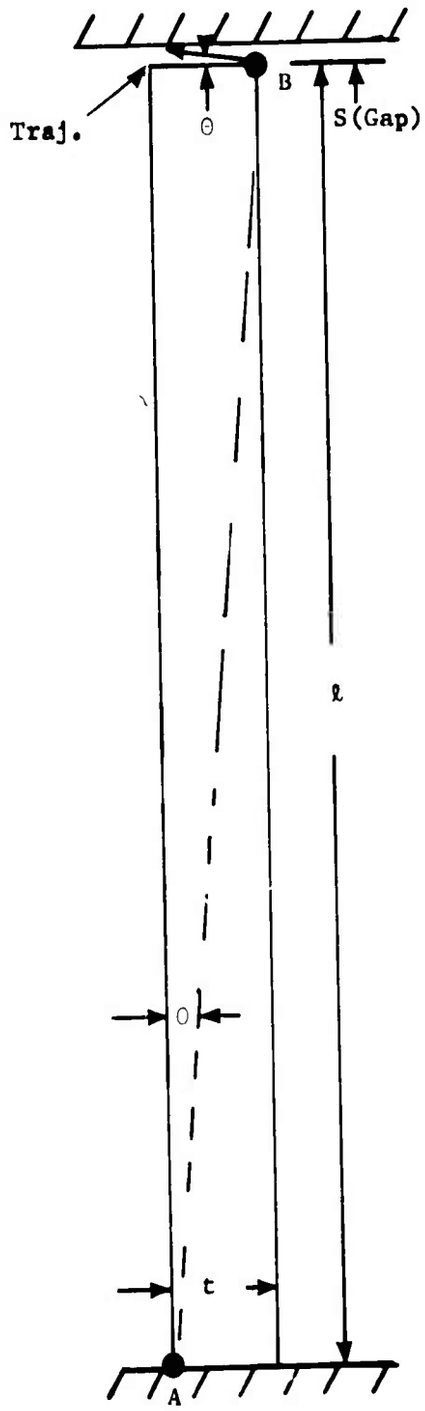

ℓ in. inches

t in. inches

S in. inches

$\Theta = \frac{t}{\ell}$ in. radius

Traj. Trajectory

Fig. 2-8. Phase 1 - Cantilever Wall.

Ψ = Slope of beam at free end

S_ℓ = Lengthening of tension side

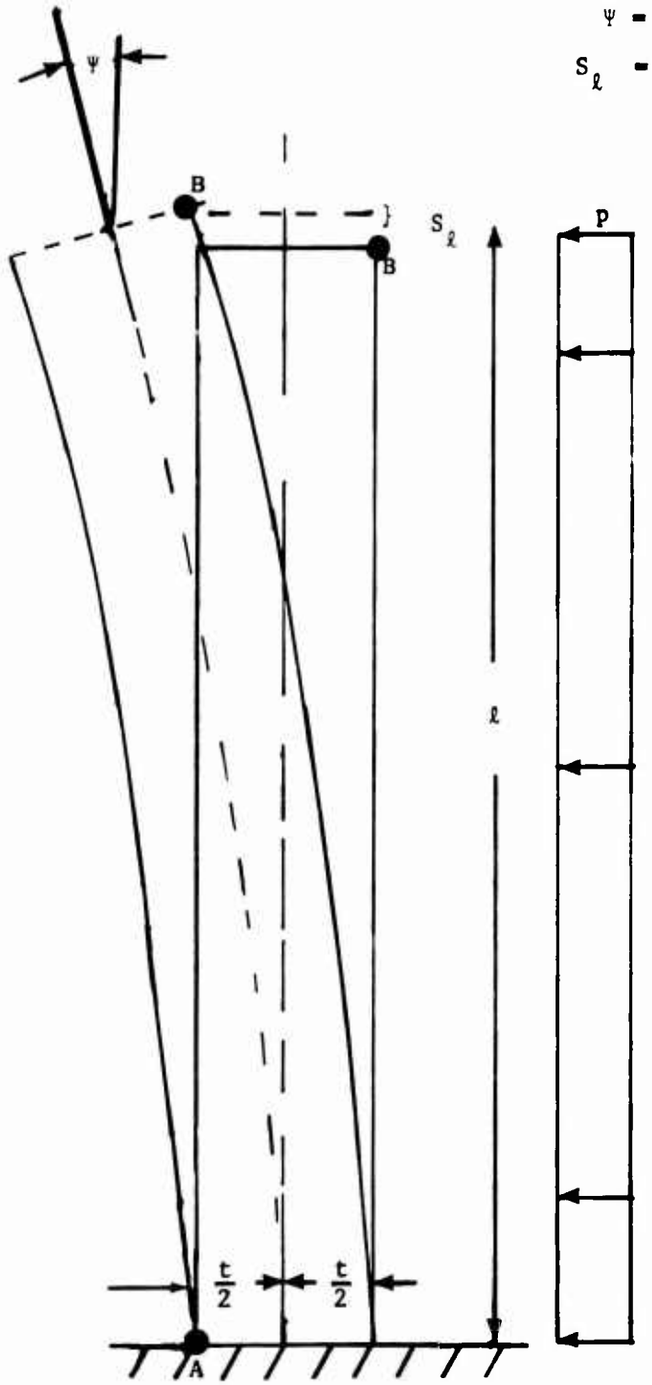

Fig. 2-9. Cantilever in Bending.

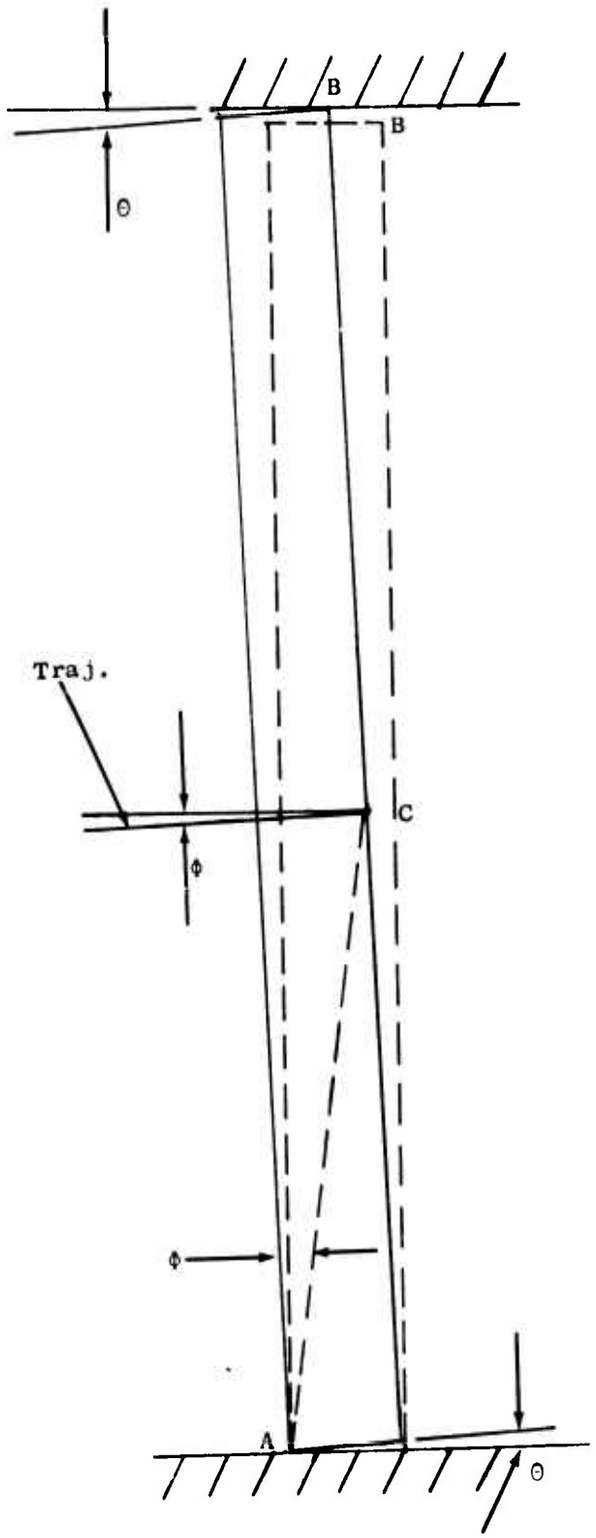

$\Theta = \frac{t}{\ell}$ in radians

$\Phi = \frac{2t}{\ell}$ in radians

Fig. 2-10. Phase II - Gapped Wall "Arched."

$$S_\ell = \frac{p\ell^3}{Et^2}$$

or for our wall

$$S_\ell = \frac{0.25(96)^3}{400{,}000(8)^2}$$

$$S_\ell = 0.00864 \text{ in.}$$

Hence, any gap greater than 0.00869 in., i.e., greater than about 0.01 in., allows the wall to assume the orientation shown in Fig. 2-10, Phase II. It appears that there is a three hinged arch, as with a non gapped wall, but the arch depth is only one-half that with a nongapped wall, i.e., t/2 instead of t.

The next thing that should be investigated is the system statics to thoroughly understand the loading system and the restraint mechanisms.

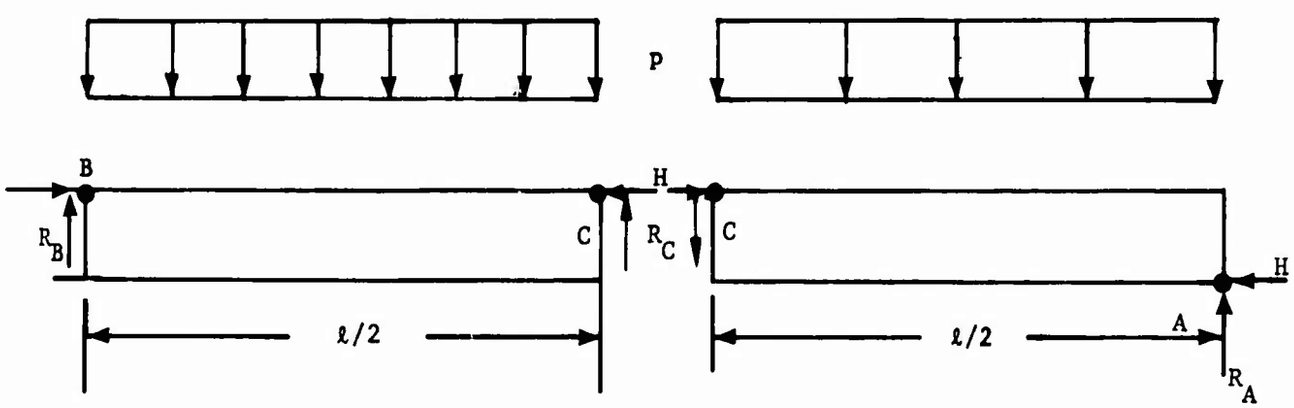

Frqm the above free body diagram in which "C" represents the line along which fracture occurs, and the laws of statics we find:

$$H = \frac{p\ell^2}{4t}$$

$$R_B = R_c = \frac{p\ell}{4}$$

and

$$R_A = \frac{3}{4}\, p\ell$$

compare these to equivalent values for the nongapped arch where

$$H = \frac{p\ell^2}{8t}$$

$$R_A = R_B = \frac{p\ell}{2}$$

$$R_C \approx 0$$

This raises some interesting points. It is observed that the thrust "H" is twice as large in the case of a wall with a gap which indicates that the wall can be no more than one-half as strong as a wall with no gap. For example, let ℓ = 96 in. and t = 8 in. (close to value used in the Shock Tunnel) and compare the arching forces for gapped and nongapped walls.

Gapped

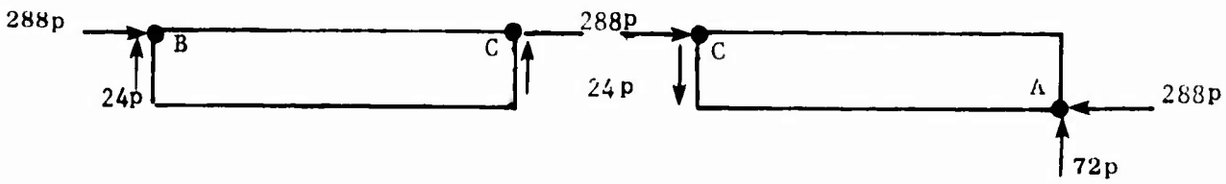

Nongapped

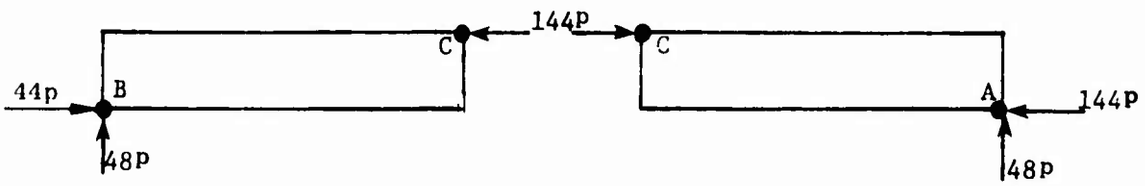

At the base (Point A) the directions of resultant force application are similar for both gapped and nongapped walls, though their magnitudes (for the same applied loads) are different.

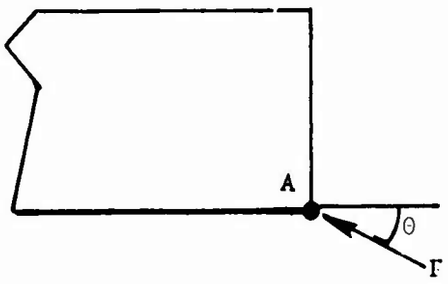

Gapped: F = 296p

θ = 14°

Nongapped: F = 153

θ = 19°

From this, it would be expected that at the base (Point A) gapped and nongapped failures would be similar, except that gapped walls would fail at only about one-half the applied load as for the nongapped condition.

At point C, however, one finds far different conditions. In the nongapped wall the force at C is a pure thrust acting on an initially nonopened crack, i.e. there is no shear to be carried across the cracked joint.

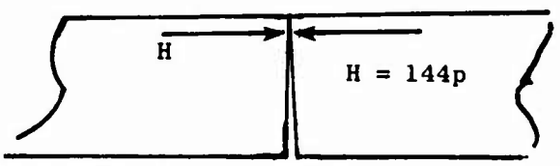

Nongapped

Joint C in the gapped wall is a great deal different. First there is a shear (24 p) to be carried across the cracked joint,

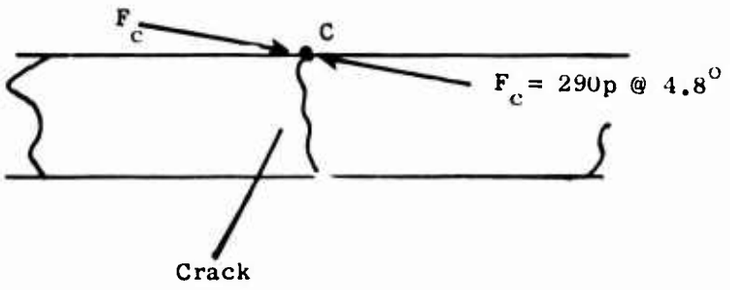

and second, the arching force F_c is not only at the face but acts in a direction tending to spall off the edge of the brick. In the nongapped case, the arching force acts along the face.

Joint B in the gapped wall case is also far different than in the non-gapped case. In the nongapped case the force is identical to that at Joint A, however, in the gapped case it is more like the left portion of Joint C. In fact the force not only acts outward from the face but it acts on a corner that is probably damaged as shown in the sketch below:

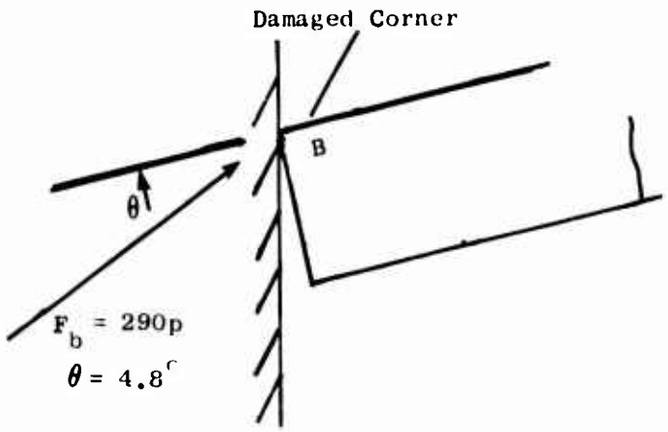

Even if the wall can provide shear resistance at B and C, one still must determine local failure values for a region like B to make some estimate of arching resistance of this degenerate arch.

RESISTANCE PREDICTIONS - GAPPED WALLS

At this early stage of problem definition it is economical to make use of as much previous work as possible. Hence, we will borrow from the prediction scheme presented previously for nongapped walls and modify it for the gapped walls.

One of the first things needed to modify the nongapped arching prediction to a gapped arching prediction is to obtain a strength estimate of the degenerate form of line load developed as at Joint B. To do this crudely, two series of static tests were conducted in the geometry shown in Fig. 2-11, with the "line load" applied in two widths (Δt) of 1/4 and 1/2 in. on an 8-1/2 x 8-1/2 x 8-1/2 in. specimen.

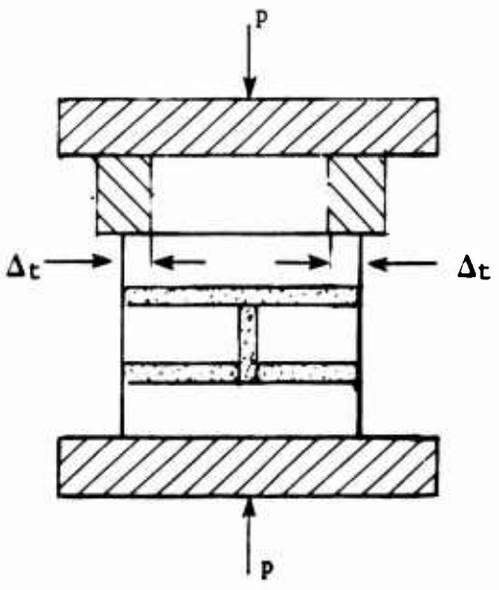

Fig. 2-11. Geometry for Determination of "Degenerate" Static Line Load.

p (lbs)	$f_c' = p/A$ (psi)	$f_\ell = p/16$ (lbs/in.)
10,900	171	680
13,465	211	840
13,990	217	875
15,200	237	950
		use average

For Δt = 1/4 in.

p	$f_c' = p/A$ total	$f_\ell = p/16$
13,980	268	975
33,000	515	2,070
34,500	540	2,160
19,000	297	1,191
		use average

For Δt = 1/2 in.

From the above test results, it is obvious that the failure mode changes from spalling of the face to local crushing at a Δt of about 1/2 in. Of course, it will be necessary to devise a static test which more closely models the actual condition at Joint B; the reaction vector should be outward from the wall centerline and not parallel to it as in this test series. However, from actual wall failures and from the above static tests it appears that a spalling type of failure should occur most commonly.

From the above we see that a line load of f_ℓ = 1,000 lbs (near the spalling value for Δt = 1/2 in.) might be a reasonable strength for a place like region B. Using the analogy of the nongapped wall we can now make an estimate of the resistance of the gapped wall. The resistance moment for the arch can be written R.M. = $H(h-\delta)$ where H is the arching thrust, h the arch height, and δ the deflection of the center.

If one assumes that 1/2 in. is a reasonable spall (crushing) area, it then follows that h = 3.5 in. and t = 8 in initialy and that H = 330 lbs. per in. for a 1 psi applied pressure. (See Page 2-26) Prorating the deflection calculations for the nongapped wall, shown on Page 2-14, one predicts δ = 0.25 in. at 1 psi. Following a step-by-step resisting moment, deflection, line load calculation one finds the maximum resistance of 2.56 psi at f_ℓ = 1,000 lbs. This quickly decays to zero at a centerline displacement of 4 in. shown in Fig. 2-12.

Experimentally all our solid, one-way arched, brick, 8-in. walls (nongapped) have failed in the 12-16 psi (reflected) range. Hence, it is believed that an 8-in. brick wall with a gap will fail at about 2.5 psi reflected.

Only one gapped wall test has been conducted to date. This was wall 95, an 8-in brick wall with a doorway. Unfortunately, this wall was tested at a much higher pressure (p_r approximately 17 psi) than is indicated by the theoretical work described above. However, this wall failed catastrophically where a similar wall (number 86) survived two tests at a p_r of 12.2 and 16.8 psi.

ARCHED WALLS WITH DOORWAYS

The rigid wall and wall-with-a-gap, beam mode (one-way) arching theories described in the preceding two subsections for walls with no openings, have been extended to the case of walls with doorways. This was done by first assuming that the total energy content put into a wall in the beam mode, whether the wall is solid or has a doorway, must be the same per unit width. Further, it has been observed that at threshold loading pressure (the pressure at which a wall just does fail) peak resistance must be overcome before the load decays. For the 8-in. thick walls, peak resistance occurs after about 2 in. of deflection, or at a time of about 50 msec. The flat top portion of our loading pulse is about 50 msec long.

When the first 50 msec of loading for a wall with a doorway is compared to that for a solid wall, it is found that the average pressure differential over the surface of the wall with a doorway is about 25 percent less than that of a solid wall. (Refs. 7 and 8.) This information permits the construction of the resistance function for a nongapped brick wall with a doorway shown on Fig. 2-13.

Wall No. 86, an arching wall with a doorway, was hit by a blast wave from 6 strands of Primacord (a 6 strand blast) which generated a peak reflection pressure, p_r of 16.8 psi. The wall survived that loading as it should about 95 percent of the time with our materials.

The mean resistance function for a gapped wall with a doorway can be derived from reasoning similar to that used for nongapped walls. The result is also shown on Fig. 2-13. Unfortunately Wall No. 95, which might have been used to test the correct use of the curve for a gapped wall in Fig. 2-12, was tested before the theory had fully evolved. From Fig. 2-13, it is obvious that a 3 strand shock wave ($p_1 \simeq 7$ psi) would have a high probability of failing the wall. Wall 95, however, was hit with a 6 strand blast (p_r = 17.2 psi) and failed dramatically. Recall that wall 86, a wall with no gap, survived a 6 strand blast.

TWO-WAY ARCHED WALLS

Little original work has beer done by URS on the theory of two-way arching. It is planned to first complete the one-way arching theory during the year following the reporting period and then extend it to two-way arching. However, from an engineering standpoint, the approximation suggested by Bockholt and Wiehle (Ref. 6) of using the ACI (American Concrete Institute) 1963 code provision for two-way slabs, seems to be sound. This approach suggests that an 8 ft x 12 ft, two-way, interior slab (arched wall in our case) would be 1.4 times as strong as a one-way slab (arched wall). URS test walls suggest that this is a valid appproximation, but the data is limited. Wall No. 68 was a 4-in. thick one-way arched brick wall. This wall survived a 1.5 psi reflected pressure

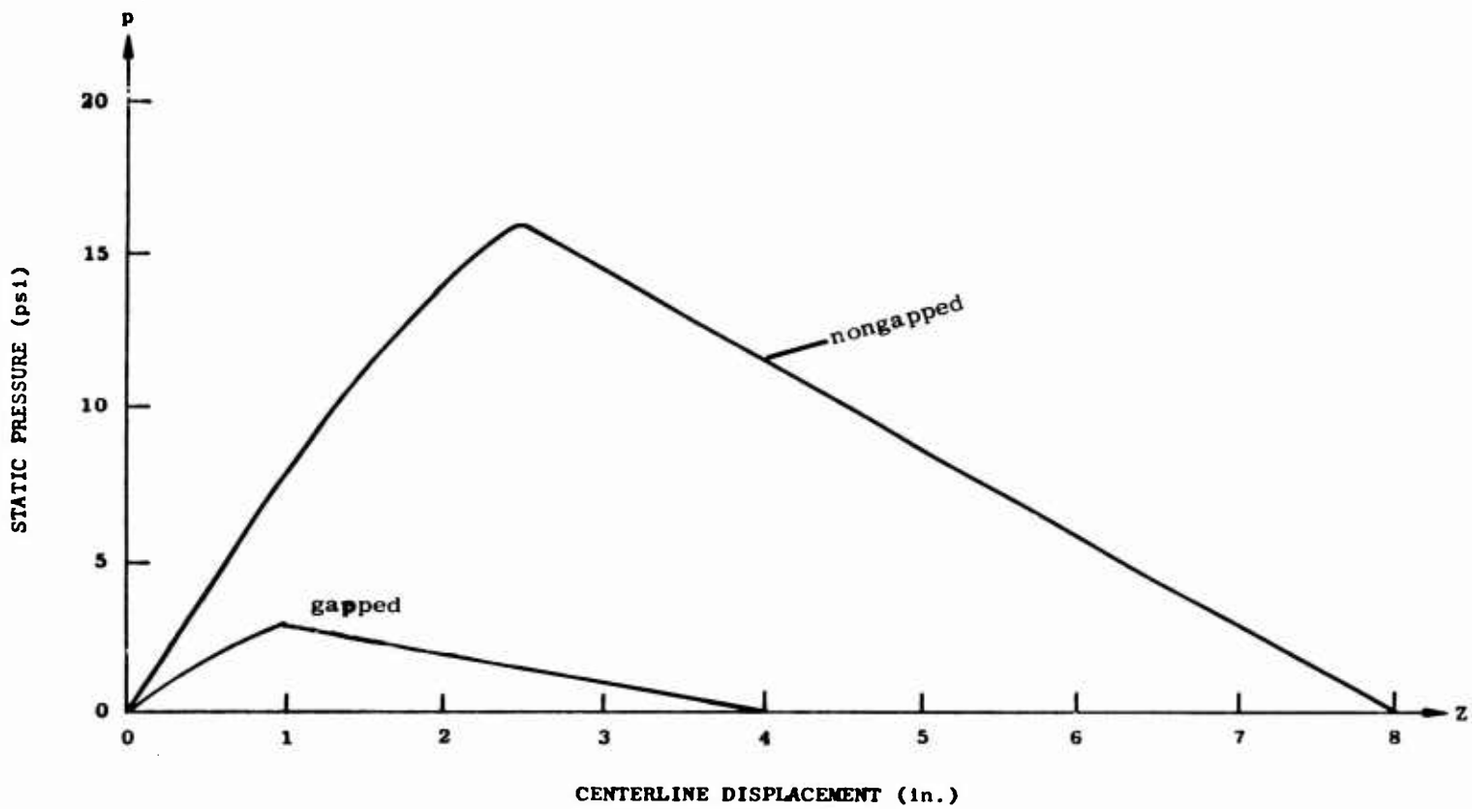

Fig. 2-12. Arched Brick Wall, Static Resistance

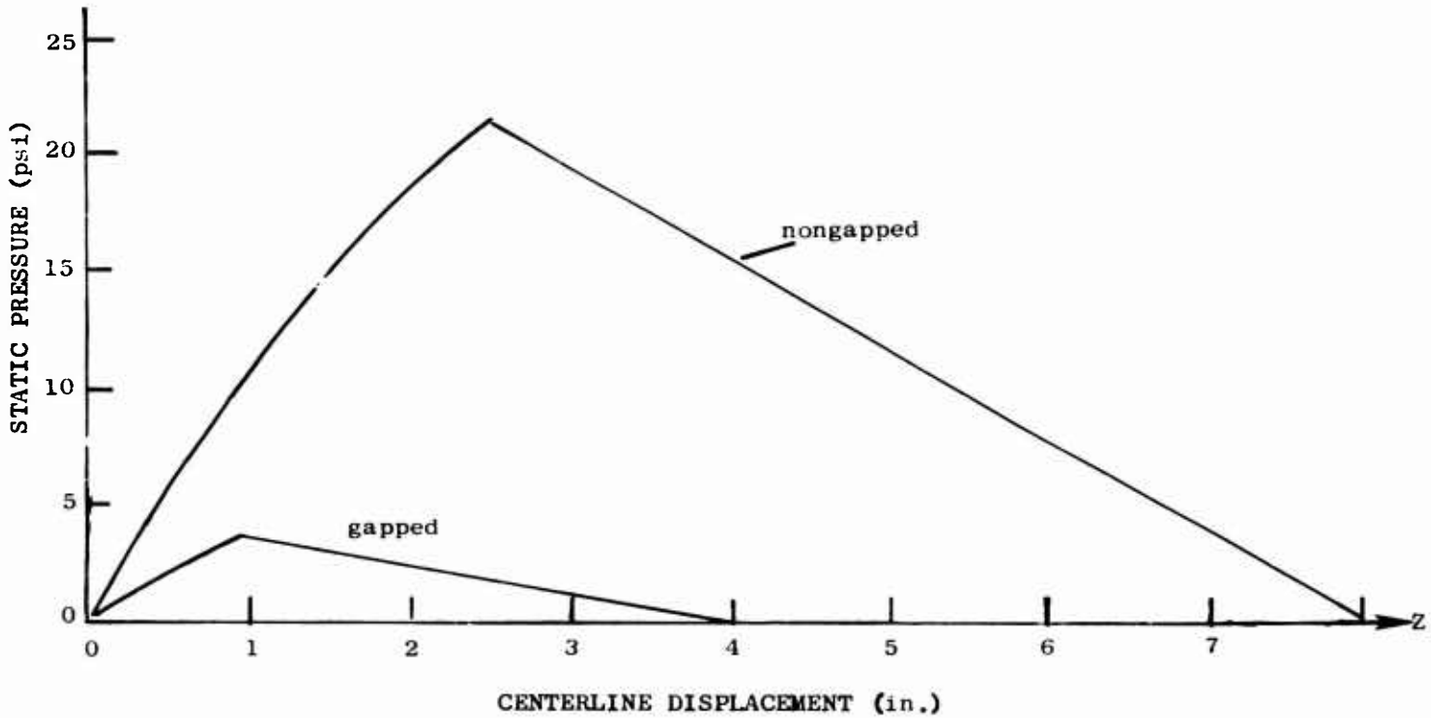

Fig. 2-13. Arched Wall, With Doorway Static Resistance

with flexural cracks at top, bottom and center-line. It then dramatically failed at 3.4 psi, hence, one would suspect that the failure threshold was somewhere around 3 psi. Wall No. 83 was a two-way arched 4 in. brick wall which survived 4.4 psi but exhibited rather dramatic flexural cracking. The wall then failed at 4.2 psi which implies about a 40 percent increase in strength over the one-way case. Of course one would like to have more data to make a stronger case.

Another important feature of this particular test is the crack pattern that was generated. From theoretical mechanics we would expect the downstream cracking to look like the sketch in the upper part of Fig. 2-14.

The photograph in the lower part of Fig. 2-14 shows the flexural cracking after the first 4.4 psi shot. Note how similar the patterns are.

Similarly, mechanics indicate that the upstream flexural cracking should look like the sketch in the upper part of Fig. 2-15.

The photograph in the lower part of that figure shows the corners remaining in the tunnel after the second shot of 4.2 psi had removed the wall. Again predicted and actual results are very close.

These very orderly results indicate that theoretical mechanics can indeed be used to predict both the flexural mode and the arching force. This means that yield-line theory developed for the ultimate strength of slabs will indeed be valid for walls. The major problem in using yield-line theory seems to be the determination of proper material properties to use to predict the yield-line moment capacity. Hence, it seems desirable to continue some of static test work and theory to evolve a good material model for determining the line-load resistance of brittle materials.

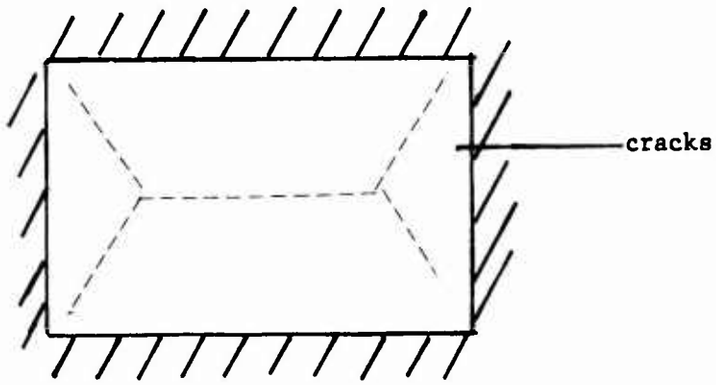

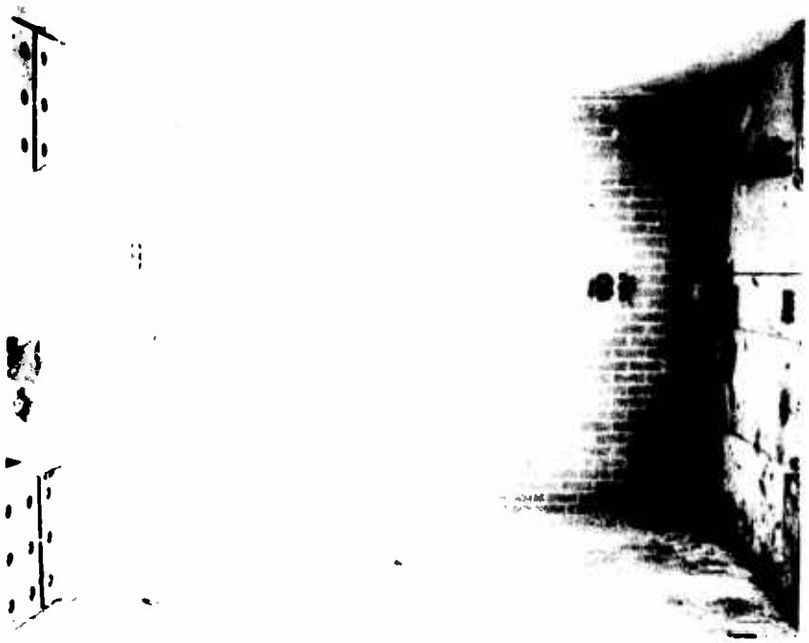

Fig. 2-14. Posttest Photographs and Crack Patterns (first test) for Test 83.

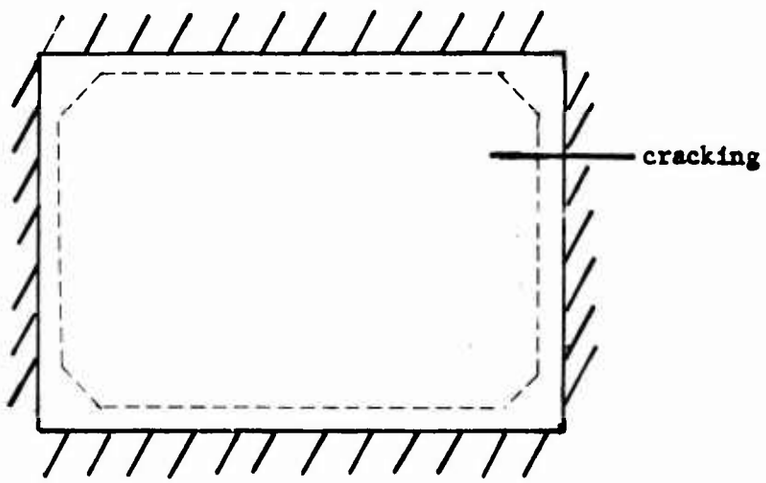

Fig. 2-15. Posttest Photographs and Crack Pattern (second test) for Test 83.

Section 3
LOADING STUDIES

Loading studies have been conducted throughout the program to obtain both calibration data and on the air blast loadings on wall panel geometries used in the response tests of full-scale wall panels. The primary emphasis of the loading study tests conducted and analyzed during this reporting period was on: those test geometries that were investigated several years ago prior to the time that the improved instrumentation and data analysis system was obtained for the tunnel program; those cases that had never been investigated; or those cases where additional pressure measurements and or loading strengths were necessary to aid in the analysis of the wall panel test results. The geometries used included one with no wall in place, i.e., the open tunnel; one with an instrumented, solid, nonfailing wall in place; and one with an instrumented nonfailing wall containing a window opening.

The data for the open tunnel and solid nonfailing wall tests have been completely analyzed. Analysis of the data for the window geometry tests is approximately 30 percent complete and will be included in a later report.

A summary of the loading study data which has been completely analyzed this period is discussed below. All of the digitized pressure vs time, and impulse vs time data for these tests are too voluminous to include in this report and therefore, will be published in a separate report which will be available for review at the Hazard Evaluation and Vulnerability Reduction Division of the Defense Civil Preparedness Agency.

OPEN TUNNEL TESTS

The open tunnel calibration test series is a repeat of a series conducted in early 1967 when the tunnel was first put into operation. The

data acquisition system at that time consisted of oscilloscopes equipped with Polaroid cameras and the data reduction and analysis was done largely by hand.

The data acquisition system that has been used the past few years includes a 14 channel tape recorder which facilitates the digitizing and computer processing of the data. In addition the pressure gauges, amplifiers, and other elements of the system have gone through considerable upgrading since the time of the earlier tests. Because of all these changes, as well as the passage of time, it seemed prudent to include a basic calibration of the tunnel as part of this year's work.

This series consisted of 6 test conditions, each repeated three times for a total of 18 tests. The 6 conditions employed 1 through 6 strands of Primacord 60 ft long. Sample gauge traces are presented in Fig. 3-1. Because this test series was limited in scope, some effort was devoted to obtaining additional open tunnel type data from tests conducted using a nonfailing wall in the tunnel. In these tests, the data from gauges in the tunnel wall located upstream from the nonfailing wall were analyzed only up to the time of the return of the reflected wave from the nonfailing wall. The combined data from these tests are summarized below and plotted in Fig. 3-2.

Summary of Incident Peak Overpressure Data

Number of Strands	Peak Overpressure (psi)	psi/strand of Primacord (approximate)
1	1.0	1.0
2	2.0	1.0
3	3.5	1.2
4	4.9	1.2
5	6.0	1.2
6	7.2	1.2

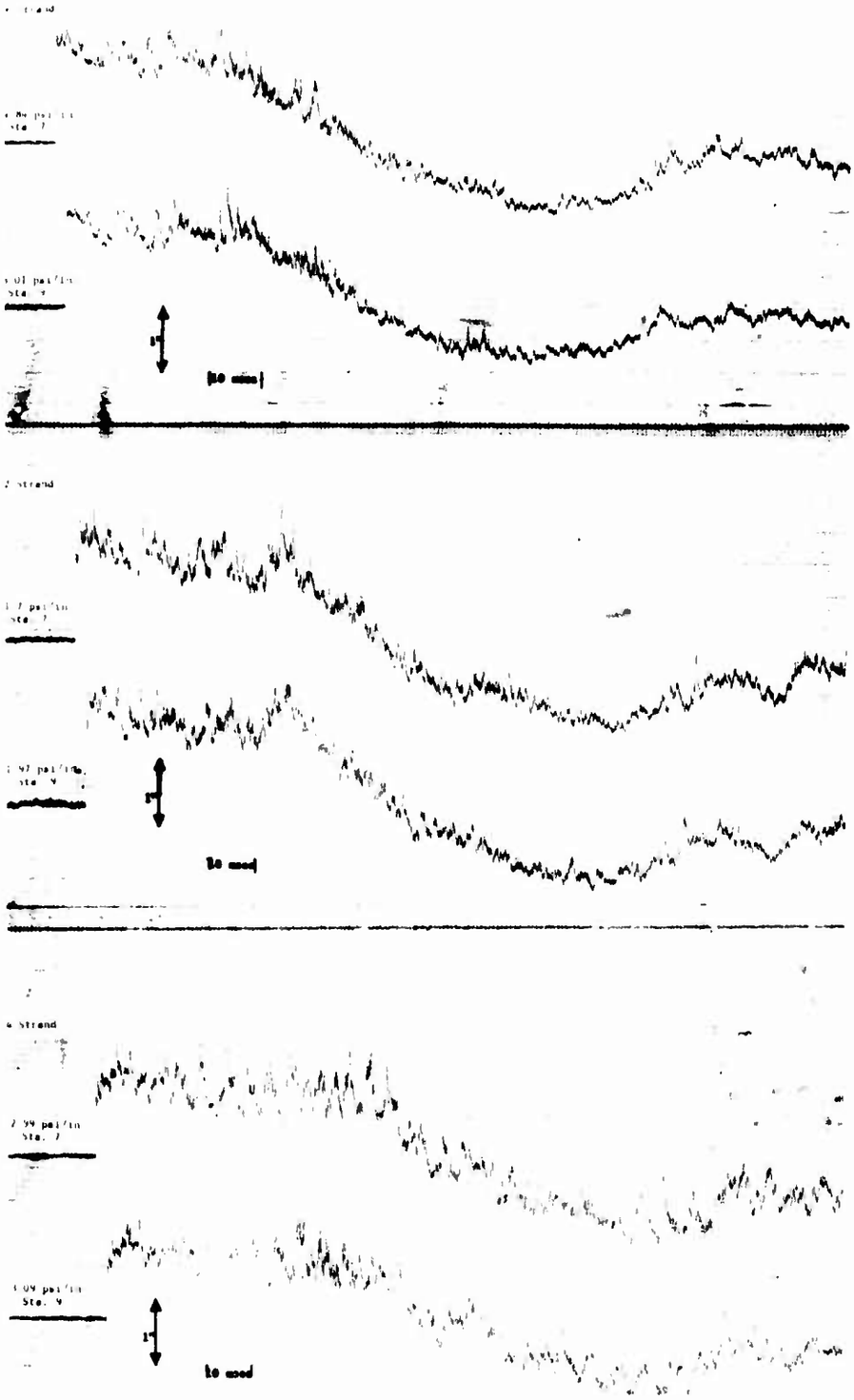

Fig. 3-1. Sample Traces From Open Tunnel Calibration Test Series.

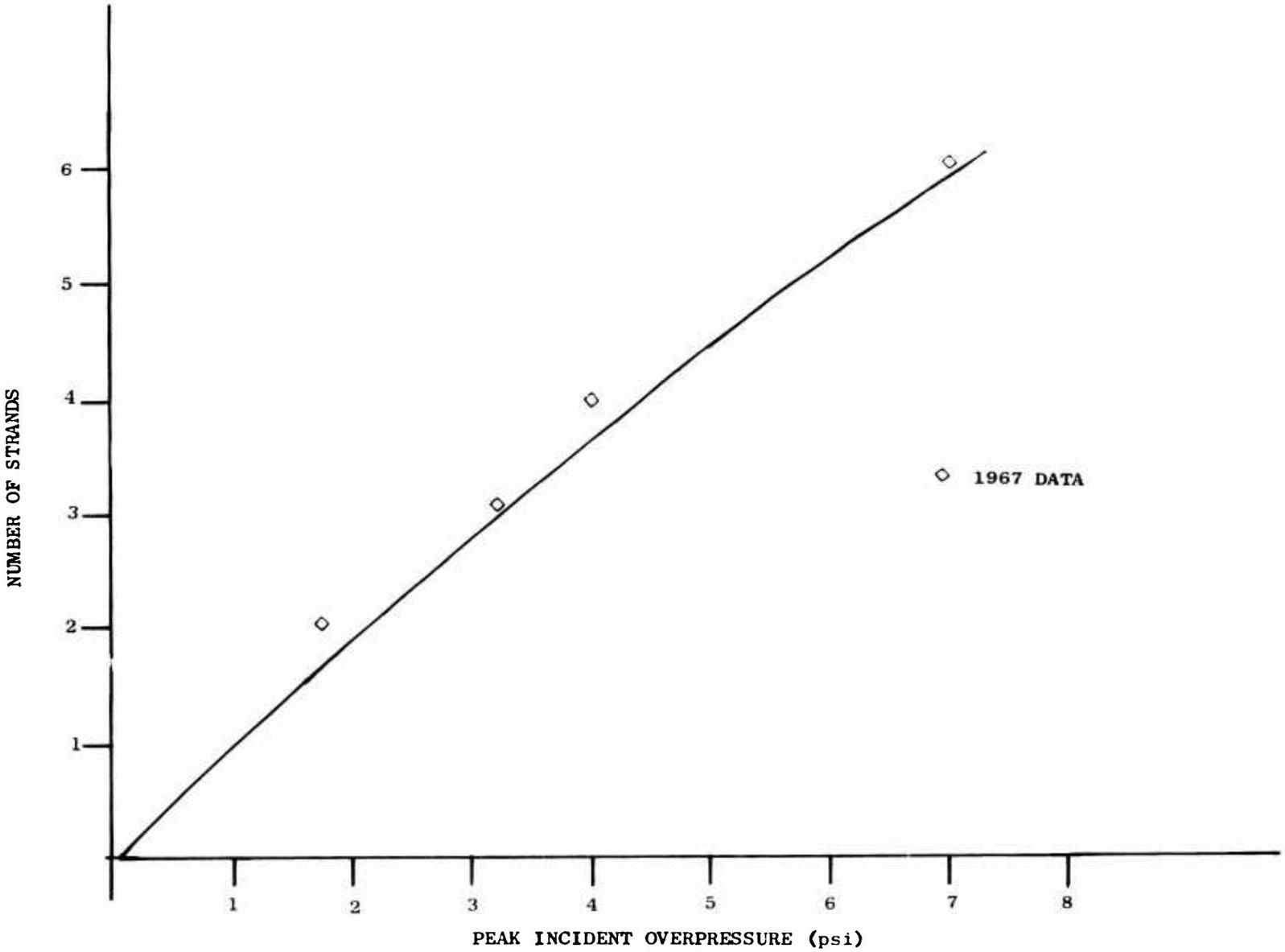

Fig. 3-2. Summary of Peak Incident Overpressure (psi) as a Function of Number of Parallel Strands of Primacord Detonated Simultaneously in the Compression Chamber.

Also plotted in Fig. 3-2 are the data points from the 1967 test series. Note that the latest values are quite close to the 1967 values, i.e., about 1.0 to 1.2 psi per strand.

CLOSED TUNNEL TESTS

The data from 14 closed tunnel tests conducted late in 1972 were analyzed during this reporting period. These tests were run to obtain loading data on a solid wall located at the rear of the support trusses, a location which has been used for recent preloaded and arched failing wall tests. The tests used an instrumented nonfailing wall. The 4 gauge locations used on the tunnel wall are shown in Fig. 3-3.

Summary plots of the closed tunnel test data are shown in Fig. 3-4 through Fig. 3-8. These plots are the averaged data from all the gauges on the nonfailing wall for the specified quantities of explosive. The same data is also plotted in Fig. 3-9, a plot of peak reflected overpressure as a function of number of strands of primacord. It is interesting to compare this experimental data with values calculated from the open tunnel data shown in Fig. 3-2. These calculated peak reflected values have also been plotted on Fig. 3-9. The correlation between the two sets of data is quite good.

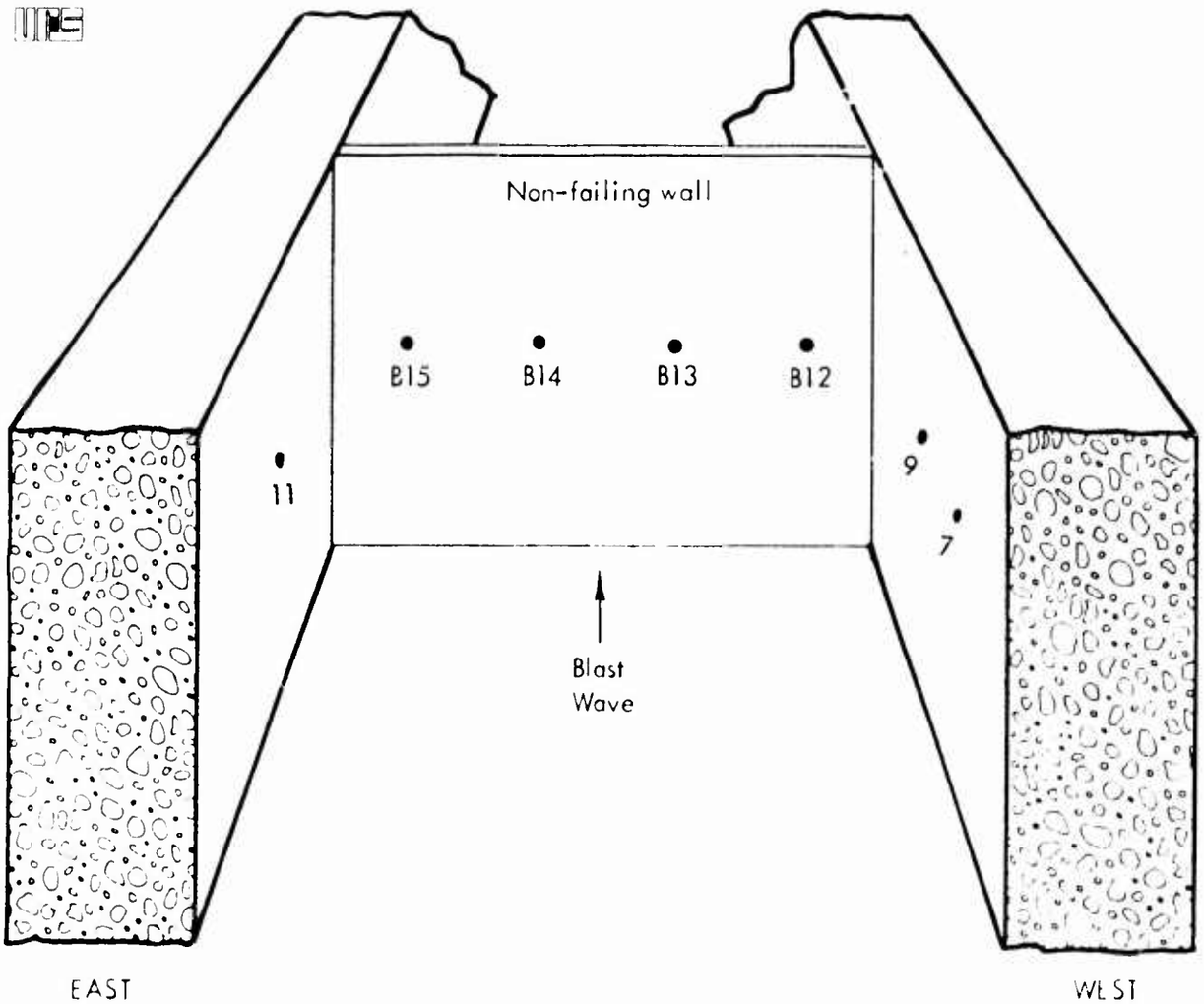

NONFAILING WALL GAGES

GAGE NO.	DISTANCE FROM FLOOR	DISTANCE FROM WEST WALL OF TUNNEL
B-12	51"	14-1/4"
B-13	51"	47 "
B-14	51"	95-1/4"
B-15	51"	127-1/2"

TUNNEL WALL GAGES

GAGE NO.	DISTANCE FROM FLOOR	DISTANCE FROM NON-FAILING WALL
7	45"	156"
9	45"	116"
11	49"	174"

Fig. 3-3. Gauge Locations for Closed Tunnel Tests.

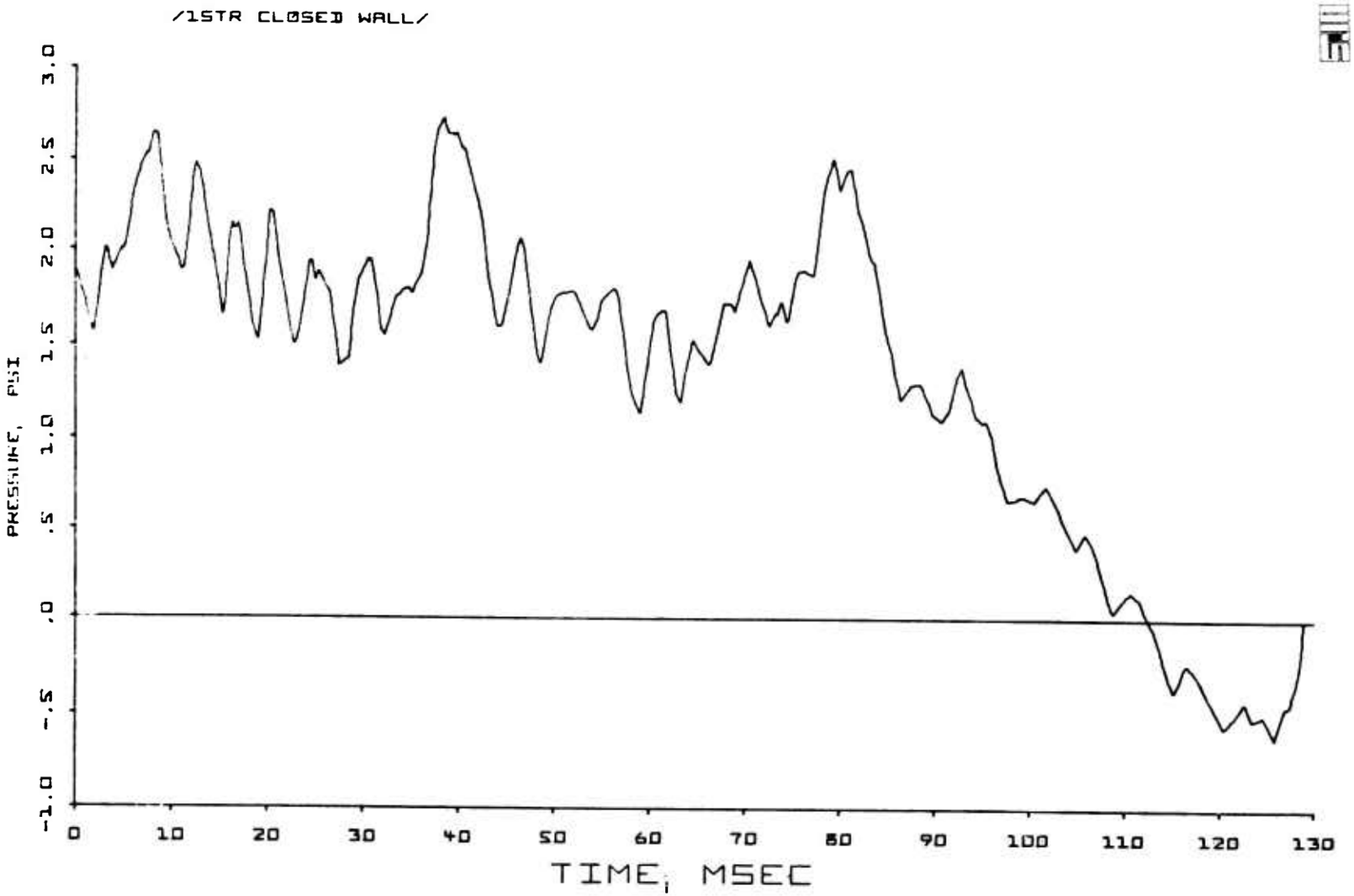

Fig. 3-4. Average Peak Overpressure vs Time for one Strand Solid Wall Loading Study Test 10-19-72-07, 08 and 09, Gauges B-12, B-13, B-14 and B-15.

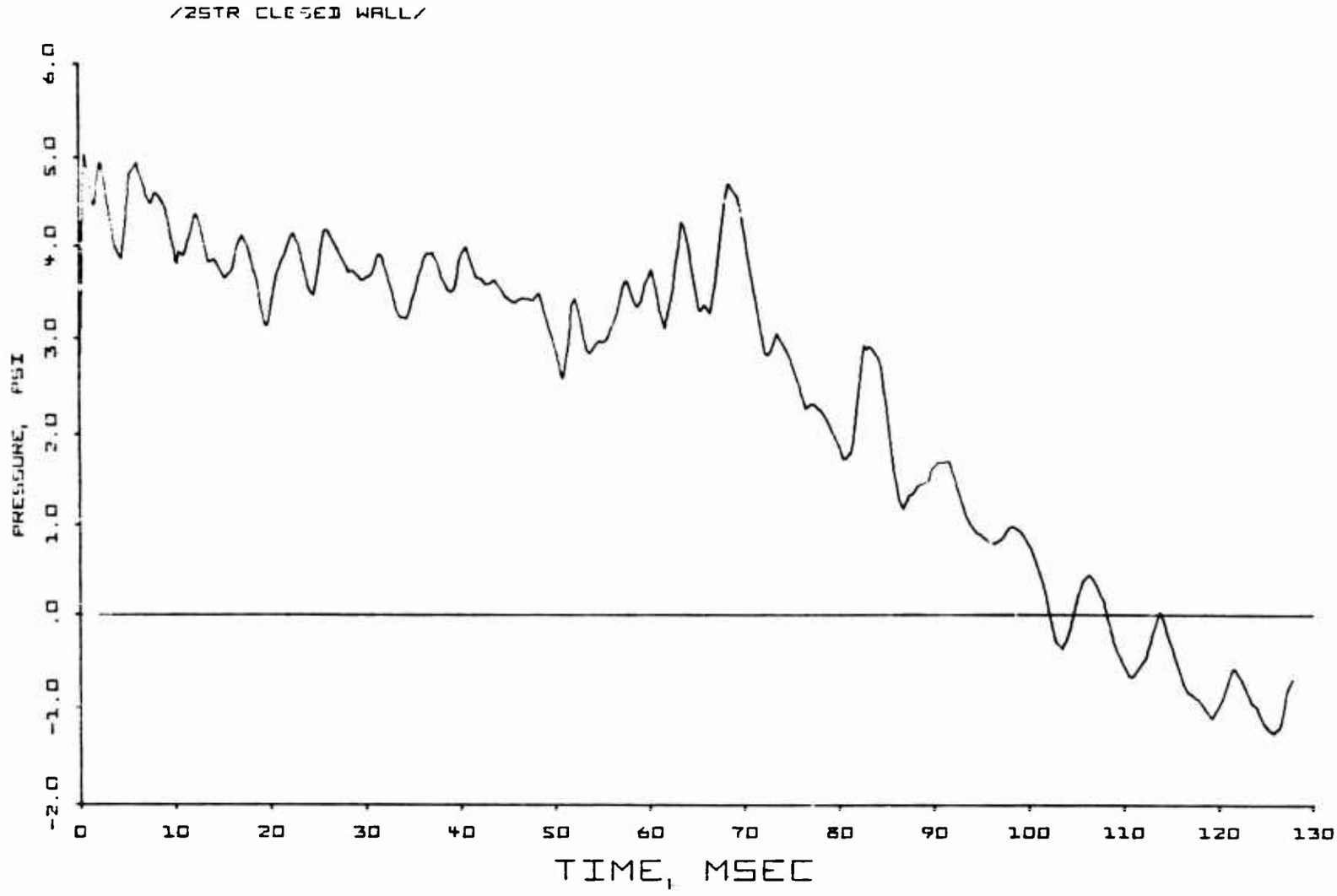

Fig. 3-5. Average Peak Overpressure vs Time for two Strand Solid Wall Loading Study Tests 10-19-72-04 and 06; Gauges B-12, B-14 and B-15.

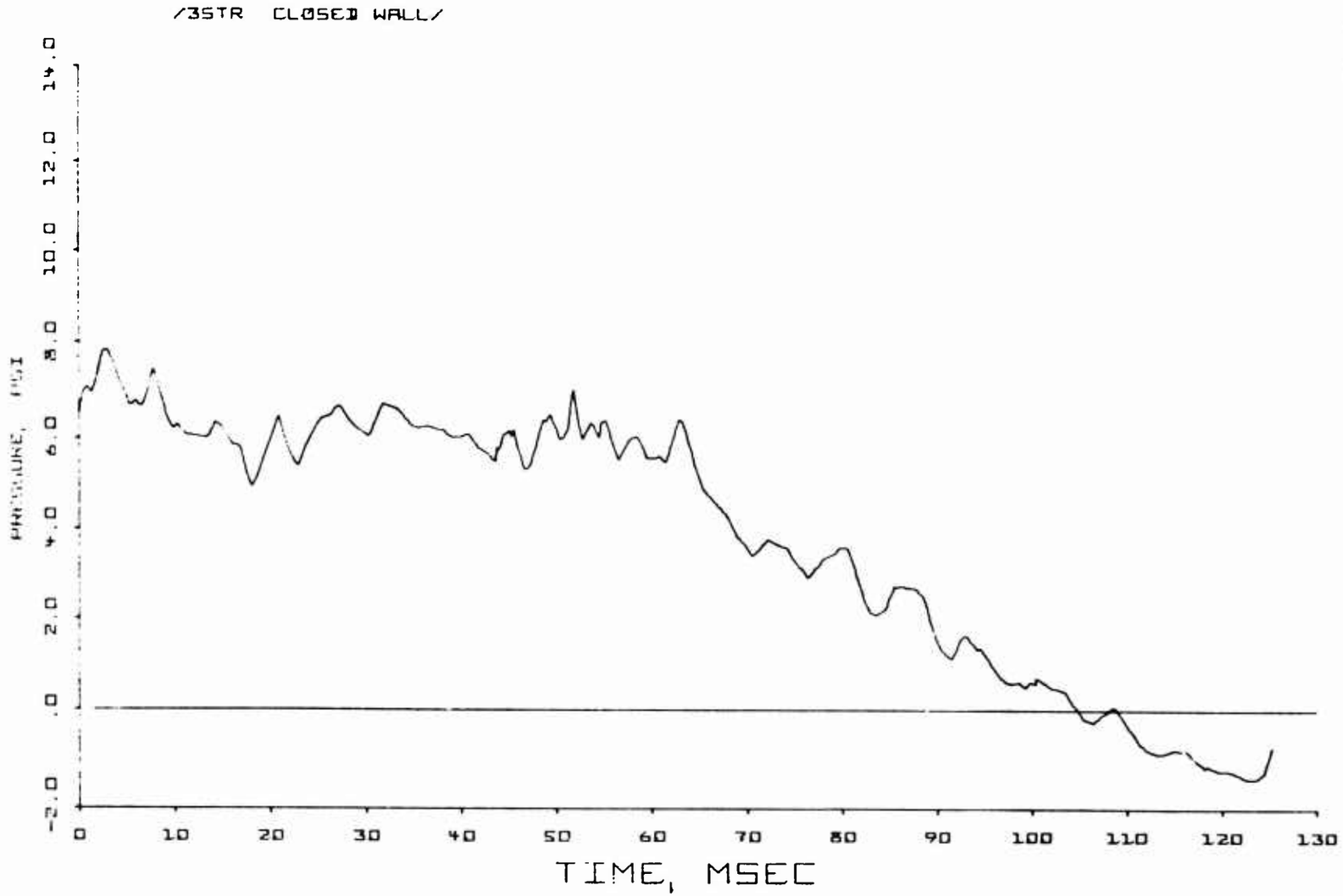

Fig. 3-6. Average Peak Overpressure vs Time for Three Strand Solid Wall Loading Study Tests 10-19-72-01, 02 and 03; Gauges B-12, B-13, B-14 and B-15.

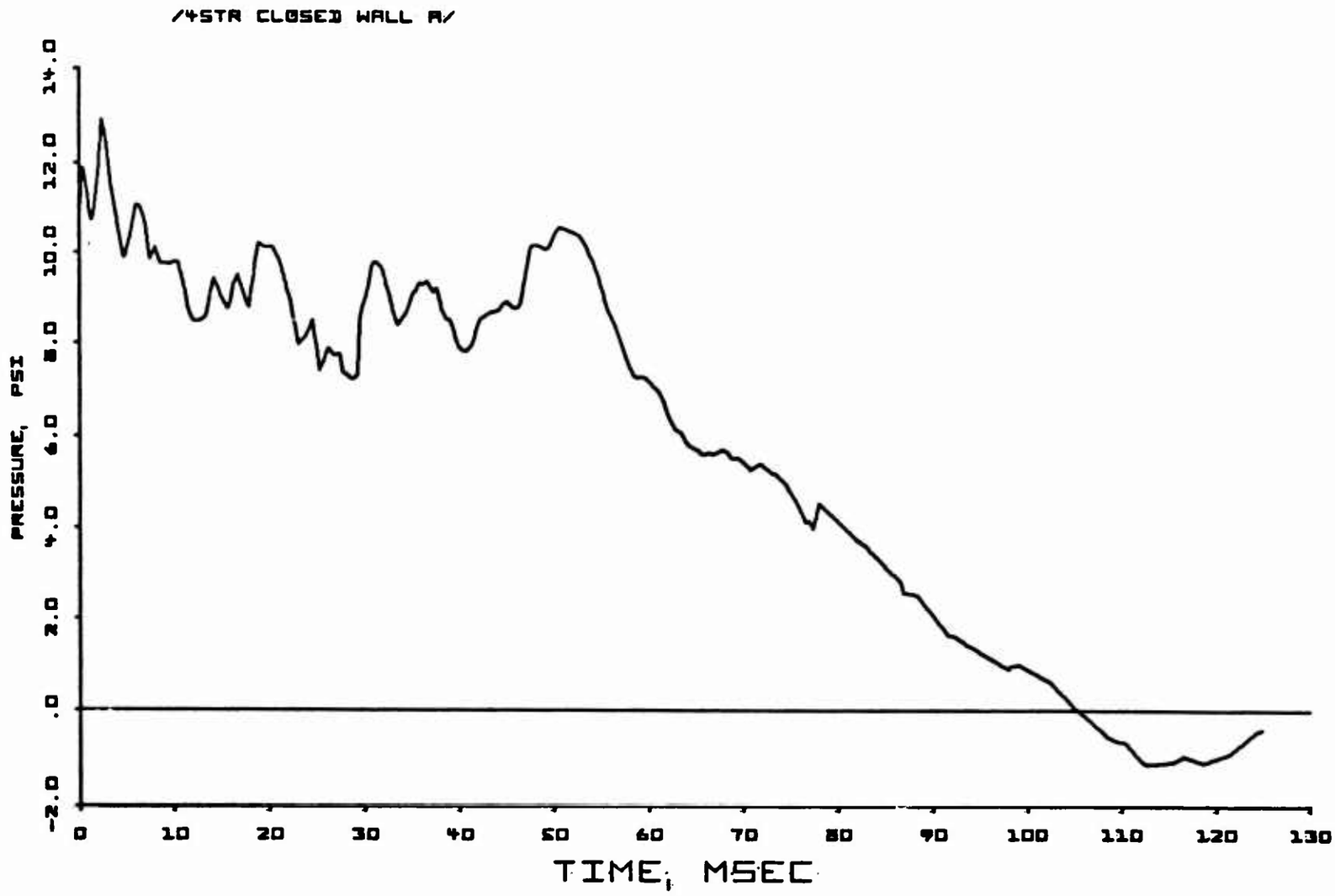

Fig. 3-7. Average Peak Overpressure vs Time for Four Strand Solid Wall Loading Study Tests 10-17-72-03, 10-17-72-04 and 10-18-72-01.

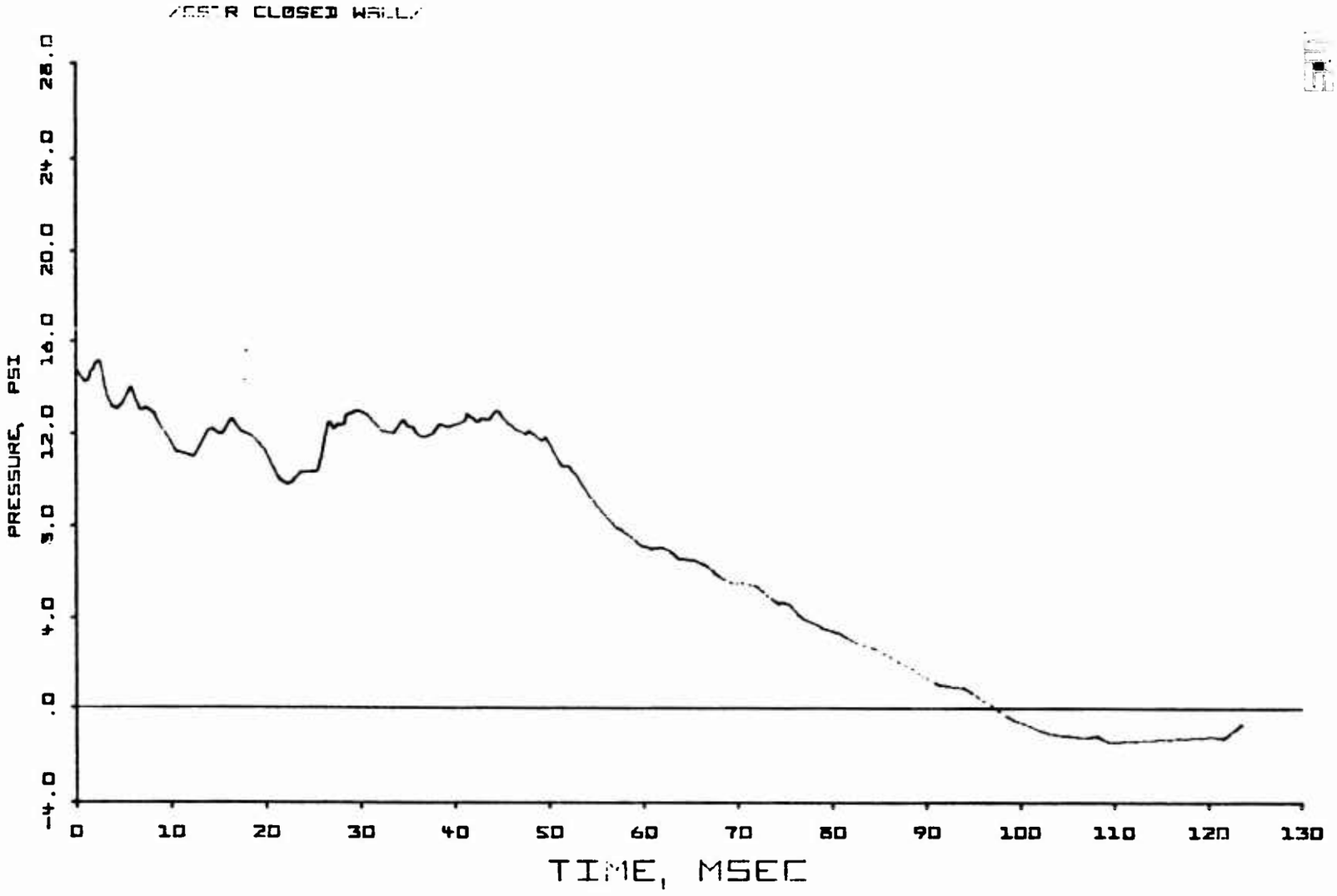

Fig. 3-8. Average Peak Overpressure vs Time for Five Strand Solid Wall Loading Study Tests 10-16-72-01, 10-17-72-01 and 02; Gauges B-12, B-13, B-14 and B-15.

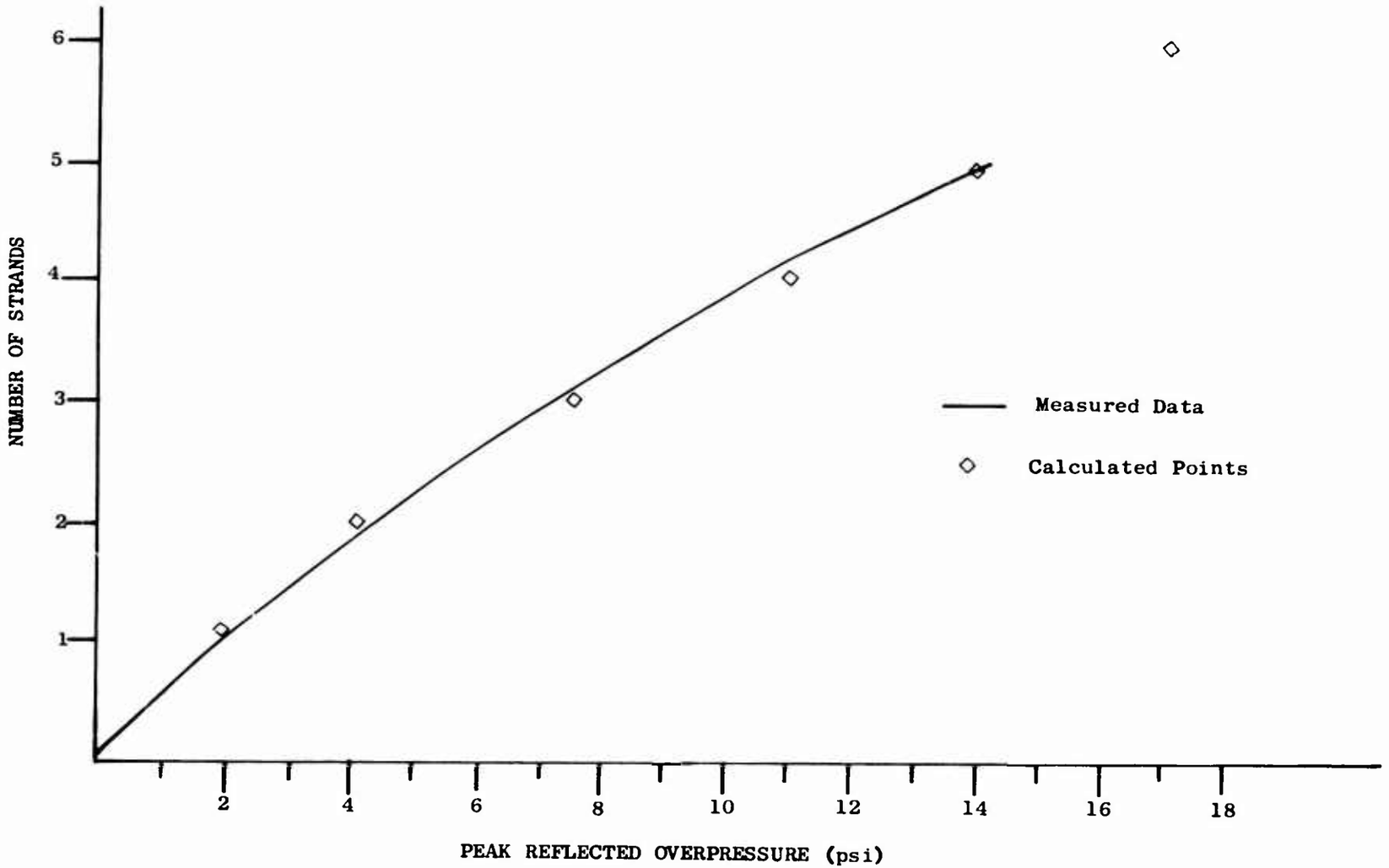

Fig. 3-9. Peak Reflected Overpressure (psi) as a Function of the Number of Parallel Strands of Primacord detonated Simultaneously in the Compression Chamber.

Section 4

WALL PANEL PROGRAM SUMMARY, CONCLUSIONS AND RECOMMENDATIONS

GENERAL

One of the major problems facing the designer, war gamer, or shelter analyst when attempting to design and/or analyze a structure in an explosive environment is the paucity of failure theories that are supported by actual test data. For some time URS has been involved in a program to alleviate some of this problem. That is, URS has been involved in a program to develop and improve methods of predicting the mechanics of structural failure and fragmentation of walls. The basic purpose of the program was to provide information for the development of improved casualty, damage and debris models.

Although a major element in the program was the testing of full-scale wall panels, test information alone could not satisfy the program goals, if only because of the economic infeasibility of testing all possible combinations of wall types, mounting conditions, openings, and of blast loading conditions. (The NSS survey typed over 30 exterior walls and 15 interior walls.) Instead the test program is being used to guide, support, and confirm an analytical program, which can be used to predict failure strengths and mechanisms of failures of walls not tested in the Shock Tunnel.

While not yet complete, the program to date has resulted in a significant increase in knowledge of failure mechanism, and of our ability to predict wall failures. This, therefore, seemed an appropriate time to summarize the more important results of the program, and to make recommendations for future directions that will maximize the amount of information produced, and minimize its costs.

In the next subsection, the entire program is briefly described; this is followed by a summary of important results, and conclusions and recommendations.

PROGRAM DESCRIPTION

The program is divided into four basic parts

- Static tests
- Loading study tests (using nonfailing walls instrumented with pressure gauges)
- Theoretical analyses
- Full-scale dynamic tests (using walls constructed with conventional materials and with conventional building practices)

Static Test Program

The static test program is conducted in conjunction with the shock tunnel dynamic tests to assure quality control in the construction of the test panels, and to obtain estimates of the strengths of the panels at the time they are tested in the tunnel. For a complete description of the static test program and a great deal of data, see Appendix A.

Loading Study

This portion of the effort is concentrated on developing an accurate and complete description of the loading on structural elements. Obviously, shock wave overpressures with either the fully closed or fully open tunnel are quite simple - merely a step pulse for about 40 msec followed by a

decaying exponential. These modes have been used extensively in instrumentation evaluation and development. The most interesting cases, however, are loadings on wall panels with openings, and on rooms. These more complex cases, coincidentally, are the cases for which the least is known. The loading information, of course, is vital to the structural analysis of the test wall and support system, as well as analyses of other walls with similar configurations; for this year's data, see Section 3.

Theoretical (Structural) Analyses

With the foregoing pressure (loading) data, structural analyses and response predictions can be attempted. We have been using a computer code (SAMIS)* developed by Philco-Ford Corporation, which is capable of dynamic analysis of finite element structural systems, for wall analysis. In addition, some work has been done with MACE** on local effects of arching. Appendix B gives a rather complete description of these programs and their results.

Full Scale Dynamic Wall Panel Tests

Full scale (8-1/2 ft x 12 ft) walls with and without openings (doors and windows) have been subjected to a blast environment in a large shock tunnel. Some of the walls, used for calibration purposes, were specifically designed not to fail under blast loadings. The others, the test walls, were built using standard practices and materials. Test walls were made of brick, concrete block, tile, timber studs and sheetrock, and reinforced concrete, with emphasis to date on the brittle materials. The walls

---

* Structural Analysis and Matrix Interpretive System.

** Mechanical Analysis of Continuous Elastic Systems.

were mounted as beams (supported on two sides) and plates (supported on all four sides), and were also preloaded* and arched.**

To the multiplicity of openings, support conditions, and loadings we add the fact that the NSS survey typed over 30 exterior walls and 15 interior walls. Obviously this provides a huge number of permutations and combinations. Of course, many types were eliminated by lack of popularity, etc. To aid in ordering this array of information the three-part Failure Matrix appearing in Figs. 4-1, 4-2, and 4-3 was created.

SUMMARY OF IMPORTANT RESULTS

It has been found that the useful way of organizing and presenting the information from the program is in the form of the "Failure Strength Matrix" shown in Figs. 4-1, 4-2, and 4-3. Contained in these figure are the geometries, support conditions, materials, and the loading (reflected) overpressures encountered in the test program plus extrapolations made by the authors to untested conditions. It should be noted that the basic aim of the program was to develop reliable means of predicting the failure strengths of untested geometries (that is, of extrapolating from tested geometries) using a minimum of tests.

The foregoing provides the input information for the full scale dynamic tests and the Failure Strength Matrix, Figs. 4-1, 4-2, and 4-3. A tabular summary of test data is also provided in Table 4-1. This table

---

* A preloaded wall is one in which vertical forces, simulating weight of walls above the wall of interest, are applied prior to shock wave loading.

** Arching of a wall panel loaded by a shock wave normal to its face takes place when the panel supports permit essentially no motion in the direction of the plane of the panel. This can occur when a wall is tightly supported in a rigid frame.

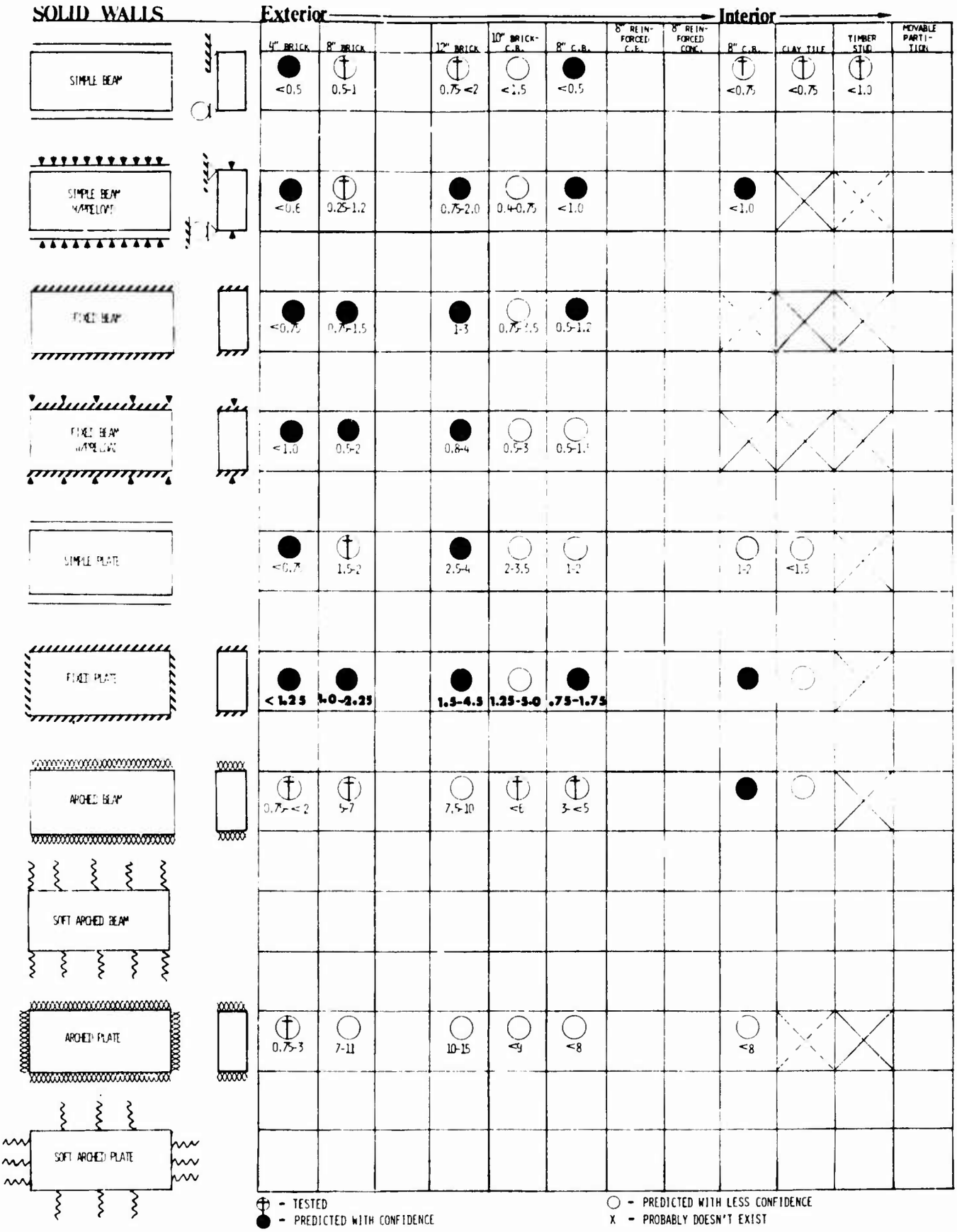

Fig. 4-1. Failure Strength Matrix - Solid Walls.

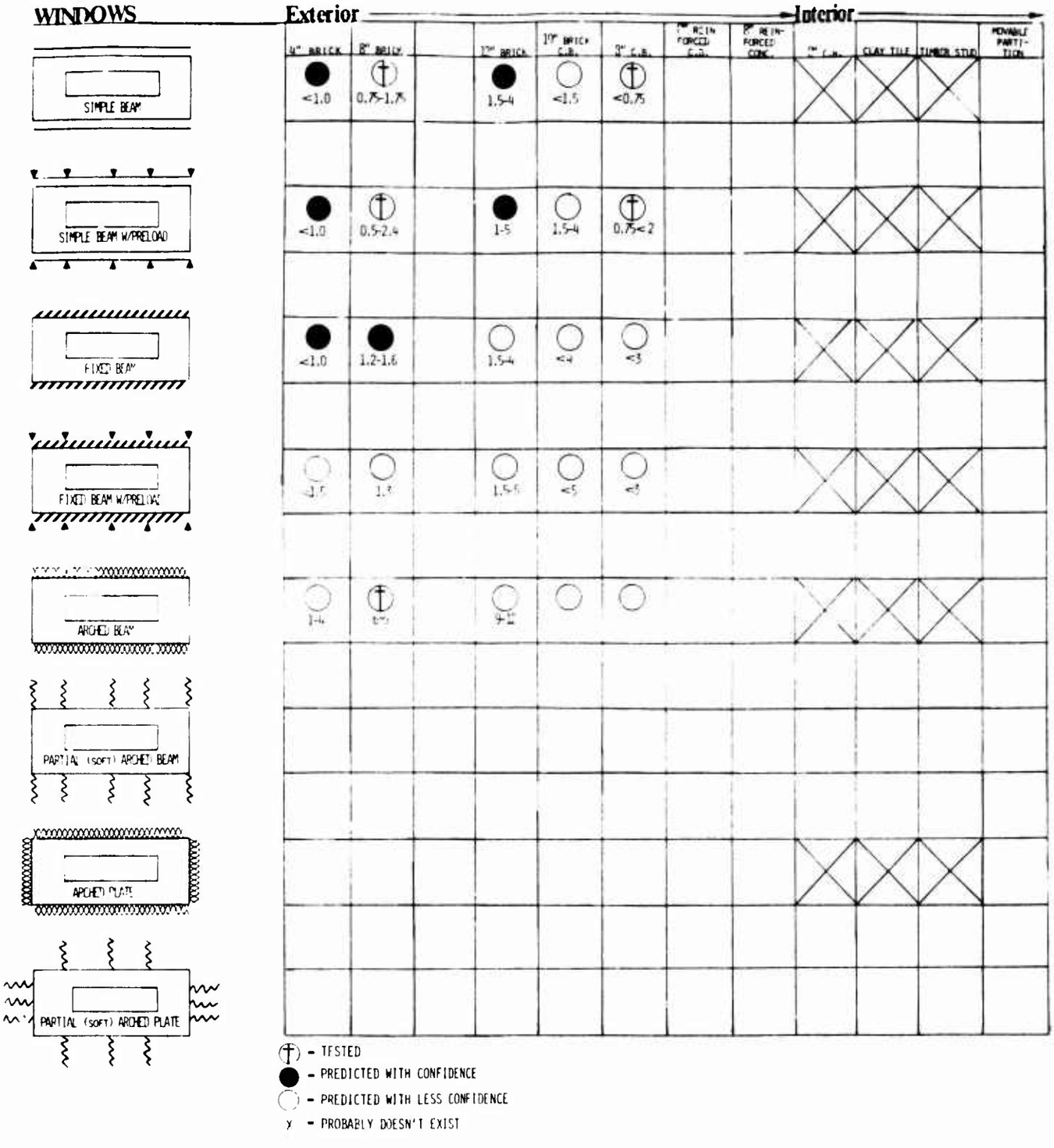

Fig. 4-2. Failure Strength Matrix - Windows.

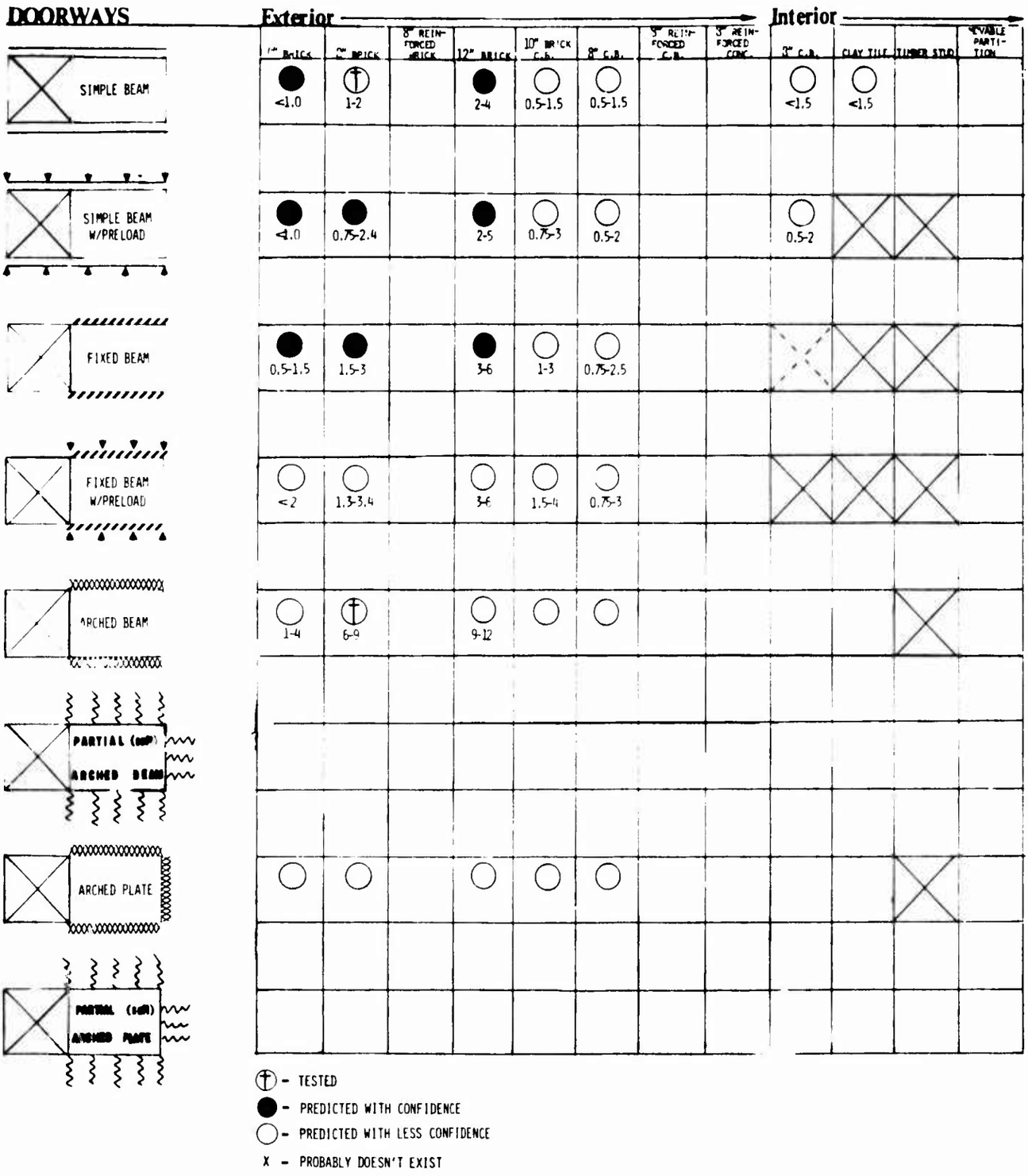

Fig. 4-3. Failure Strength Matrix - Doorways.

Table 4-1

SUMMARY OF SHOCK TUNNEL TEST DATA

Test No.	Incident Overpressure p_i - (psi)	Remarks
1. SOLID WALLS		8 in. Brick Simple Beam Wall
1	1.5	Wall failed
2	1.7	" "
3	1.7	" "
5	1.8	" "
7	1.8	" "
21	1.7	" "
4	4.3	" "
6	4.4	" "
20	4.6	" "
22	3.5	" "
		12 in. Brick Simple Beam Wall
50	1.9	Wall failed
51	2.1	" "
52a	0.75	No sign of failure
52b	0.75	" " " "
52c	0.75	" " " "
52d	2.0	Wall failed
		8 in. Brick Simple Beam Wall with Preload (to simulate high curtain bearing walls)
64a	0.75	Wall cracked full width but did not come out of frame (preloaded to 16,500 lbs*)
64b	0.75	Wall collapsed
65	0.75	Wall collapsed (preloaded to 16,500 lbs)
66	0.75	Wall cracked full width; did not collapse and not reloaded (preloaded to 23,500**)
67	6.1	Wall failed
81	0.8	Wall cracked (preload to 28,500)
82a	0.8	" " " " "
82b	2.0	Wall failed (preload to 28,500)

* Equivalent to a two-story curtain wall.

** Equivalent to a three-story curtain wall.

Table 4-1 (Cont'd)

Test No.	Incident Overpressure p_i - (psi)	Remarks
1. SOLID WALLS (Cont'd)		8 in. Brick Simple Plate Wall
24a	1.6	Did not collapse, but severely cracked in yield line pattern
24b	1.5	Wall failed
25	1.7	Did not fail, but a large piece was removed; severely damaged, so not retested
29a	1.9	Wall did not collapse, but cracked in yield line pattern
29b	2.0	Wall collapsed
28	1.9	" "
23	4.0	" "
32	3.9	" "
33	3.9	" "
		4 in. Brick Arched Wall (one-way)‡
68a	.75	Wall cracked
68b	1.7	Wall failed
2. SOLID WALLS (Arched)		8 in. Brick Arched Wall (one-way)‡
71a	1.9	Test for natural period
71b	2.9	Wall cracked
71c	4.3	Cracks enlarged
74	5.5	Wall failed
75	5.9	Wall failed
76	5.6	Wall failed
87a	5.7	Wall cracked
87b	6.3	Cracks enlarged
87c	8.2	Wall failed
88a	7.8	Wall cracked
88b	3.6	Cracks enlarged
94	7.8	Wall failed
96	6.7	Wall failed (Pre-Split)
		8 in. Concrete Block Arched Wall (one-way)
77	3.3	Wall cracked
77	2.0	No additional damage
77	3.4	Wall failed
78	4.5	Wall failed

‡ Geometrically restrained on Top and Bottom.

Table 4-1 (Cont'd)

Test No.	Incident Overpressure p_i - (psi)	Remarks
2. SOLID WALLS (Arched) (Cont'd)		10 in. Composite Brick and Concrete Block Arched Wall (one-way)*
79	5.6	Wall failed
92a	3.5	Wall cracked
92b	3.5	No additional damage
92c	5.0	Cracks enlarged
		4 in. Brick Arched Wall (two-way)‡‡
83a	2.2	Wall cracked
83b	2.1	Wall failed
		8 in. Concrete Block Arched Wall (two-way)‡‡
89	5.0	Wall failed
90	4.0	Wall failed
3. WALLS WITH DOORWAY		8 in. Brick Simple Beam Wall
46	1.7	Wall failed
44	4.0	" "
45	1.8	" "
48a	0.75	No visible damage
48b	0.75	" " "
48c	0.75	" " "
48d	1.7	Wall failed
		8 in. Brick Arched Wall (one-way)
86a	6.1	Wall cracked
86b	8.4	Cracks enlarged
		8 in. Brick Arched Wall (with gap)
95	8.6	Wall failed

‡ Geometrically restrained on all four sides.

Table 4-1 (Cont'd)

Test No.	Incident Overpressure p_i - (psi)	Remarks
4. WALLS WITH WINDOWS		8 in. Brick Wall With Window (38" x 62")
56	1.8	Wall failed (Simple Beam)
57a	0.65	Wall cracked " "
57b	0.65	Wall crack enlarged " "
57c	0.65	" " " " "
57d	1.9	Wall failed " "
		8 in. Concrete Block With Window (39" x 62"
60a		"Plink" * for period -- cracked (Simple Beam)
60b	0.75	Wall failed " "
61a		"Plink" * for period -- wall cracked " "
61b	0.75	Cracks enlarged " "
61c	0.75	Wall failed " "
		Preloaded 8 in. Brick Wall With Window (39" x 62")
69a	0.8	No damage (preload to 22,500)
69b	2.0	Wall failed (preload to 22,500)
70a	0.8	No damage (preload to 22,500)
70b	2.0	Wall failed (preload to 22,500)
		Preloaded - 8 in. Concrete Block Wall With Window (39" x 62")
72a	0.8	Wall cracked (preload to 22,500)
72b	2.0	Wall failed (preload to 22,500)
73a	0.8	Wall cracked (preload to 22,500)
73b	2.0	Wall failed (preload to 22,500)
		One-Way Arched 8 in. Brick Wall with Window (38"x62")
80a	5.7	Wall cracked
80b	6.3	Wall failed
84a	6.4	Wall cracked
84b	7.8	Wall failed
85a	6.2	Wall cracked
85b	5.8	Cracks enlarged
85c	7.5	Slight additional cracking
85d	9.5	Wall failed

* See Page 4-12.

Table 4-1 (Cont'd)

Test No.	Incident Overpressure p_i - (psi)	Remarks
	Room With Front Window (62" x 33-1/2") and Solid Back Wall	
5. ROOMS WITH WINDOWS		Back Wall 8 in. Concrete Block Simple Beam
58a		"Plink" * for natural period -- Wall cracked
58b	0.75	Wall failed
59	0.75	Wall failed
		Back Wall 6 in. Hollow Clay Tile Simple Beam
62	0.75	Wall failed
63	0.75	" "

* A "Plink" test is conducted with a short length of primacord (approximately 10 ft) to determine the natural period of a particular wall as installed in the Shock Tunnel.

provides the background data from all wall tests for filling in the "Failure Strength Matrix" entries labeled Ⓣ (tested). As can be seen from this table, a great number (nearly 100) of walls have been tested. The data in more detailed form can be found in **Refs. 1, 7, 8 and 9.**

Summary, Conclusions, Recommendations

Study of the "Failure Strength Matrix" shows that only a few of the important combinations have been tested. However, these tested conditions have been selected to maximize the number of conditions we predict with confidence, that is, the many entries in the "matrix" marked by ●.

There still remain gaps, of course, and the filling of those must be done in a prudent manner, i.e., a manner designed to maximize the sponsor's gains.

The major gaps in the nonreinforced masonry walls appears to be that of partial or "soft" and interior partitions. Interior partitions are being emphasized in the current year's work which will help fill in some of these gaps.

Reinforced masonry and reinforced concrete have been almost completely neglected because currently accepted techniques of analysis seem to be far more adequate than they were with the nonreinforced walls, with their many unknowns. Thus, far fewer tests with these materials need be carried out.

Section 5

REFERENCES

1. Wilton, C., and B. L. Gabrielsen, Shock Tunnel Tests of Preloaded and Arched Wall Panels, URS 7030-10, Final Report, June 1973, URS Research Company, San Mateo, California.

2. Huntington, Whitney Clark, Building Construction Materials and Type of Construction, John Wiehle & Sons, Inc., New York, 1966.

3. Manual of Steel Construction," American Institute of Steel Construction, Inc.," New York, 1967.

4. Plummer, Harry C., Brick and Tile Engineering, Structural Clay Products Institute, Washington, D.C., 1967.

5. Time Saver Standards, A Handbook of Architectural Design, McGraw-Hill, 1966.

6. Wiehle, C. K., J. L. Bockholt, Existing Structures Evaluation, Part IV: Two-Way Action Walls, Technical Report, Stanford Research Institute, Menlo Park, California, September 1970.

7. Willoughby, A. B., C. Wilton, B. L. Gabrielsen, J. V. Zaccor, A Study of Loading, Structural Response, and Debris Characteristics of Wall Panels, URS 680-5, Final Report, URS Research Company, San Mateo, California, July 1969.

8. Wilton, C., and B. L. Gabrielsen, Shock Tunnel Tests of Wall Panels, URS 7030-7, Technical Report, URS Research Company, San Mateo, California, January 1972.

9. Wilton, C. and J. Boyes, Shock Tunnel Tests of Wall Panels, Data Report - Room Geometry Loading Study Tests, URS 7030-11, Limited Distribution Data Report, URS Research Company, San Mateo, California, April 1973.

Appendix A

TEST DATA

ARCHED SOLID WALL TESTS

Eight solid wall panels were investigated. Five of these were arched one-way (i.e., fixed top and bottom with the sides free to move) and three were two-way arched (i.e., fixed on all four sides).

One-Way Arched Brick Walls

Four of the walls (Wall Nos. 87, 88, 94 and 96) were 8-inch non-reinforced brick one-way arched. These walls were constructed on steel frames and cured outside the shock tunnel. The walls when cured (more than 28 days) were then moved into the tunnel, and the top grouted with a high-early strength type grout and raised to the ceiling as shown in Figure A-1, A and B. The bottom was then blocked and a high-early type cement beam was poured as shown in Figure A-1, C. The sides of the wall panels were gapped to insure one-way arching.

Test Results, Wall No. 87 (8-inch non-reinforced brick wall, arched one-way)

Three tests were conducted on this wall. The first, using four 60-foot strands of primacord (P_r approximately 10 psi) cracked the wall with a horizontal crack appearing at about the center of the wall on the downstream side (away from the blast) and some spalling occurring along the top and bottom of the wall at the grout lines. On the upstream side of the wall some spalling was noted along the horizontal center crack. Crack gauges which were mounted vertically at about the one-third points on the downstream side of the wall indicated crack times of 4.6, 4.8 and 5.0 msec. On the second test, using five strands

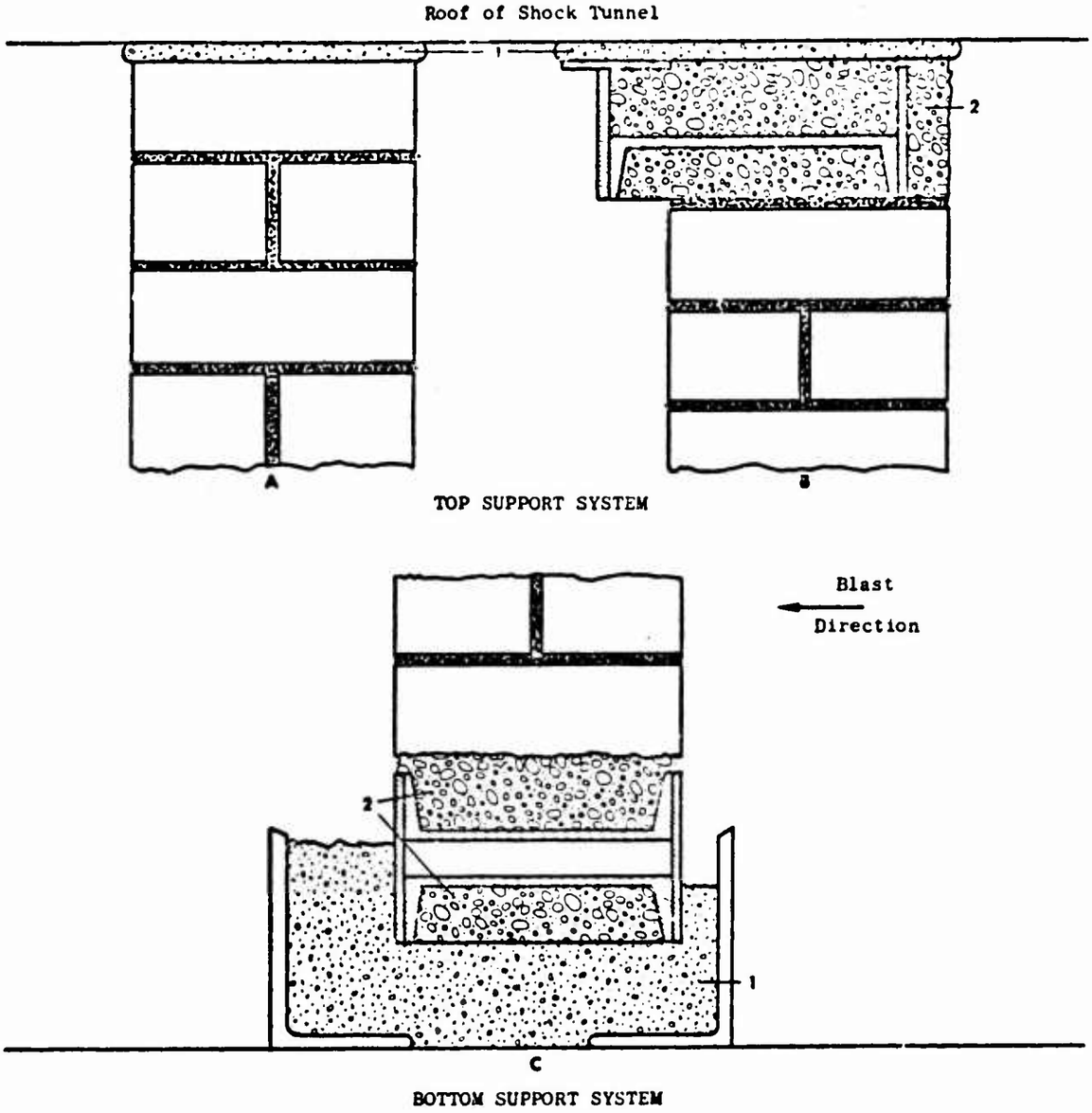

Fig. A-1. Top and Bottom Support Systems for Arching Walls Constructed and Cured Outside Shock Tunnel. Note: 1. Mortar installed when wall placed in Shock Tunnel. 2. Mortar installed when wall was constructed.

of primacord (P_r approximately 13 psi) some additional spalling was noted at the grout line along the bottom of the wall. During the third test, using six strands of primacord (P_r approximately 16 psi) the wall failed, scattering debris to 80 feet with approximately 70 to 80 percent of the total debris landing within the first 30 feet.

A series of pre- and post-test photographs of this wall are presented in Figures A-2 and A-3. Figure A-2 shows the downstream side of the wall and the location of the crack gauges (the vertical narrow strips of gray). The bottom poured beam also from the downstream side can be seen in Figure A-2 B. Post-test photographs of this test are given in Figures A-3 A and B. Figure A-3 A shows the amount of debris which landed in the casement a considerable distance from the wall and Figure A-3 B shows the debris that landed within the first 20 feet. Note also in this photograph that all the brick was removed from the frame. A displacement gauge is located near the center of the upstream face of the wall. Data from this gauge for the three tests are presented in Figure A-4.

A

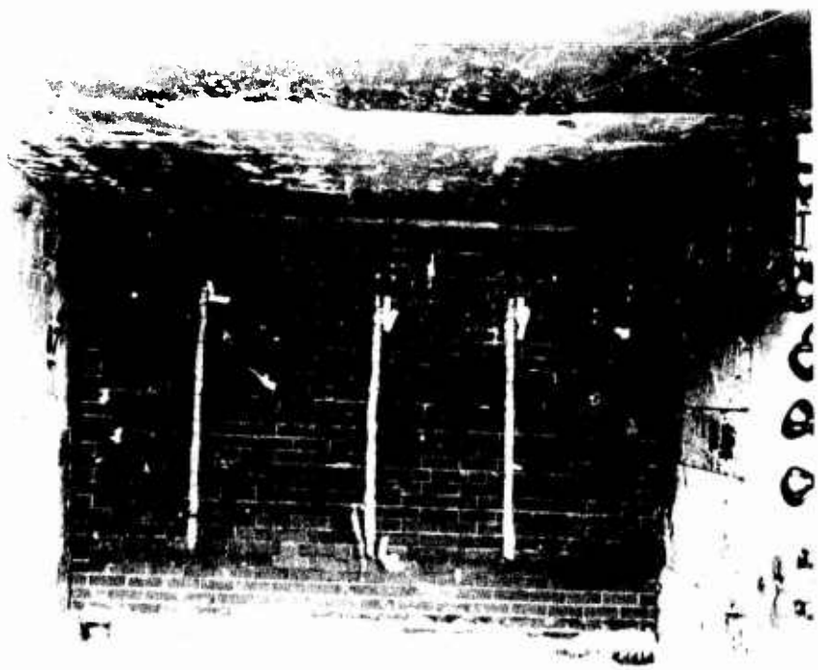

B

Fig. A-2. Pre-Test Photographs of Wall No. 87

A

B

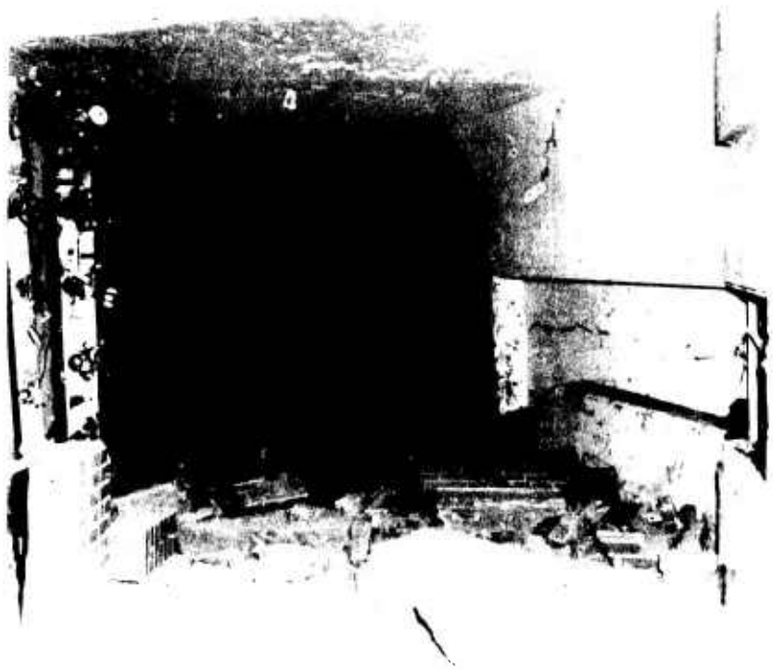

Fig. A-3. Post-Test Photographs of Wall No. 84

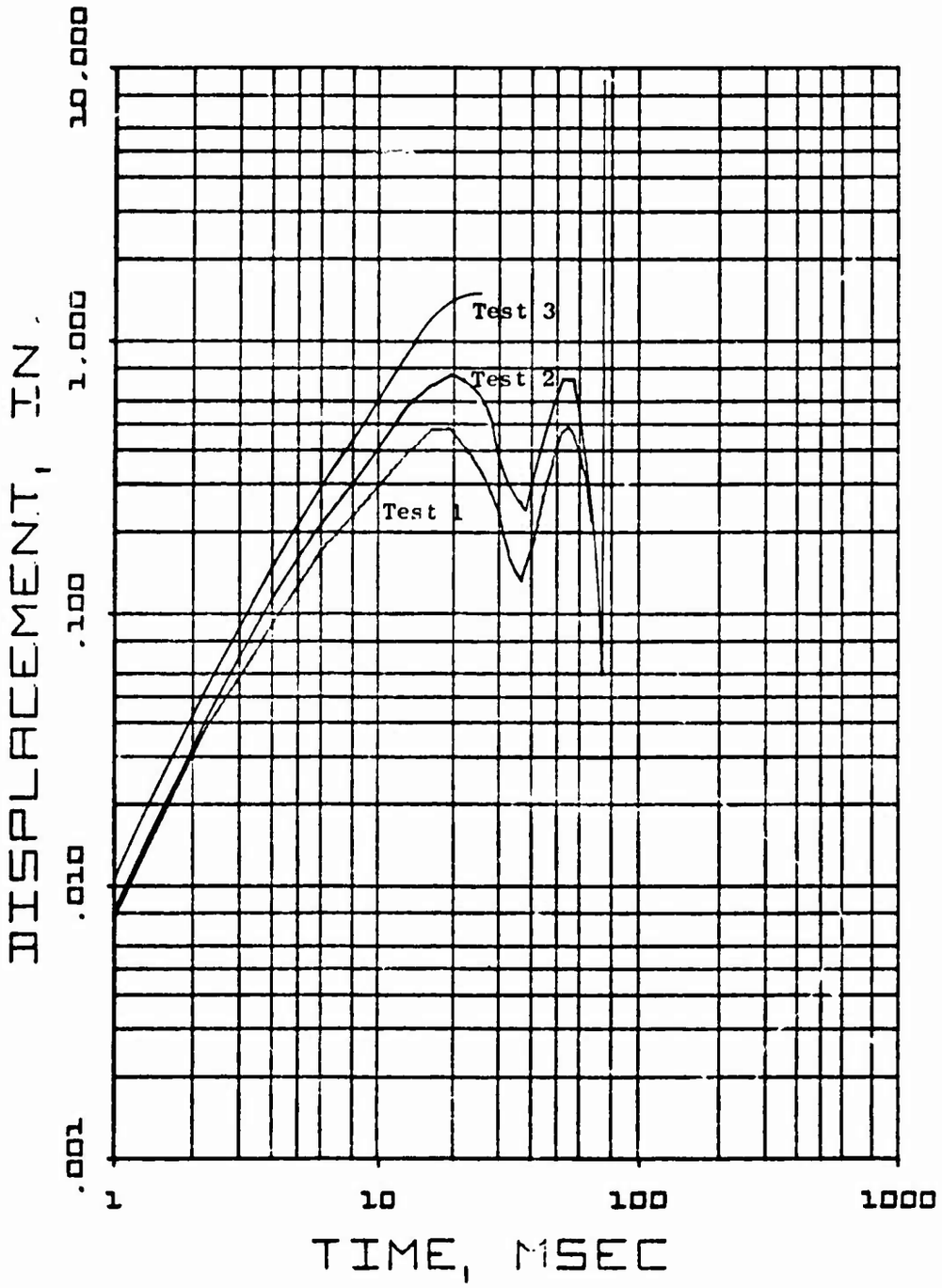

Fig. A-4. Displacement as a Function of Time, Wall No. 87, Tests 1,2 and 3

Test Results, Wall No. 88 (8-inch non-reinforced brick wall, arched one-way

Two tests were conducted on this wall. The first test, using six 60-foot strands of primacord (P_r approximately 16 psi), cracked the wall with a horizontal crack near the center and a diagonal crack from the center to the bottom. The bottom concrete beam was cracked along the entire wall and spalling of the brick was noted at the bottom corners. The crack gauges indicated crack times of 4.0, 5.6 and 5.8 msec. In the second test using three 60-foot strands of primacord (P_r approximately 7 psi), the horizontal crack was enlarged and a brick piece was removed. Considerably more spalling of the brick was noted at the lower corners and some spalling occurred along the top edge.

Post-test photographs of this wall are given in Figure A-5 and the displacement data for Test 1 is given in Figure A-6.

Test Results, Wall No. 94 (8-inch non-reinforced brick wall, arched one-way)

One test was conducted on this wall using six 60-foot strands of primacord (P_r approximately 16 psi) which catastrophically failed the wall spreading debris to 80 feet (the far wall of the casement) as shown in the post-test photograph in Figure A-7. Displacement gauge data for this test is presented in Figure A-8.

Fig. A-5. Post-Test Photographs of Wall No. 88

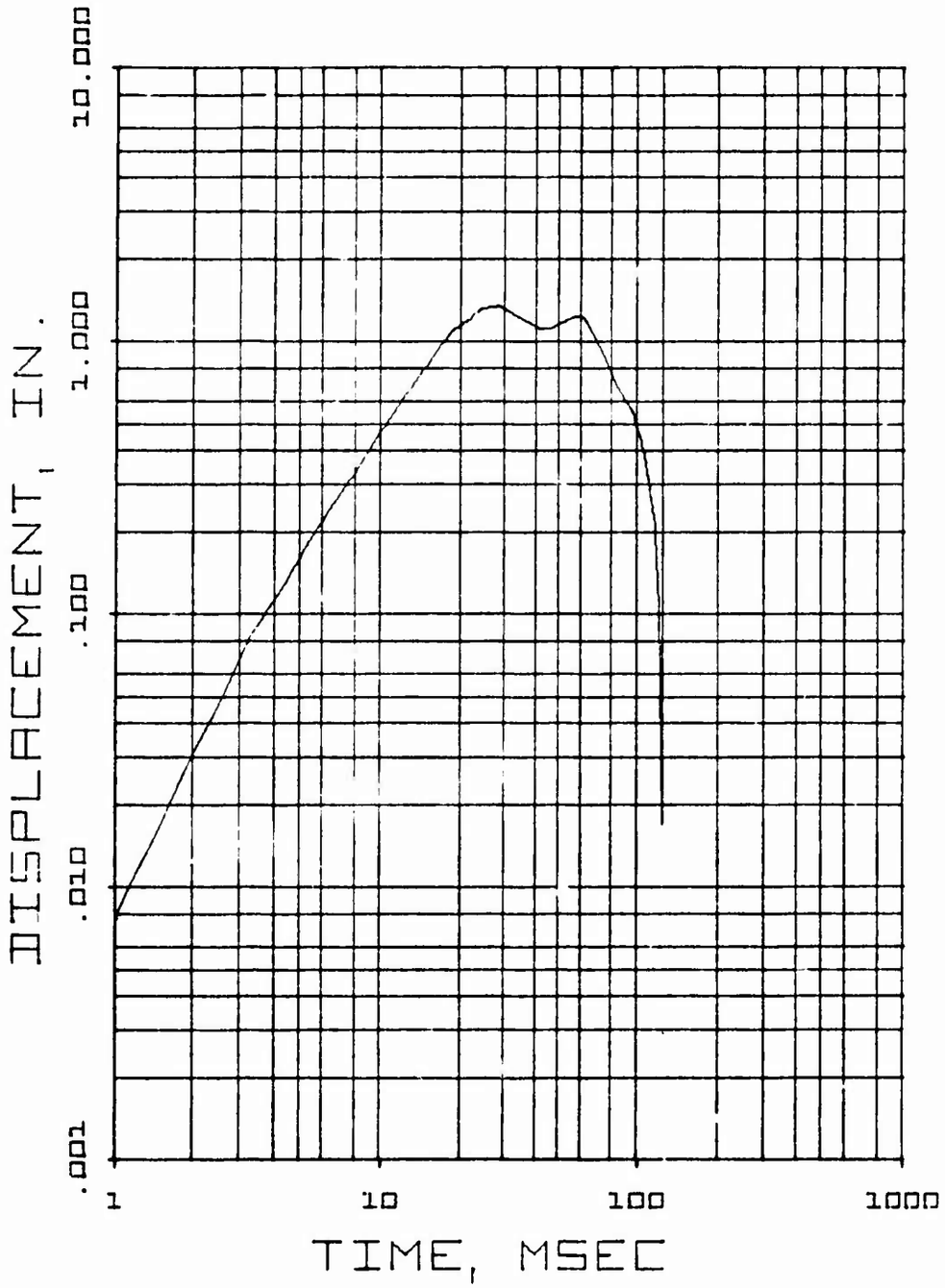

Fig. A-6. Displacement as a Function of Time, Wall No. 88

Fig. A-7. Post-Test Photographs of Wall No. 94

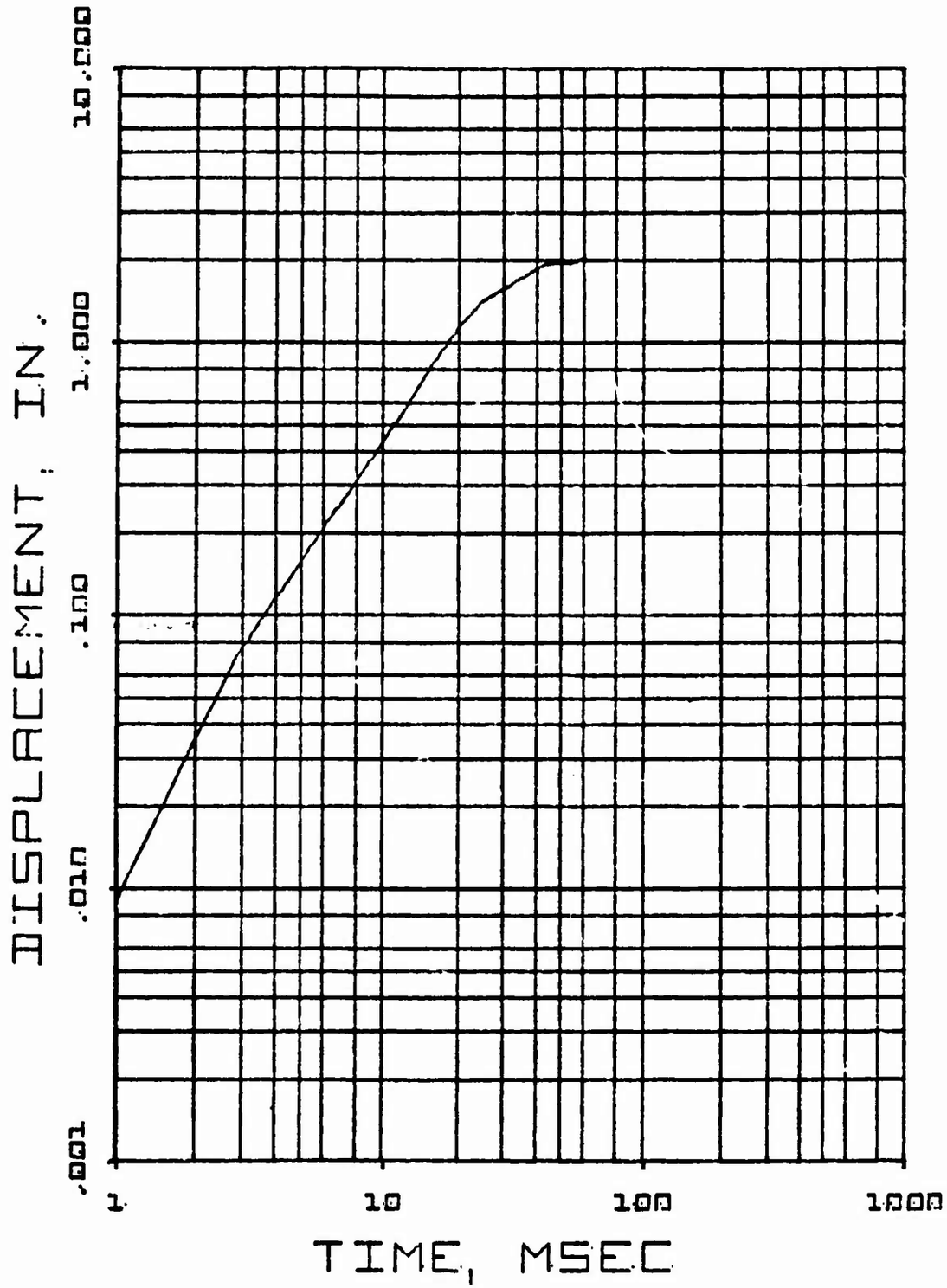

Fig. A-8. Displacement as a Function of Time, Wall No. 94

Test Results, Wall No. 96 (8-inch non-reinforced brick wall, arched one-way)

The fourth wall in this series was important in that it had a built-in flaw, a crack across the horizontal center of the wall. This was created during the construction of the wall by placing a sandwich of two layers of tar paper with a layer of plastic film between them in the wall at the center.

One test was conducted on this wall using five 60-foot strands of primacord (P_r approximately 13 psi). After the test, the debris was well scattered with large pieces 70 to 80 feet away (as far as the back wall of the facility).

Post-test photographs of this debris can be seen in Figure A-9. Displacement data for this test is presented in Figure A-10.

One-Way Arched Composite Walls

One composite wall (Wall No. 92), which consisted of 6-inch concrete block with a 4-inch brick facing on the side toward the blast, was investigated during this year's series. This wall was constructed on a steel frame outside the tunnel. The wall when cured (more than 28 days) was then moved into the shock tunnel and mounted as shown in Figure A-11.

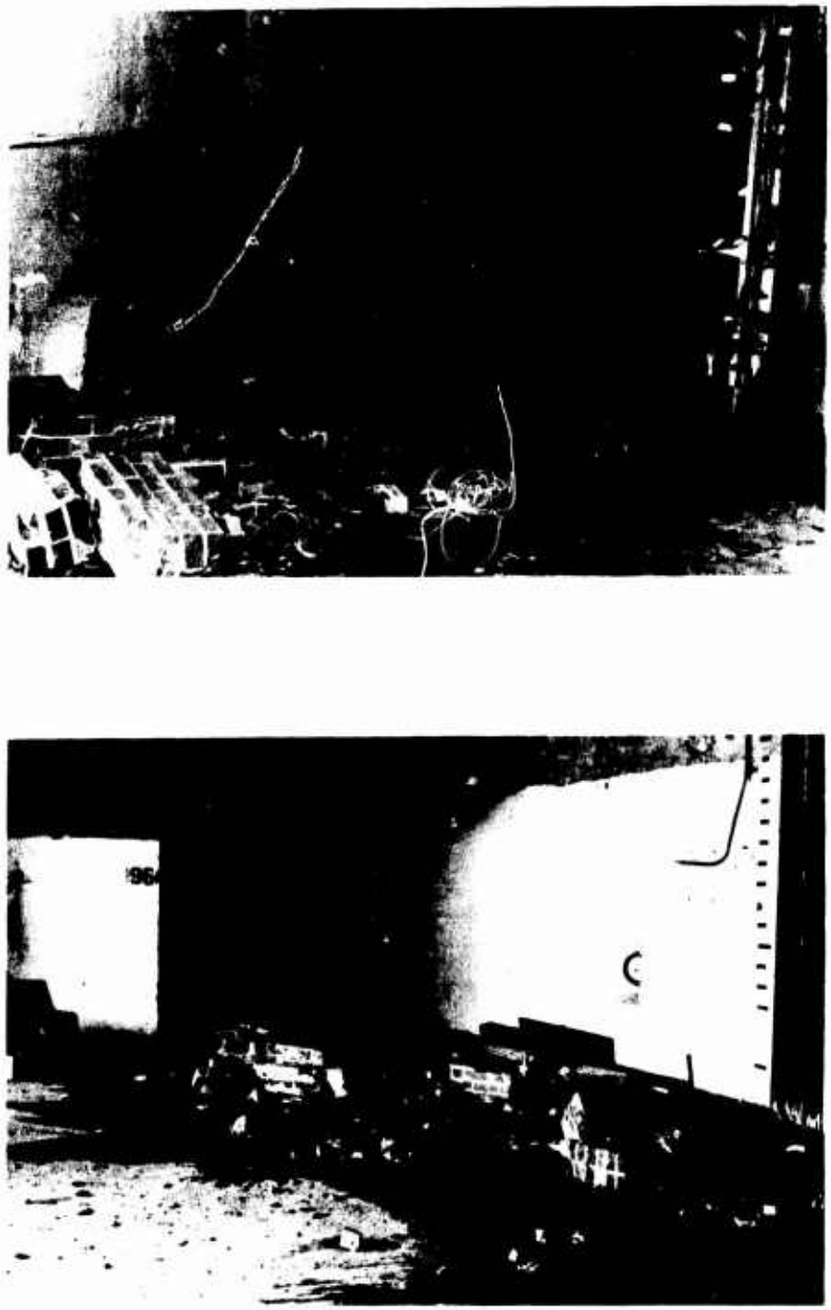

Fig. A-9. Post-Test Photographs of Wall No. 96

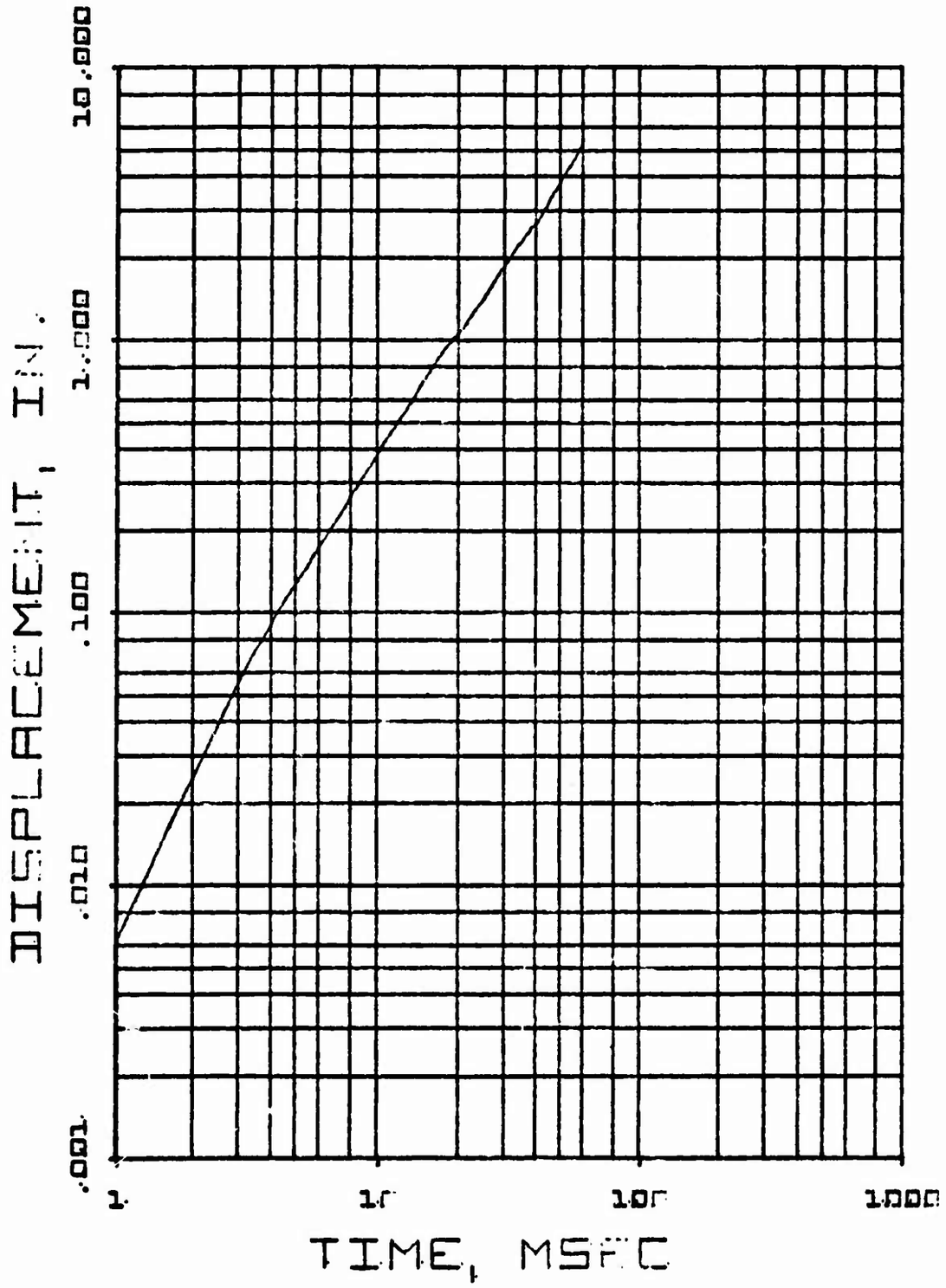

Fig. A-10. Displacement as a Function of Time, Wall No. 96

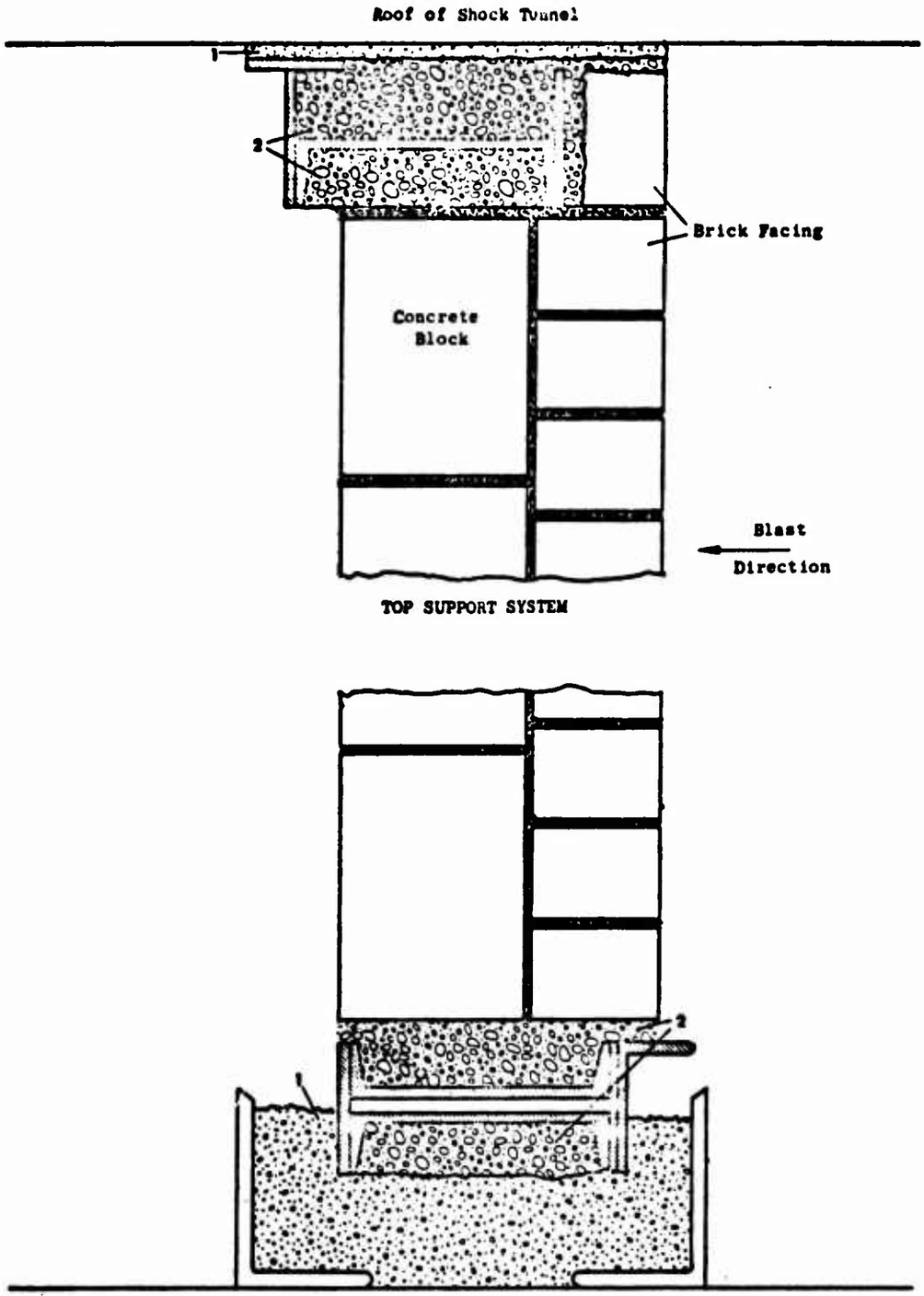

Fig. A-11. Support Systems for Wall 92, 6-in. Concrete Block with 4-in. Brick Facing. Note: 1. Mortar installed when wall placed in Shock Tunnel. 2. Mortar installed when wall was constructed.

Test results, Wall No. 92 (10-inch non-reinforced concrete block wall with a brick facing).

Three tests were conducted on this wall. The first test, using three 60-foot strands of primacord (P_r approximately 7 psi) created a small horizontal crack along the horizontal center of the wall, and some spalling of the concrete block along the lower edge of the wall. The crack gauges measured crack times of 4.6, 7.4 and 10.3 msec suggesting that the crack gauges progressed from left to right (as you face the back side of the wall). It is also interesting to note that the intervals between the crack times are almost equal.

The second test, using three 60-foot strands of primacord (P_r approximately 7 psi) produced no additional apparent damage. The third test, using four 60-foot strands of primacord (P_r approximately 10 psi) enlarged the center horizontal crack and created considerable spalling of the concrete block at the lower right-hand corner, as shown in the photographs in Figure A-12. The displacement data for the three tests on this wall are presented in Figure A-13.

Two-way Arched Walls

Three two-way arched walls (i.e., fixed on all four sides) were investigated during this reporting period. These were a 4-inch non-reinforced brick (Wall No. 83) and two 8-inch non-reinforced concrete block walls (Wall Nos. 89 and 90). These walls were constructed in the tunnel and allowed to cure a minimum of 28 days before testing.

Test results, Wall No. 83 (4-inch non-reinforced brick two-way arched).

Two tests were conducted on the wall, each using two 60-foot strands of primacord. The first test cracked the wall with the three crack gauges indicating times of 7, 8 and 20 msec. On the downstream side (away from

Fig. A-12. Post-Test Photographs of Wall No. 92

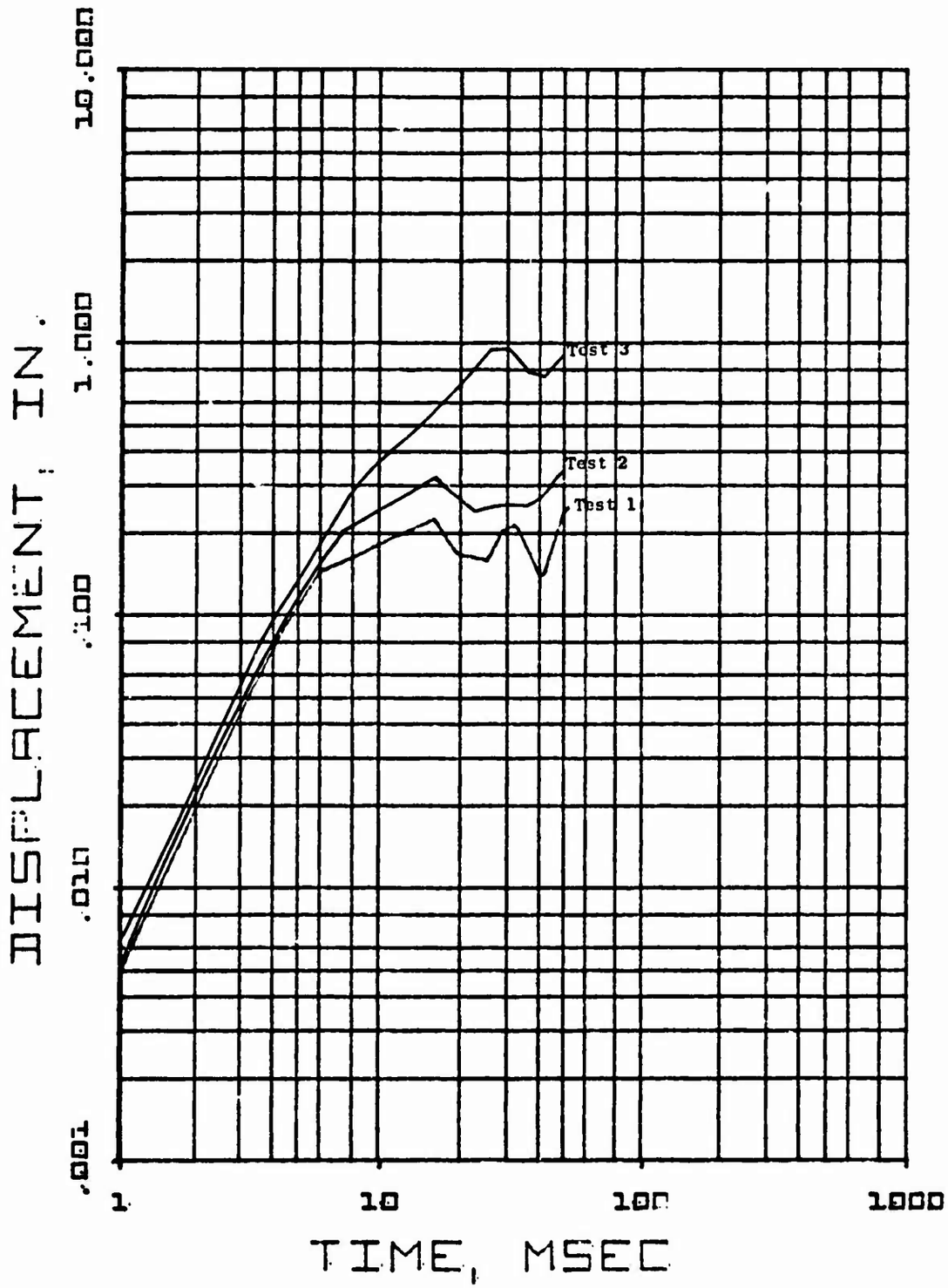

Fig. A-13. Displacement as a Function of Time, Wall No. 92, Tests 1,2 and 3

the blast), numerous cracks were noted in the center of the wall, and seven long cracks radiated from this center area towards the corners. On the upstream side, there was a little spalling near the center which detached the velocity gauge, and there were also cracks at each corner.

In the second test, the wall failed catastrophically, leaving the corners attached to the Shock Tunnel, as shown in the two post test photographs in Figure A-14.

Test results, Wall No. 89 (8-inch non-reinforced concrete block two-way arched).

One test was conducted on this wall using four 60-foot strands of primacord (P_r approximately 10 psi). The wall failed catastrophically, with debris scattered throughout the tunnel and casement area. Approximately 10 percent of the debris landed within the first 30 feet, approximately 70 percent between 20 and 70 feet, and approximately 20 percent piled up against the back wall at 80 feet. The crack gauges recorded crack times of 6.5, 4.3 and 4.25 msec.

Displacement gauge data for this test is presented in Figure A-15. Post test photographs of this wall are presented in Figures A-16 and A-17.

Fig. A-14. Post-Test Photographs of Wall No. 83

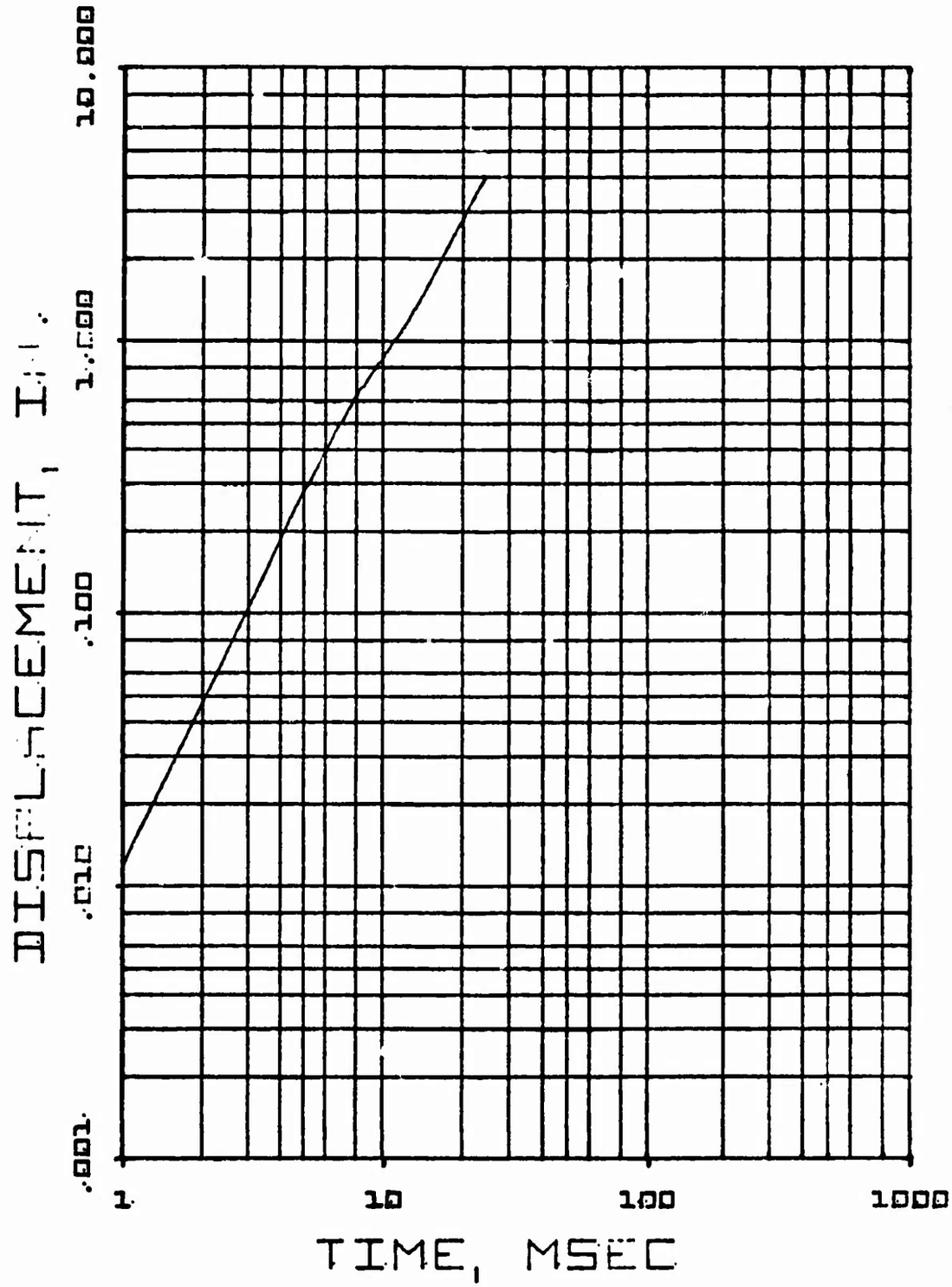

Fig. A-15. Displacement as a Function of Time, Wall No. 89

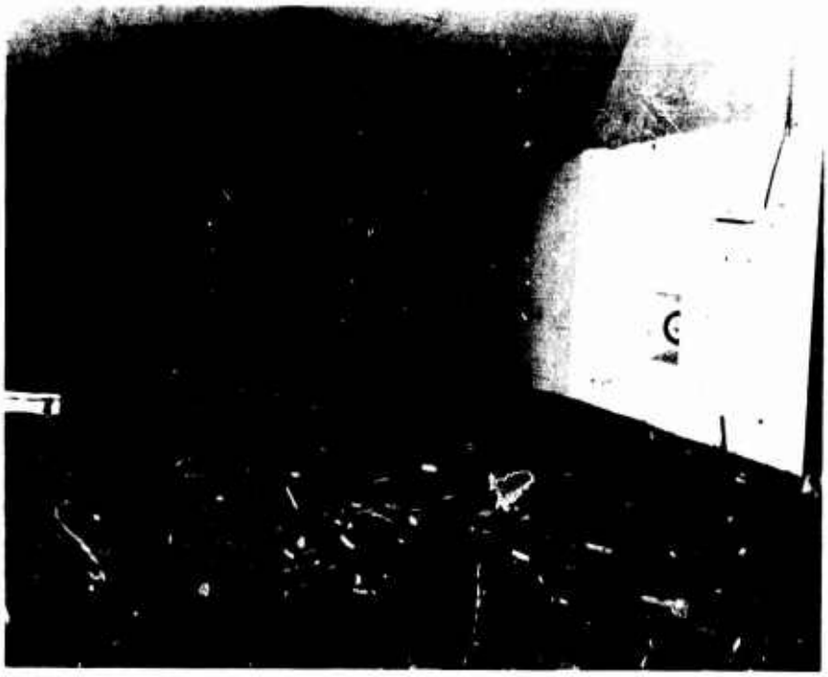

Debris Within First 60 Feet

Debris Against Back Wall

Fig. A-16. Post-Test Photographs of Wall No. 89

Right Edge of Wall

Fig. A-17. Post-Test Photograph of Wall No. 89

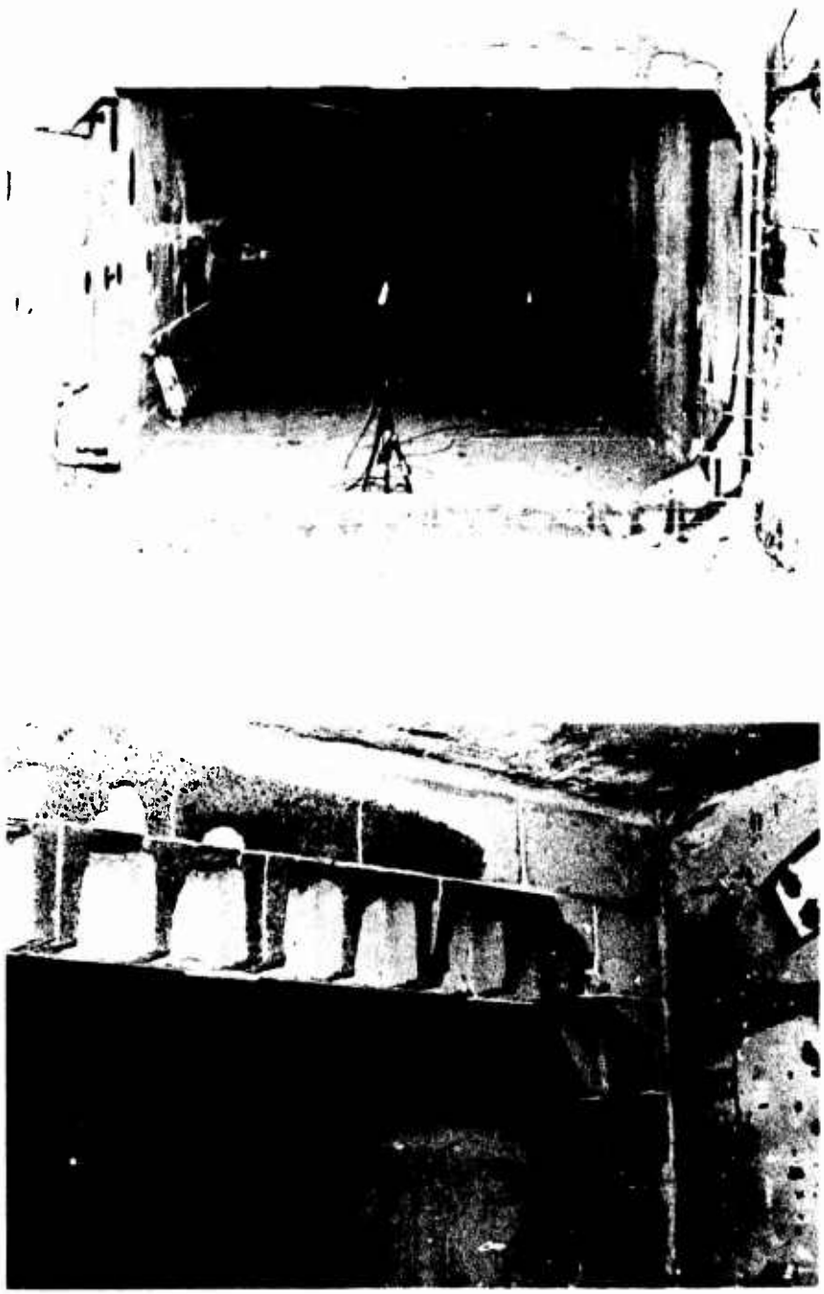

Fig. A-18. Post-Test Photographs of Wall No. 90

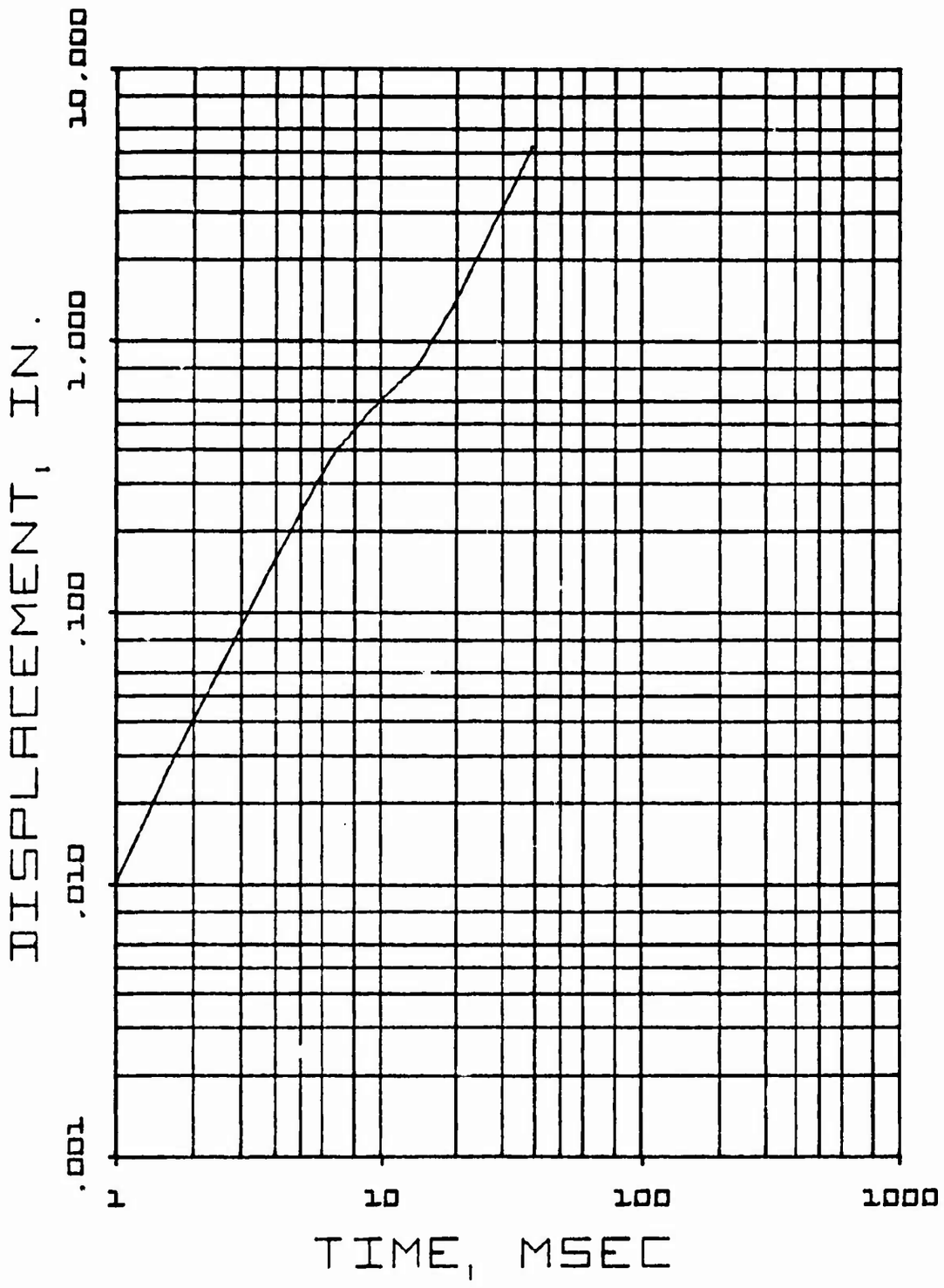

Fig. A-19. Displacement as a Function of Time, Wall No. 90

Test results, Wall No. 86 (8-inch non-reinforced brick one-way arched with doorway opening).

Two tests were conducted on this wall. The first, using five 60-foot strands of primacord (P_r approximately 12 psi), cracked the wall with indicated crack times from the three crack gauges of 5.8, 5.9 and 5.0 msec. In the second test using six strands (P_r approximately 17 psi), additional cracking occurred but they were still very small and no spalling of the brick was noted. No further tests were conducted on this wall.

The displacement data for these two tests on Wall No. 86 are shown in Figure A-20.

Test results, Wall No. 95 (8-inch non-reinforced brick one-way arched with a doorway opening).

This one-way arched wall had an approximately 1/3-inch gap between the top of the wall and the ceiling. Since only minimal damage was caused to Wall No. 86 (a like wall without a gap), the decision was made to test this wall at six strands. The six strand test (P_r approximately 17 psi) completely failed the wall with the majority of the debris landing within the first 30 feet.

Analytical work conducted since this test have indicated that this wall should be much weaker than first surmised. The crack times for this test were 6, 8.8 and 9 msec. The displacement data is presented in Fig. A-21 and post test photographs in Figure A-22.

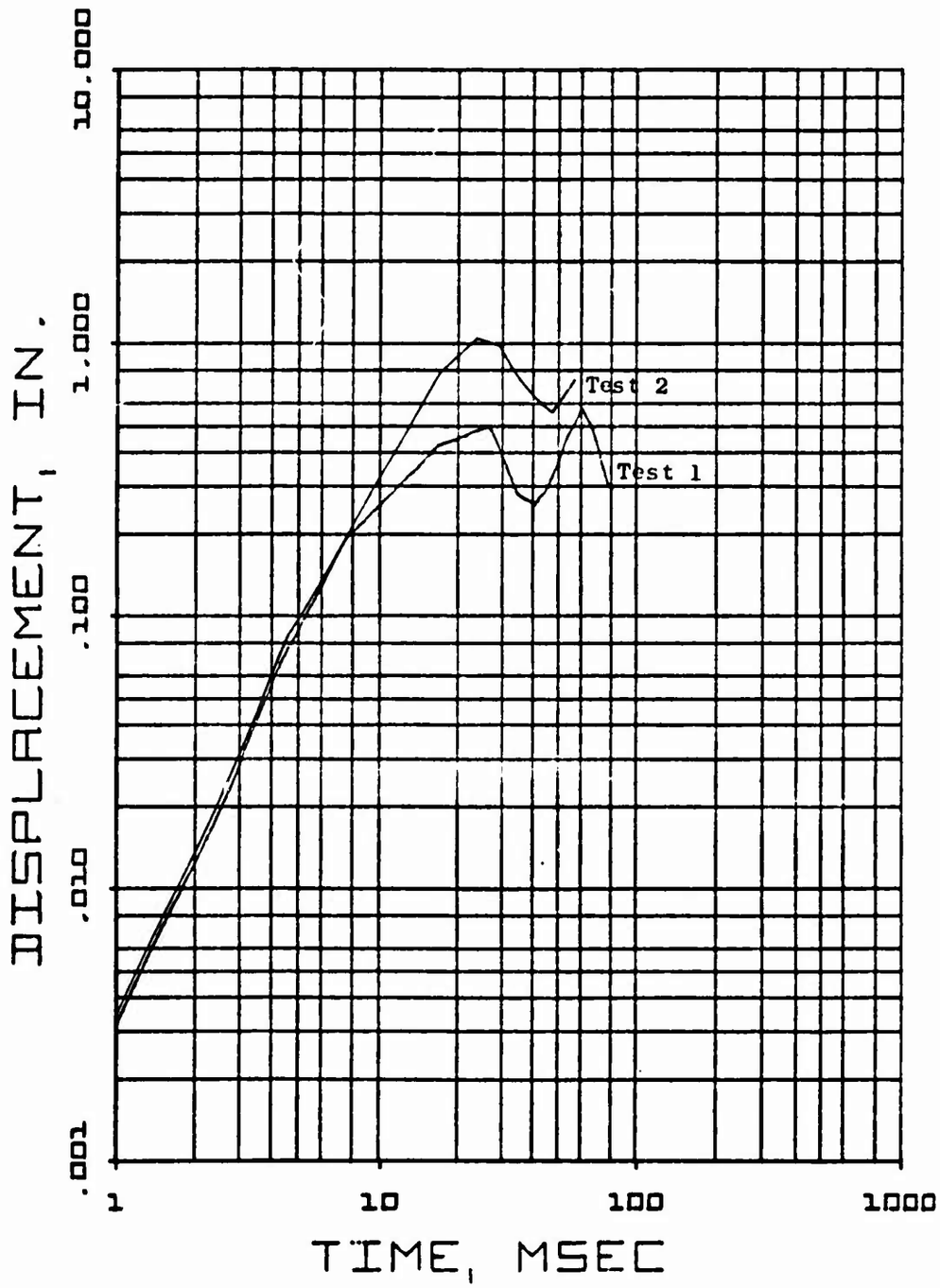

Fig. A-20. Displacement as a Function of Time Wall No. 86, Tests 1 and 2

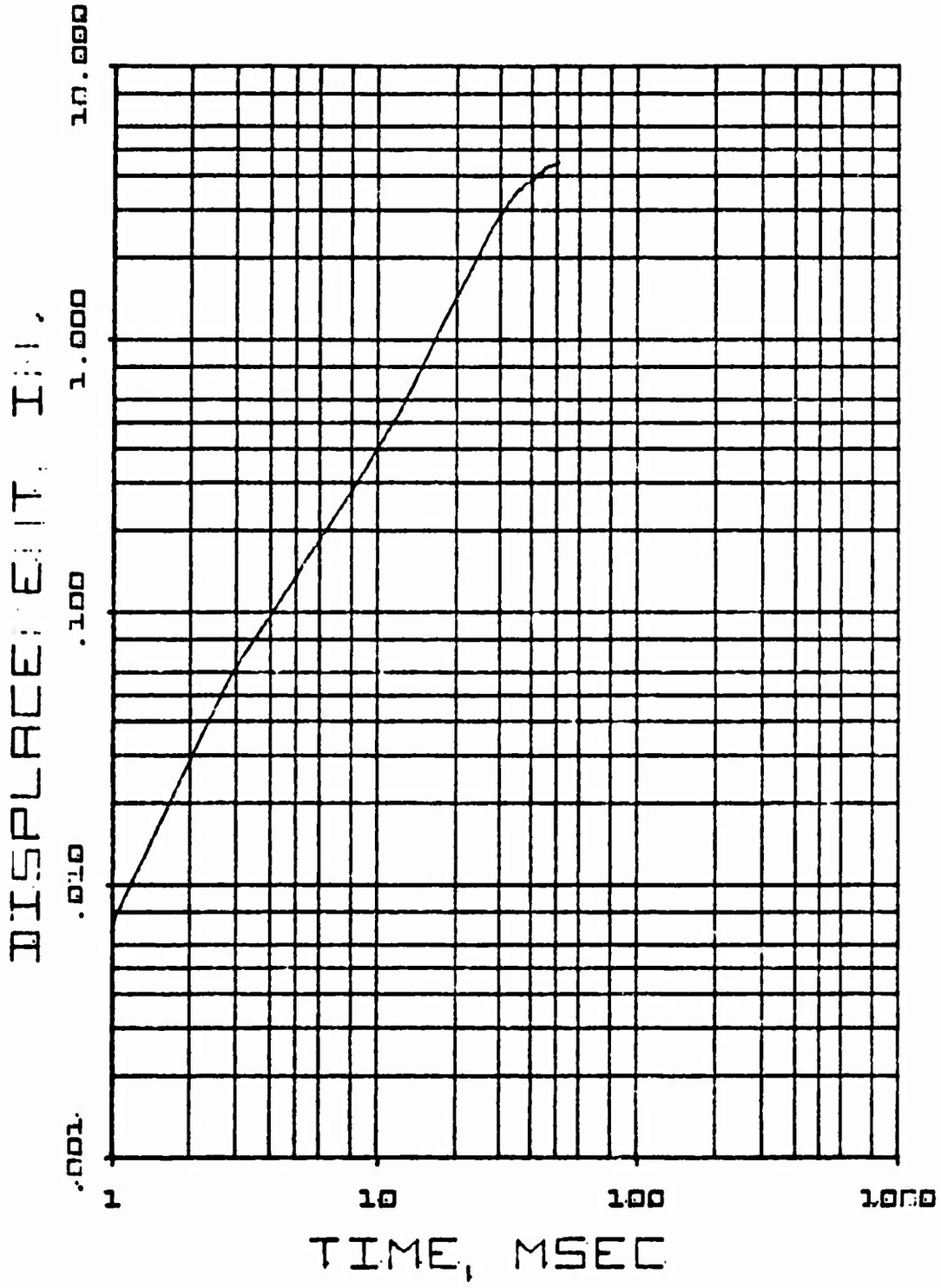

Fig. A-21. Displacement as a Function of Time, Wall No. 95

Fig. A-22. Post-Test Photographs of Wall No. 95

Arched Walls With a Window Opening

Two non-reinforced brick walls (Wall Nos. 84 and 85) and two non-reinforced concrete block walls (Wall Nos. 91 and 93) with window openings were tested in this series. The window openings were located in the center of the walls and were 38 inches high and 60 inches wide, creating a hole approximately 16 percent open. These walls were also constructed on frames and were mounted in the tunnel as shown in Figure A-1, A and C.

Test Results, Wall No. 84 (8-inch non-reinforced brick, one-way arched with a window opening)

Two tests were conducted on this wall. The first test, using five 60-foot strands of primacord (P_r approximately 13 psi), cracked the wall with indicated crack times of 7.6, 7.8 and 8.6 msec. The second test, using six strands of primacord (P_r approximately 16 psi), failed the wall, scattering debris to 80 feet with 70 to 80 percent of the debris remaining within the first 30 feet. Post-test photographs of this test are shown in Figure A-23. Displacement gauge data for Tests 1 and 2 are shown in Figure A-24.

Test Results, Wall No. 85 (8-inch non-reinforced brick, one-way arched with a window opening

Four tests were conducted on this wall. The first test, using five 60-foot strands of primacord (P_r approximately 12 psi), cracked the wall with two cracks running across the entire wall at the 15th and 16th course (a typical wall is 31 courses high). Measured crack times for this test were 4.2, 6.3 and 6.8 msec.

The second test, also using five strands of primacord (P_r approximately 11 psi), caused additional cracks at the 13th and 18th courses. The third test, using six strands of primacord (P_r approximately 15 psi), caused the crack at the 16th course to widen and a one-foot wide spalling and cracking was noted along the bottom of the wall.

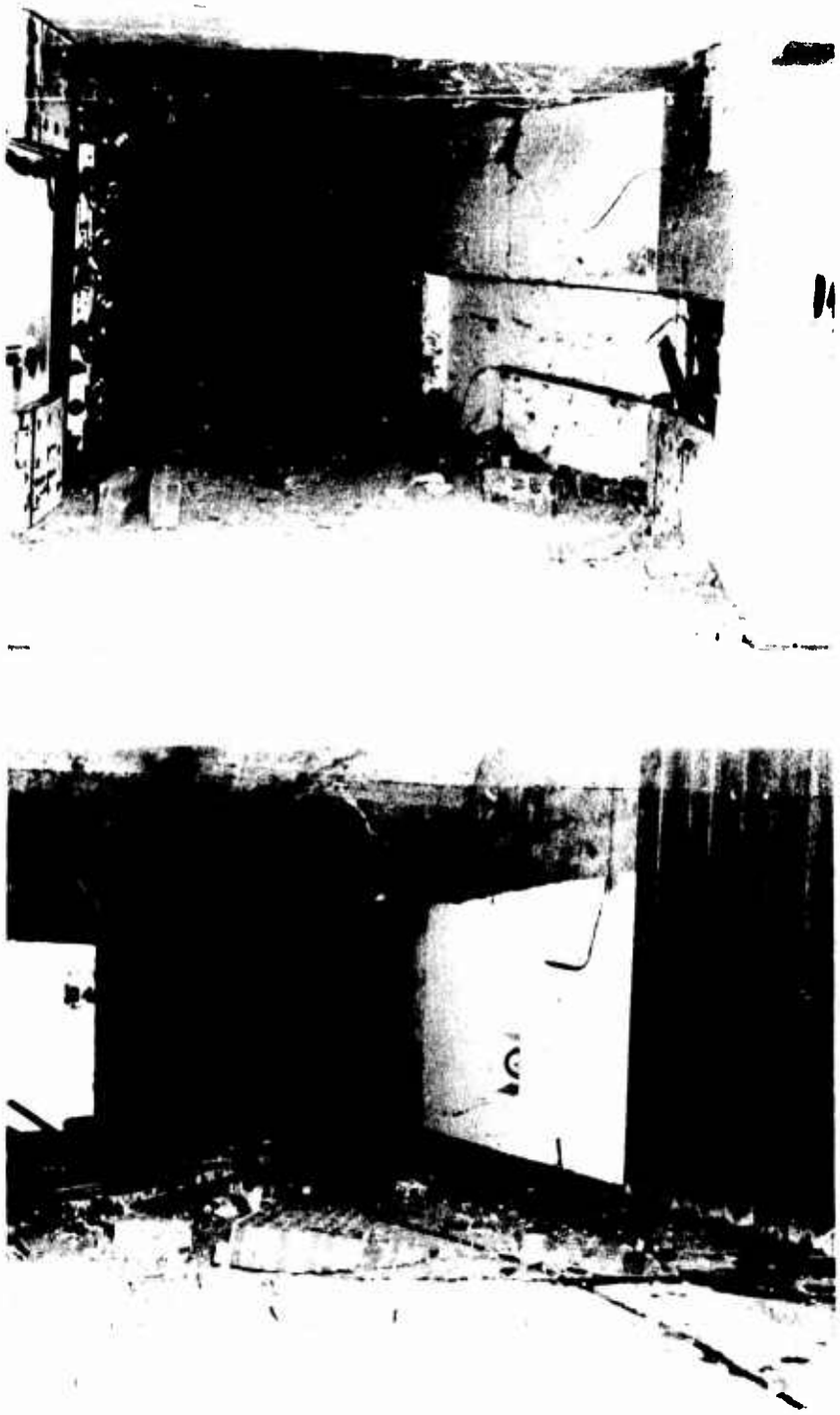

Fig. A-23. Post-Test Photographs of Wall No. 84, Second Tes.

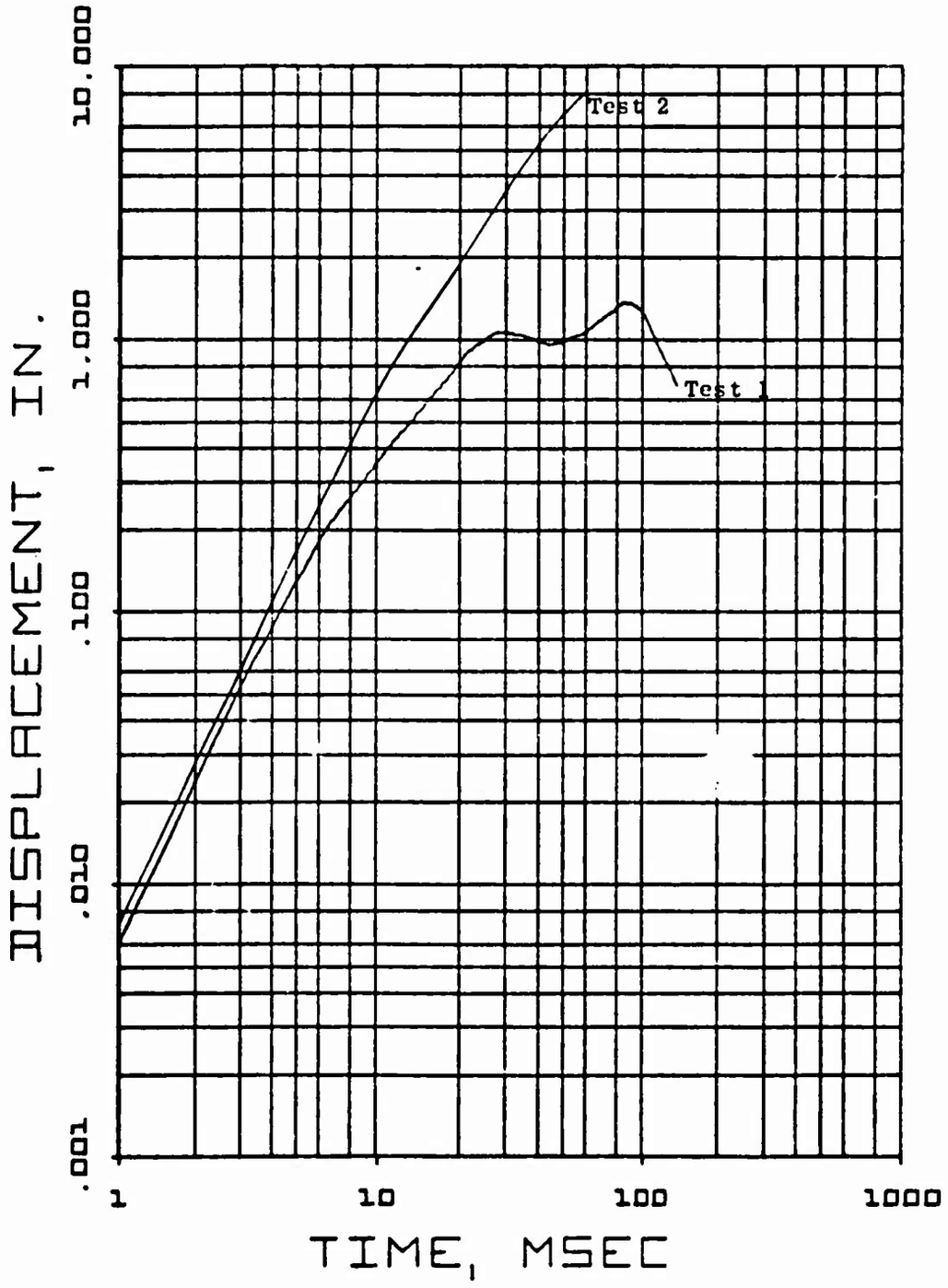

Fig. A-24. Displacement as a Function of Time, Wall No. 84, Tests 1 and 2

The fourth test, using seven strands of primacord (P_r approximately 19 psi), failed the wall as shown in Figures A-25 and A-26, a selection of pre- and post-test photographs.

Test Results, Wall No. 91 (8-inch non-reinforced concrete block with window opening)

One test was conducted on this wall using three 60-foot strands of primacord (P_r approximately 7 psi). The wall failed as shown in the post-test photos, Figure A-27. A crack gauge on the section that collapsed indicated a crack time of 7.3 msec and two crack guages on the portion remaining standing after the test indicated crack times of 5.1 and 5.2 msec. Displacement gauge data for this test is given in Figure A-28.

Test Results, Wall No. 93 (8-inch non-reinforced concrete block with a window opening

One test was conducted on this wall using three 60-foot strands of primacord (P_r approximately 6 psi). The crack gauges indicated times of 8.1, 5.9 and 6.0 msec. The wall did not fall down; however, post-test inspection showed very extensive cracking at four or more levels across the wall, with at least one crack across the entire wall near the top. There were also vertical cracks on both sides of the window and diagonal cracks from the top corners to the window corners.

Displacement gauge data for this test is presented in Figure A-29.

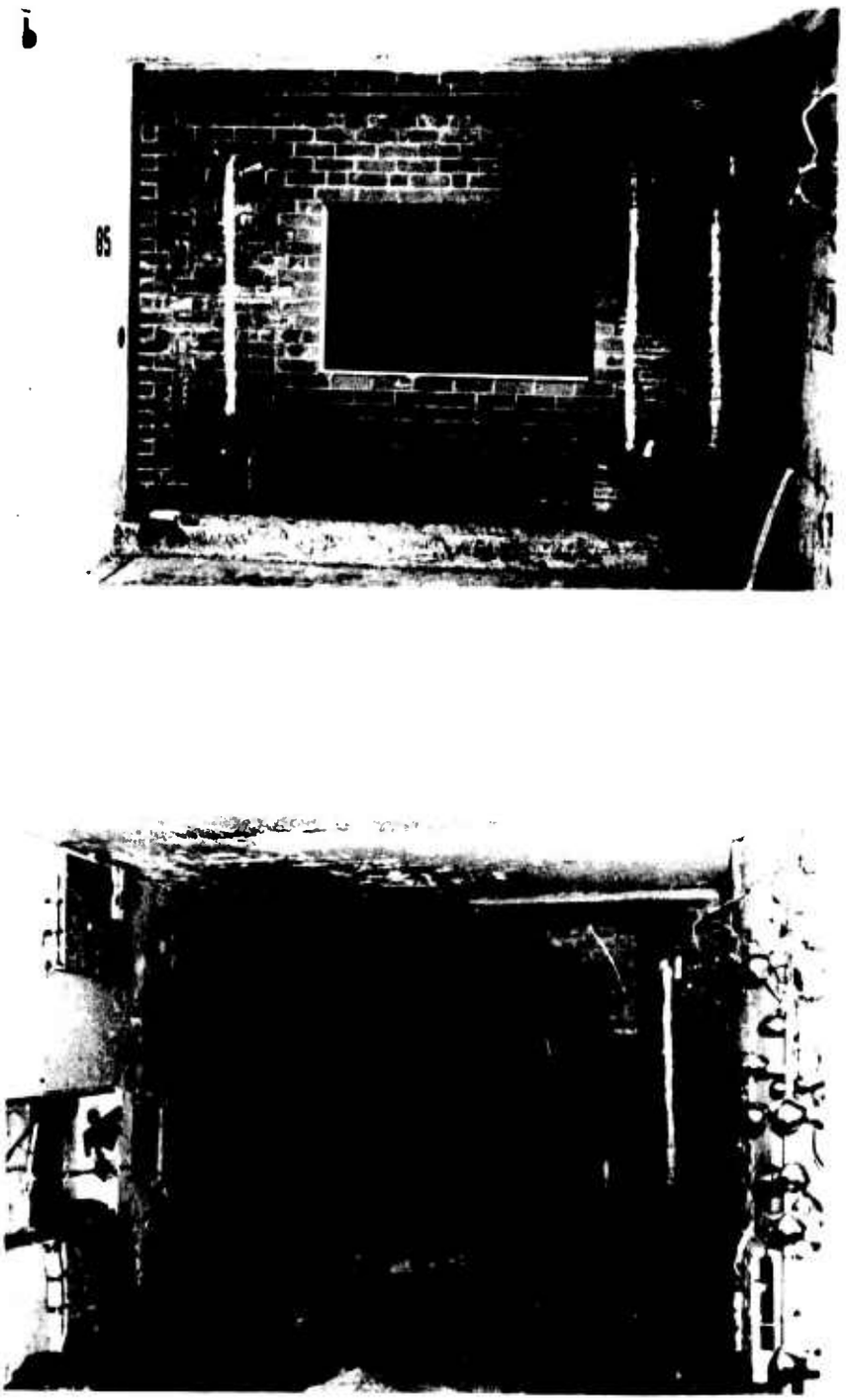

Fig. A-25. Pre- and Post-Test Photographs of Wall No. 85

Fig. A-26. Post-Test Photographs of Wall No. 85

Fig. A-27. Post-Test Photographs of Wall No. 91

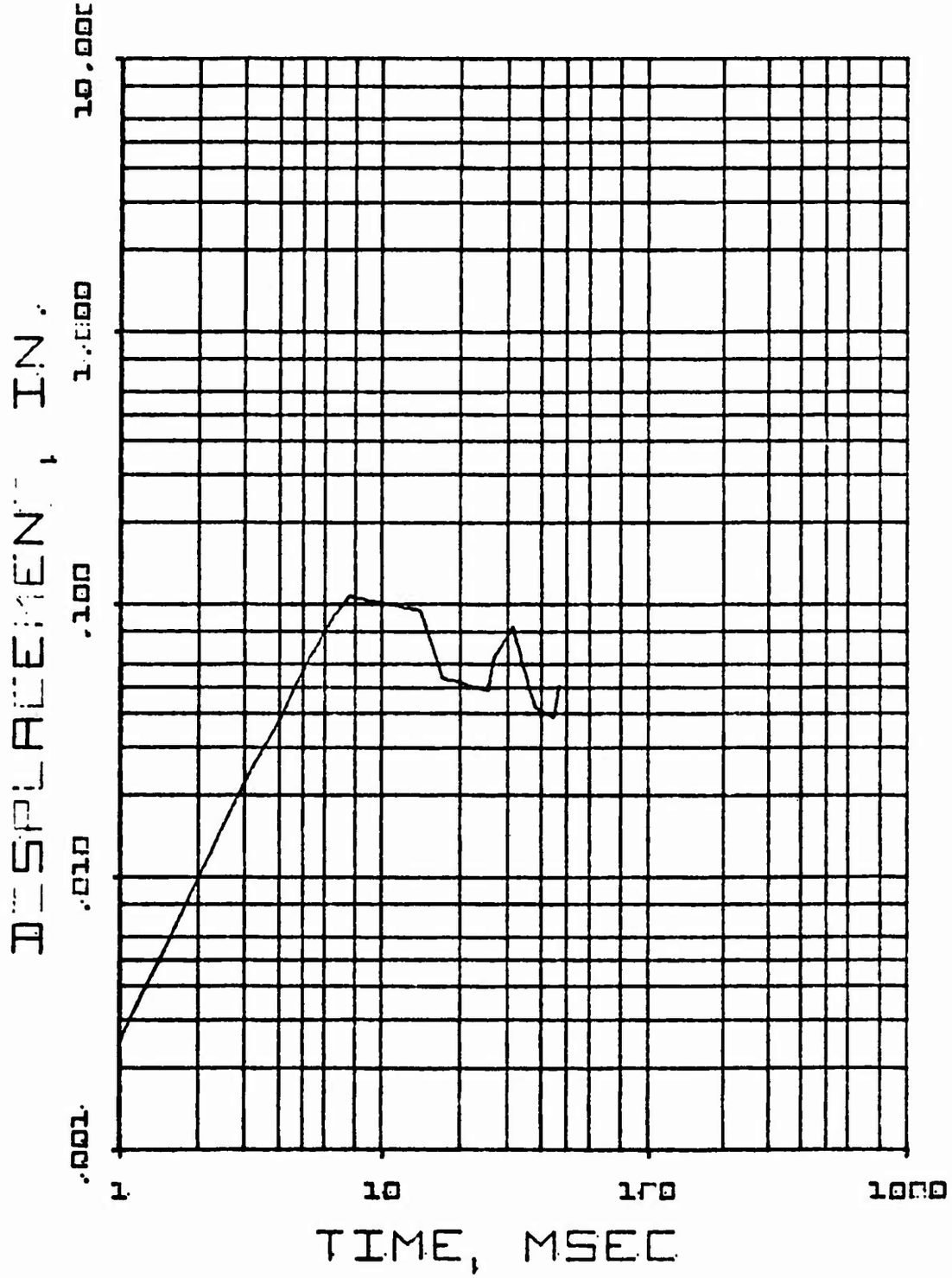

Fig. A-28. Displacement as a Function of Time, Wall No. 91

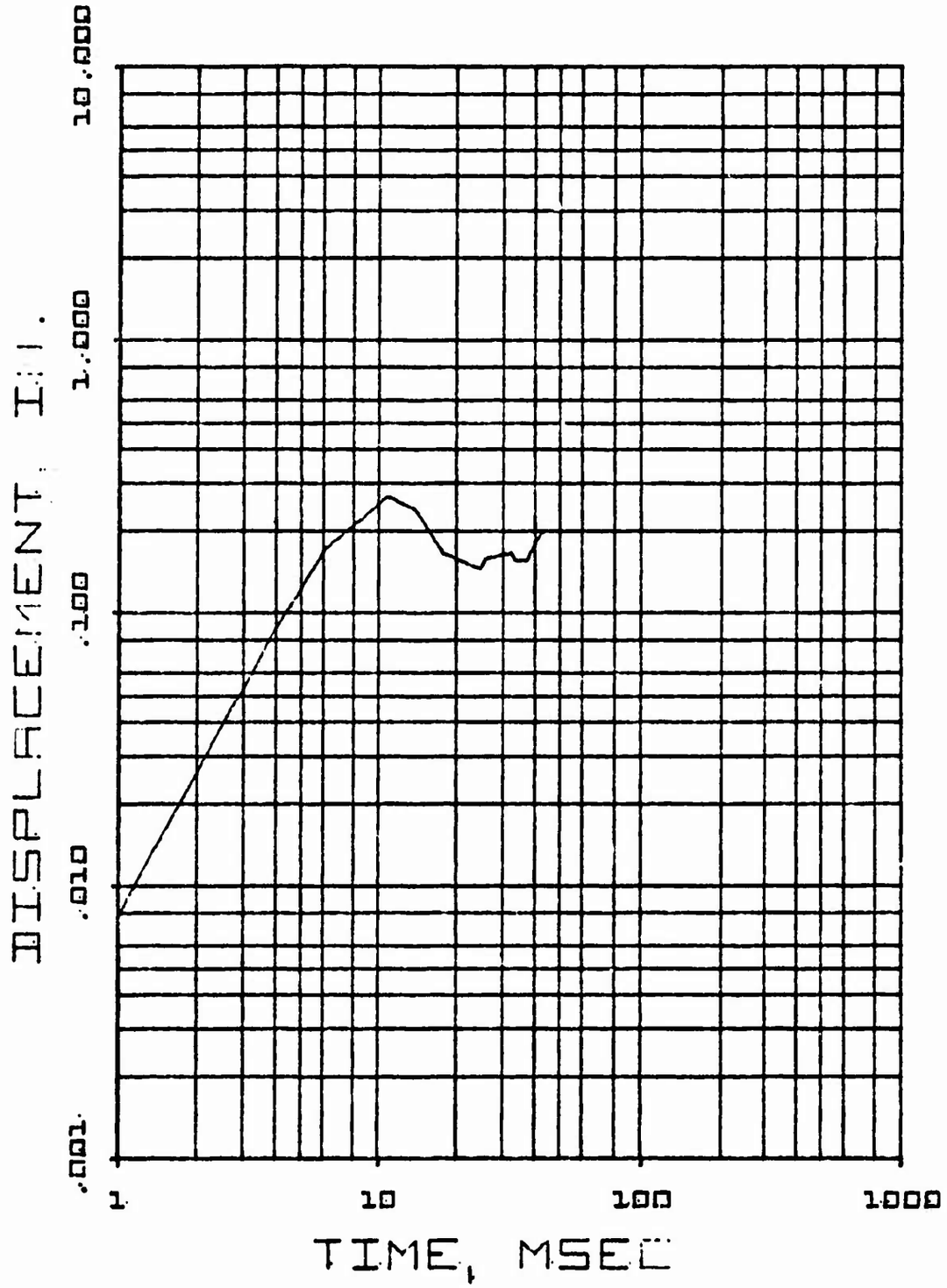

Fig. A-29. Displacement as a Function of Time, Wall No. 93

Appendix B

SUMMARY OF THE COMPUTER EFFORT

INTRODUCTION

For several years, a rather complete analytical effort of full-scale response of wall panels to blast loading was conducted in conjunction with the test program. Information such as failure times, energy or impulses transmitted to a building frame, and the influences of support conditions and wall geometry are required for casualty and injury predictions, debris prediction, etc. This section concentrates on comprehensive analytical investigation of the loading and response of structural nonreinforced building wall panels constructed of brittle materials.

From the beginning, a computer orientated effort was recognized as the most practical and economical way of obtaining the dynamic structural response of wall panels. A sufficiently sophisticated computer program could produce the desired structural response data for each wall panel permutation more succinctly than experimental test results, provided computer input reflected real-life conditions. Thus an experimental test program was run parallel to computer and theoretical efforts to accurately determine material properties and blast loading histories used as computer input. Also, the experimental and computer efforts complimented each other, in that experimental tests on walls similar to those considered by the computer code verified computer results and these results directed the experimental test program to examine closer certain behavioral characteristics of some wall panels.

Two different computer programs were used in analyzing structural behavior of wall panels. One program, known as the Mechanical Analysis of Continuous Elastic Systems, or MACE, is used in analyzing structural behavior of arched walls. The second program, known as the Structural Analysis and Matrix Interpretive System, or SAMIS, provides data on deflections at a point and stresses on an element of wall at incremented time intervals for three wall geometries -- solid walls, walls with doorways and window openings. For each wall form, four different support conditions were considered:

- Simple (pinned) supports top and bottom of wall
- Moment resisting (fixed) supports top and bottom
- Simple (pinned) supports four sides
- Moment resisting (fixed) supports four sides.

Some of the data from SAMIS on the above wall forms and support conditions for wall deflections and stresses has been compiled into this report.

DESCRIPTION OF SAMIS

The computer code used in predicting wall behavior was the Structural Analysis and Matrix Interpretive System (SAMIS). SAMIS was developed by Western Development Laboratories of the Philco-Ford Corporation under contract to the Jet Propulsion Laboratory and utilizes the finite-element method of analysis.

The finite-element method of analyzing continuums, such as plates and shells, is based upon the premise that a continuum with an infinite number of degrees of freedom can be accurately approximated by an equivalent continuum with a finite number of degrees of freedom. Thus, an equivalent continuum is divided into small areas or elements which are interconnected at a finite number of points, known as nodal points or nodes. The total number of the degrees of freedom is the sum of the degrees of freedom of

each node. And each node has a maximum of 6^{D} of freedom (3 translational in x, y, and z; and 3 rotational about x, y, and z axis). Knowing the forces on the continuum and the physical and material properties of that continuum, matrices are written and operated on to obtain the element stresses and node displacements.

SAMIS is a segmented or chain program composed of 16 segments or links. The user selects the links to be used to give his desired output. The user specifies the order of the selected links by writing a set of instructions called pseudo instructions. A pseudo instruction calls for a set of subprograms to perform the necessary matrix operations.

SAMIS has two phases, a generation phase and a manipulative phase. The generation phase (one link) uses the geometric and material input data to generate:

- Element stiffness and stress matrices
- Fixed-node forces due to temperature gradients
- Equivalent gridpoint forces due to a unit uniform pressure
- Gravity loading vectors from imposed acceleration
- Element mass matrices for uniformly distributed masses within each element.

The manipulative phase of SAMIS is made up of 15 links. Five perform standard matrix algebra, i.e, addition and subtraction, multiplication, transportation, triangular decomposition and row-column scaling. Three others operate on simultaneous algebric equations and find the roots and vectors of the matrix. The remaining 7 links are special purpose programs for input and output of data.

The solution of a typical structural program involves the following steps. First, material tables defining the mechanical properties of all materials of interest are made. Then a listing of the element data is made defining local geometry (thickness, cross-sectional area, moment of intertia), gridpoints, coordinate systems, temperatures, weight and pressure on each element. Thirdly, boundary and loading conditions in matrix form are put in. And finally, the pseudo instructions are used to direct the operation of SAMIS to achieve the desired results.

INPUT DATA

Input to SAMIS consisted of material properties, pressure loading data and a wall grid with line elements. A determined analytical effort was made to have input data closely reflect actual walls such that computer results could be verified by experimental tests. Therefore, wall dimensions (8 ft x 12 ft x 8 in.) and material properties chosen for the computer code were the same as walls tested at the URS Shock Tunnel Facility.

Material Properties

For steel

$$\text{Young's Modulus} = E = 30 \times 10^6 \text{ psi}$$

$$\text{Poisson's Ratio} = \mu = 0.3$$

$$\text{Coefficient of Thermal Expansion} = \beta = 6.5 \times 10^6 \text{ in./in. } ^{o}F$$

$$\text{Temperature} = 60^{o} \text{ F}$$

For brick

$$E = 1 \times 10^6 \text{ psi}$$

$$\mu = 0.1$$

$$\text{Specific Weight} = 120 \text{ lbs/ft}^3$$

$$\beta = 3.4 \times 10^{-6} \text{ in./in. } ^{o}F$$

The properties for steel were obtained from the AISC Manual. For brick, Young's Modulus was determined by static tests on common brick using ASTM procedures. Different materials, or brick with different properties would, under loading, behave the same with different magnitudes for deflection and stress. These magnitudes would vary linearly with respect to the change in E. This is true since the motion is fundamentally in the brick wall other E values can be approximated by prorating the deflections by a E ratioed and the square root of the E ratio in the time domain.

Loading Data

The program SAMIS uses a loading matrix, i.e., the load vs time history of the blast wave on the wall to compute stresses and deflections at each predetermined time increment. For program stability, this must be no more than 1/20 of the highest natural period. By having the wall mass concentrated at every other nodal point, the minimum time interval was increased to 0.001 seconds or 1 msec from .0005 seconds or 0.5 msec.

The dynamic response prediction is a step-by-step numerical integration of structural behavior of a wall which is a function of time. Thus loading must be supplied to each element at each time increment used in numerical integration. The load-time history is different for each wall form because the wall openings allow blast pressure to be relieved on the front and creates a small pressure on the back side of the wall. Hence, extensive loading tests were required to obtain the best load time history for the computer loading matrix for each wall form. For the solid wall, a step load of 1 psi uniformly distributed across the surface closely reflected the results of load time surveys.

Walls with an opening require more complex loading information. In the case of a doorway each facet or element is loaded differently at each time interval. Loading studies resulted in Fig. B-1 for the loading vs time input for the wall with a doorway. Fig. B-2 is a comparison of SAMIS

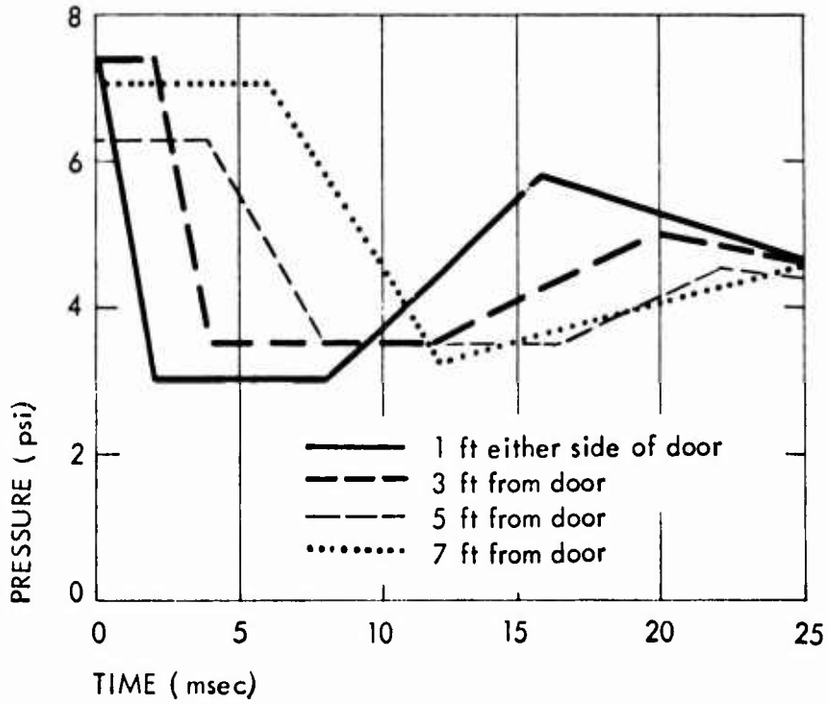

Fig. B-1. Loading Input for SAMIS for Wall with a Doorway.

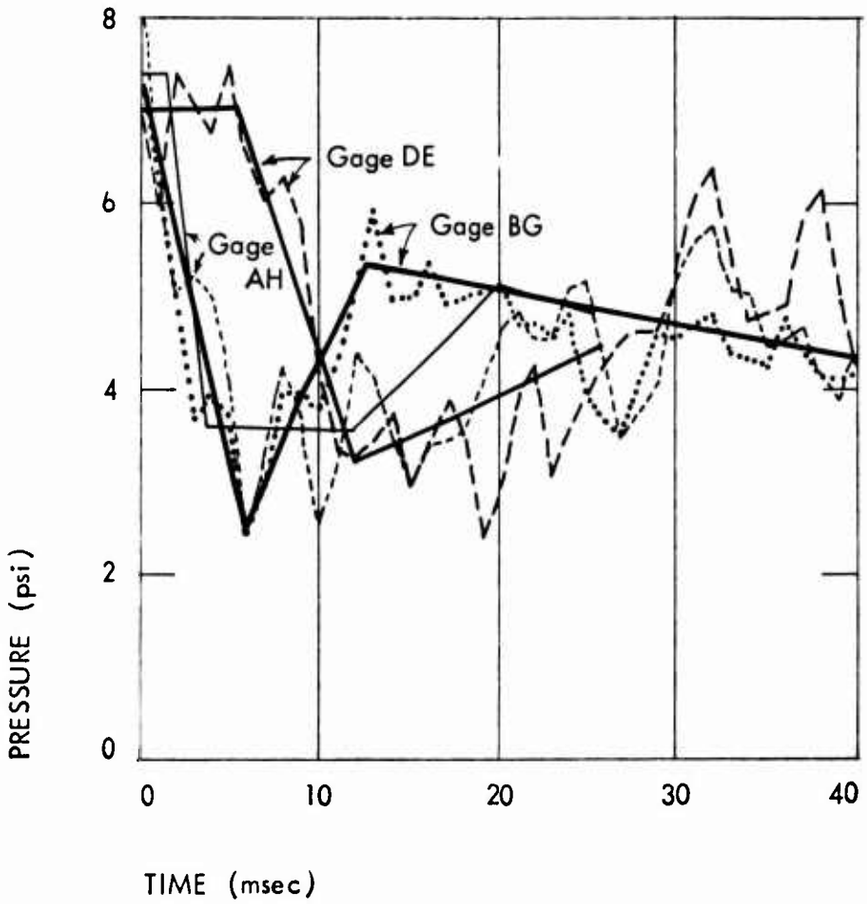

Fig. B-2. Comparison of SAMIS Input Data in Fig. B-1 with Loading Study Data From Ref. 1.

input data with the loading study data. The loading time history was normalized to 1 psi pressure when fed to the computer. For a window, the load time history for SAMIS input is shown in Fig. B-3. This history also was normalized to 1 psi before deflections and stresses were completed.

Support Conditions

SAMIS provided deflections and stresses for each wall form for each of four different types of support:

1. Simple (pinned) supports top and bottom of wall
2. Moment resisting (fixed) supports top and bottom
3. Simple (pinned) supports four sides
4. Moment resisting (fixed) supports four sides.

Figure B-4 shows what is meant by a pinned and fixed support. Simply supported walls are more prevalent and weaker than moment resisting types as a comparison of graphs in following subsections (Solid Wall, Wall With a Doorway, Wall With a Window) will correlate. However, it should be noted that the "fixed supports" conditions are idealized as moment resisting supports with no deformation of the support. In actual construction such supports are difficult to achieve.

SOLID WALL SOLUTION

The solid wall dimensions are 8 ft x 12 ft x 8 in. and is made of non-reinforced mortared brick. For structural modeling the node and element pattern of Fig. B-5 was chosen, being the most accurate yet economical with respect to computer time. A smaller element size would be only slightly more accurate, but much more expensive. Due to symmetry about x and y axis, additional savings were realized by considering only 1/4 panel of the wall by the computer. Loading used was a 1 psi step dynamic load.

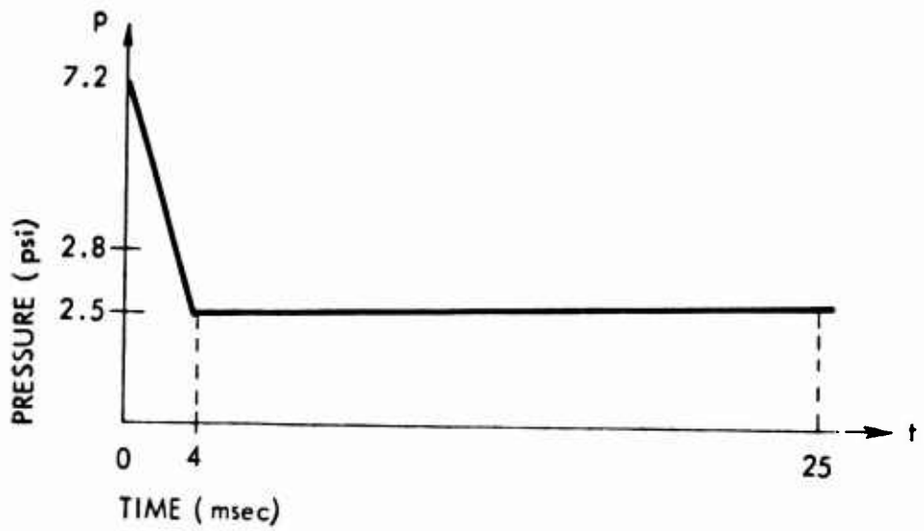

Fig. B-3. Average Input Loading for Wall With a Window.

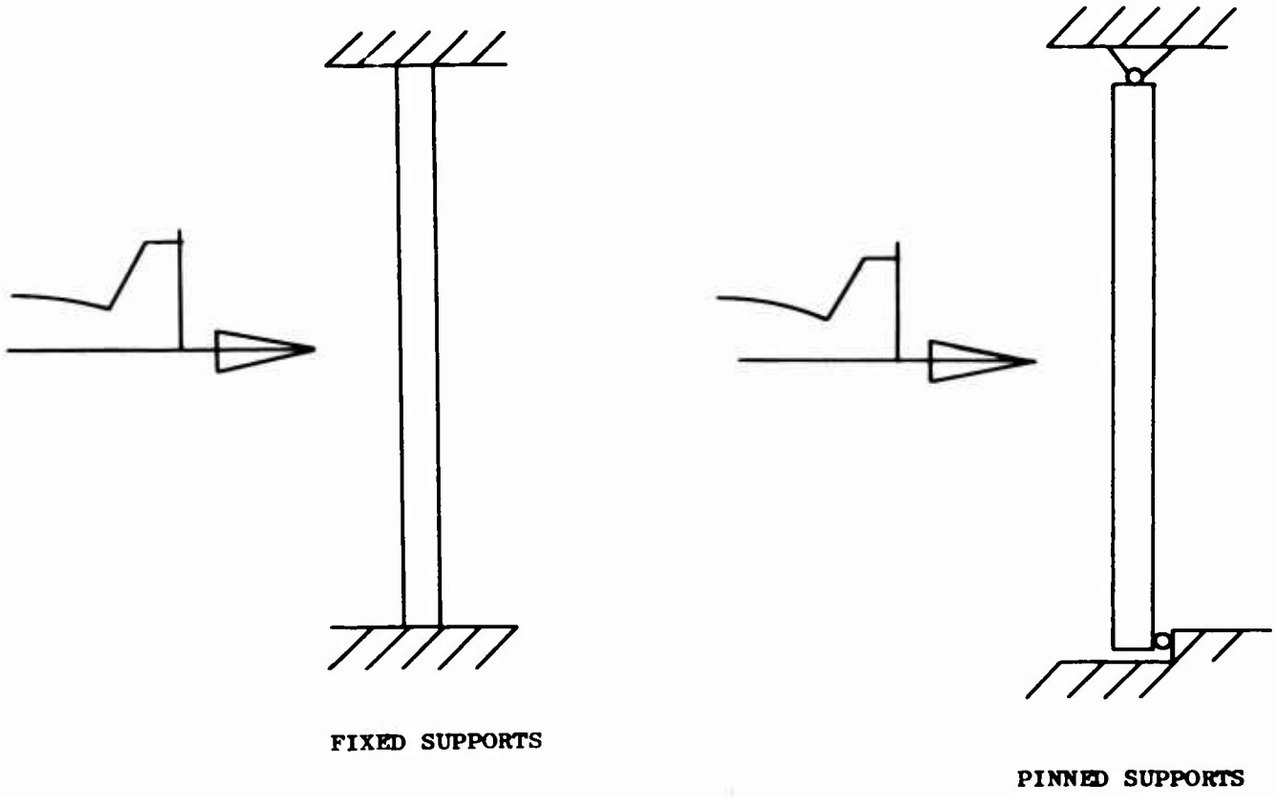

Fig. B-4. Simple (Pinned) and Moment Resisting (Fixed) Supports Top and Bottom.

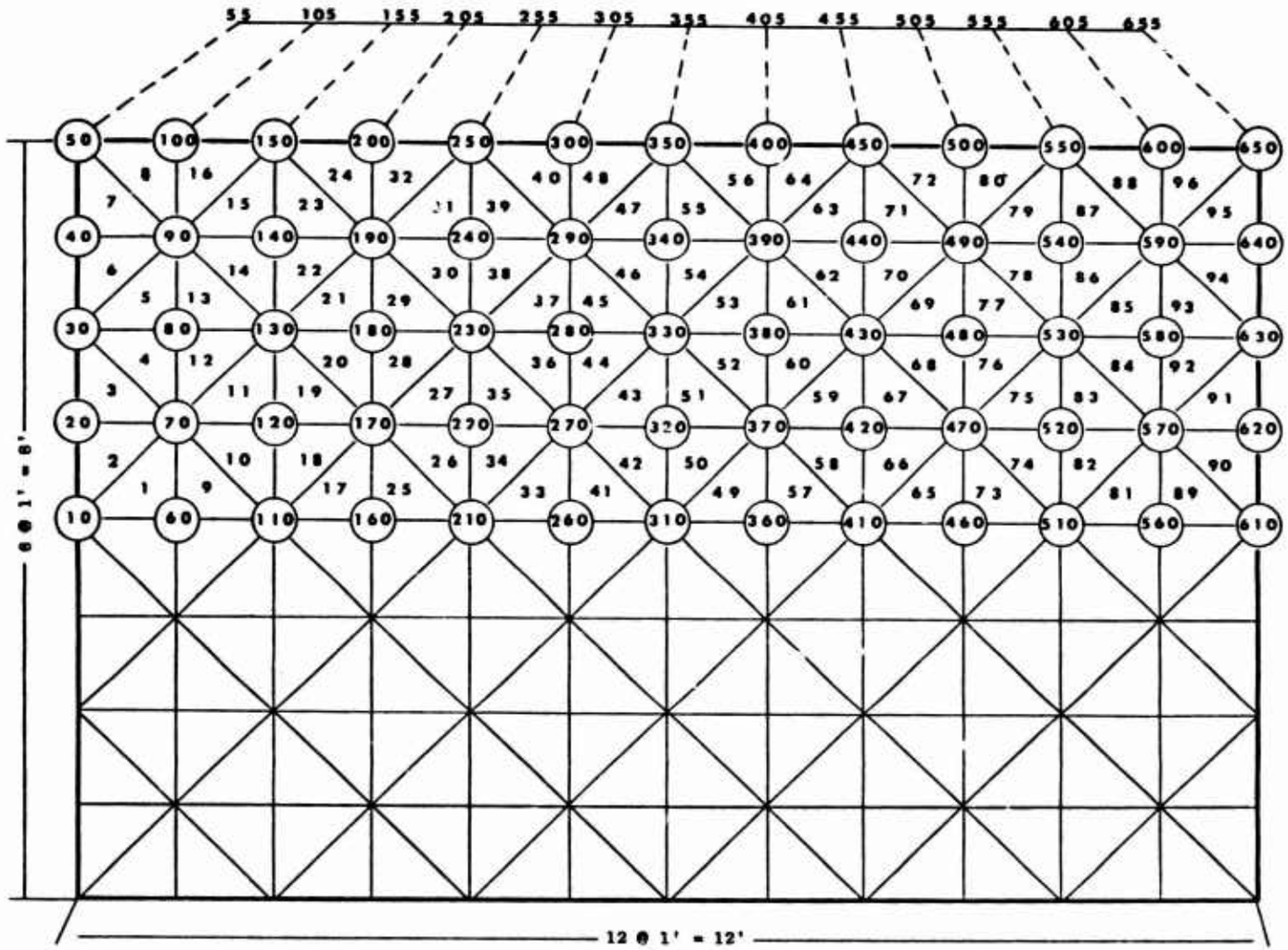

Fig. B-5. Node and Element Locations for Solid Walls

Since tests of the typical shock tunnel loading pulse show an essentially uniform pulse of 40 to 50 msec duration, we need to only consider 25 msec of that pulse, as failure will occur before this time.

Since the resulting deflections and stresses are for a 1 psi load, the deflections or stresses for any reflected pressure can be obtained by multiplying these results by the actual reflected pressure.

Figure B-6 shows the coordinate axis for each element and how the principal stresses are located from the x and y axis. The angle shown is positive. For the stress contour maps, only the maximum tensile stress of the principal stresses is shown. Other sign conventions are t for tensile stresses and - for compressive. Deflections are positive in the +Z (downstream) wall surface.

Pinned Top and Bottom

Figure B-7 is a graph of both velocity and displacement (deflection) vs time of Node 360. The location of Node 360 is shown in Fig. B-6. Figure B-7 shows that the wall has a period of 35 msec under a typical blast load; and that maximum deflection at this point on the wall is 0.052 in. Figure B-8 also shows peak deflections at 17 msec and how uniform the deflections at midspan are over the length of the wall. Figure B-9 is an interesting picture of peak wall deflection, showing how the wall deforms under 1 psi blast loading.

The stress history for element No. 9 is given in Fig. B-10. As you see, for the minimum failure pressure, the wall will fail at 18 msec, where the maximum tensile stress occurs. Also note that θ is small, meaning the stresses are essentailly vertical. This is confirmed in Fig. B-11, the stress contour map at 17 msec. From the stress contours, the solid wall, simply supported, can be predicted to fail across its length at mid-height.

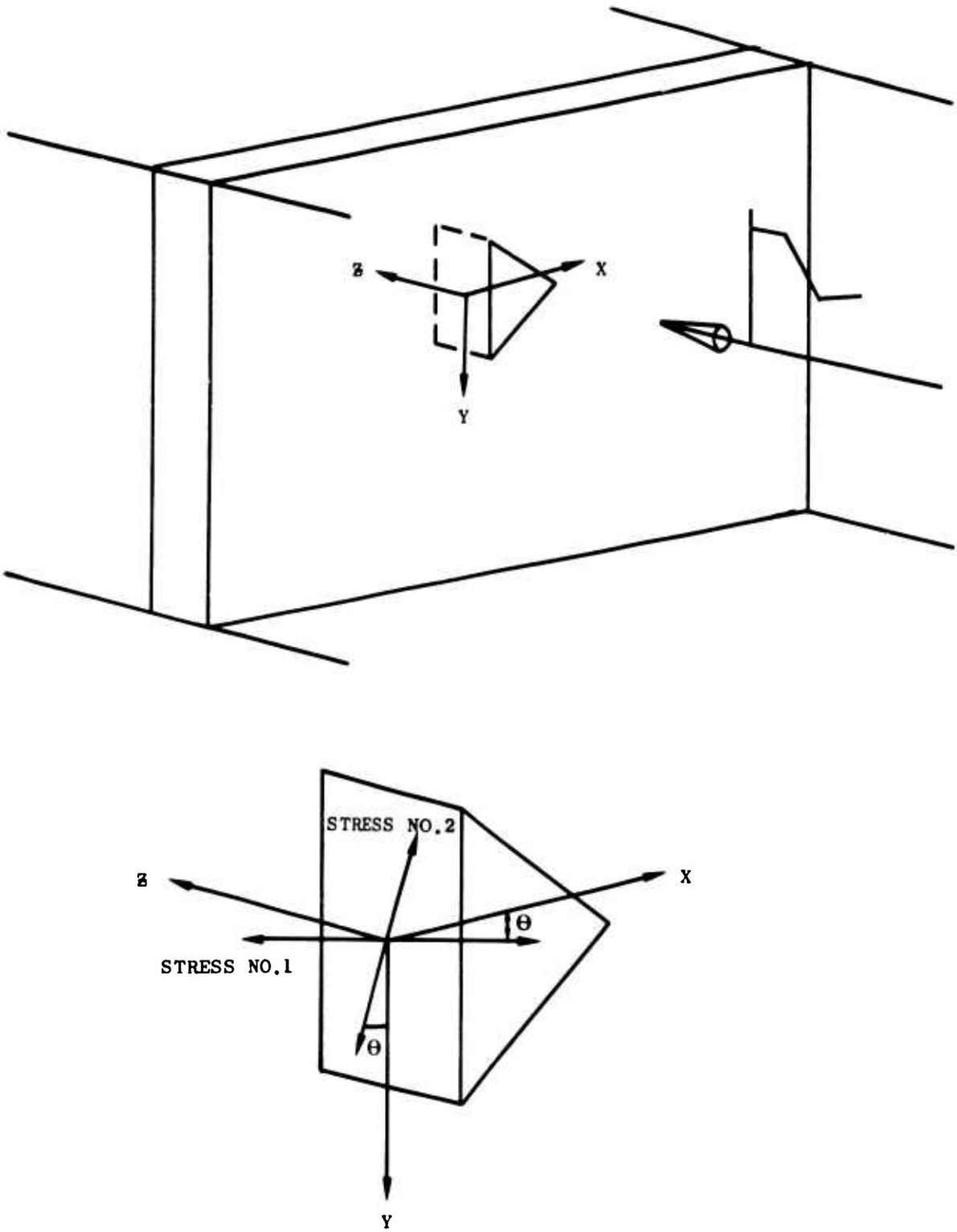

Fig. B-6. Element Coordinate System and Relation with Principal Stresses.

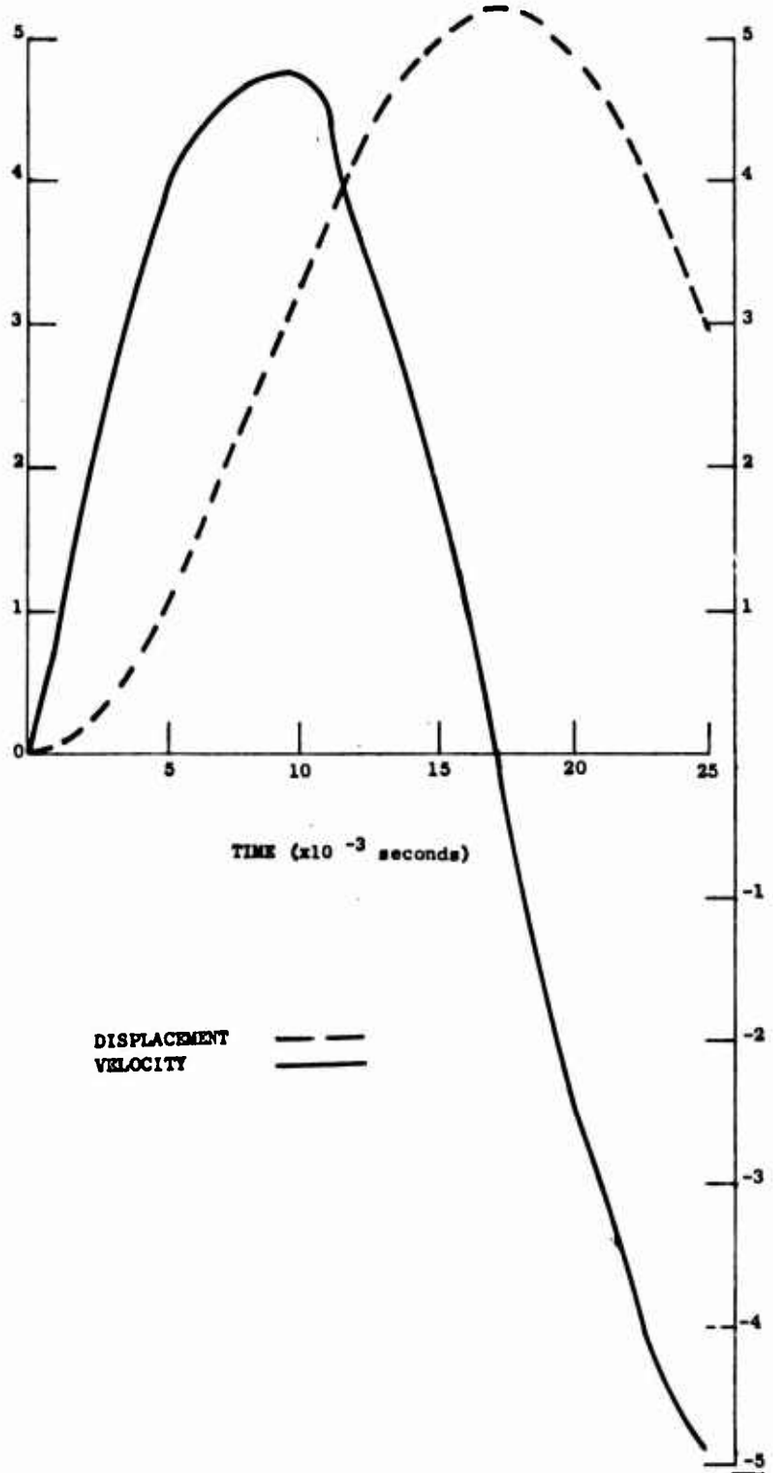

Fig. B-7. Displacement and Velocity vs Time for Node 360 on a Solid Wall Pinned Top and Bottom.

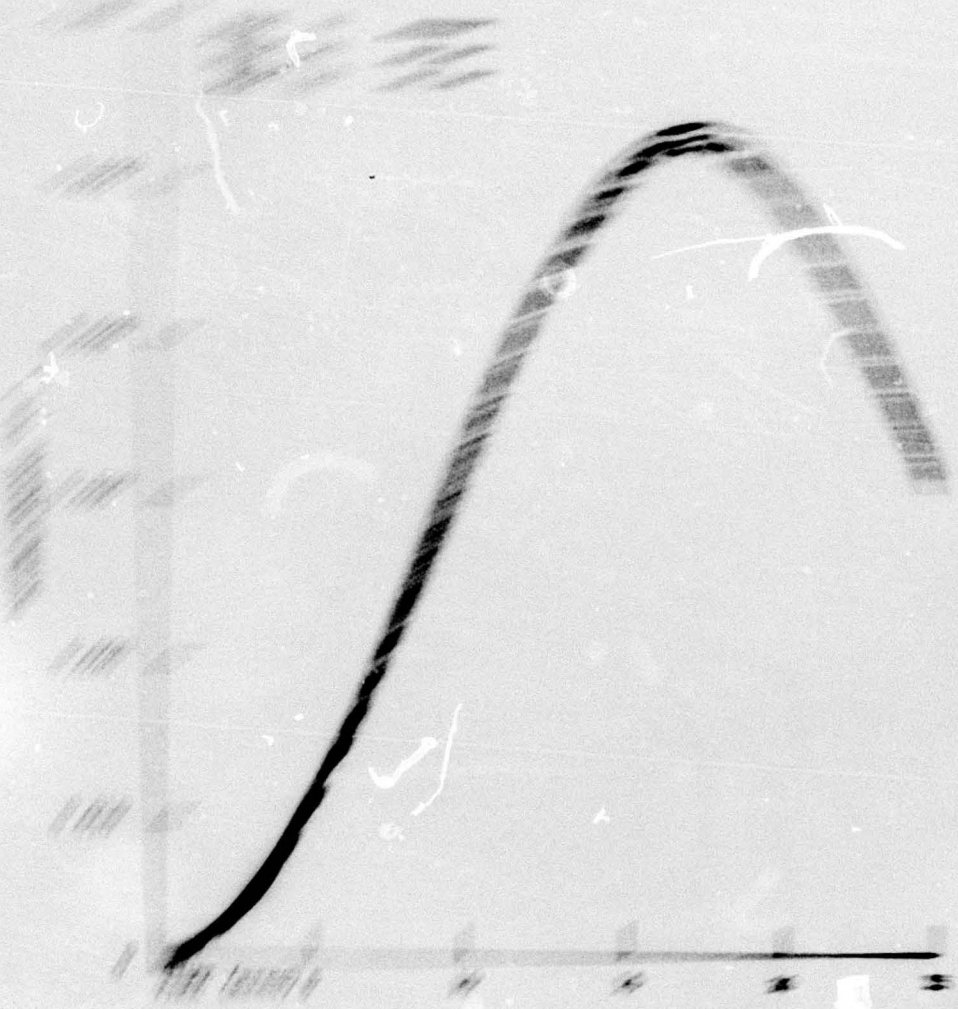

[illegible] vs Time for Nodes 10, 100 and 310 on a Solid Wall

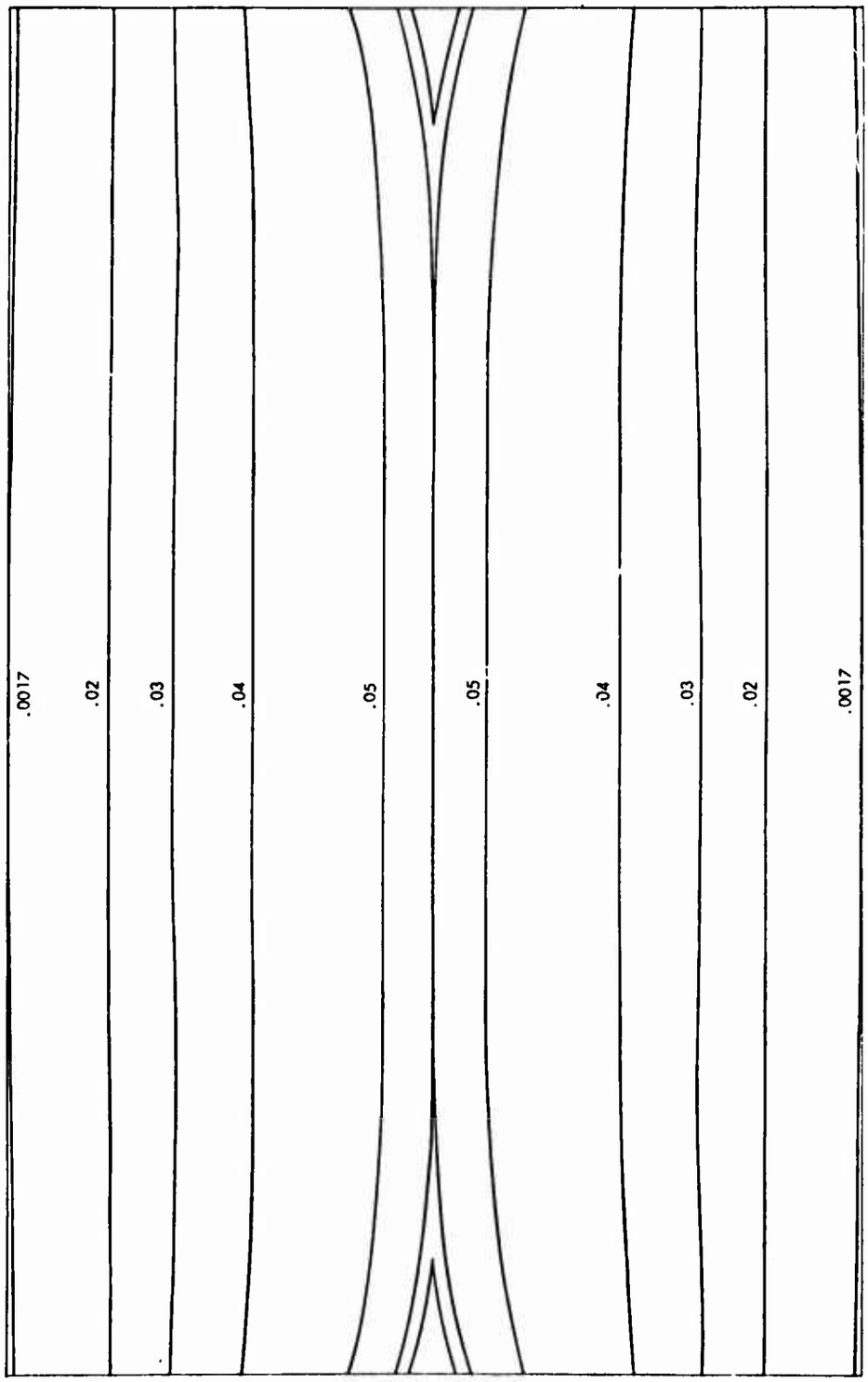

Fig. B-9. Contour Display of Maximum Deflection of Wall Surface at t = 17 msec.

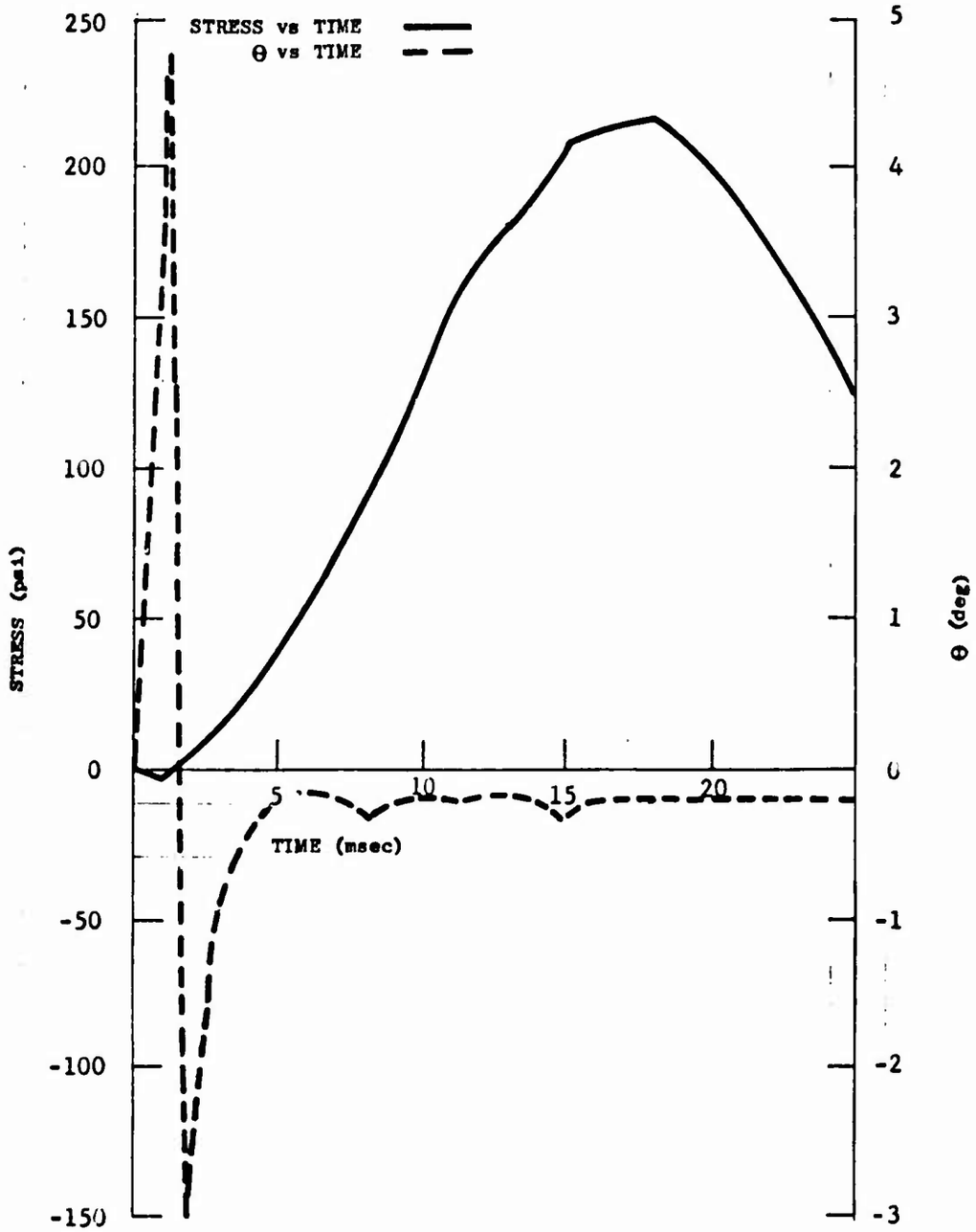

Fig. B-10. Stress and θ vs Time for Element No. 9 on a Solid Wall Pinned Top and Bottom

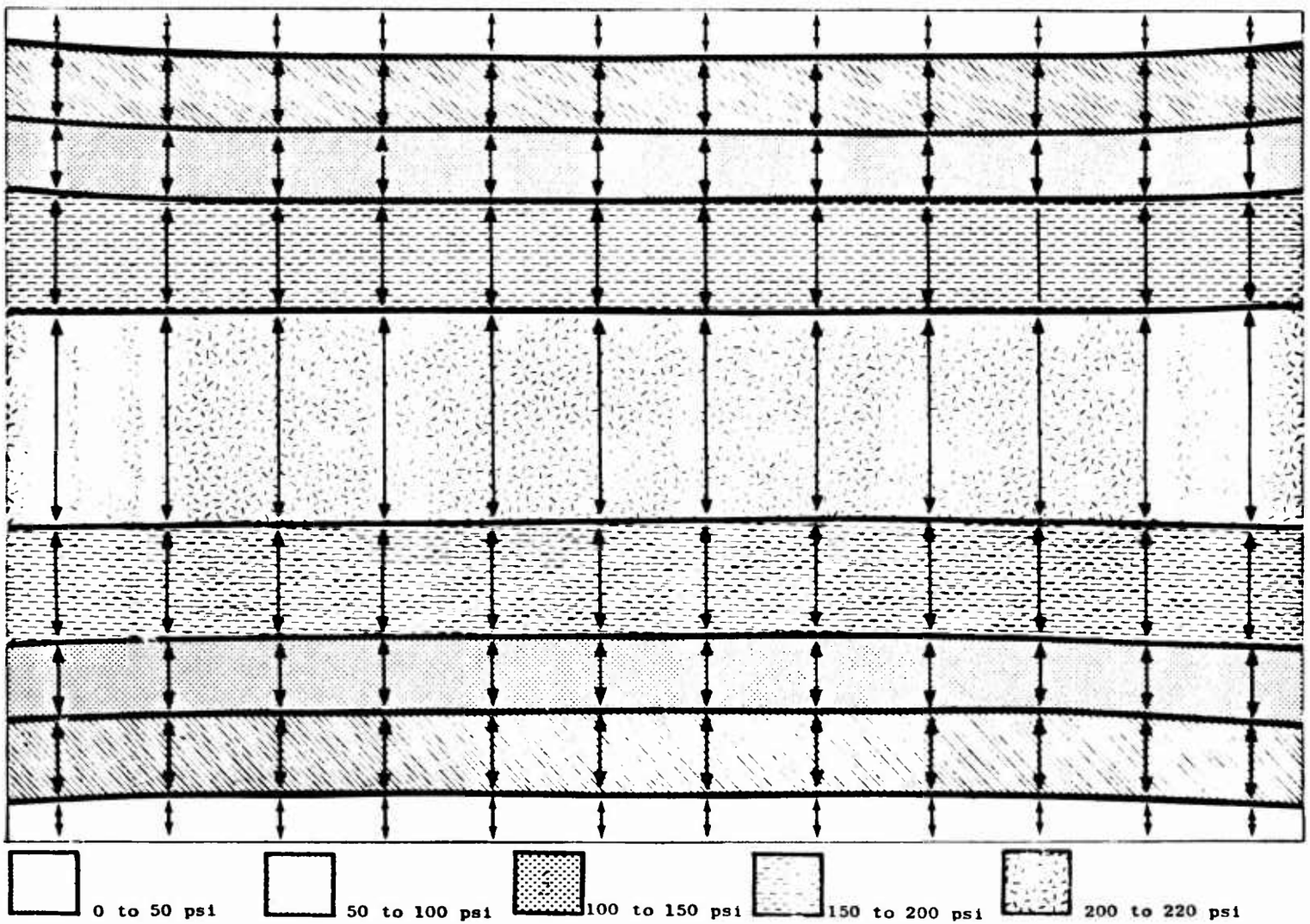

Fig. B-11. Stress Contours for Solid Wall (+ Z Face) Pinned Top and Bottom at 17 msec.

Fixed Top and Bottom

With moment resisting supports top and bottom, the velocity of the mode 360 is 1/2 of that for a simple support, and the deflection is about 1/4 that of a simply supported wall, for comparison see Figs. B-12 and B-7. Fixed supports also change the dynamic behavior by increasing the stiffness of the wall and shortening the vibration period considerably. From Fig. B-13, the solid wall has a period of 16 msec vs 35 msec for simple supports. This increased stiffness is evident in the peak deflection contours (Fig. B-14).

Figure B-15 is a stress history of an element at midspan. Peak stress is 66 psi at 8 msec. The computer predicts that wall failure will occur along the length at mid-height. The peak stress contours are given in Fig. B-16.

Pinned All Sides

With simple supports on the sides as well as top and bottom, the wall acts as a diaphragm; increasing its stiffness and decreasing the period over a simply supported wall. Figures B-17 and B-18 support this, particularly Figure B-18 which shows very small deflection for node 10 with increasing deflection of nodes toward the center of the wall. This diaphragm action is shown more clearly in the deflection contour map, Fig. B-19.

The stress and θ vs time history (Fig. B-20) is more complex with side supports. Fig. B-20 is not a typical stress history for elements on the center line as every element in a quarter panel will see different magnitudes and directions of stress. Figure B-21 reveals the stress contours at 12 msec. From this we would predict a crack propagating 4 ft long at mid-height and then continuing at approximately 45° to each corner. Figure B-22A and B are photographs of a test wall verifying the crack propagation indicated by stresses from the computer code SAMIS.

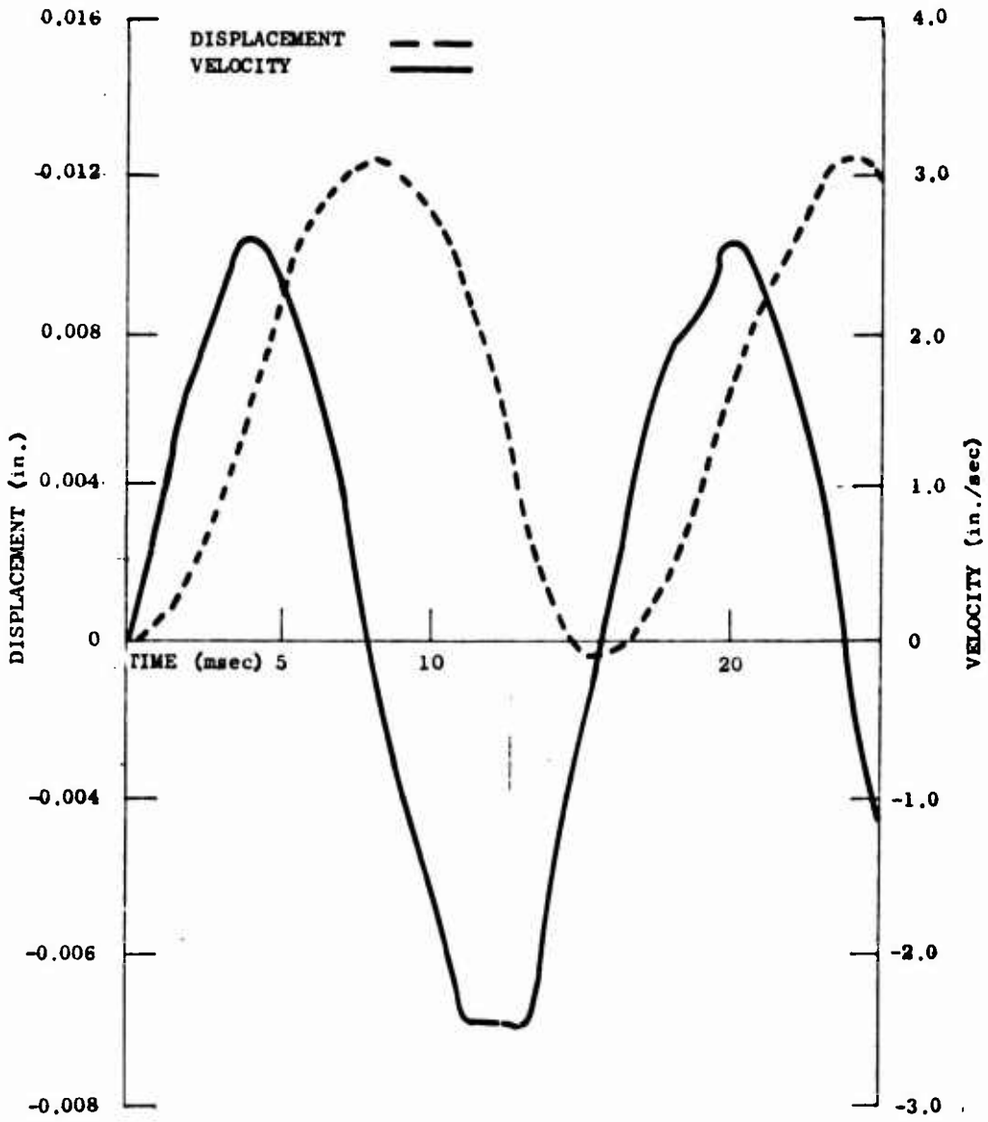

Fig. B-12. Velocity and Deflection vs Time for Node 360 with Fixed Supports Top and Bottom of Wall

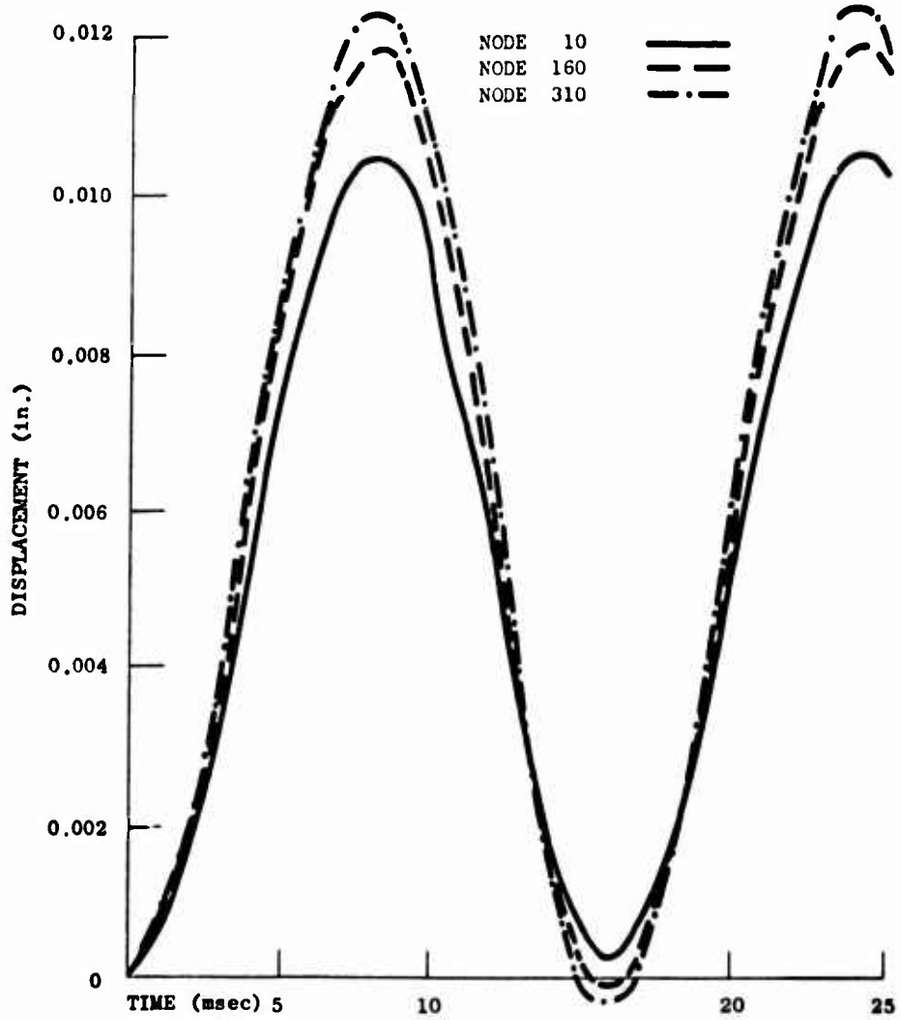

Fig. B-13. Deflection vs Time for Nodes 10, 160 and 310 with Fixed Supports Top and Bottom

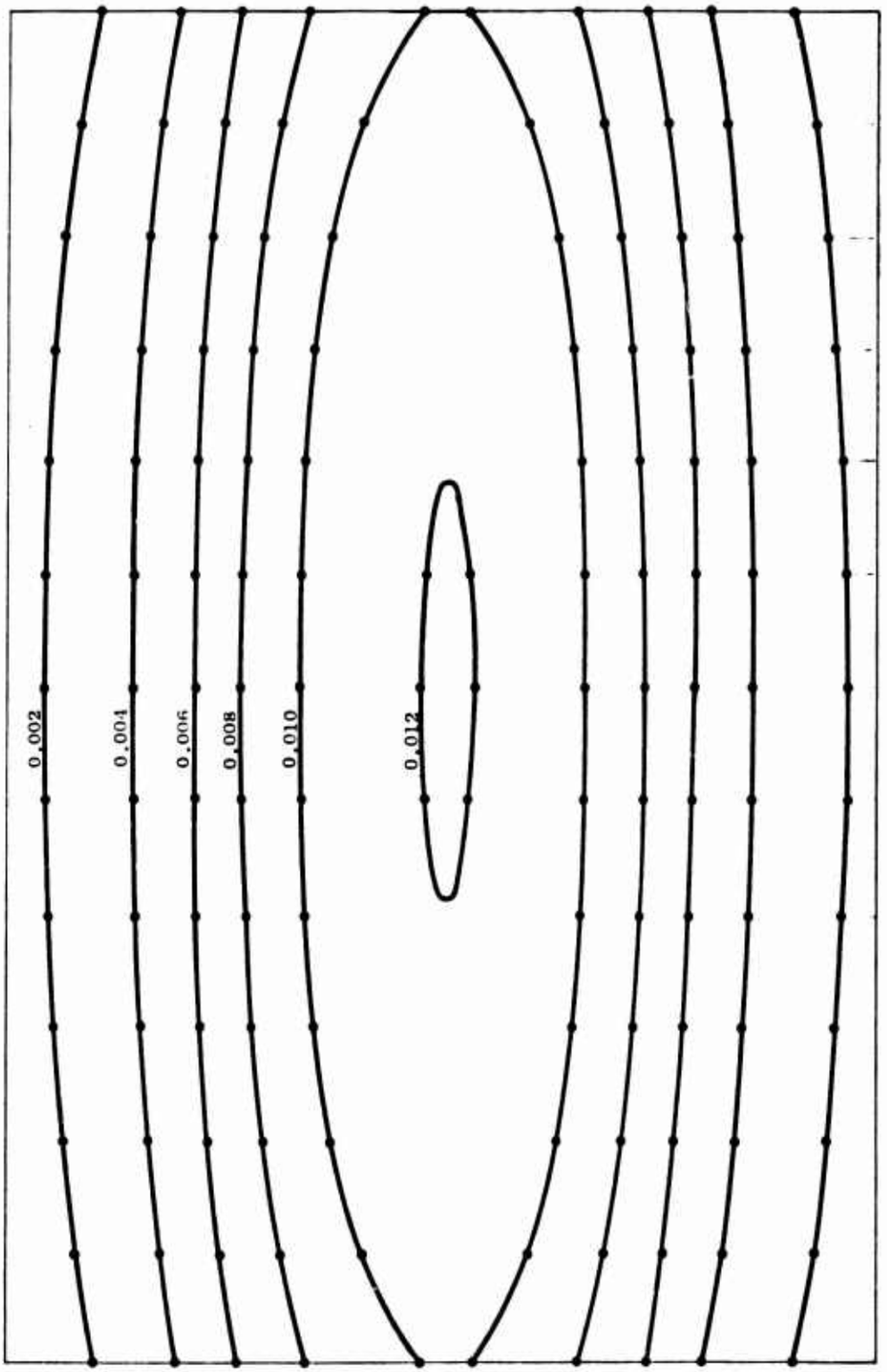

Fig. B-14. Deflection Contours (in.) for Time = 0.008 seconds with Fixed Supports Top and Bottom

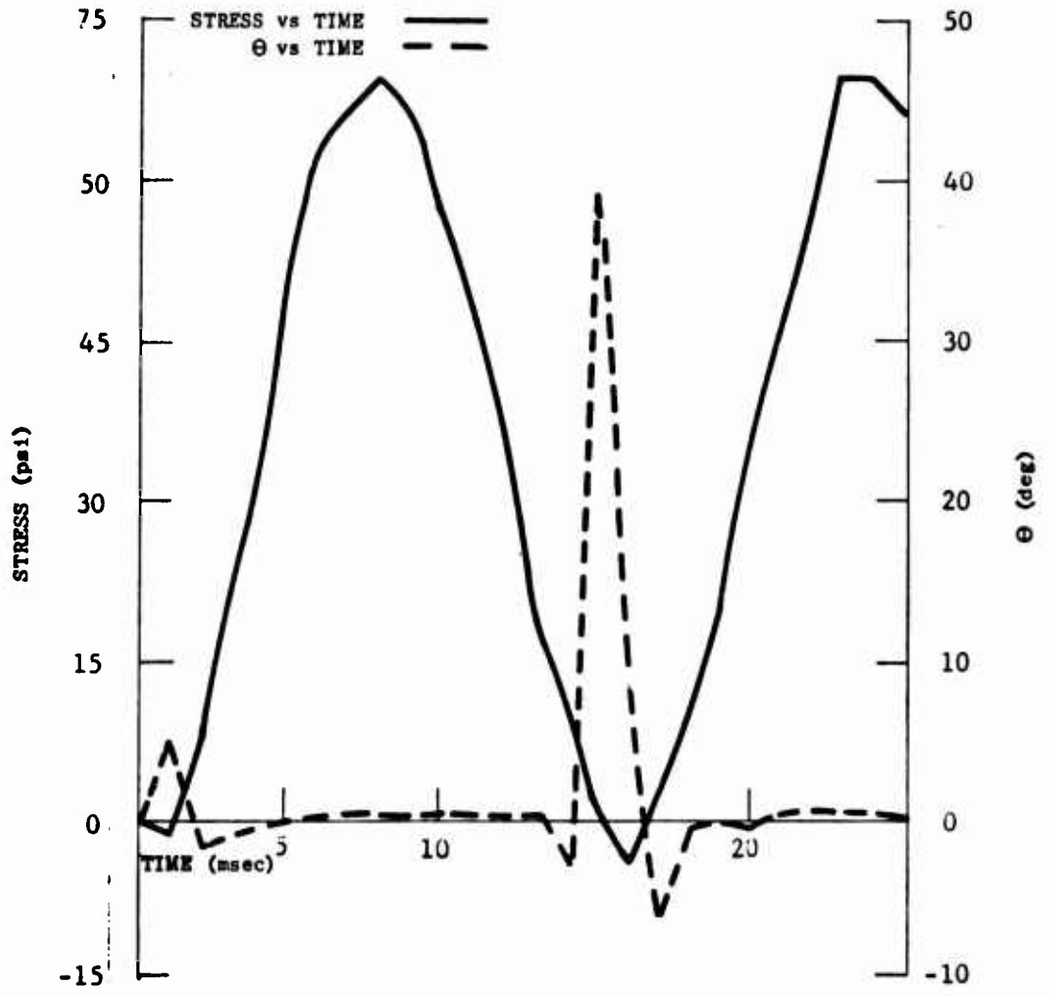

Fig. B-15. Stress and Θ vs Time for Element No. 9 with Fixed Supports-Top and Bottom

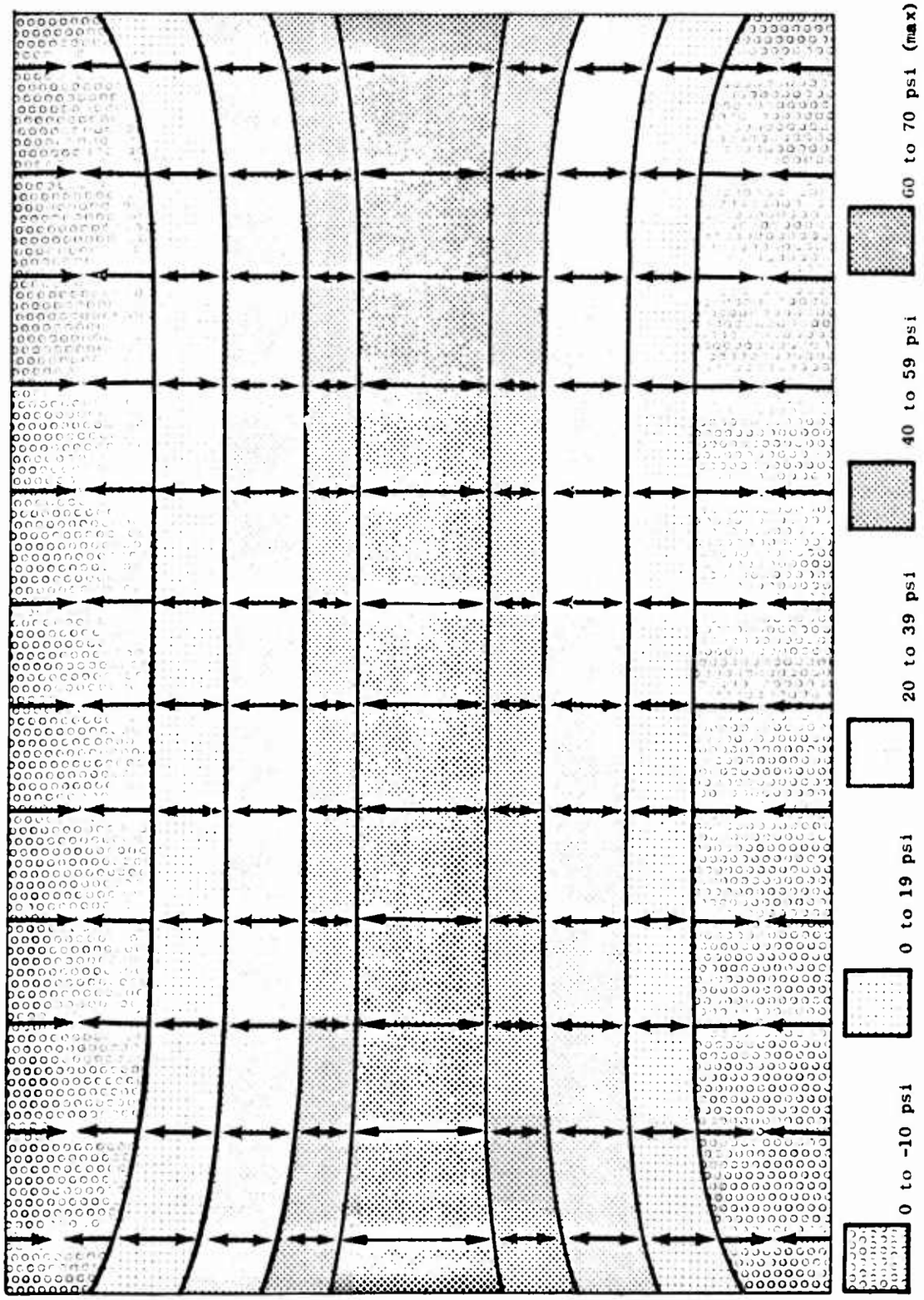

Fig. B-16. Stress Contours for Time = 0.008 seconds for Downstream (+Z) Face with Fixed Supports Top and Bottom

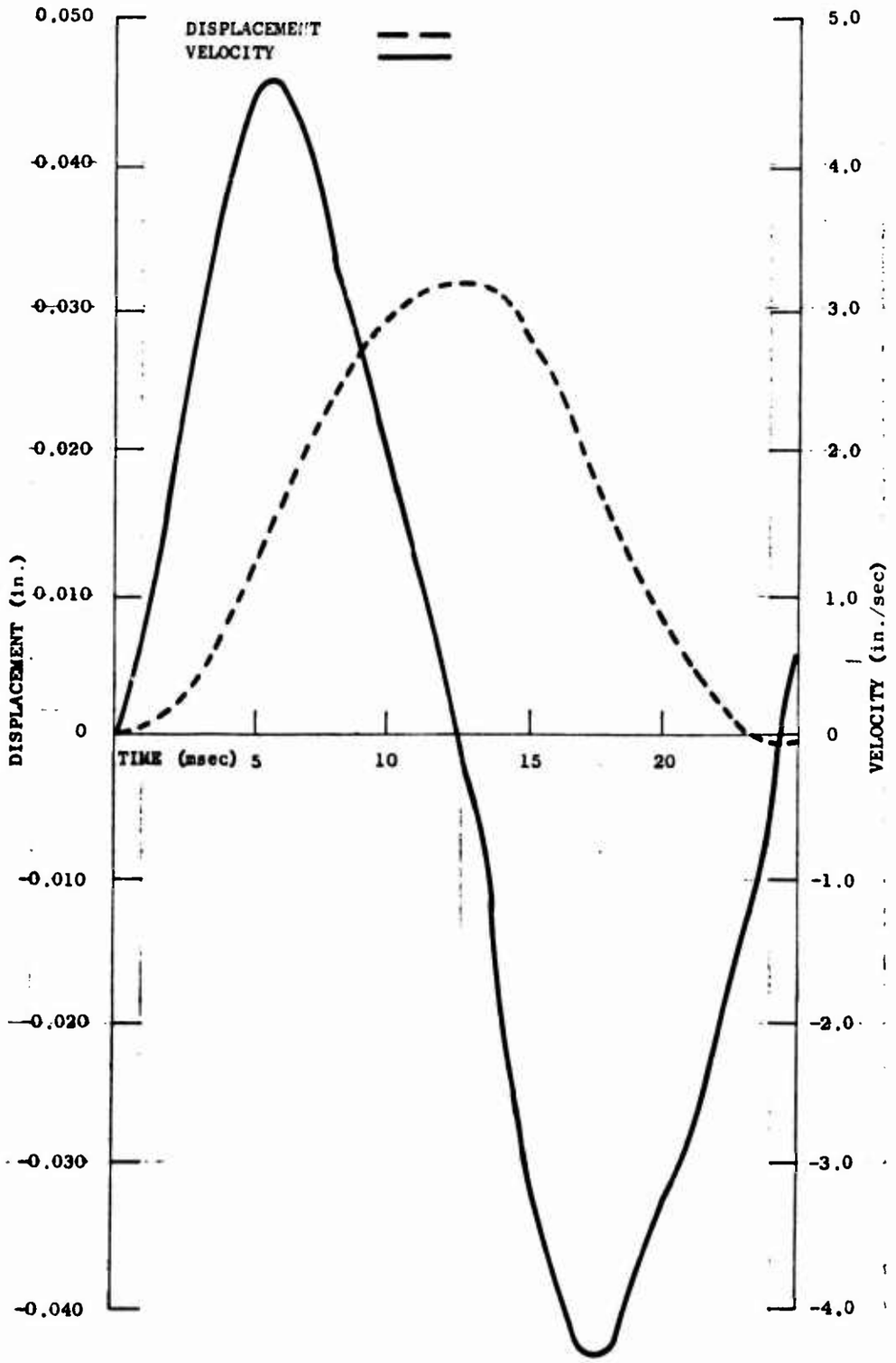

Fig. B-17. Displacement and Velocity vs Time for Node 360 on a Solid Wall with Pinned Supports on all sides

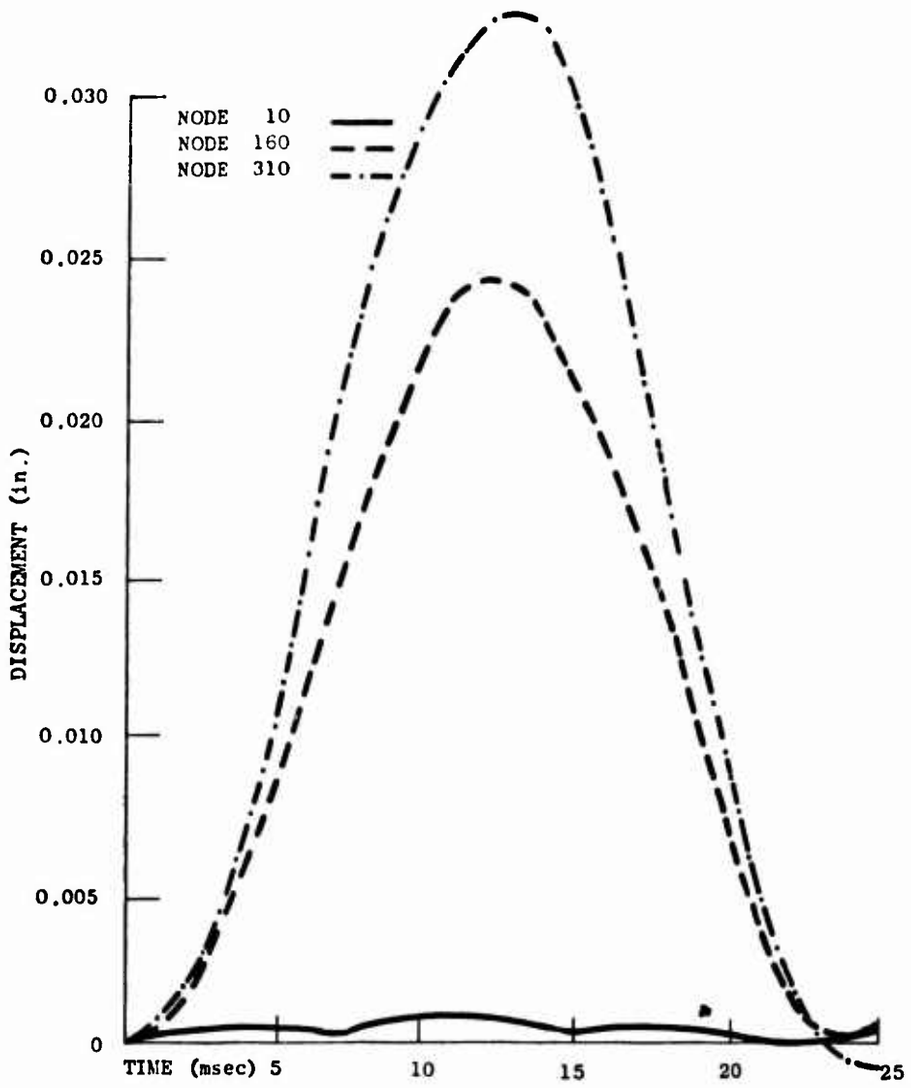

Fig. B-18. Deflection vs Time for Nodes 10, 160 and 310 with Pinned Supports All Sides

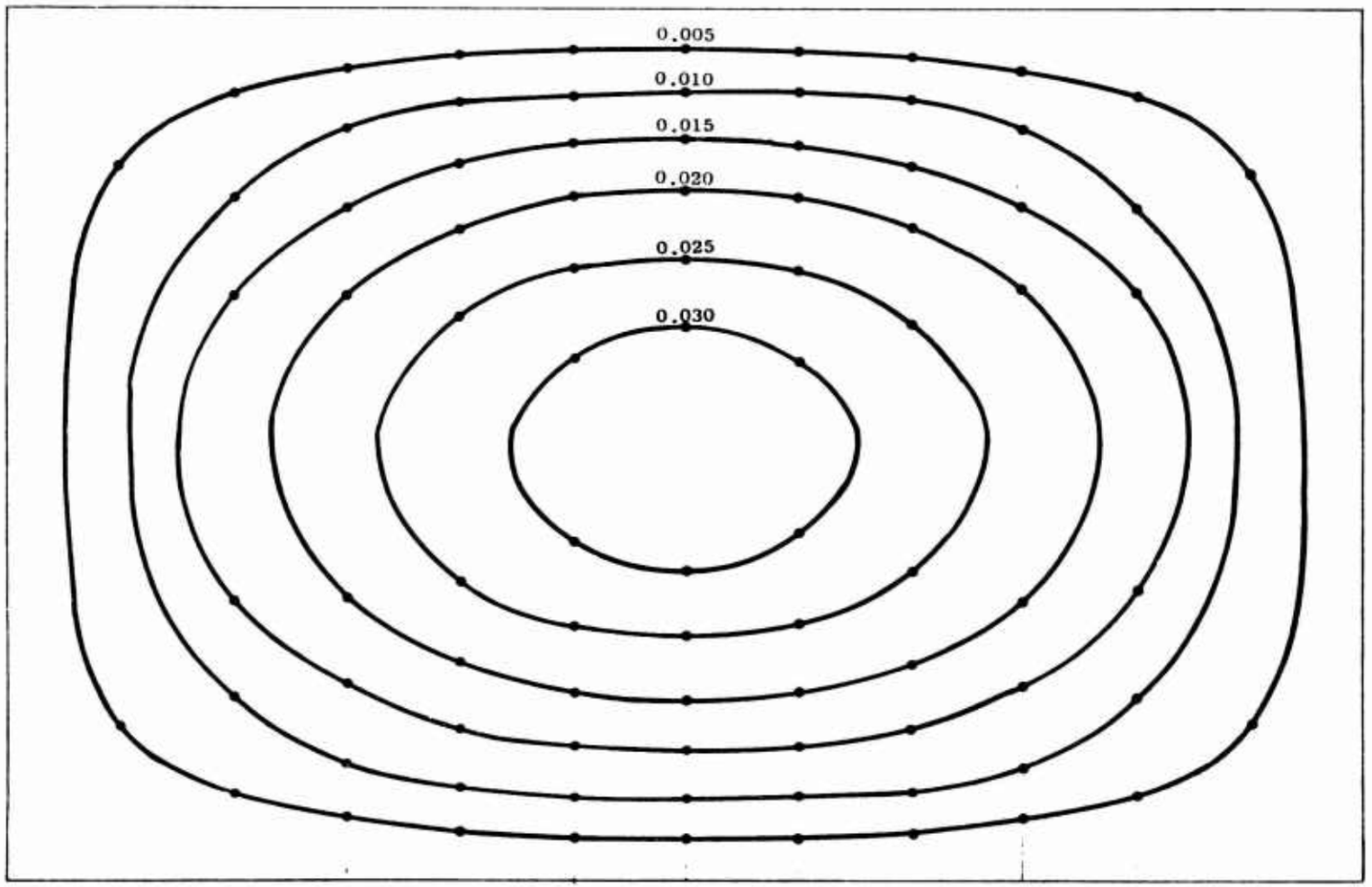

Fig. B-19. Deflection Contours (in.) for Time = 0.012 seconds with Pinned Supports on All Sides

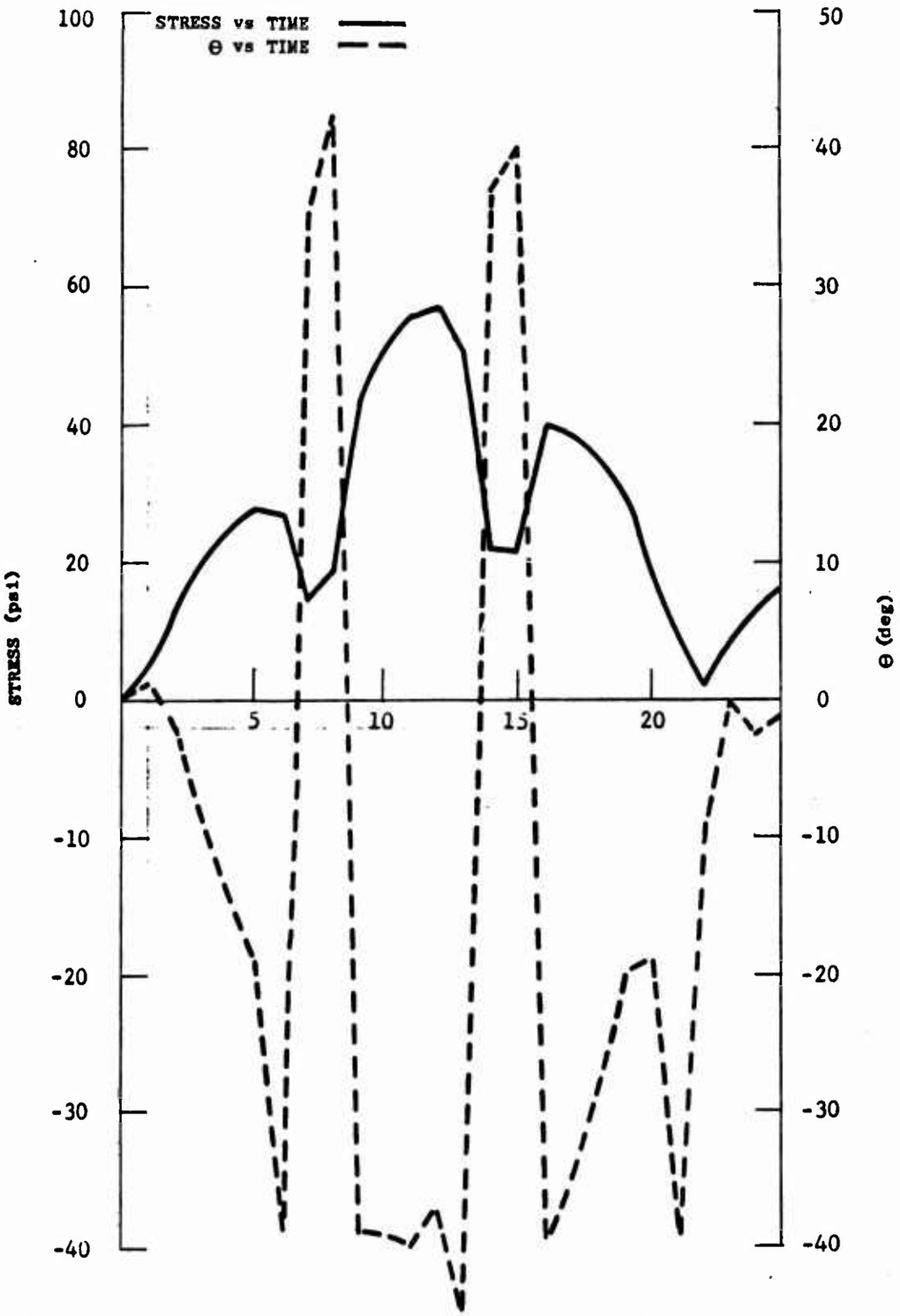

Fig. B-20. Stress and θ vs Time for Element No. 9 with Pinned Supports on All Sides

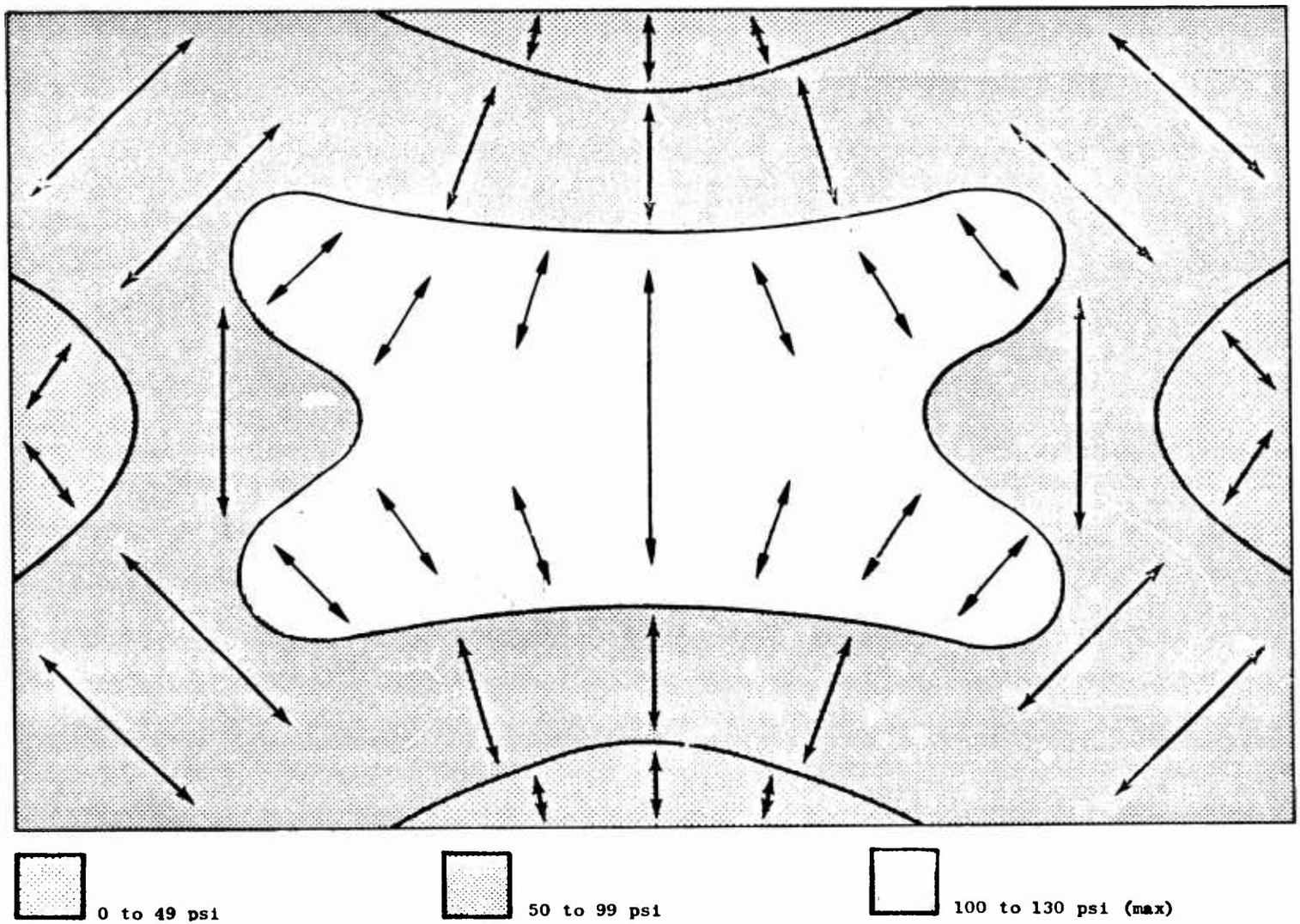

Fig. B-21. Shear Contours for Time = 0.012 sec for Downstream (+Z) Face with Pinned Support.

Fig. B-22A. Test Wall No. 24 Downstream Face Simply Supported All Sides

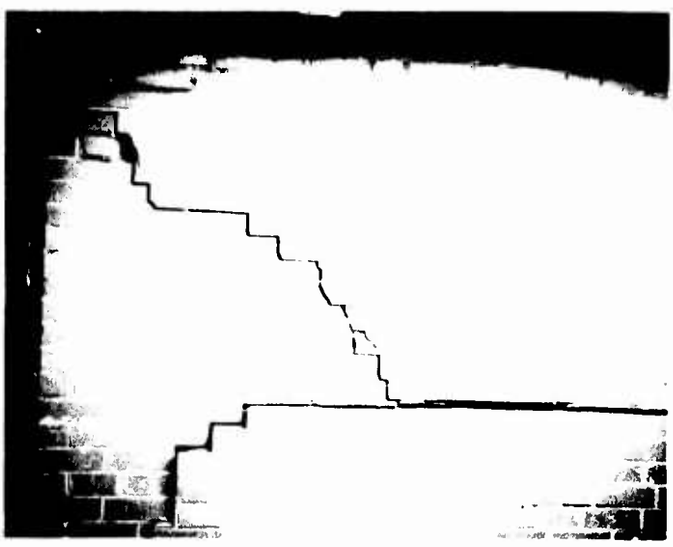

Fig. B-22B. Close-up of Cracking Towards Corners for Test Wall No. 24

Fixed All Sides

Moment resisting supports all around decreases the period to 14 msec (Fig. B-23) and maximum deflection to 0.014 in. compared to pinned all around. Figure B-24 shows the effect of diaphragm action on the deflection nodes 10, 160, and 310. Figure B-25 gives a overall view of nodal deflection with deflections between nodes linearly interpolated. With supports on all sides, a blast load will deform a solid wall into a "dish."

The stress and θ vs time history for element No. 9, Fig. B-26, has sharp jagged lines showing the influence of higher periods of vibration. Figure B-27, the stress contour at 8 msec shows the compression zones near the supports. On the upstream face, the tensile stresses are about 49 psi. Crack propagation theory for this case would predict a failure similar to that for a wall pinned all around; except that at about 1 ft from the corners the wall would fracture on a line perpendicular to the 45^{o} crack line from the center line.

WALL WITH A DOORWAY

The dimensions used for the wall with a doorway were 8 ft x 12 ft x 8 in. with a 3 ft x 8 ft doorway 1 ft from the right side of the downstream (tz) face. This represents a 25 percent opening. With the doorway, the wall is not symmetrical about the y-axis as for a solid wall, so SAMIS determined the displacement, velocity and acceleration for every nodal point above the x-axis of the wall. The structural model, Fig. B-28 for the doorway is similar to that for the solid wall except three ft of wall was blanked out in the computer. Blast loading for the wall is shown in Fig. B-1. Computations were performed for the first 25 msec of load duration. Since the resulting deflections and stresses are normalized for a one psi load, the deflections and stresses for any reflected measure can be obtained by multiplying these results by the actual reflected pressure.

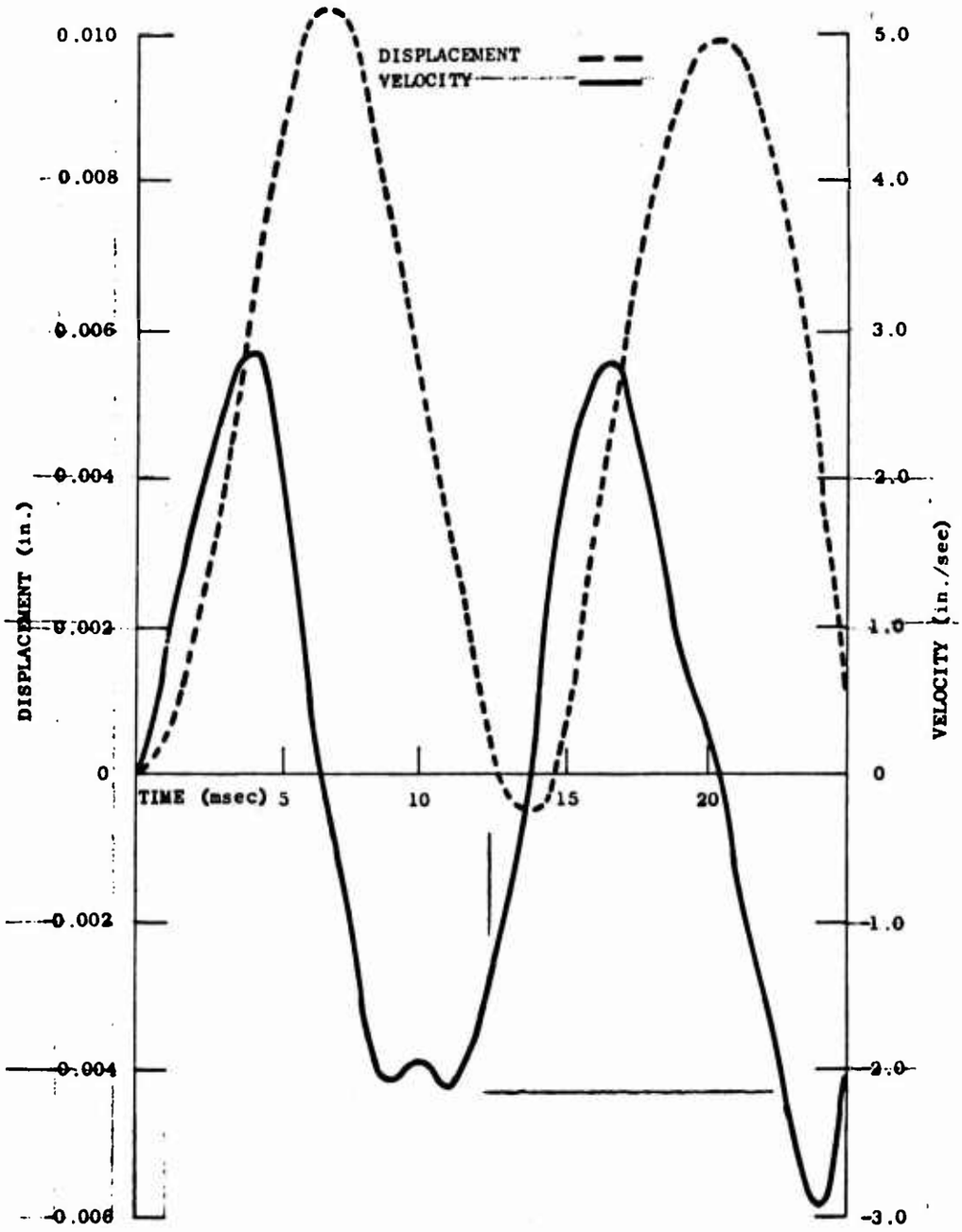

Fig. B-23. Velocity and Deflection vs Time for Node 360 with Fixed Supports on All Sides

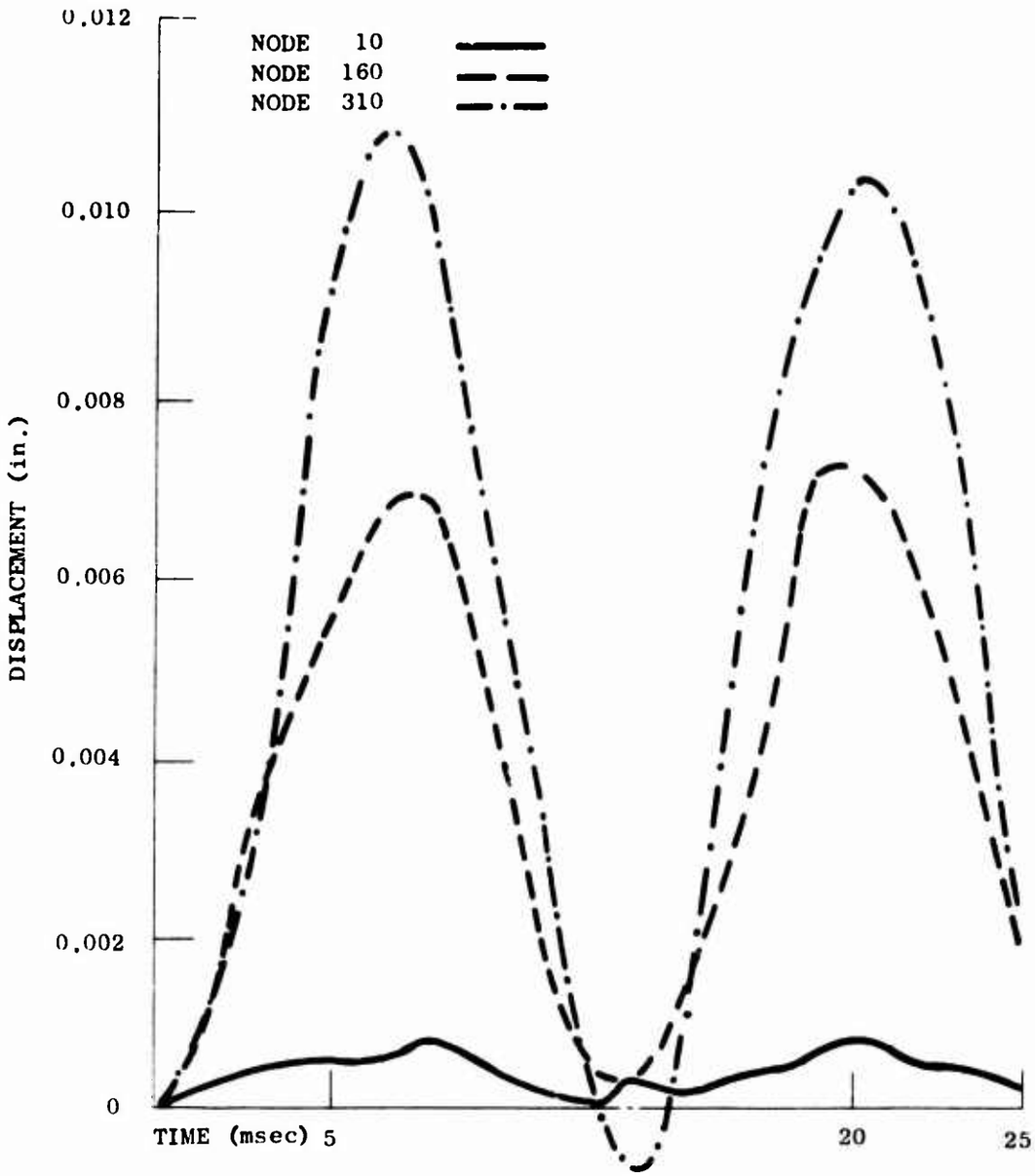

Fig. B-24. Deflection vs Time for Nodes 10, 160 and 310 with Fixed Supports All Sides

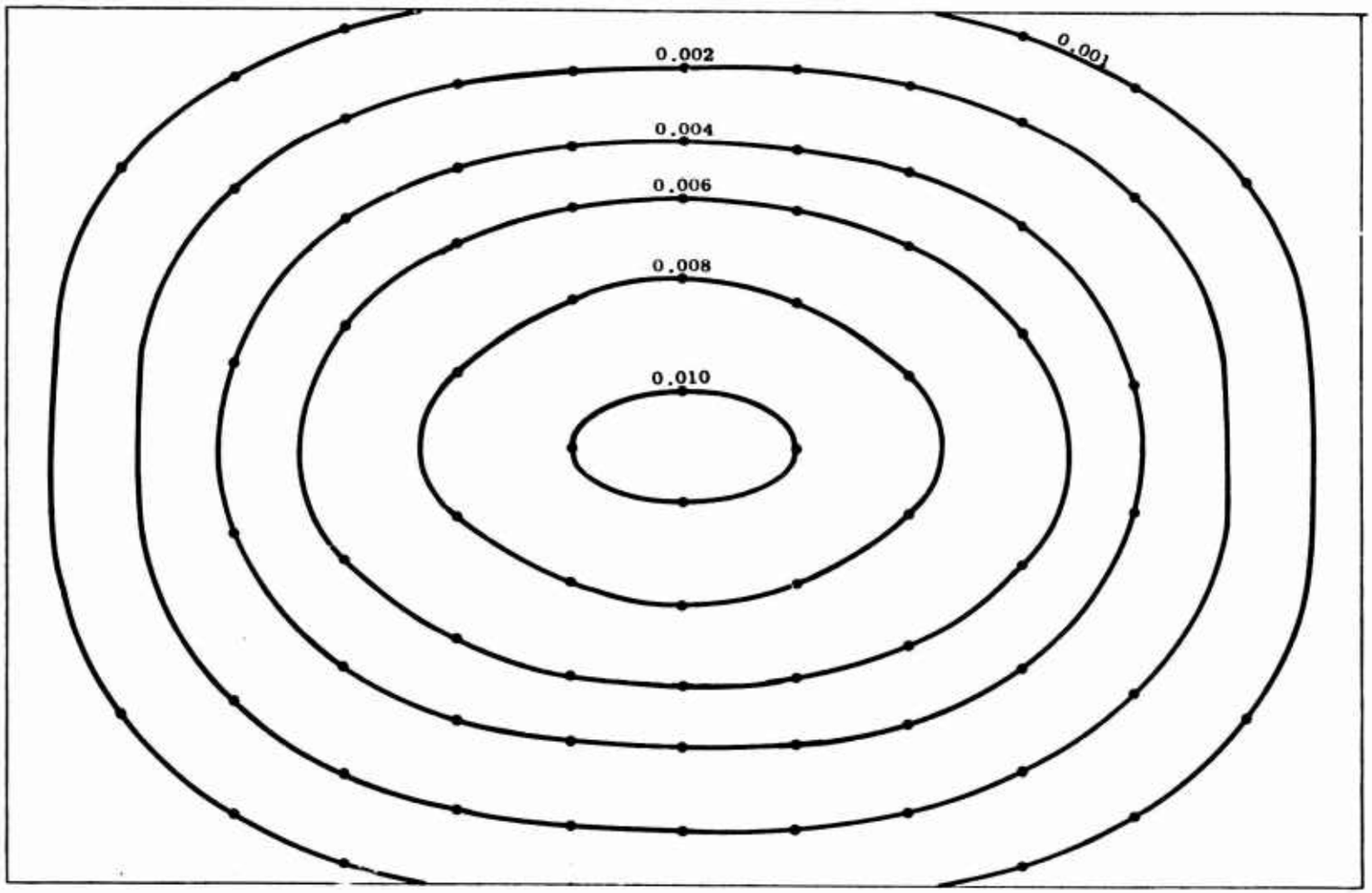

Fig. B-25. Deflection Contours (in.) for Time = 0.007 seconds with Fixed Supports on All Sides

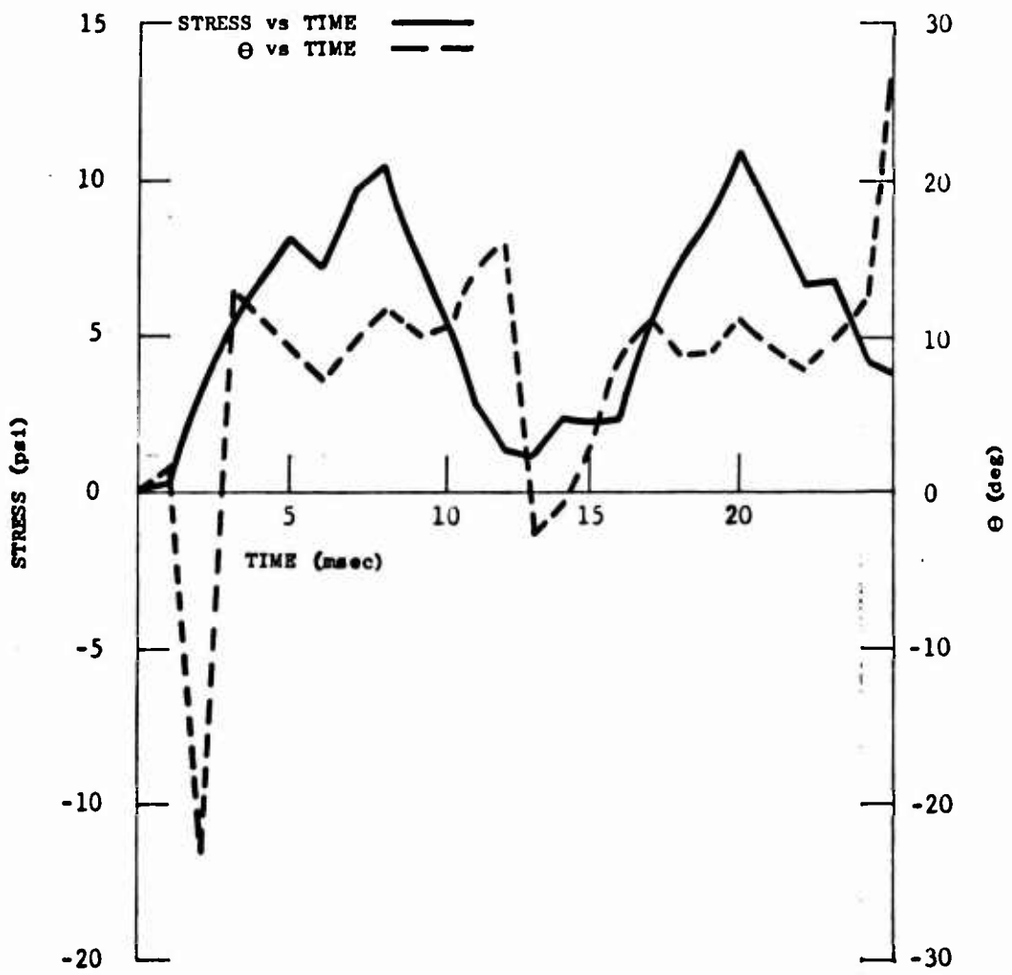

Fig. B-26. Stress and Θ vs Time for Element No. 9 with Fixed Supports on All Sides

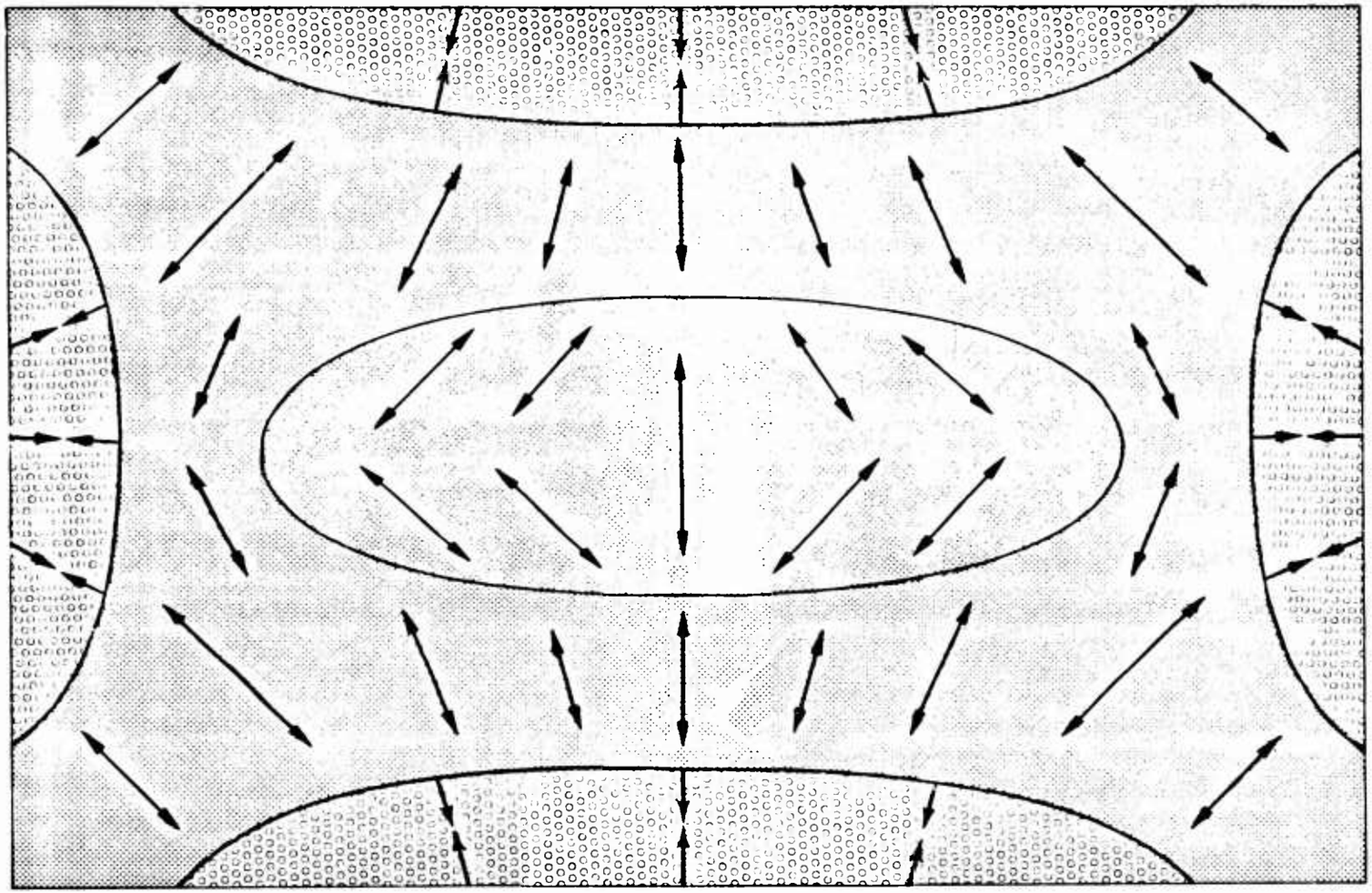

Fig. B-27. Stress Contours for a Solid Wall Fixed on All Sides at 8 msec.

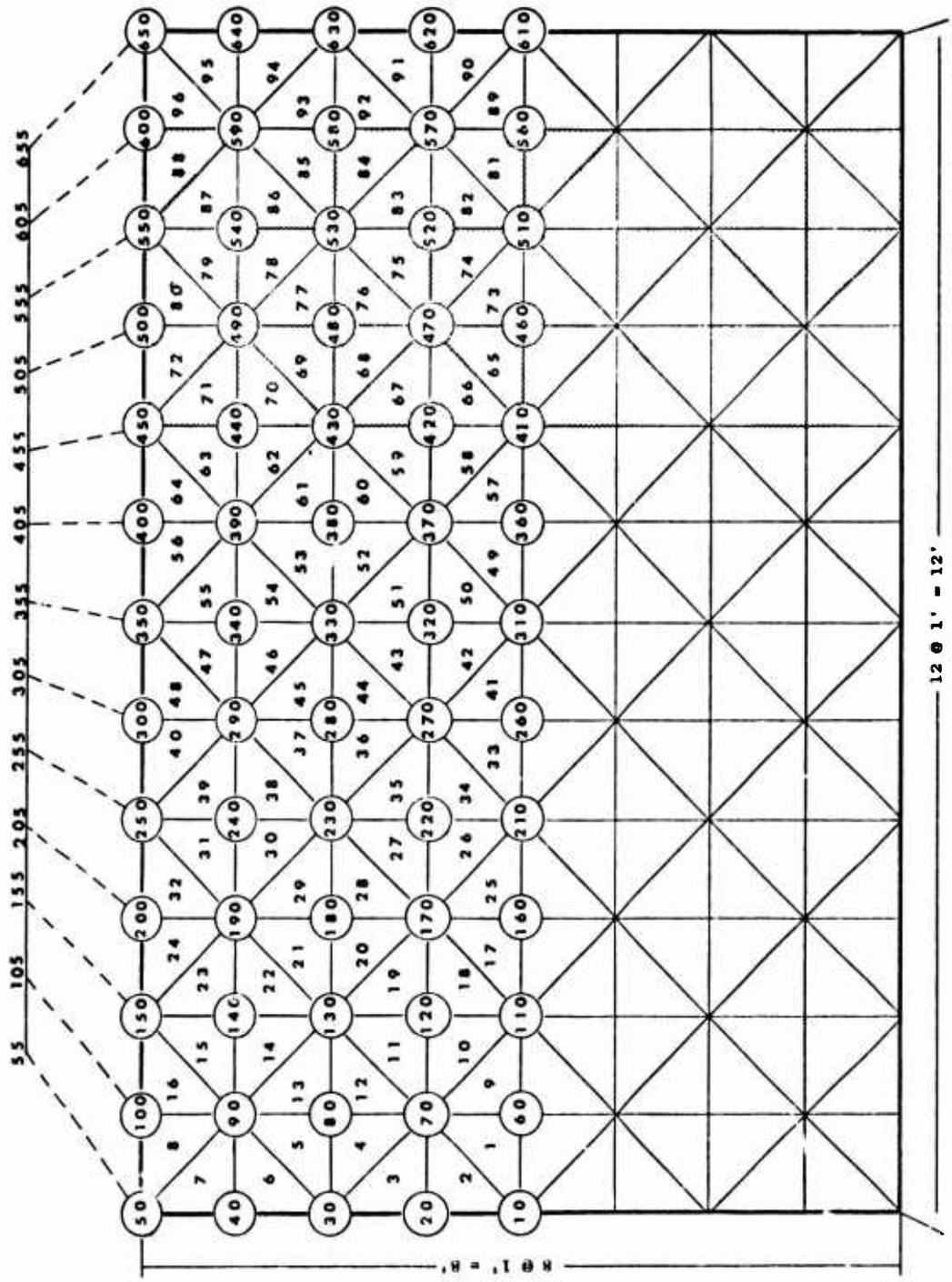

Fig. B-28. Node and Element Grid for Wall with a Doorway

Figure B-6 shows the coordinate axis for each element and how the principal stresses are located from the x and y axis. The angle shown is positive. For the stress contour maps, only the maximum tensile stress is shown except for compression fields, then the maximum compressive stress is shown. Other sign conventions are t for tensile stresses and - for compressive. Deflections are positive in the +Z direction. All graphs and contours are for stresses on and deflections of the +Z (downstream) wall surface.

Pinned Top and Bottom

Figure B-29 is a comparison of the displacements of nodes 10, 210, and 410 over 25 msec of load for a simply supported wall. When extrapolated the graphs on Fig. B-29 indicate an approximate period of 30 msec. Interpolation between displacements of nodal points will reveal a deflection contour map, Fig. B-30, at 17 msec. Figure B-31 is the stress history of element No. 9 located at mid-height. And Fig. B-32 shows the variation of stresses from supports to the center of the wall. From these two figures, and for the minimum failure pressure, the wall will fail at 12 msec across the length at mid-height where the maximum tensile stresses occur.

Fixed Top and Bottom

A comparison of Figs. B-29 and B-33 show that moment resisting supports greatly improve the wall stiffness by decreasing the period from 30 msec to 15 msec and peak deflections from 0.039 in. to 0.011 in. Figure B-34 shows how the doorway opening relieves the blast load on the wall near the openings, but still has full effect on the left side away from the door.

The stress and Θ vs time graph in Fig. B-35 is the history of an element where peak deflections occurred. The stress contour at 0.007 seconds is seen in Fig. B-36. From this and Fig. B-34 we would predict a failure node of cracking starting from the left side at mid-height and propagating to the doorway opening.

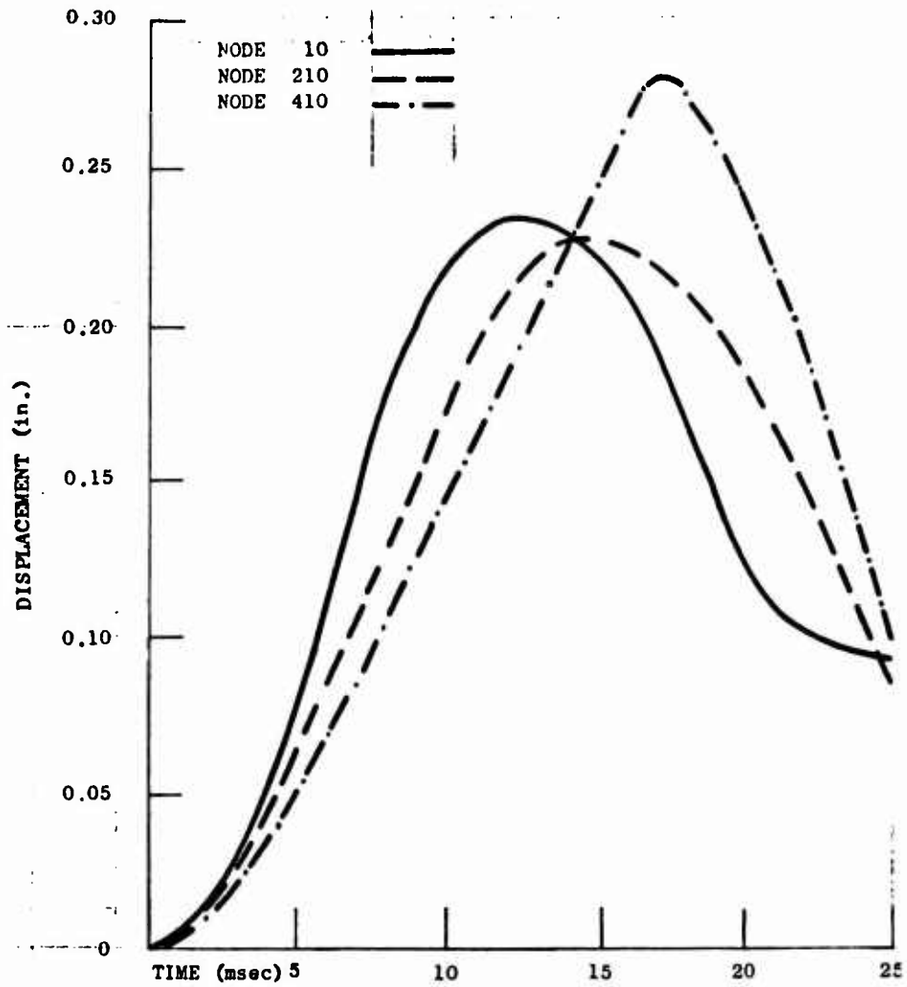

Fig. B-29. Deflection vs Time for Nodes 10, 210 and 410 with Pinned Supports Top and Bottom of Wall

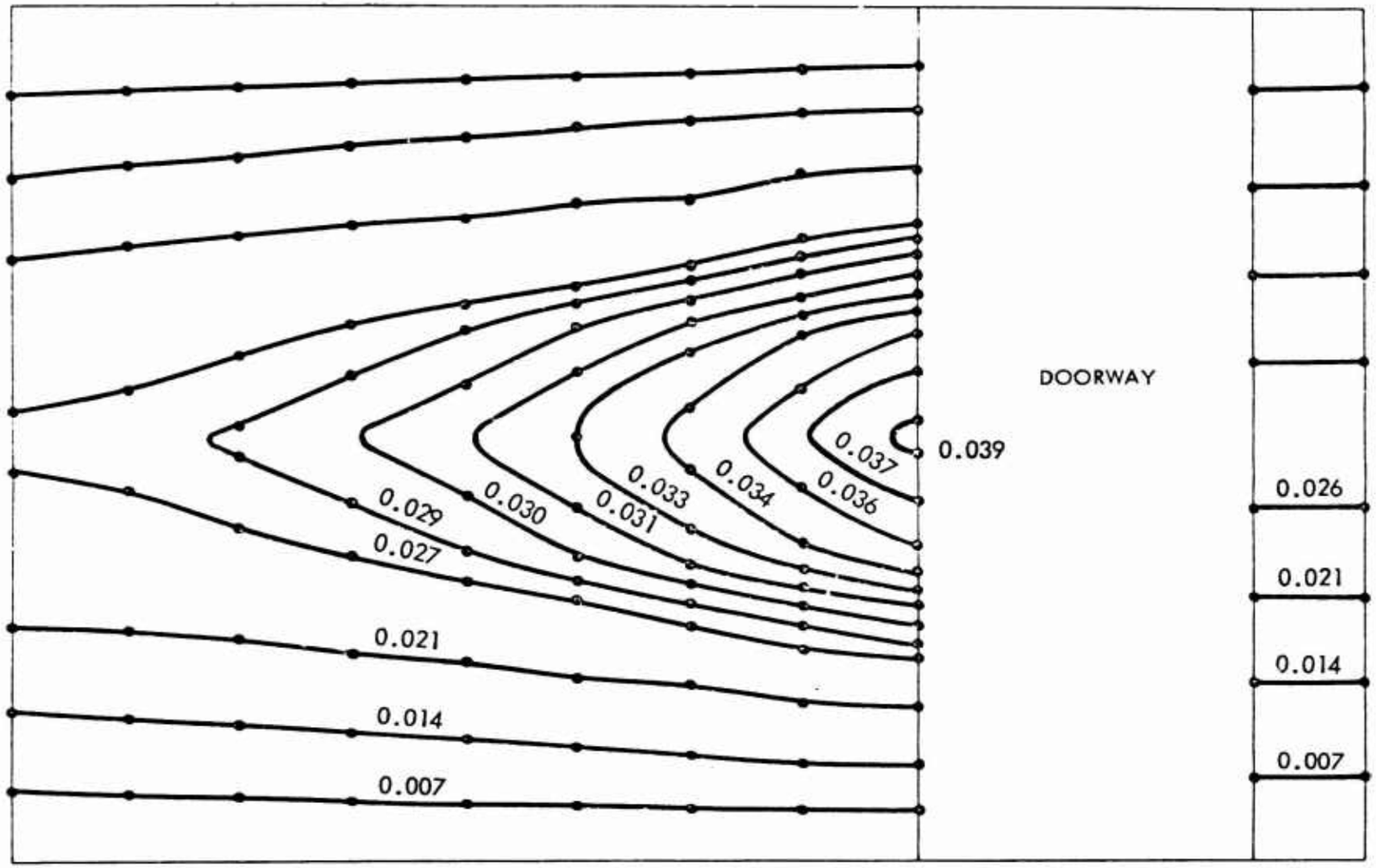

Fig. B-30. Wall With Doorway Deflection Contour (in.) at 17 msec, Normalized to 1 psi Loading

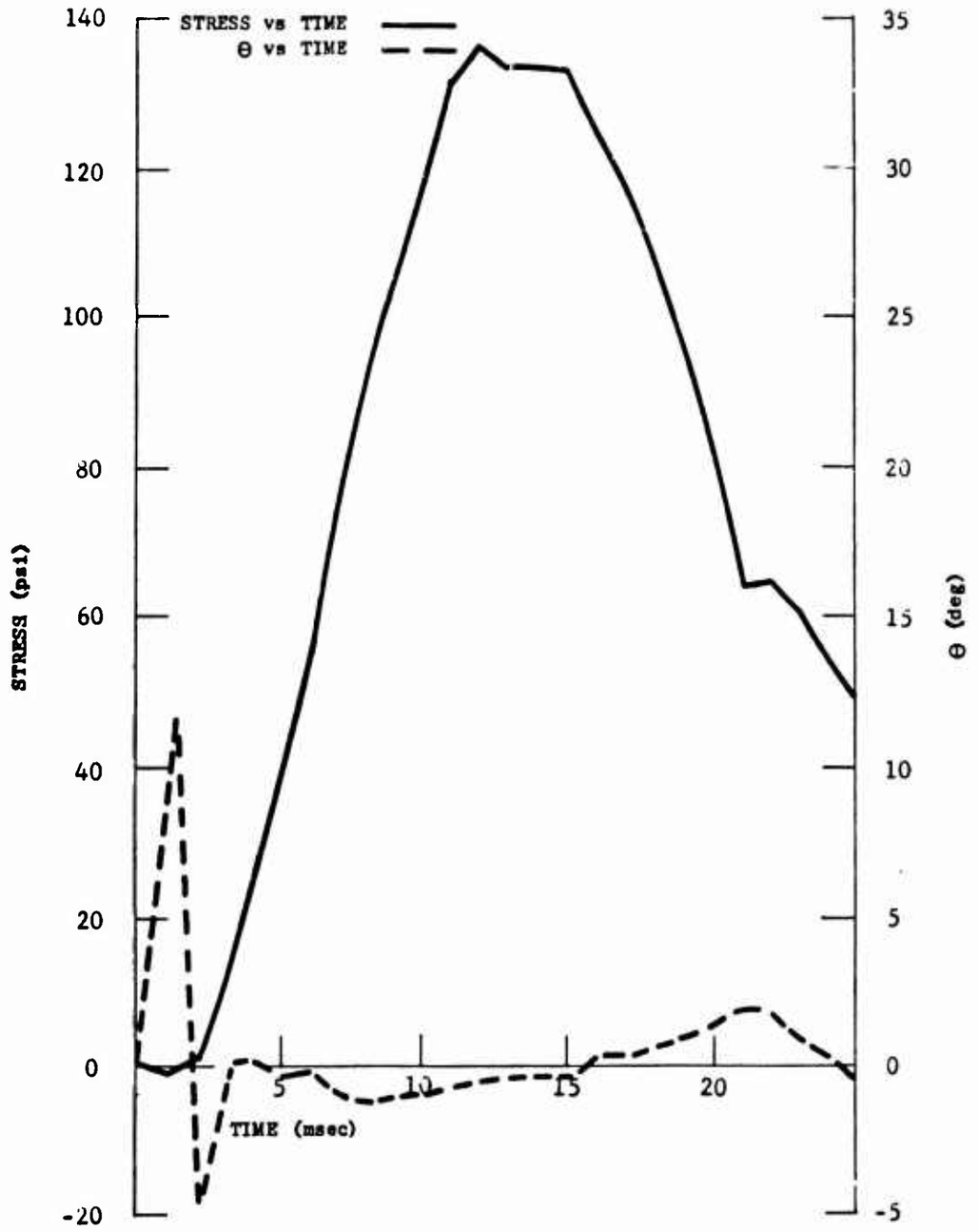

Fig. B-31. Stress and θ vs Time for Element No. 9 with Pinned Supports Top and Bottom

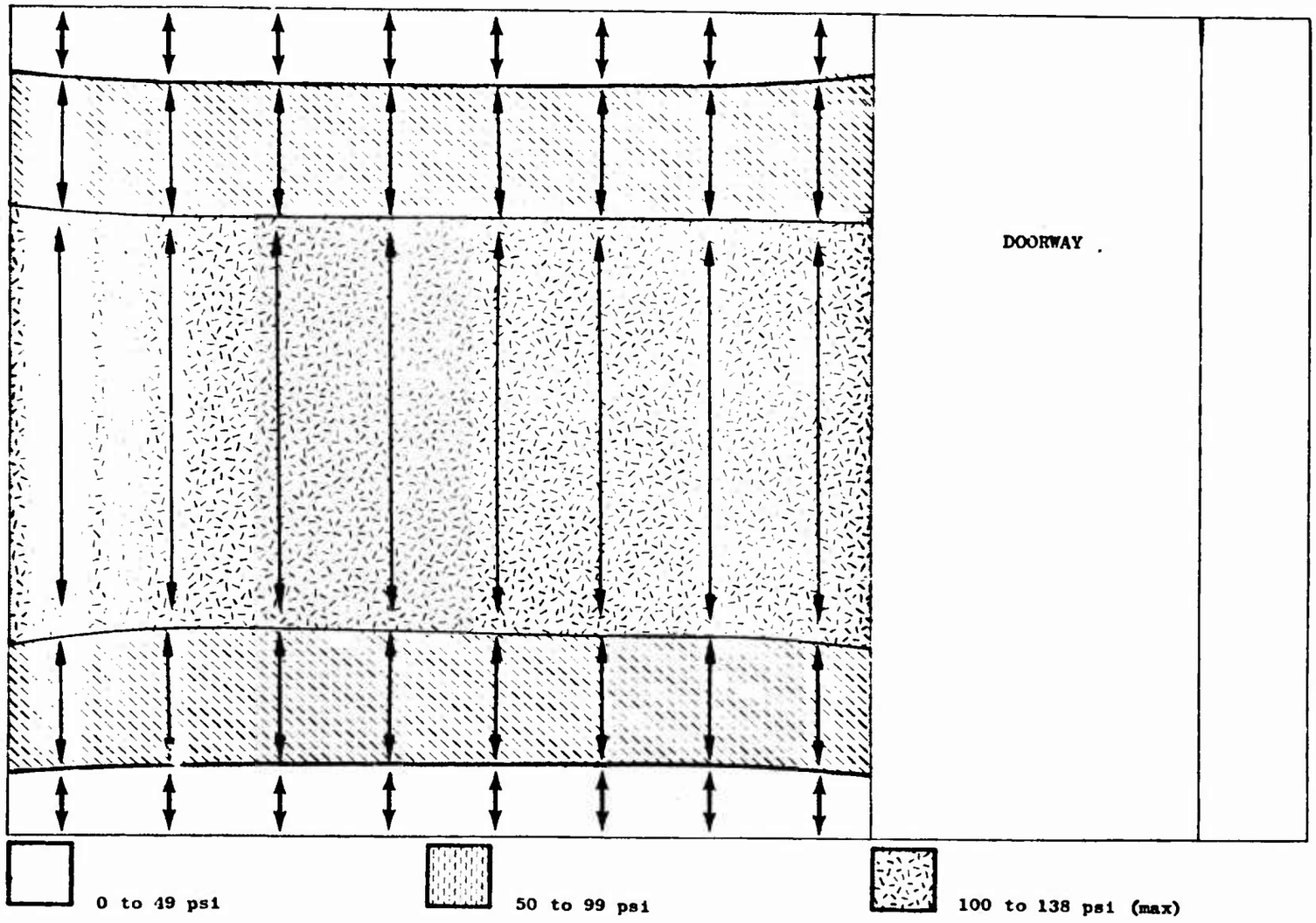

Fig. B-32. Stress Contours for a Wall With Doorway Pinned Top and Bottom at time = .017 sec on the (+Z) face.

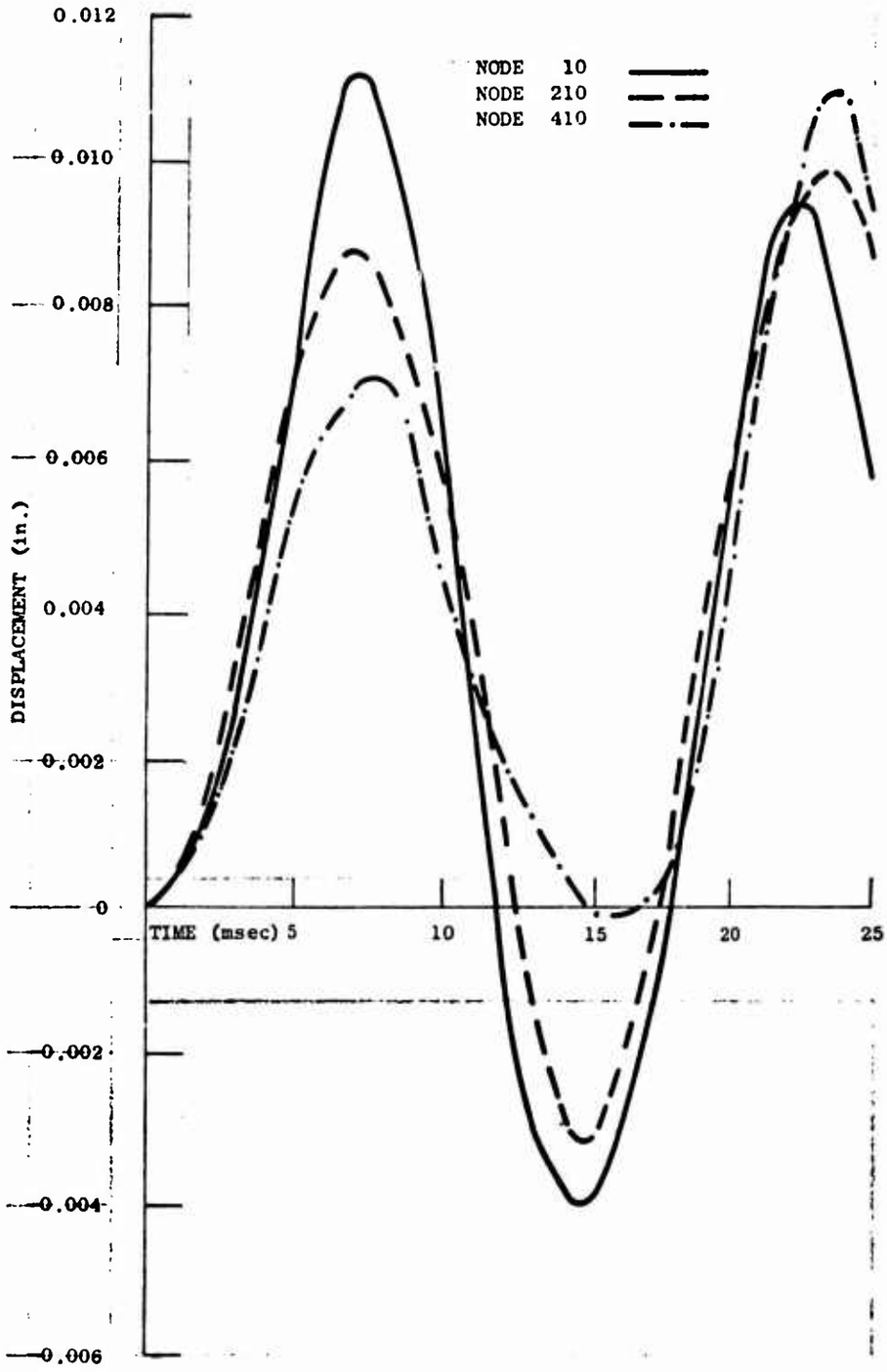

Fig. B-33. Deflection vs Time for Nodes 10, 210 and 410 with Fixed Supports Top and Bottom of Wall

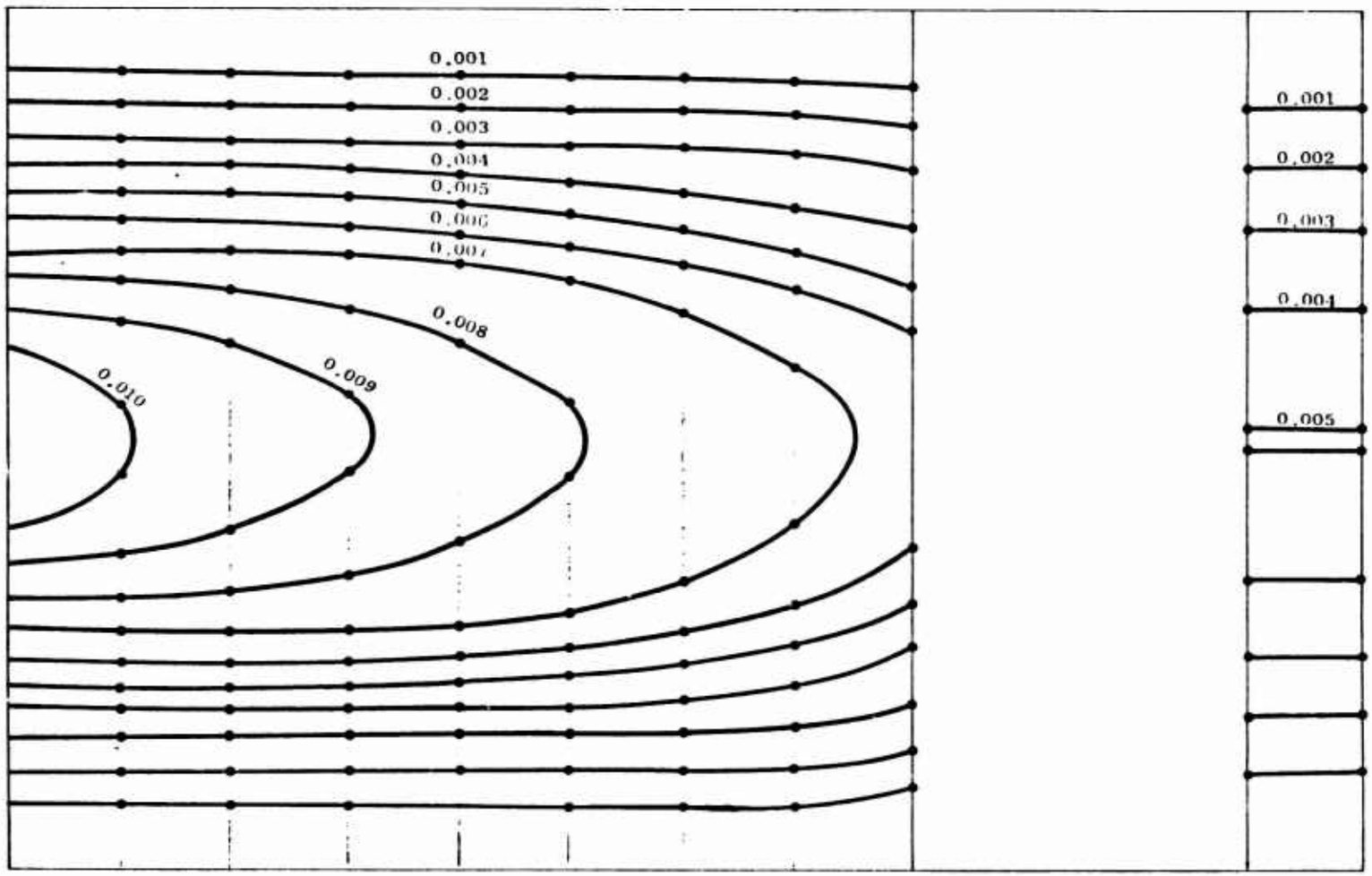

Fig. B-34. Deflection Contours (in.) for Time = 0.007 seconds with Fixed Supports Top and Bottom

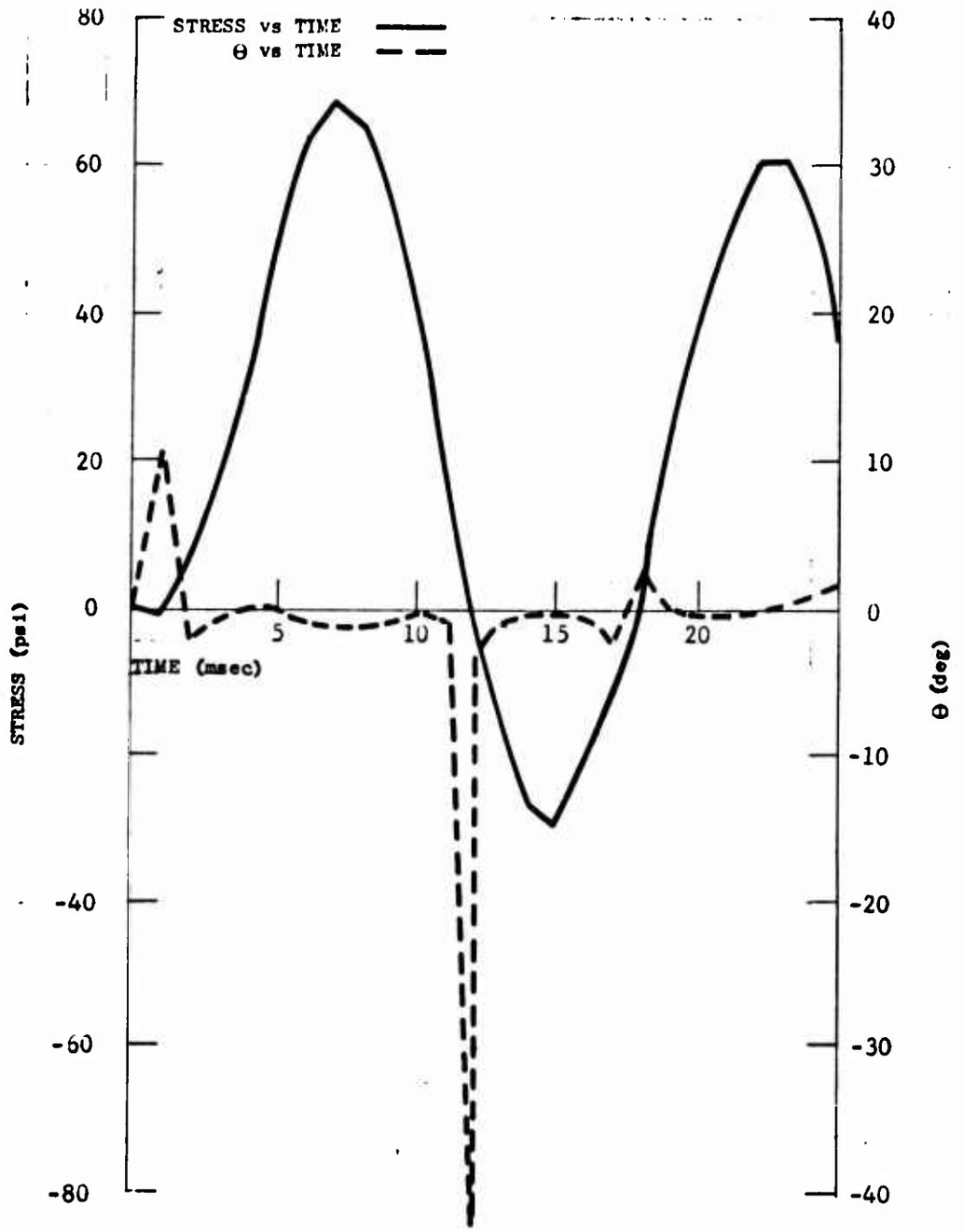

Fig. B-35. Stress and Θ vs Time for Element No. 9 with Fixed Supports Top and Bottom

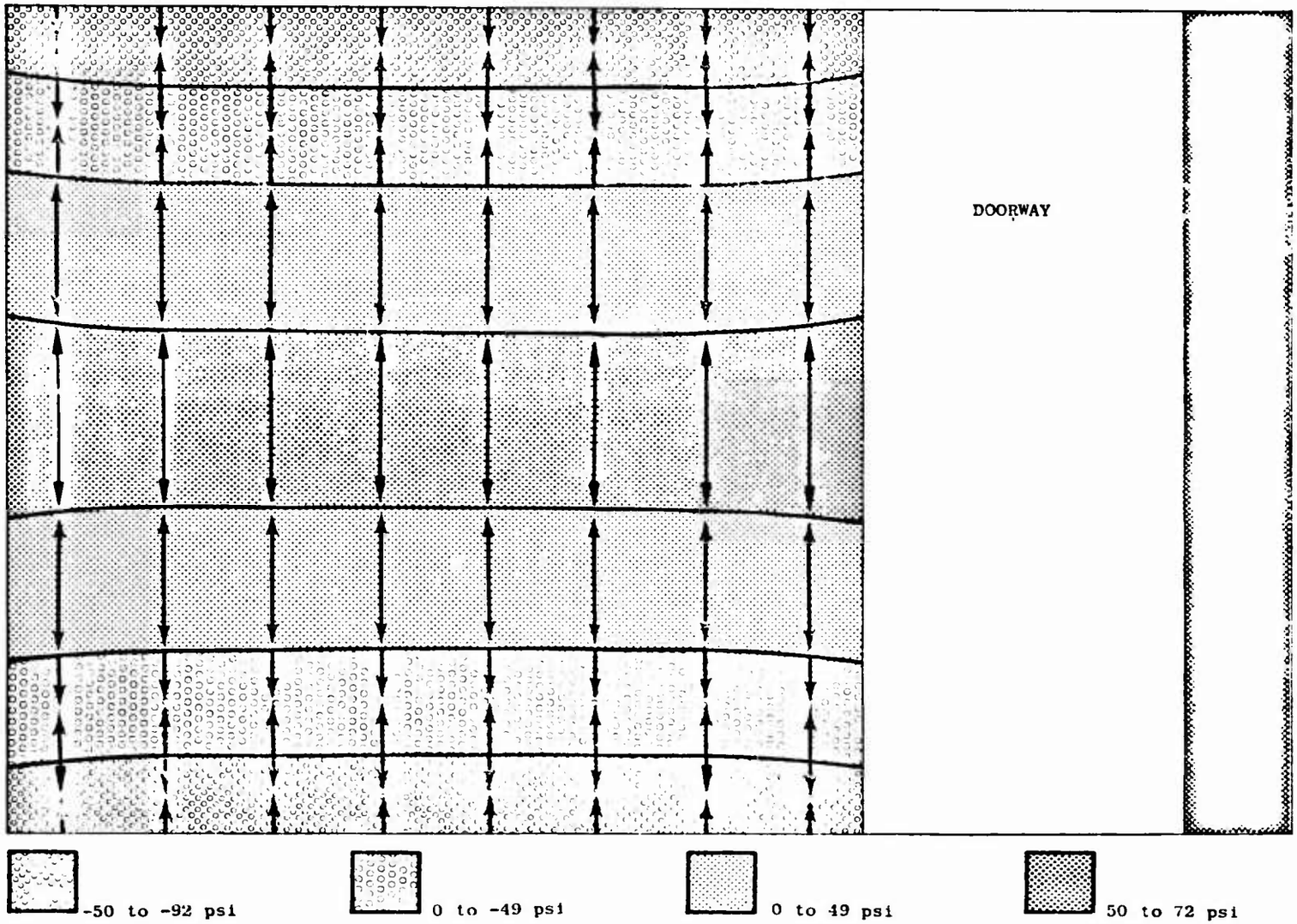

Fig. B-36. Stress Contours for Time = 0.007 seconds for Downstream (tZ) Face with Fixed Supports Top and Bottom

Pinned All Four Sides

Figure B-37 shows how pinned support on all four sides effect dynamic structural behavior. Note that the period is only slightly less for a doorway simply supported. Figure B-38 indicates how the deflection varies from the supports toward the openings.

The stress history of element No. 9, Fig. B-39 is confusing due to higher nodes of vibration and considerable changes in stress direction. The stress contours of Fig. B-40 present a clearer picture of stresses on the wall. From this, we could predict a wall failure starting at mid-height at the opening and continuing at a 45^{o} angle to each corner.

Fixed all Four Sides

With fixed supports, Fig. B-41, the nodes are displaced more toward the opening. The period is about 13 msec and peak deflections are very small being 0.0083 in. per psi of loading. Figure B-42 shows the contours of the wall at near peak displacement.

Figure B-43 is rather jagged showing high participation of the higher nodes of vibration. The stress contours at 6 msec are shown in Fig. B-44. Failure would start at the opening and proceed at 45^{o} to near the corners; there, because of high shear stresses, fracture will occur perpendicular to the 45^{o} crack.

WALL WITH A WINDOW

The window is 3 ft x 5 ft located in the center of a 8 ft x 12 ft x 8 in. nonreinforced brick wall. Being symmetrical about the x and y axis, the element and nodal pattern in Fig. B-45 models effectively the dynamic structural behavior. The small element size around the window opening provides for a more detailed investigation of deflections

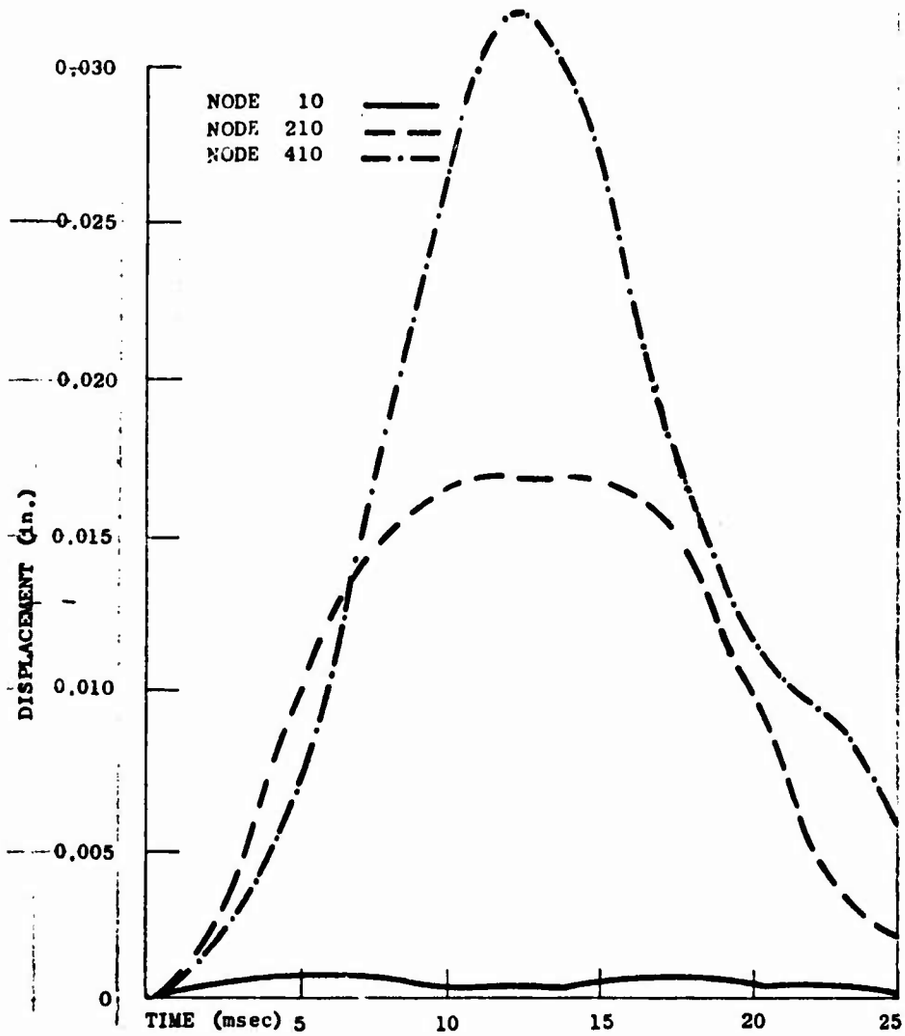

Fig. B-37. Deflection vs Time for Nodes 10, 210 and 410 with Pinned Supports on All Sides

Pinned All Four Sides

Figure B-37 shows how pinned support on all four sides effect dynamic structural behavior. Note that the period is only slightly less for a doorway simply supported. Figure B-38 indicates how the deflection varies from the supports toward the openings.

The stress history of element No. 9, Fig. B-39 is confusing due to higher nodes of vibration and considerable changes in stress direction. The stress contours of Fig. B-40 present a clearer picture of stresses on the wall. From this, we could predict a wall failure starting at mid-height at the opening and continuing at a 45^{o} angle to each corner.

Fixed all Four Sides

With fixed supports, Fig. B-41, the nodes are displaced more toward the opening. The period is about 13 msec and peak deflections are very small being 0.0083 in. per psi of loading. Figure B-42 shows the contours of the wall at near peak displacement.

Figure B-43 is rather jagged showing high participation of the higher nodes of vibration. The stress contours at 6 msec are shown in Fig. B-44. Failure would start at the opening and proceed at 45^{o} to near the corners; there, because of high shear stresses, fracture will occur perpendicular to the 45^{o} crack.

WALL WITH A WINDOW

The window is 3 ft x 5 ft located in the center of a 8 ft x 12 ft x 8 in. nonreinforced brick wall. Being symmetrical about the x and y axis, the element and nodal pattern in Fig. B-45 models effectively the dynamic structural behavior. The small element size around the window opening provides for a more detailed investigation of deflections

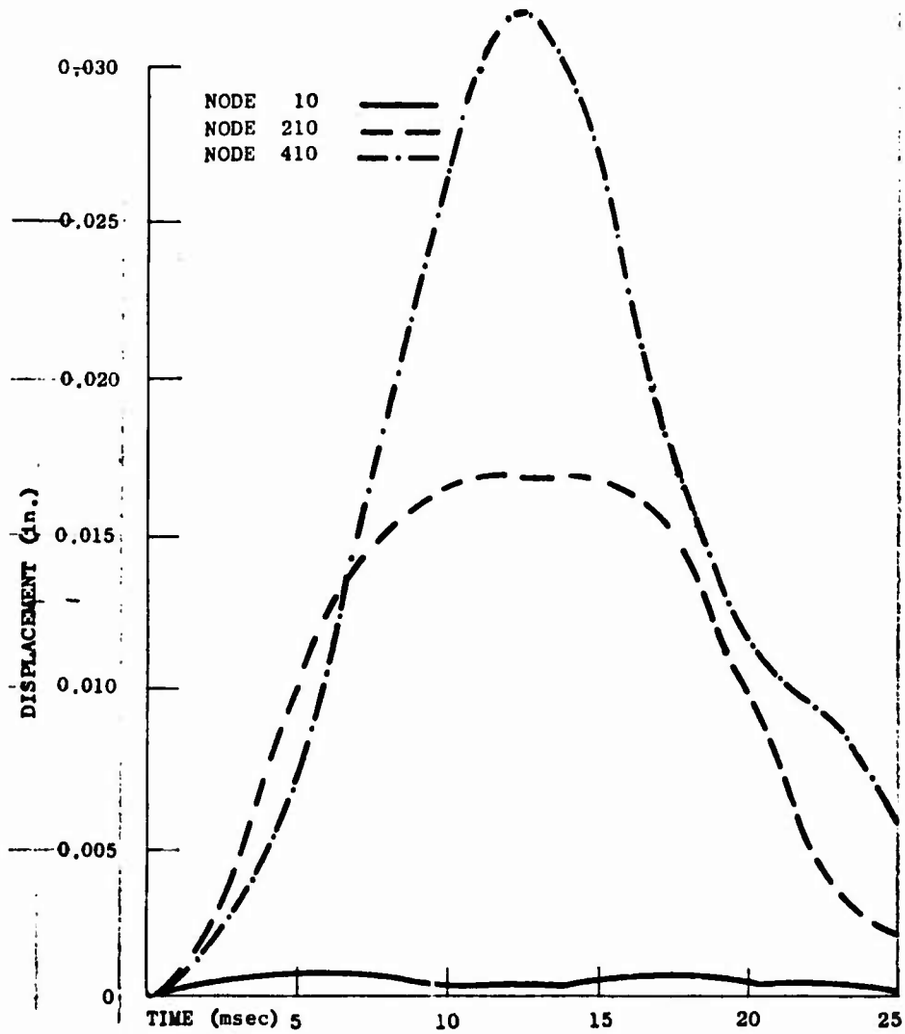

Fig. B-37. Deflection vs Time for Nodes 10, 210 and 410 with Pinned Supports on All Sides

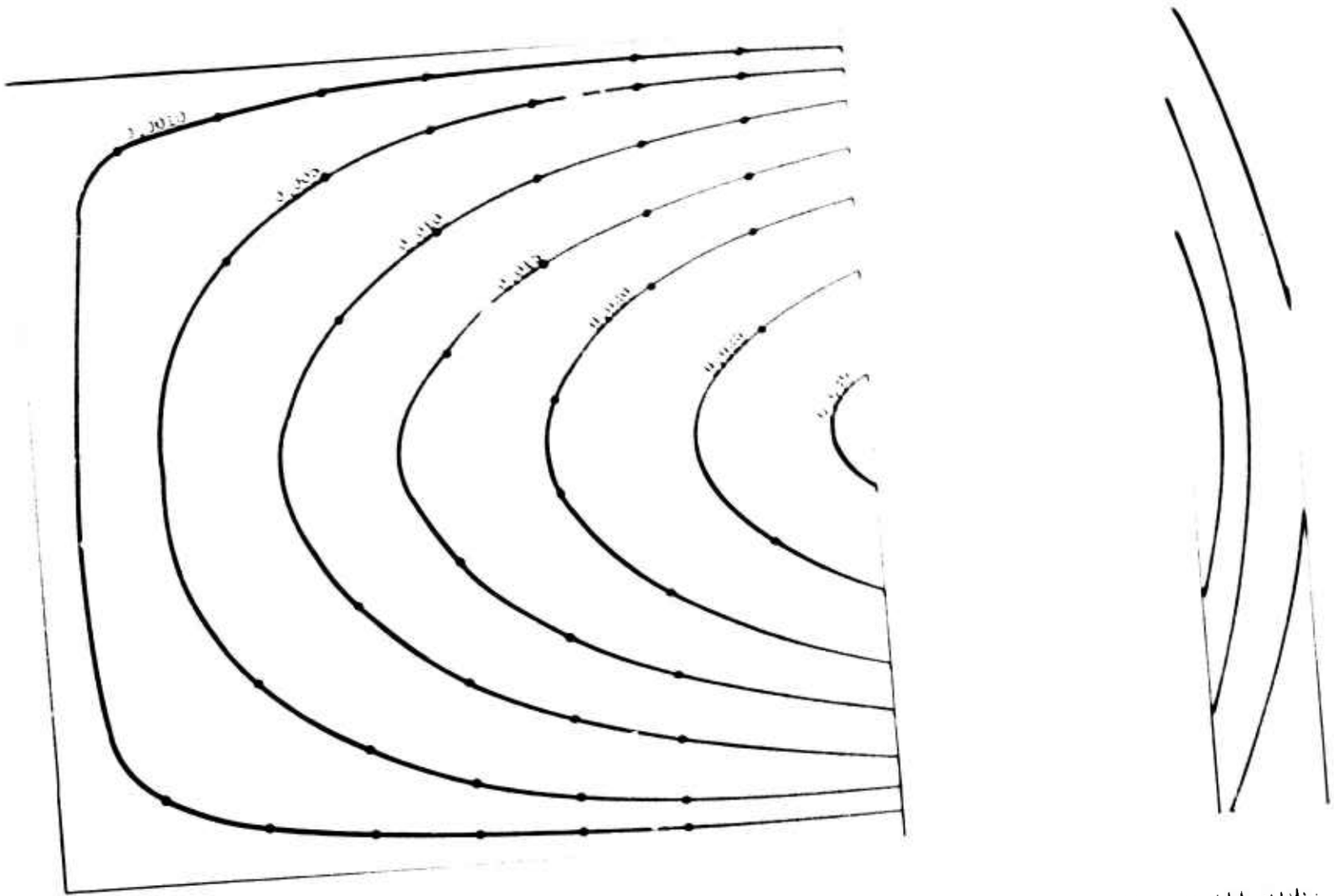

Fig. B-38. Deflection Contours (in.) for Time = 0.012 seconds with Pinned Supports on All Sides

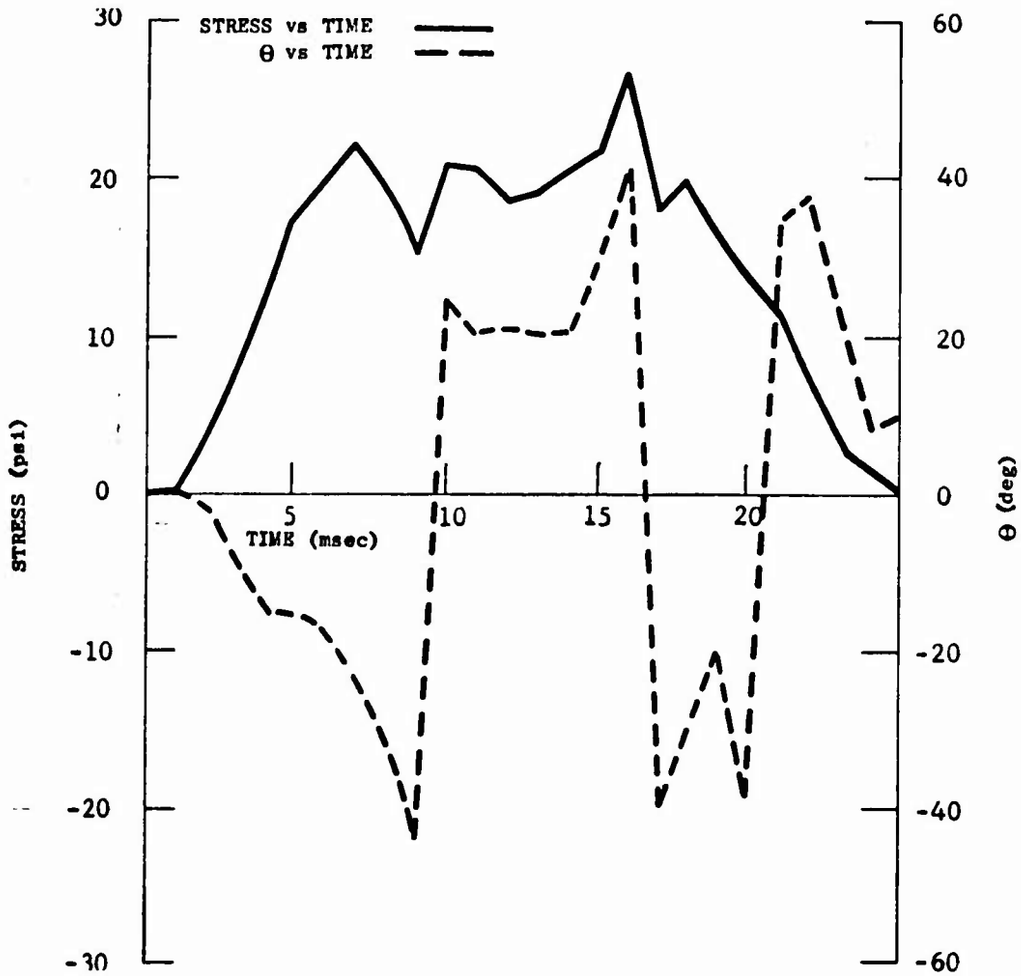

Fig. B-39. Stress and θ vs Time for Element No. 9 with Pinned Supports on All Sides

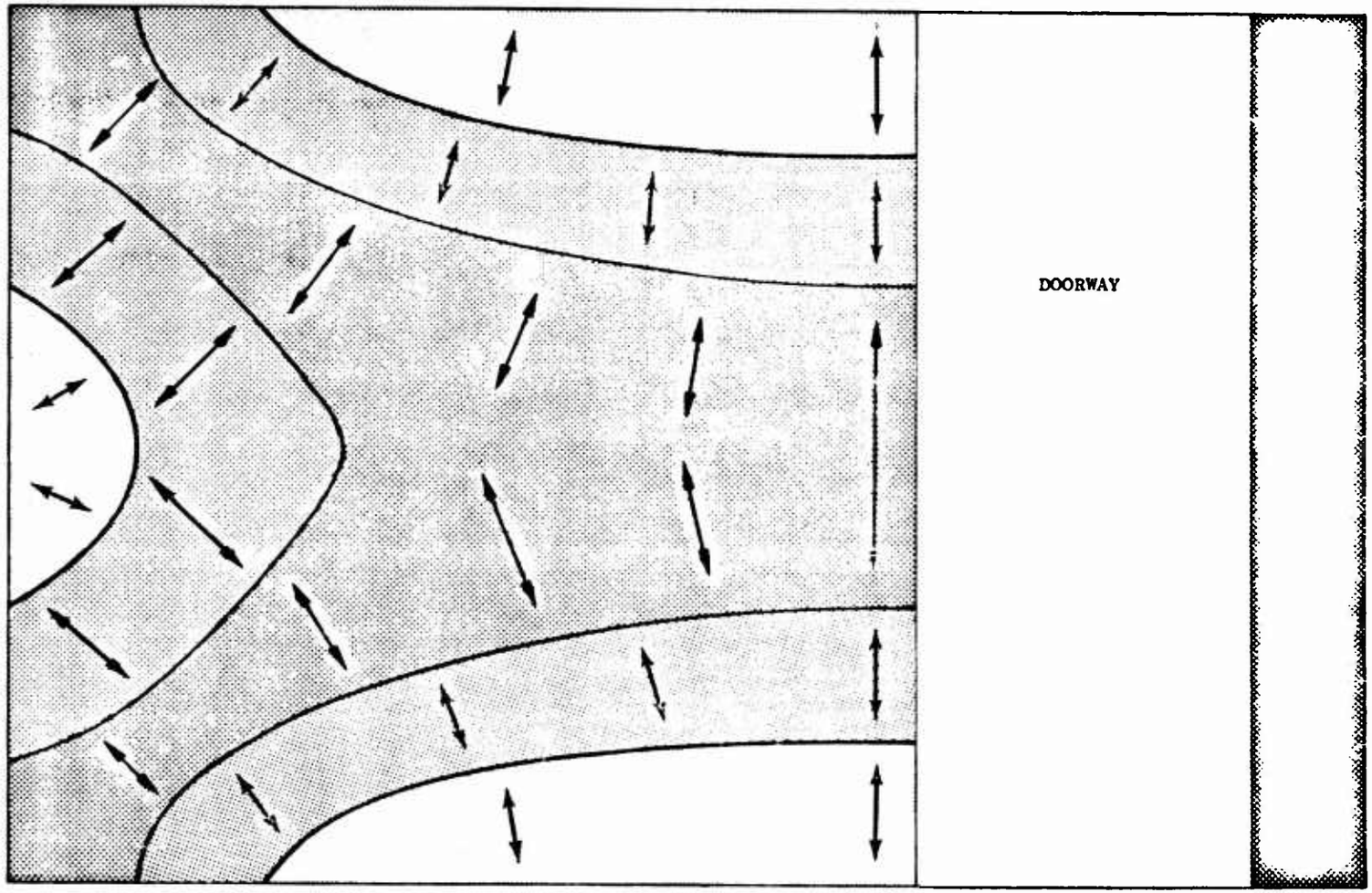

Fig. B-40. Stress Contours on (+Z) Face at Time - 0.13 Seconds for a Wall With Doorway Pinned on Three Sides.

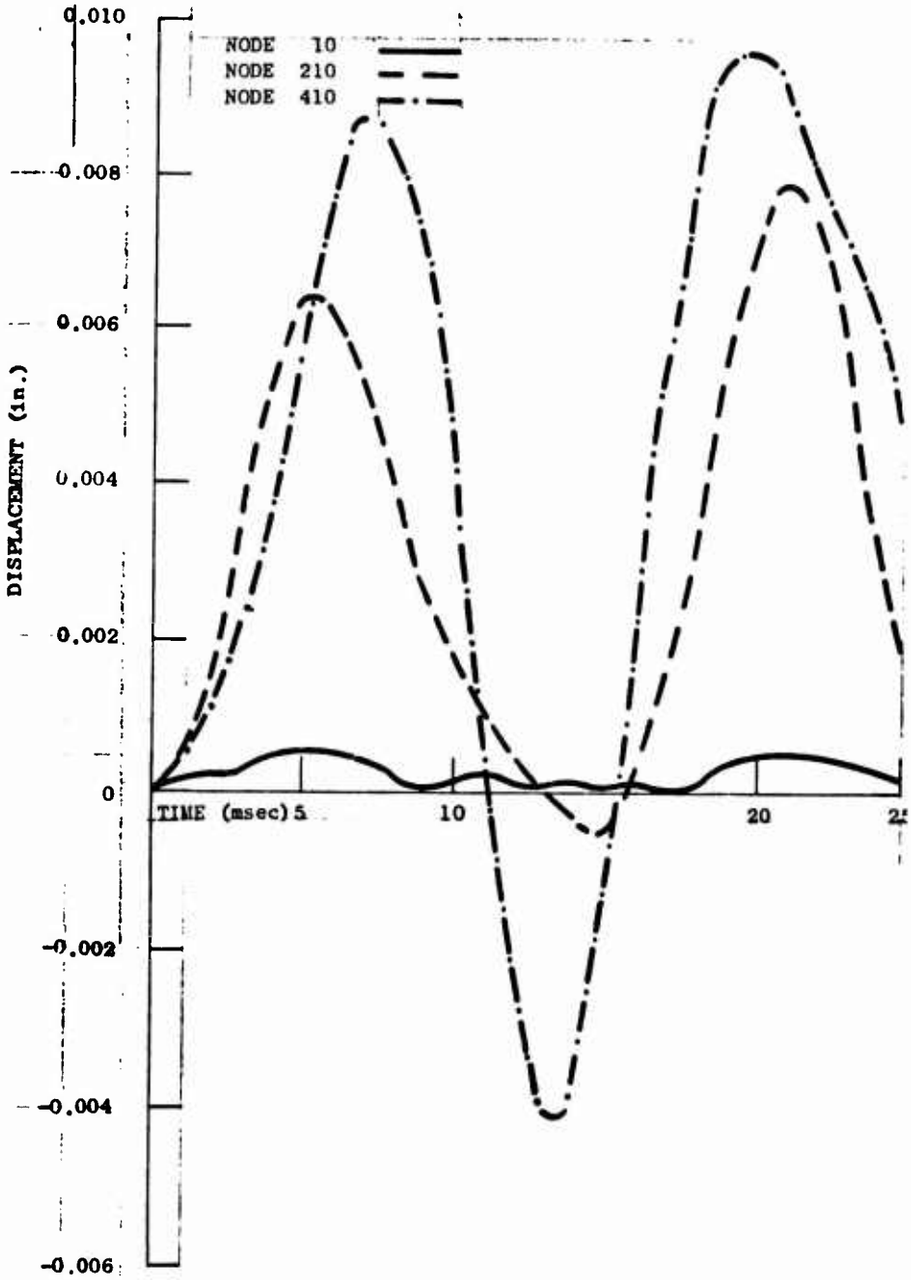

Fig. B-41. Deflection vs Time for Nodes 10, 210 and 410 with Fixed Supports All Sides

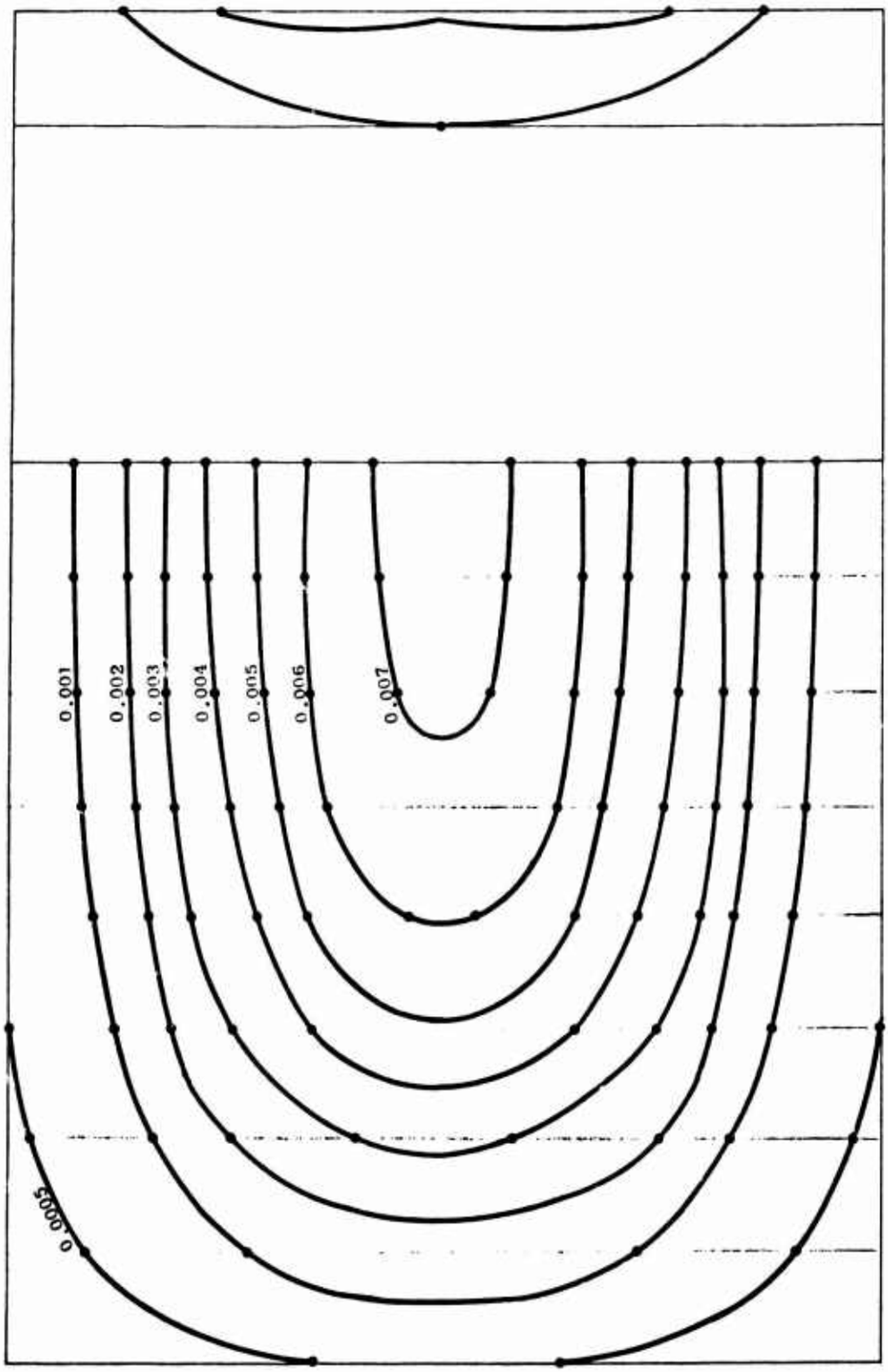

Fig. B-42. Deflection Contours (in.) for Time = 0.006 seconds with Fixed Supports All Sides

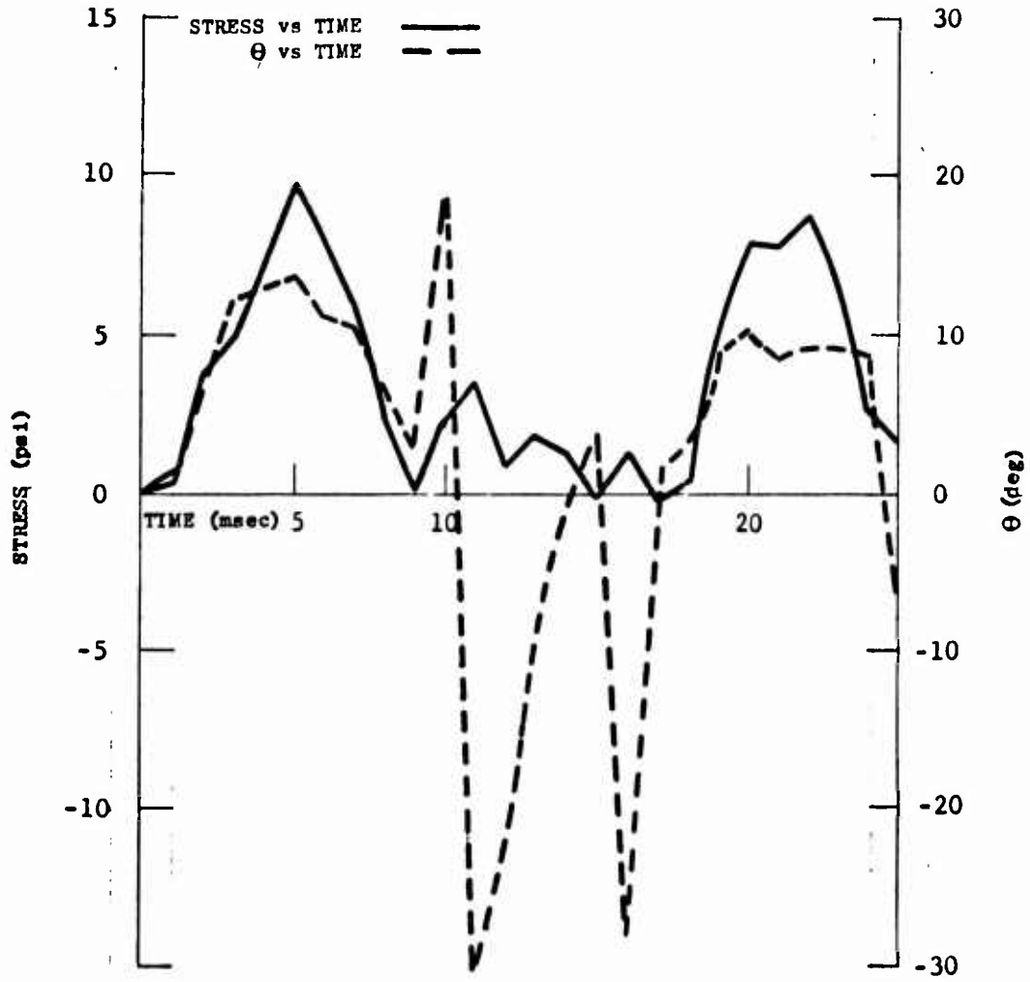

Fig. B-43. Stress and θ vs Time for Element No. 9 with Fixed Supports All Sides

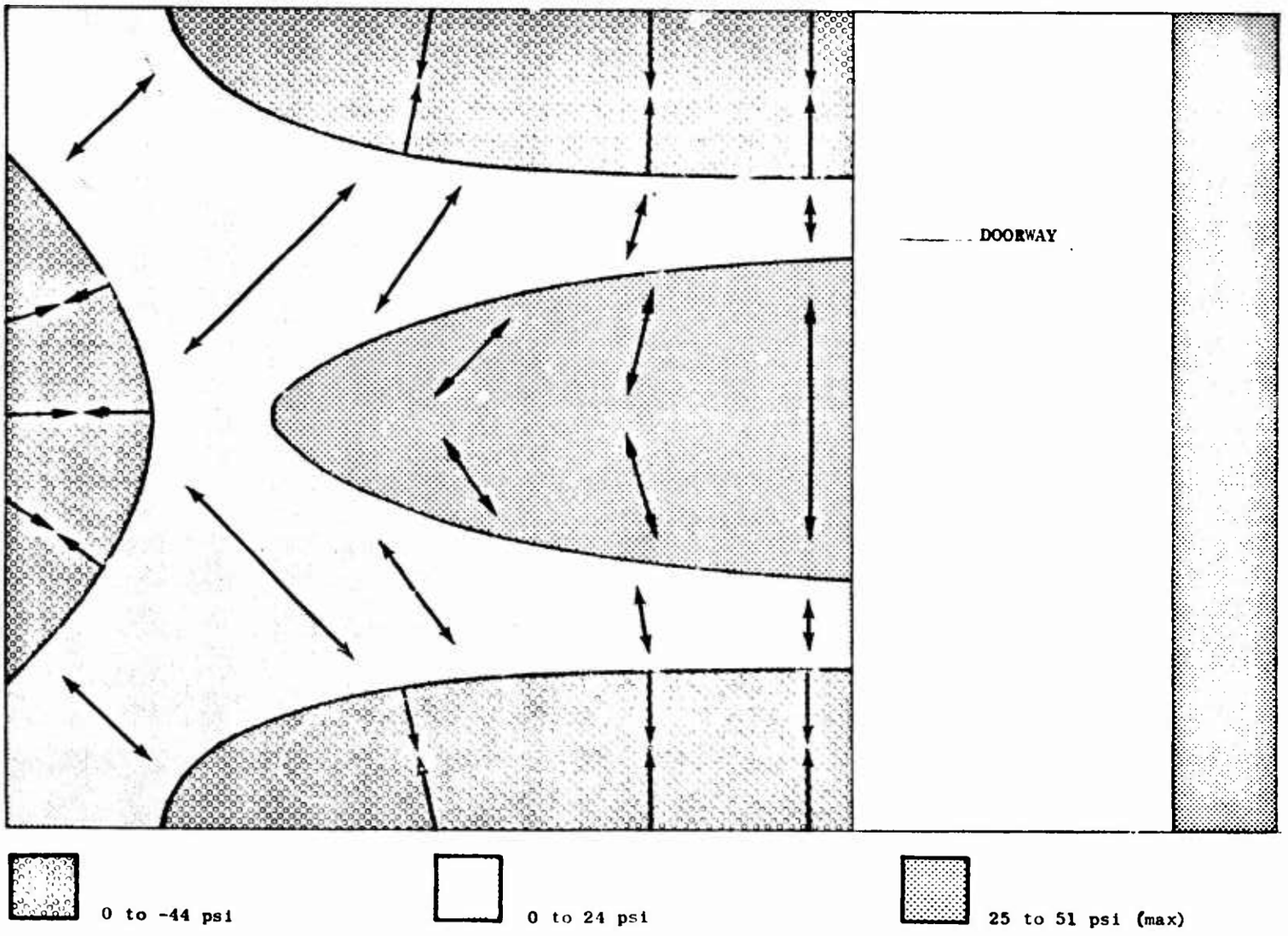

Fig. B-44. Stress Contours on the (+Z) Face at t = 0.006 sec for a Wall With Doorway Fixed on Three Sides.

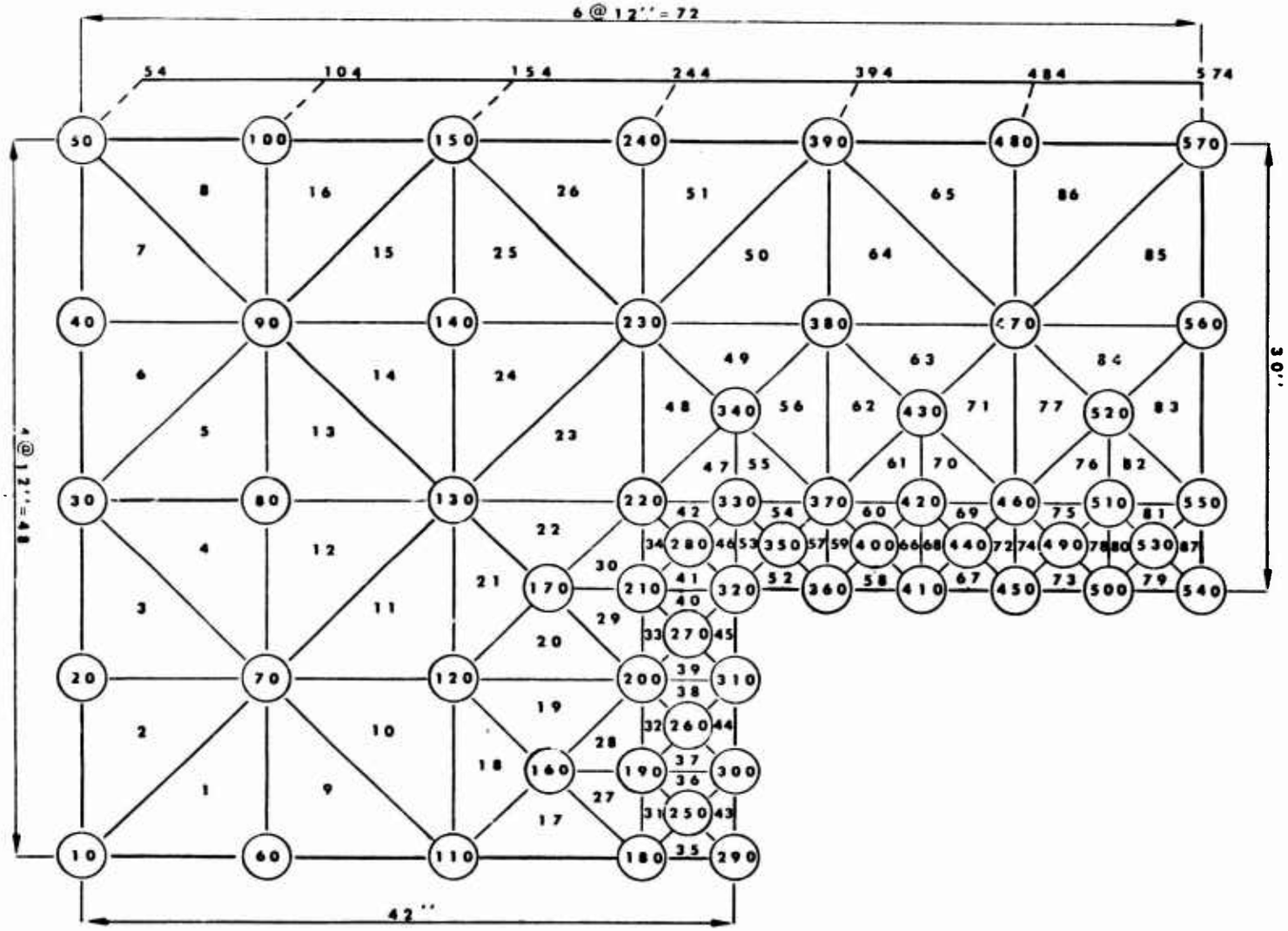

Fig. B-45. Node and Element Locations for Wall With Window.

and stresses along the window. Thus the accuracy of stress concentrations and consequently prediction of crack propagation correlates very well with actual tests. Loading on the wall with window is that of Fig. B-3 normalized by SAMIS to 1 psi.

Figure B-6 shows the coordinate axis for each element and how the principal stresses are located from the x and y axis. The angle shown is positive. For the stress contour maps, only the maximum tensile stress of the principal stresses is shown except for compression fields, then the maximum compressive stress is shown. Other sign conventions are t for tensile stress and - for compressive. Deflections are positive in the +Z direction. All graphs and contours are for stresses on and deflections of the +Z direction. All graphs and contours are for stresses on and deflections of the +Z (downstream) wall surface.

Pinned Top and Bottom

Figures B-46 and B-47 are of nodal displacement of the downstream side of the wall. The location of these nodes can be found on Fig. B-45. Figure B-48 shows displacement for the entire wall at 0.015 msec.

Figure B-49 is of stress and θ vs time for element No. 22. With an opening in the center, wall behavior is more complex with understanding and prediction becoming more uncertain. This complexity increases with these more sophisticated support conditions. Figure B-50, however, is fairly accurate giving areas of high tensile stresses near the corners of the opening; and we would predict cracking to start at the corners and propagating to the sides (see Ref. 2).

Fixed Top and Bottom

Figures B-51 and B-52 show that the period has decreased to about 13 msec and to very small deflections per 1 psi load. The deflections for this wall are shown in Fig. B-53.

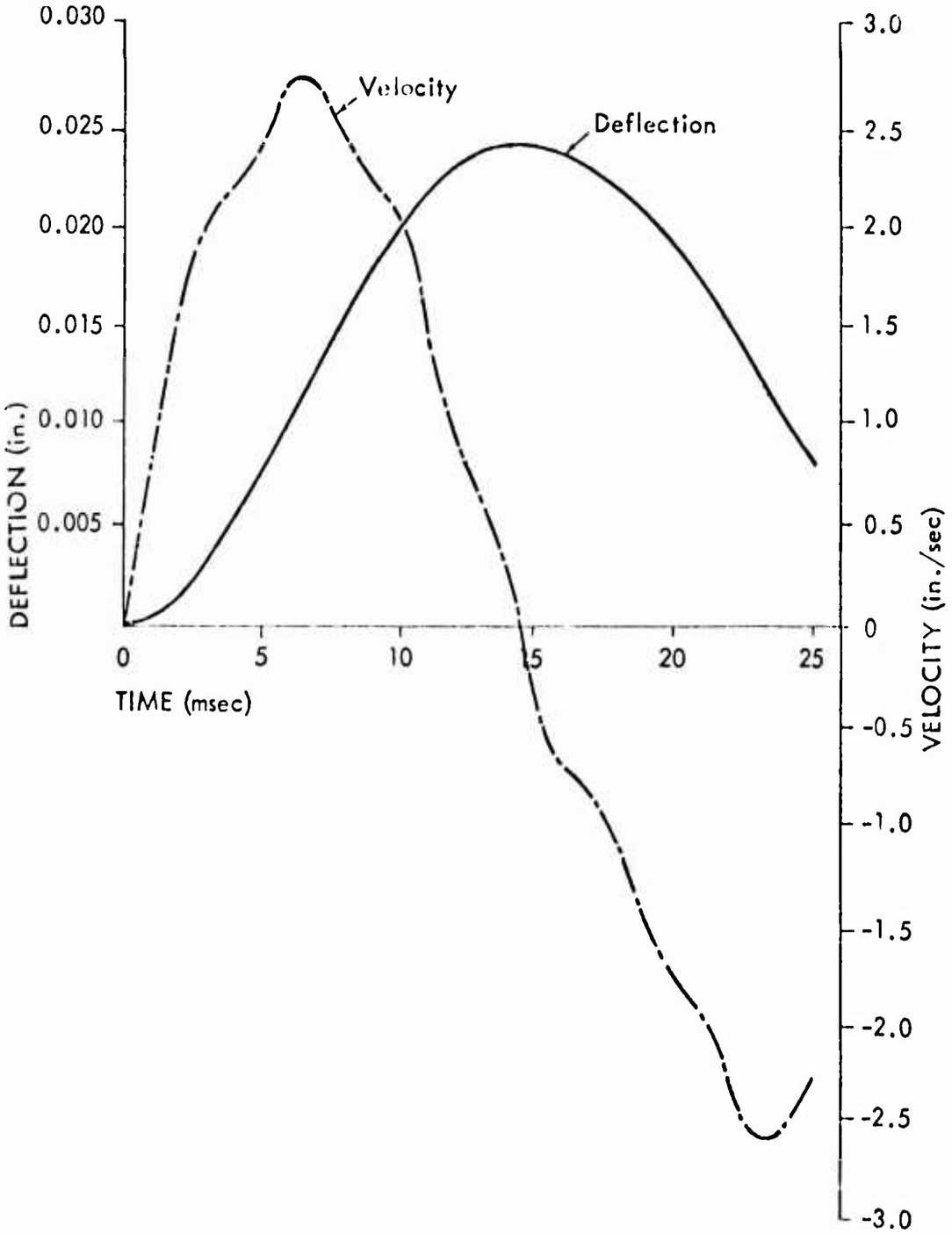

Fig. B-46. Velocity and Deflection vs Time for Node 60.

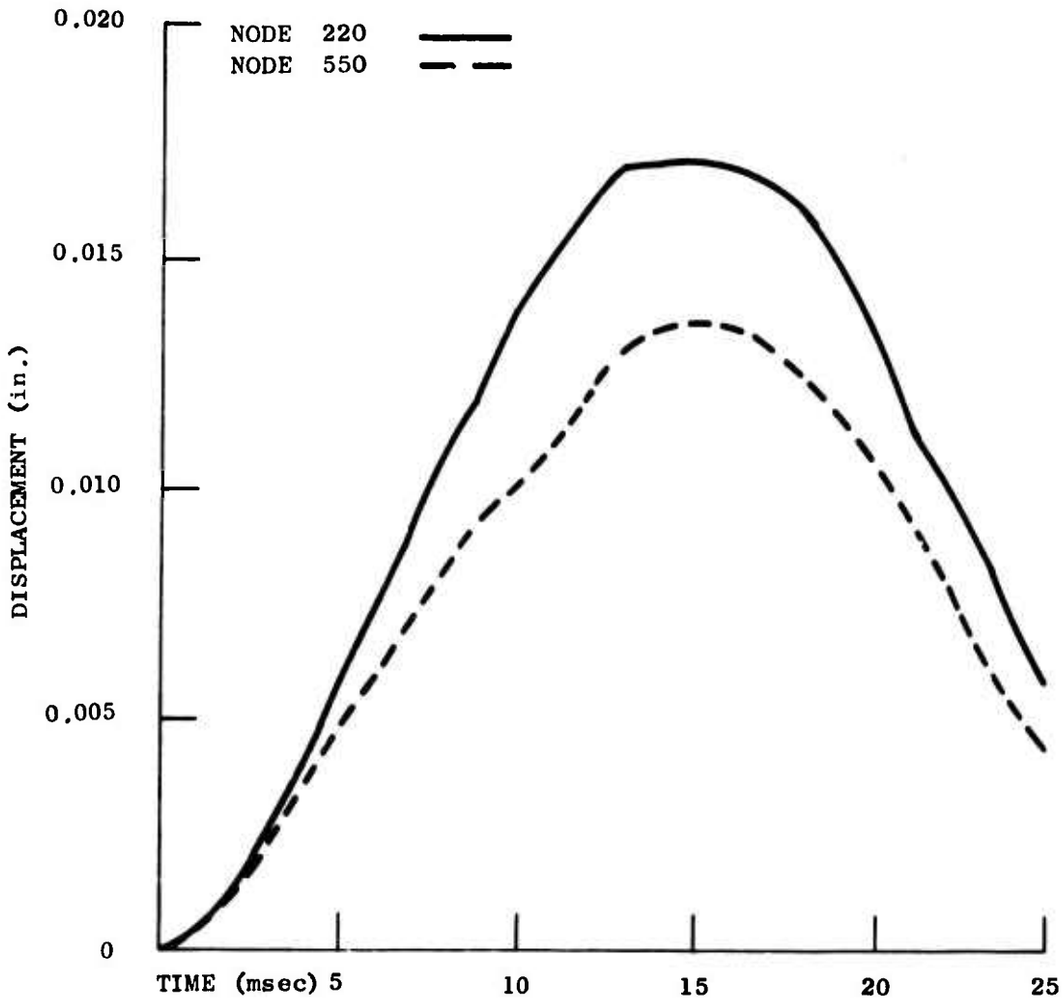

Fig. B-47. Deflection vs Time for Nodes 220 and 550 with Pinned Supports Top and Bottom

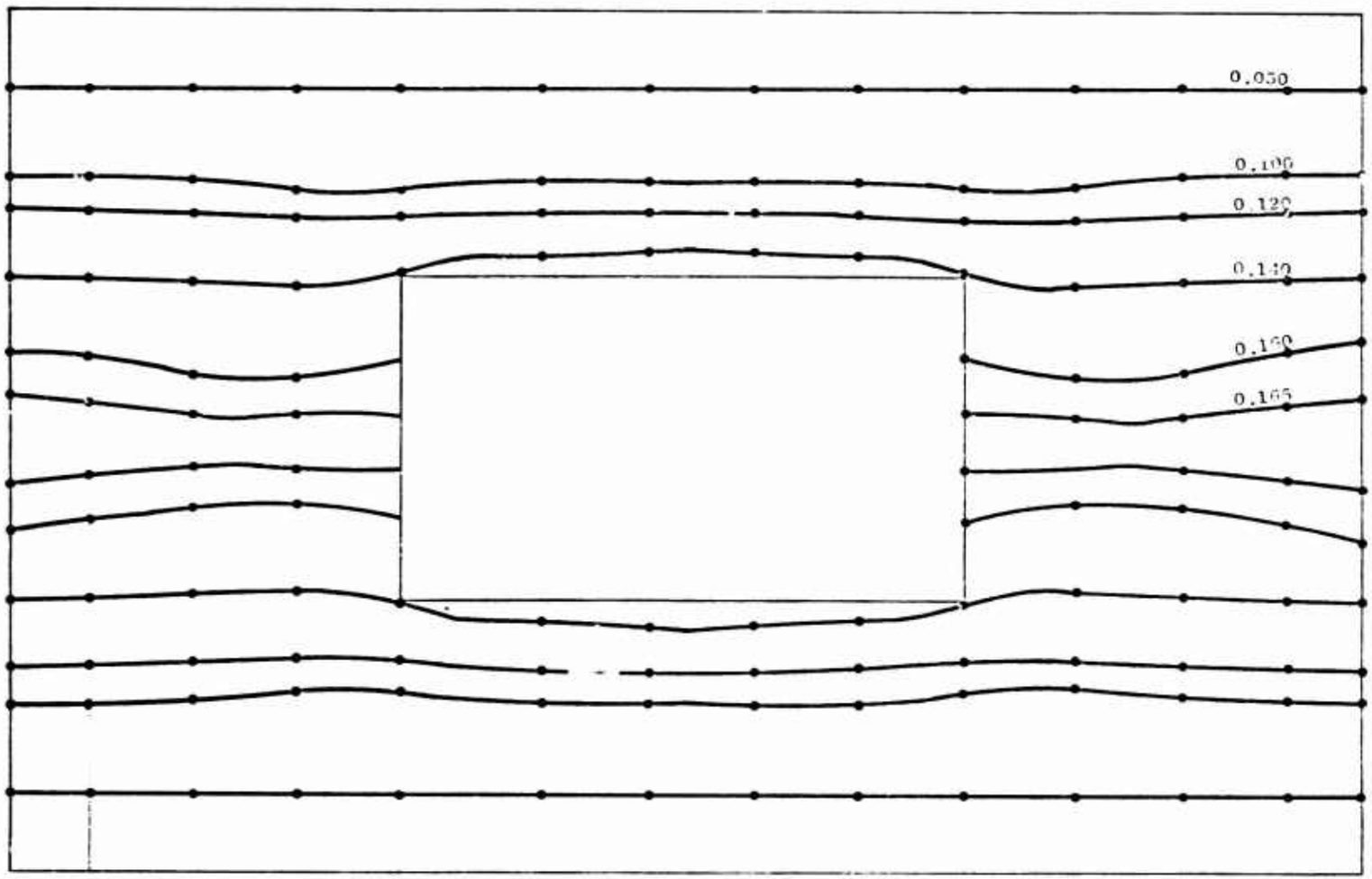

Fig. B-18. Deflection Contours (in.) for Time = 0.015 seconds with Pinned Supports Top and Bottom

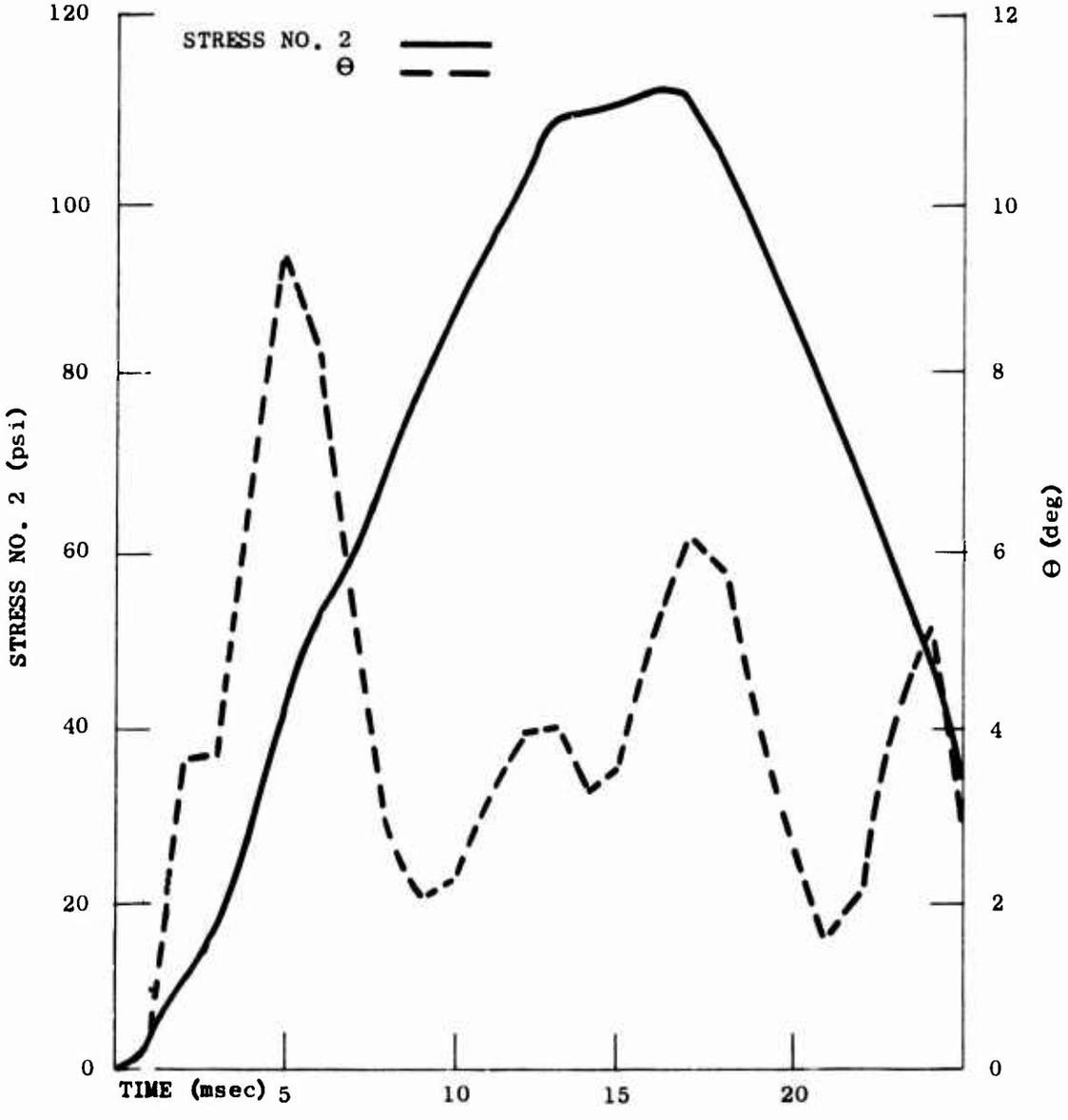

Fig. B-49. Stress and Θ vs Time for Element No. 22 with Pinned Supports Top and Bottom

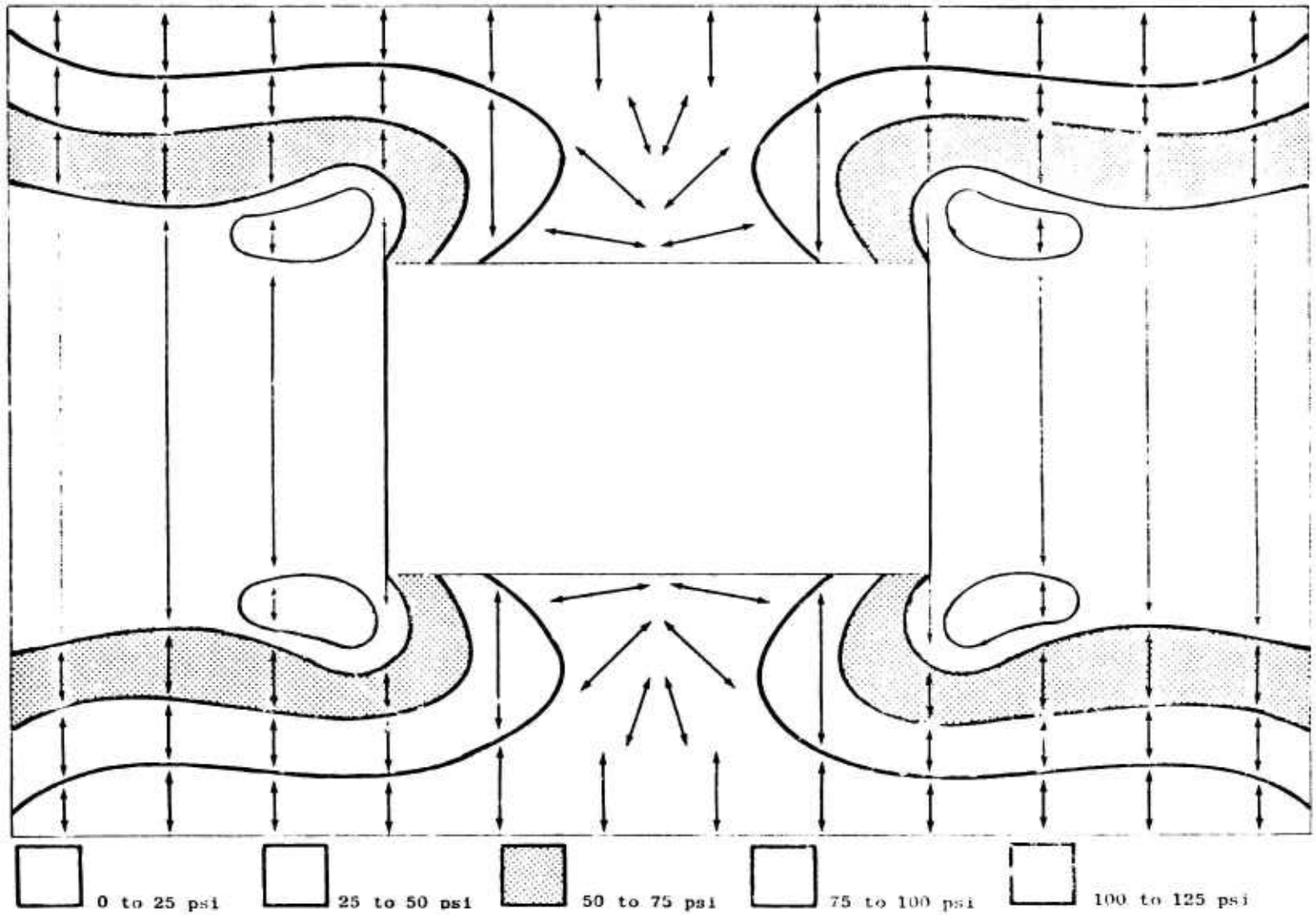

Fig. B-50. Stress Contours for Time = 0.016 seconds for Downstream (-Z) Face with Pinned Supports Top and Bottom

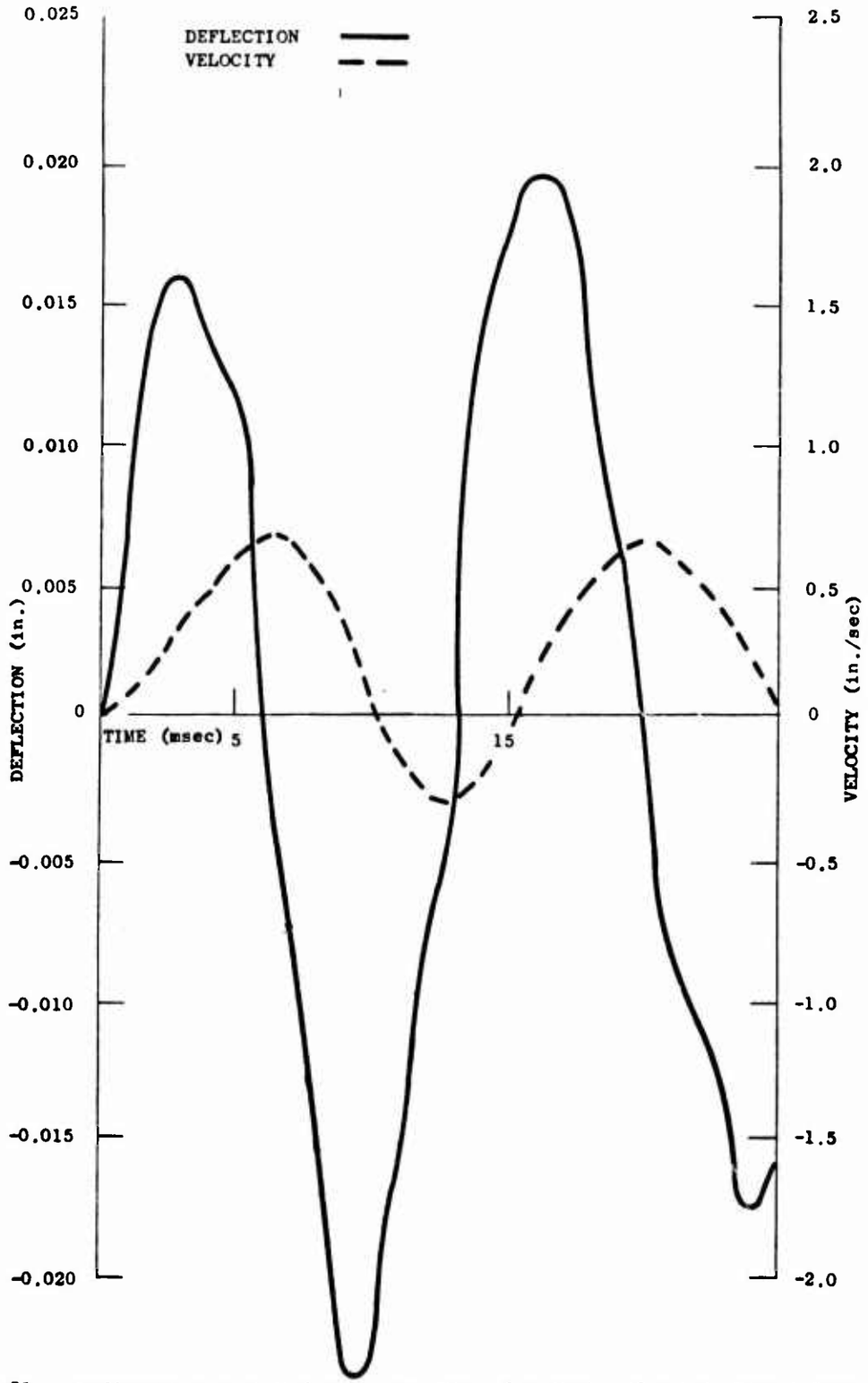

Fig. B-51. Deflection and Velocity vs Time for Node 60 with Fixed Supports Top and Bottom

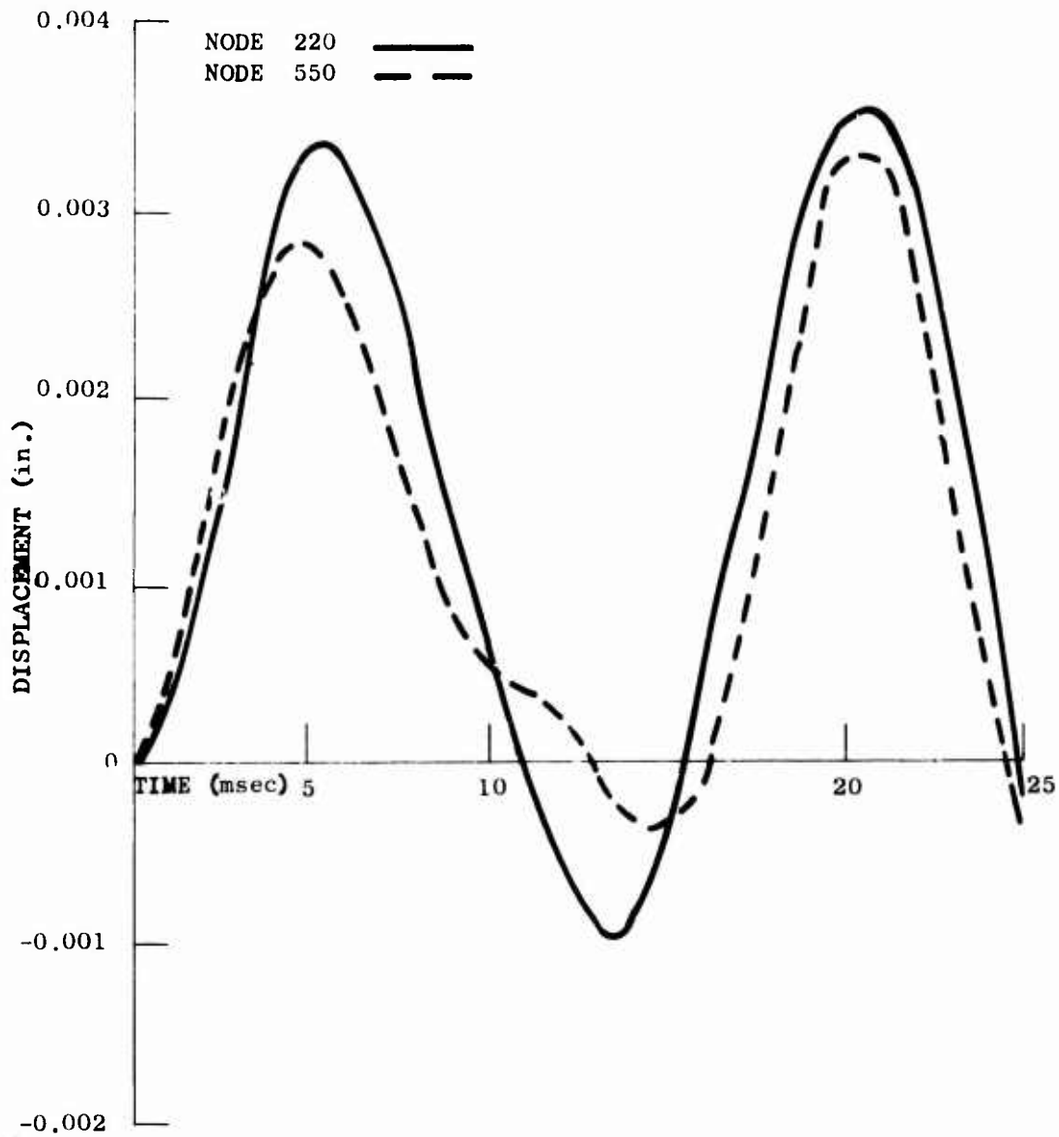

Fig. B-52. Deflection vs Time for Nodes 220 and 550 with Fixed Supports Top and Bottom

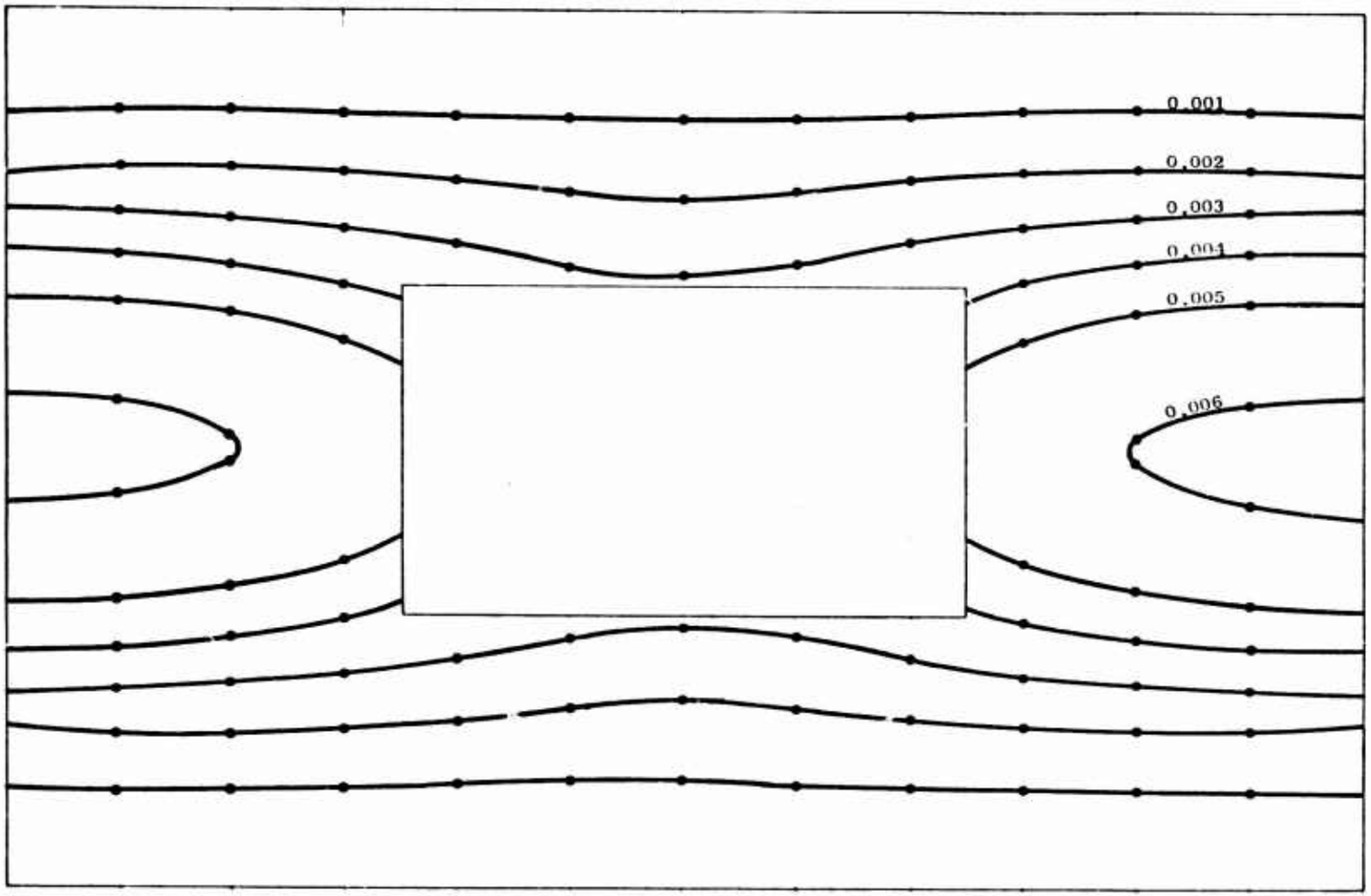

Fig. B-53. Deflection Contours (in.) for Time = 0.006 seconds with Fixed Supports Top and Bottom

Figure B-54 of element stress history is even more confused than that of the simply supported case. But from Fig. B-55 we can say that the wall will fracture first at the corners leading to wall failure.

Pinned All Four Sides

For this support condition, displacement history of some points is given by Figures B-56 and B-57. Figure B-58 shows the ponding effect caused by blast loading.

The stress and θ vs time history of element No. 22, Fig. B-59, reveals the time at which peak stress occurs. For this time of 8 msec, Fig. B-60 shows high stresses at the window corners indicating fracture first occurring there. Crack propagation beyond this is difficult to predict, but tests have shown the cracks will continue to the wall corners. It should be noted that variances in material properties would greatly affect the direction of crack propagation from the opening's corners.

Fixed All Four Sides

Moment resisting supports greatly reduce the fundamental period of the wall to about 7 msec, as substantiated by Figs. B-61 and B-62. Deflection is very low being 0.0032 in. per psi of loading. Figure B-63 is of the deflection gradients from the sides to the opening.

The change in element stress can be seen in Fig. B-64. Figure B-65 is of stress contours. We would predict fracture starting at the corners and traveling to the wall corners. High shear stresses at the corners will cause the wall to fail at about 1 ft from the corner and perpendicular to the window fracture.

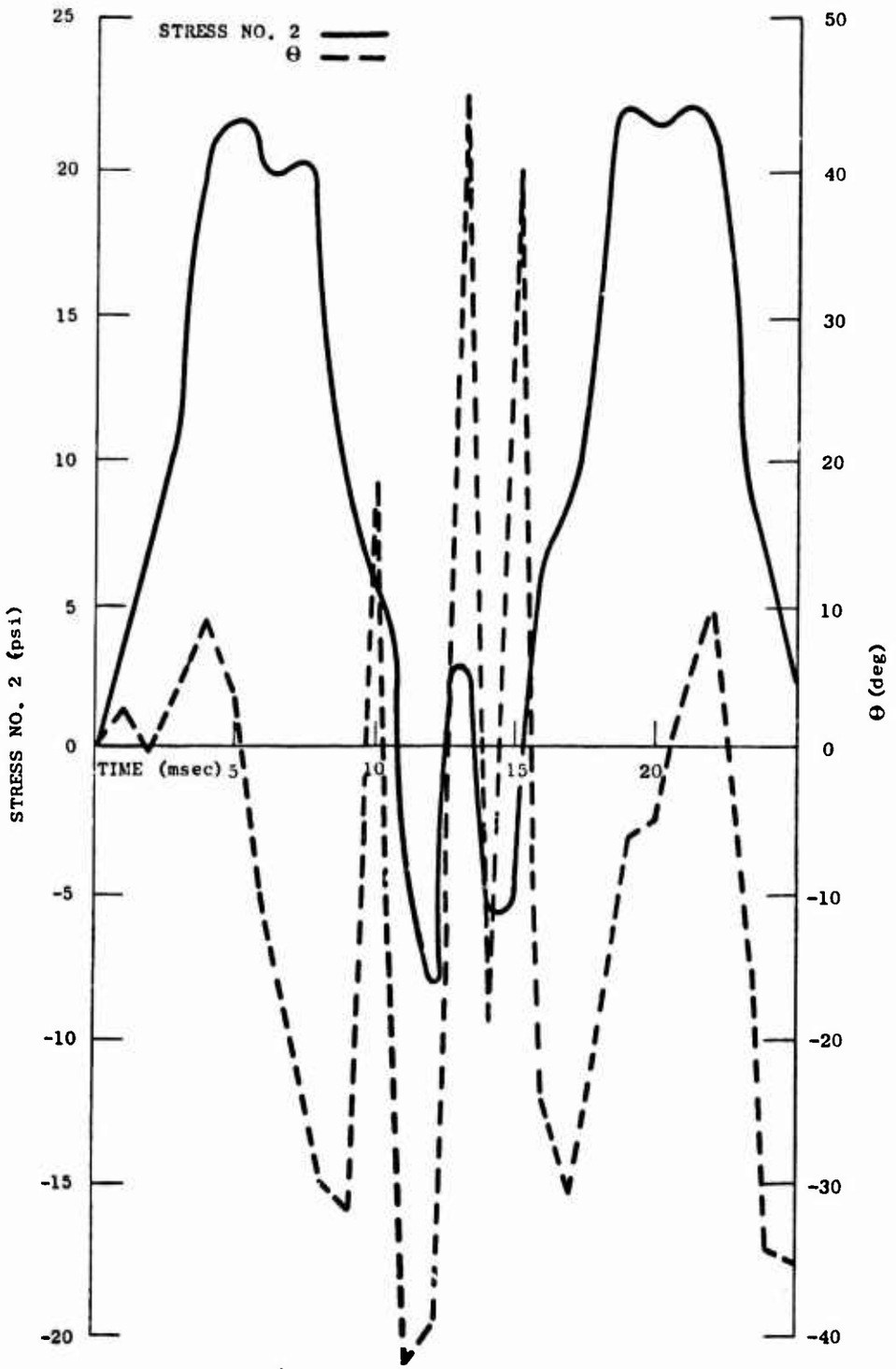

Fig. B-54. Stress and $\dot{\theta}$ vs Time for Element No. 22 with Fixed Supports Top and Bottom

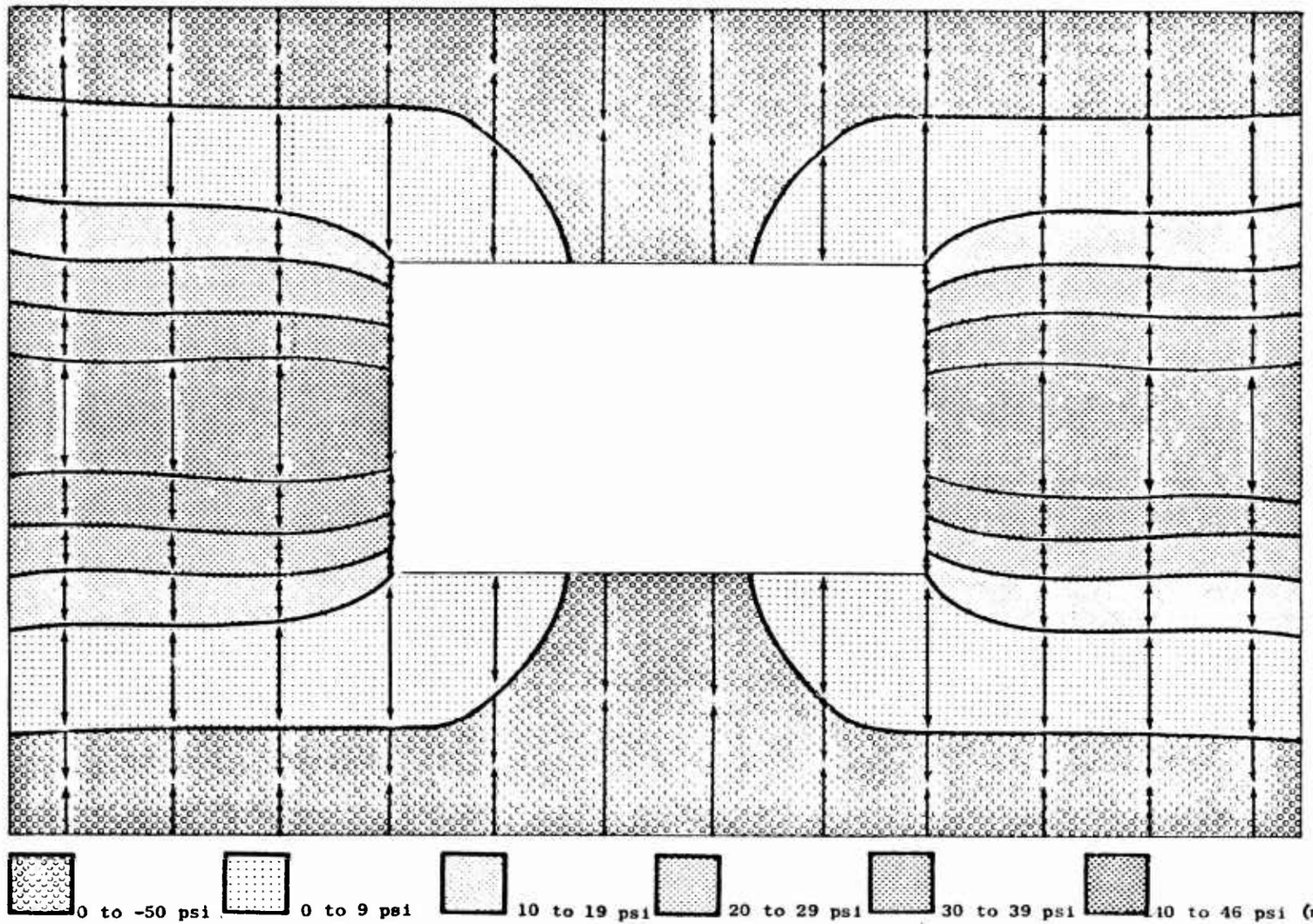

Fig. B-55. Stress Contours for Time = 0.000 seconds for Downstream (+Z) Face with Fixed Supports Top and Bottom

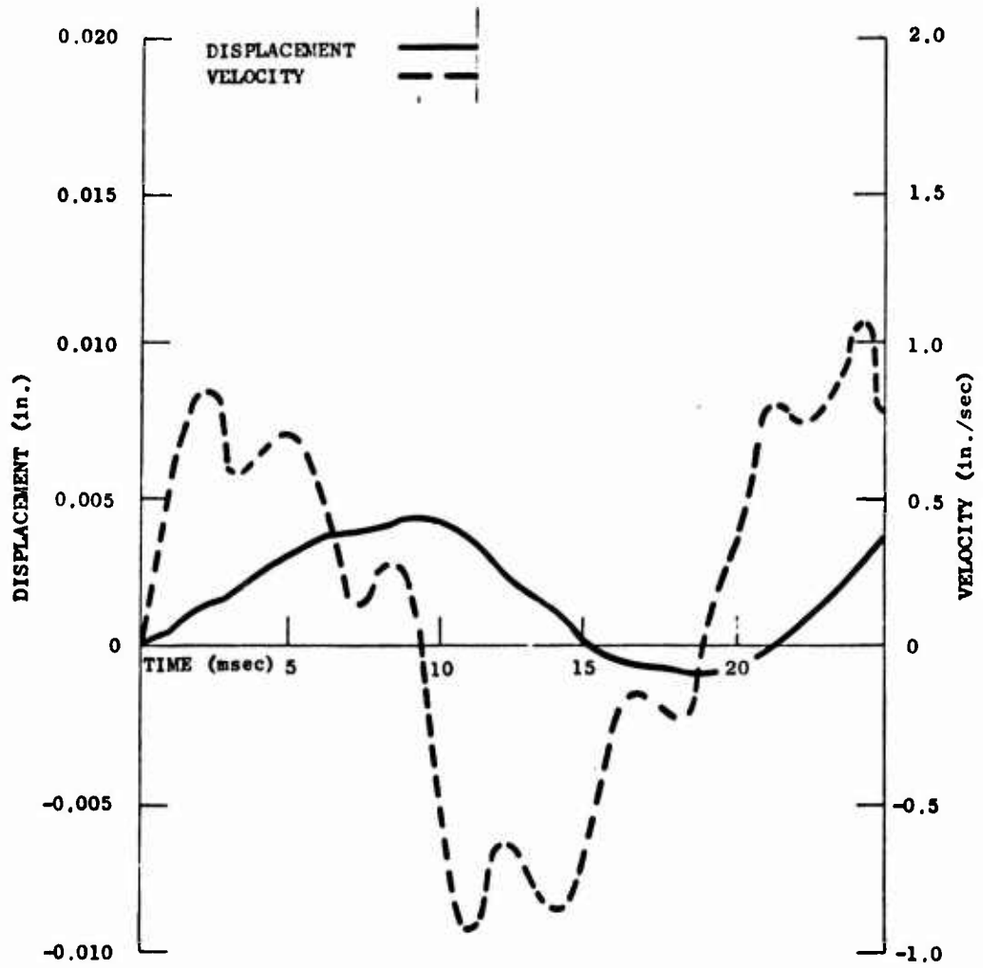

Fig. B-56. Deflection and Velocity vs Time for Node 60 with Pinned Supports All Sides

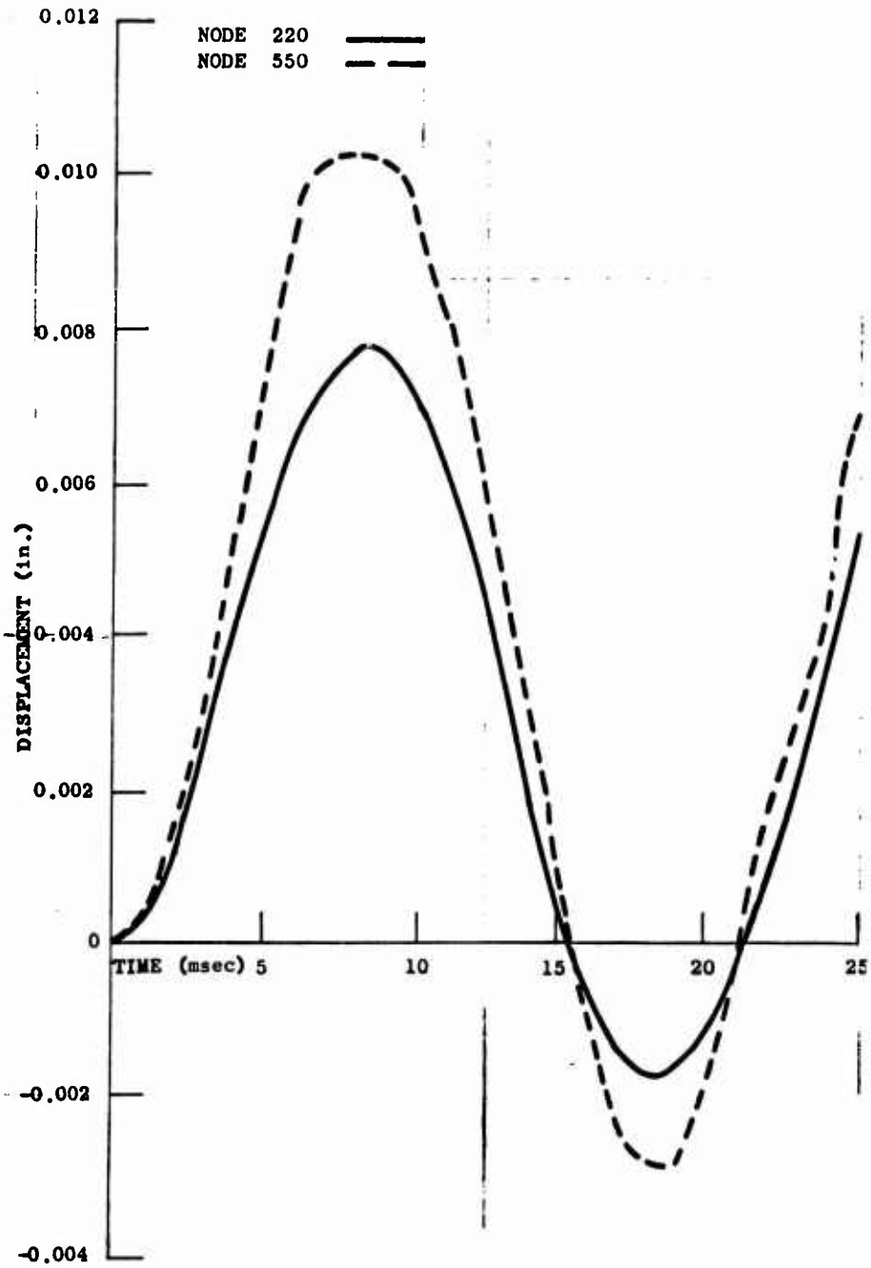

Fig. B-57. Deflection vs Time for Nodes 220 and 550 with Pinned Supports All Sides

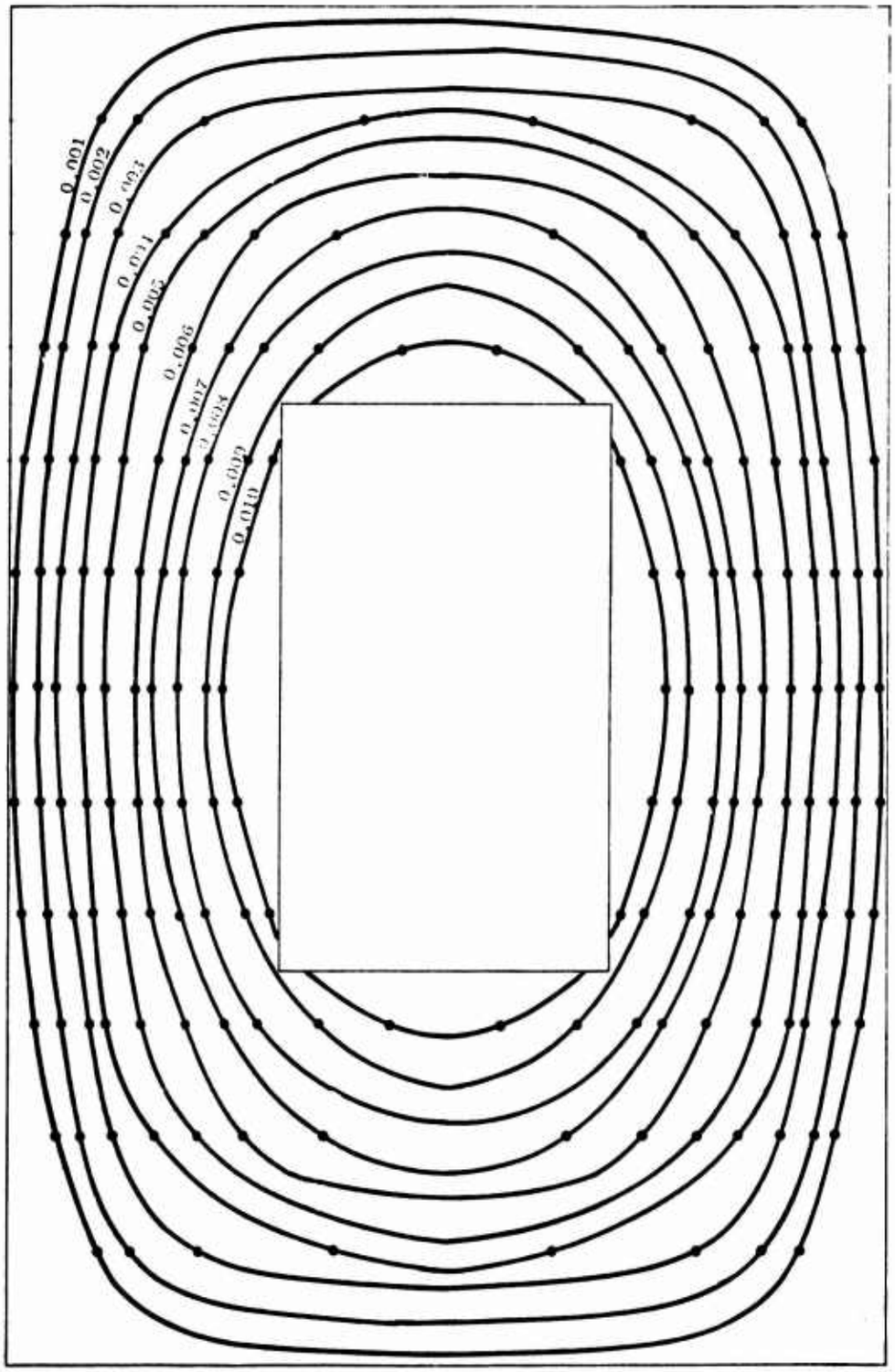

Fig. B-58. Deflection Contours (in.) for Time = 0.009 seconds with Pinned Supports All Sides

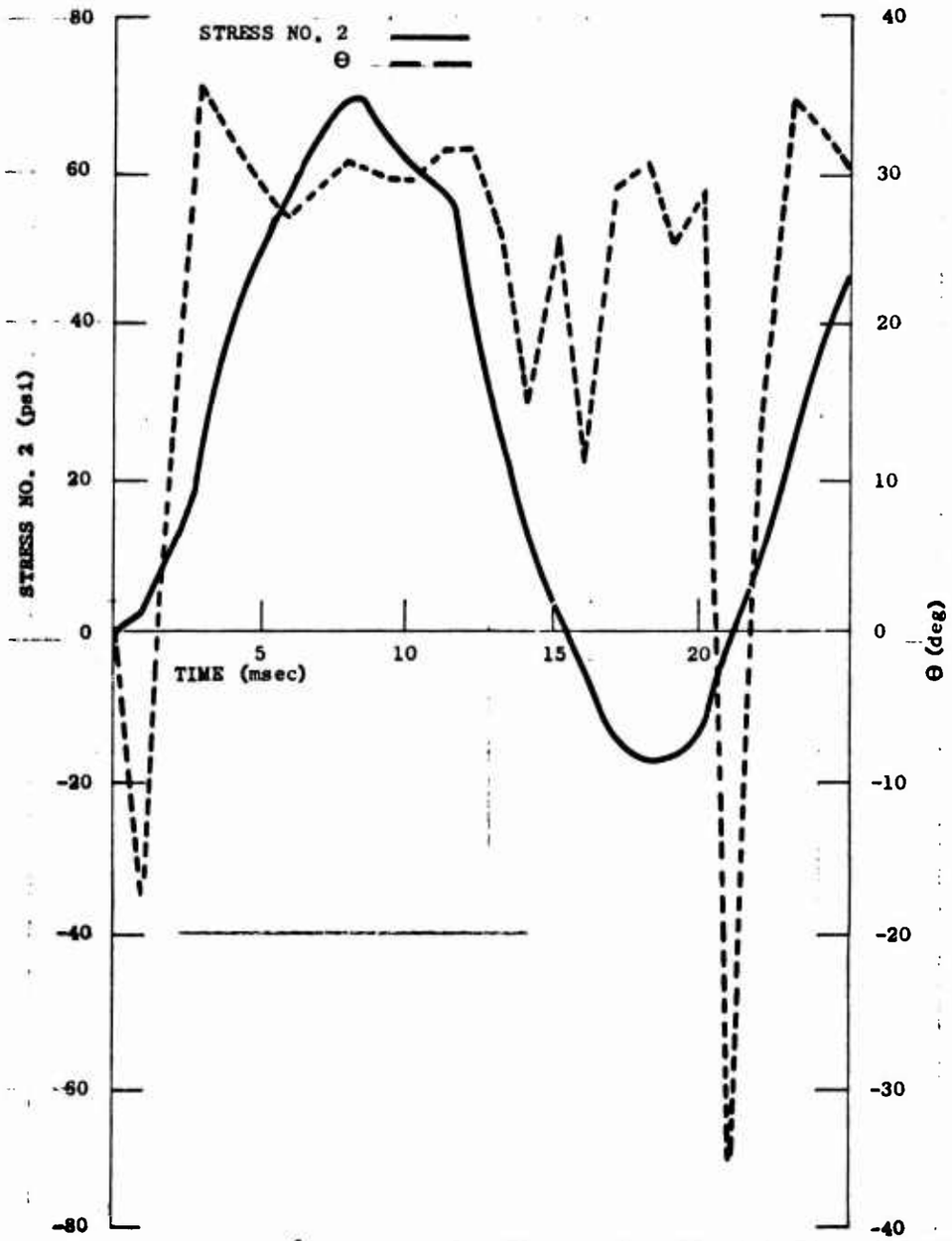

Fig. B-59. Stress and θ vs Time for Element No. 22 with Pinned Supports All Sides

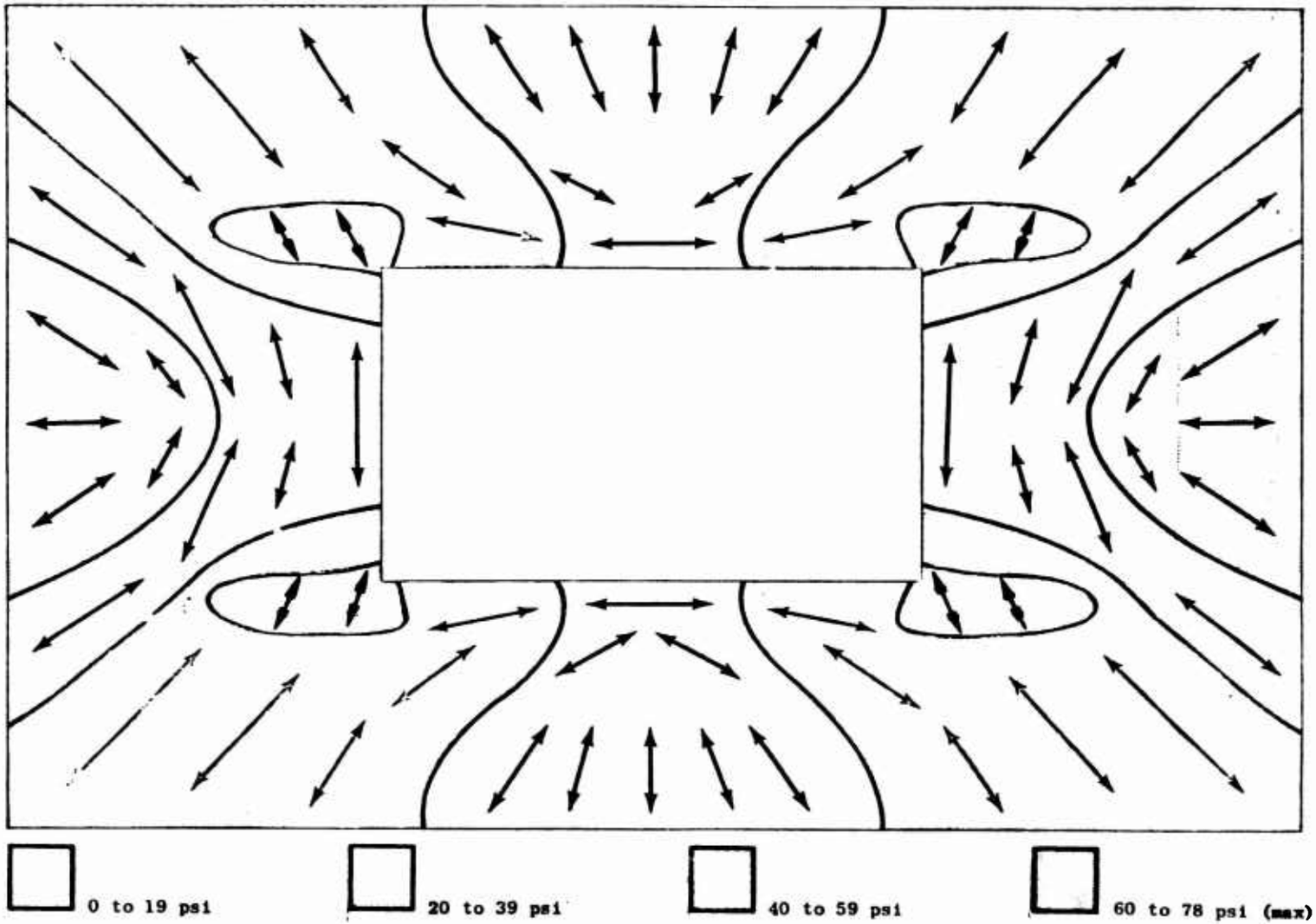

Fig. B-60. Stress Contour for Time = 0.008 seconds for Downstream (tZ) Face with Pinned Supports All Sides

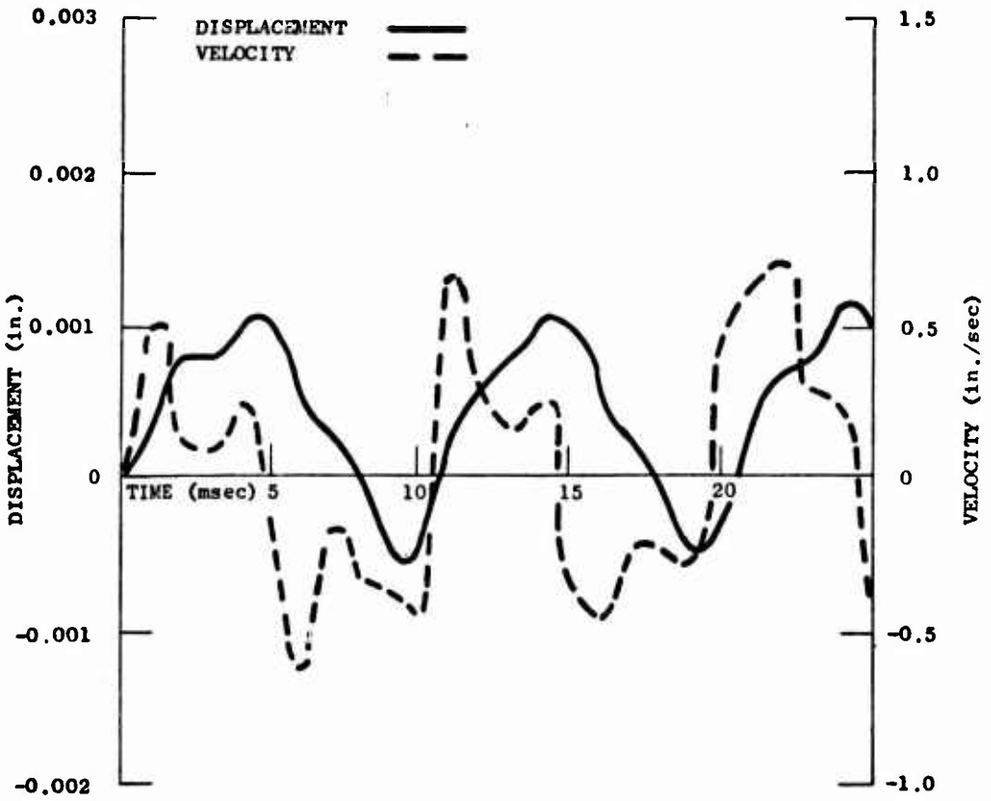

Fig. B-61. Deflection and Velocity vs Time for Node 60 with Fixed Supports All Sides

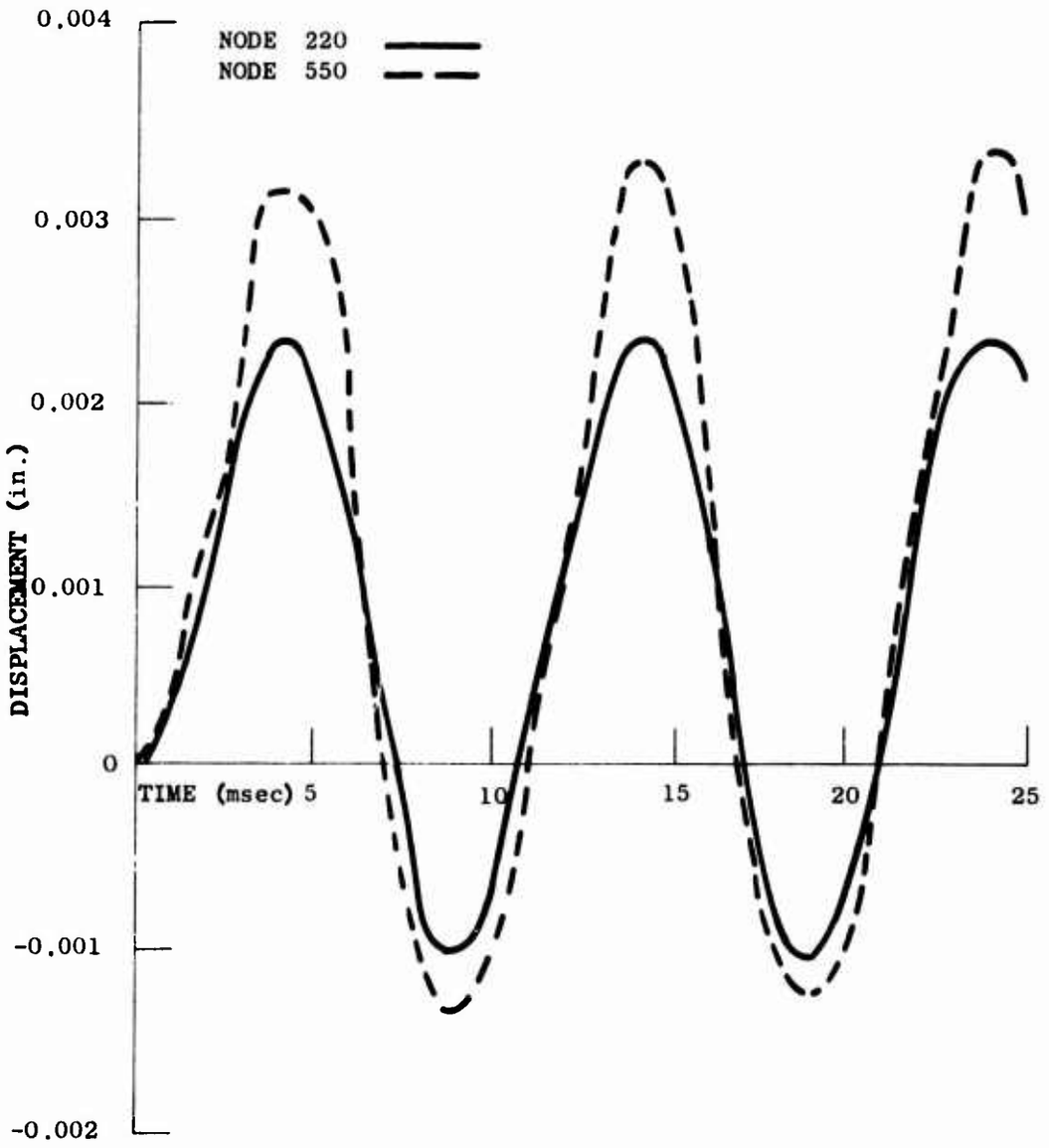

Fig. B-62. Deflection vs Time for Nodes 220 and 550 with Fixed Supports All Sides

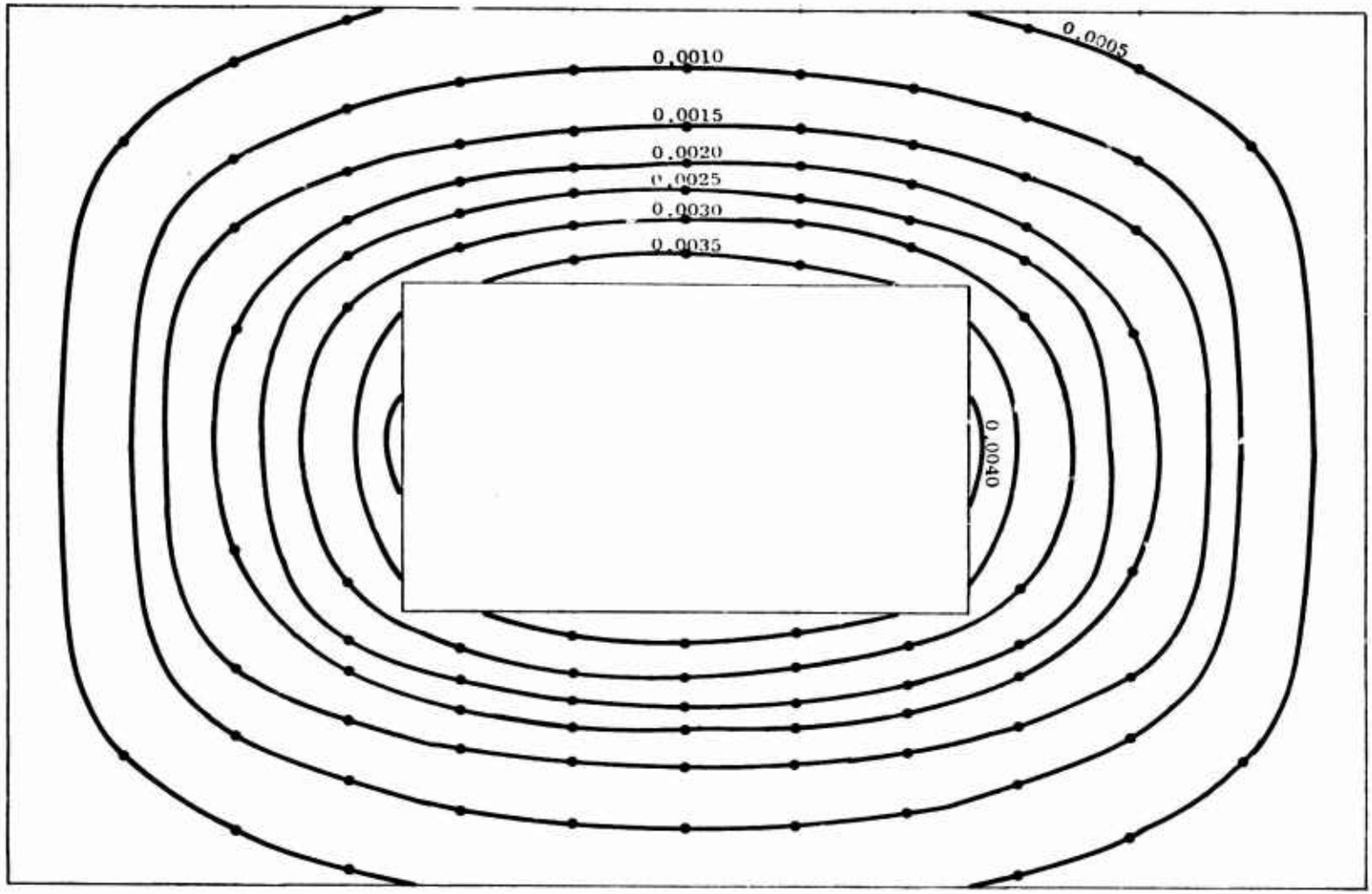

Fig. B-63. Deflection Contours (in.) for Time = 0.004 seconds with Fixed Supports Top and Bottom

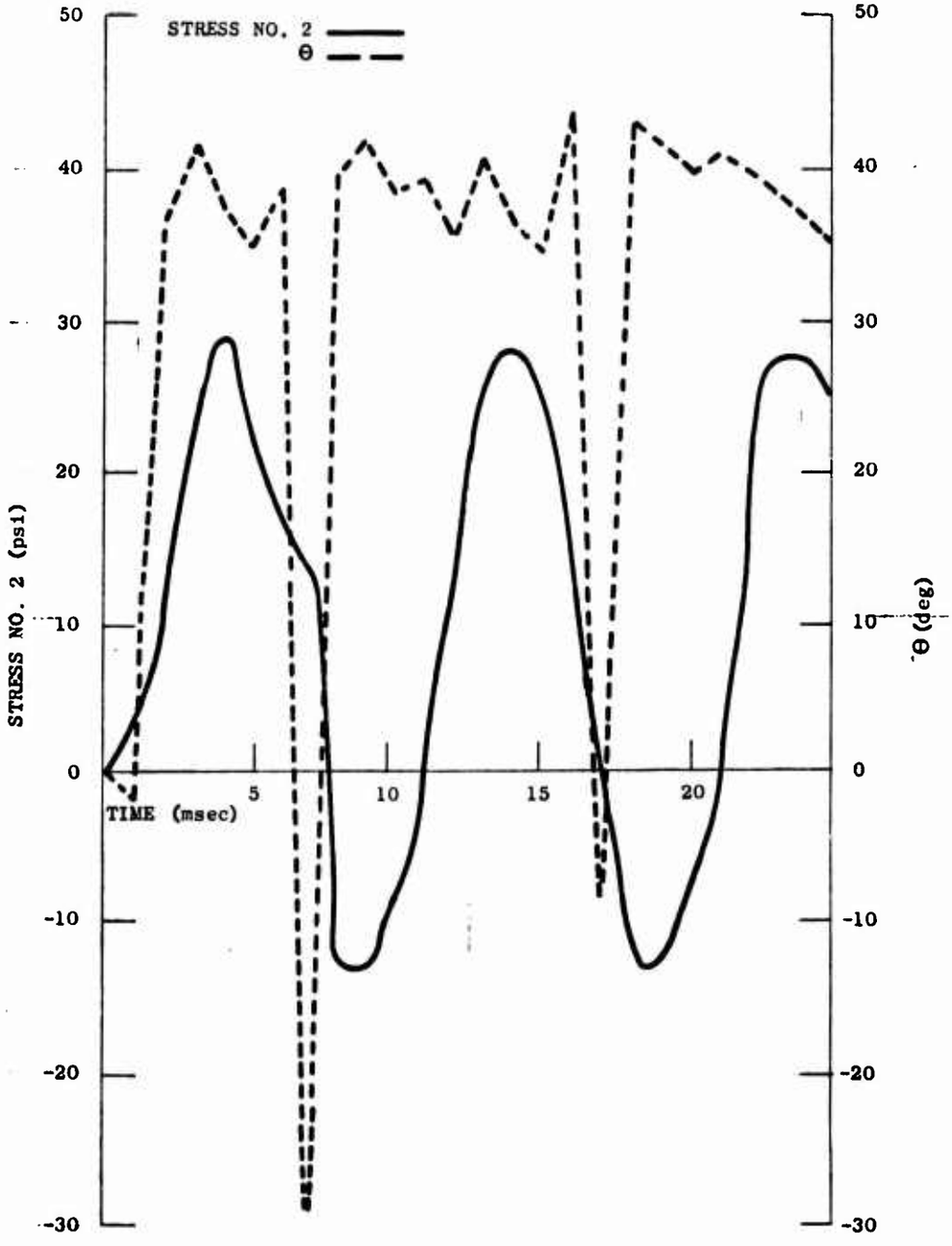

Fig. B-64. Stress and θ vs Time for Element No. 22 with Fixed Supports All Sides

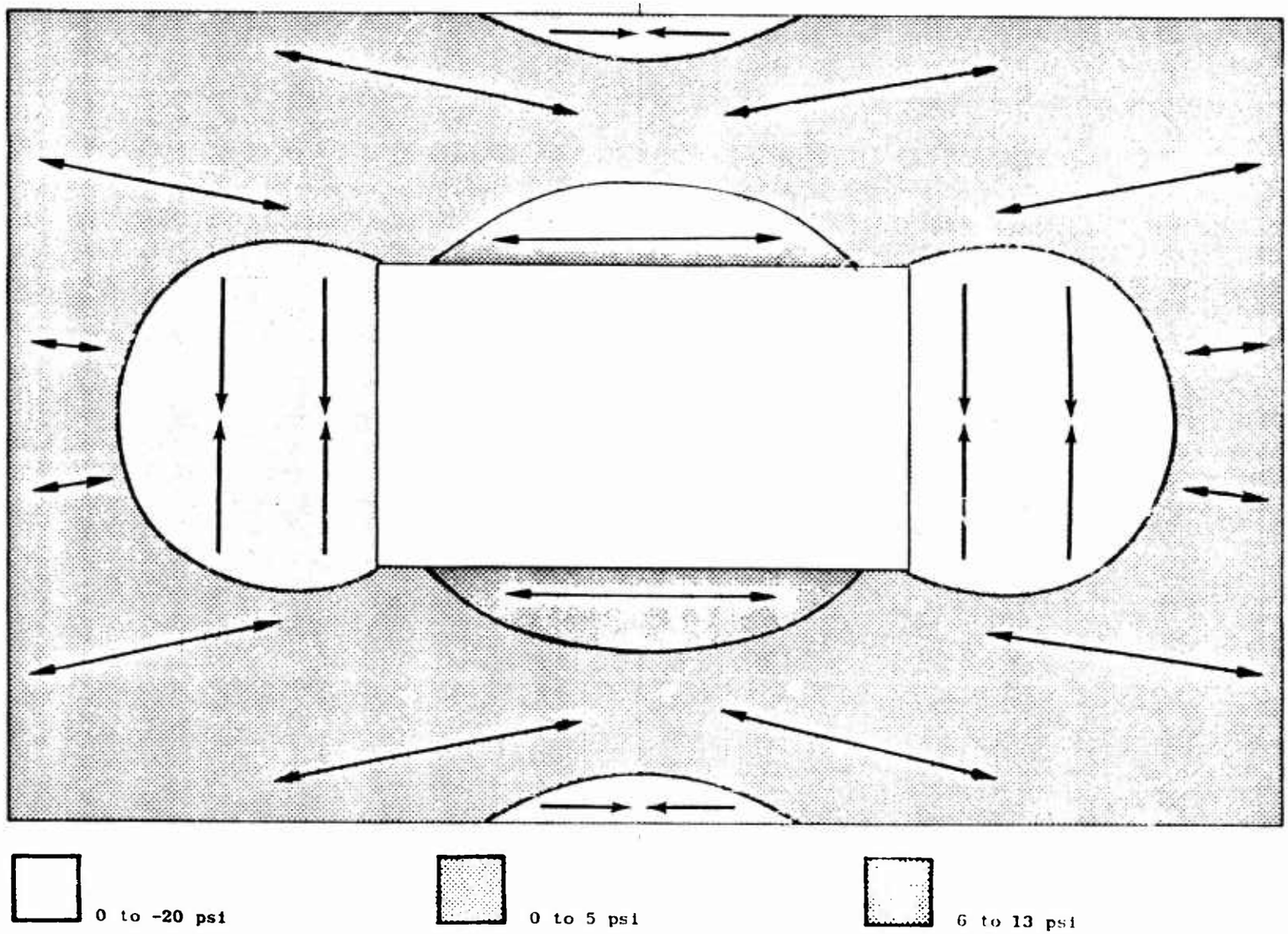

Fig. B-65. Stress Contours on (+Z) Face at time = 0.003 sec for a Wall With Window Fixed on all Four Sides.

Appendix C

STATIC TEST PROGRAM

INTRODUCTION

In conjunction with the Shock Tunnel dynamic tests, a static test program was conducted to determine the quality of construction of the test items fabricated, to obtain estimates of the strength of specimen walls prior to the dynamic tests, and to gather sufficient data to make a statistical comparison between laboratory specimens and real world constructed masonry.

Specimens for the static test program are constructed at the same time and of the same materials as the test walls. Typical specimens for the brick and concrete block walls follow:

Brick Test Specimen

1. Brick-mortar beams for flexural strength testing
2. Brick-mortar blocks for compressive and shear strength tests
3. Brick-mortar couplets for tensile bond strength tests
4. Mortar cylinders for compressive and tensile strength tests
5. Bricks for modulus of rupture and compressive strength tests.

Concrete Block Specimens

1. Concrete block-mortar beams for flexural strength tests
2. Mortar cylinders for compressive and tensile strength tests

3. Concrete blocks for compressive strength tests.

Composite walls of brick-concrete block construction are accompanied by similar specimens, except that the beams and masonry assemblies are also of composite construction.

All materials were purchased from a commercial supplier and were representative of those commonly used in local building construction. A Portland Cement meeting the requirements of ASTM Specification for Portland Cement, Type 1, (designation C150-66) was used in preparation of the mortar mixture, along with a mason's sand from the San Francisco Bay Area. No analysis of the sand properties was performed.

The walls and corresponding static test samples were constructed and stored for curing in the underground tunnel complex, where the mean temperature for July is 53 to 60°F and for January, 45 to 60°F. The mean humidity ranges from 75 to 85 percent.

Beams

Most beams were tested for flexural strength in the concrete tester equipped with the transverse beam apparatus, following the standard method for a simple concrete beam with third-point loading, ASTM designation C78-64. A diagram of a brick beam in place for this test is shown in Fig. C-1. Sketches of the various brick and concrete block beams investigated are shown in Fig. C-2. The spacing of the load-applying and support blocks were changed for the CBA and CBB concrete block beams, which were longer when four blocks were used, and shorter when only three were used. For the cype CBC concrete block beams, which were both higher and longer than the other beams, and therefore did not fit the tester when the complete transverse beam apparatus was used, a method similar to ASTM C293-64, the standard method of test for flexural strength of simple concrete beams with center point loading was used. For these beams, the load was applied at the center of the supported section through a 2 in. diameter steel roller.

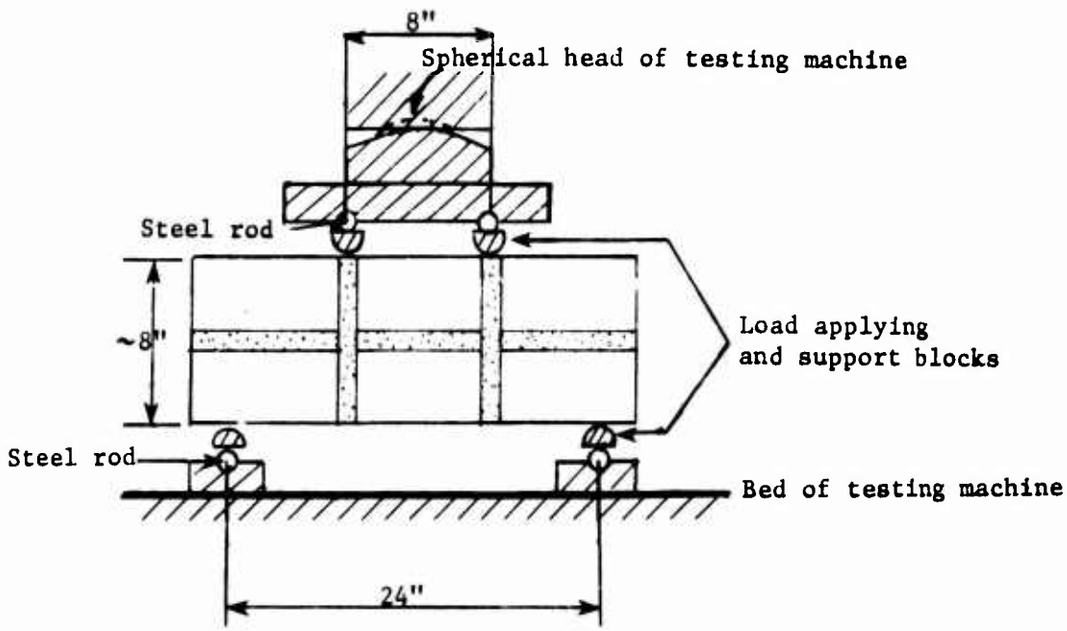

Fig. C-1. Brick Beam Flexural Test, Third-Point Loading.

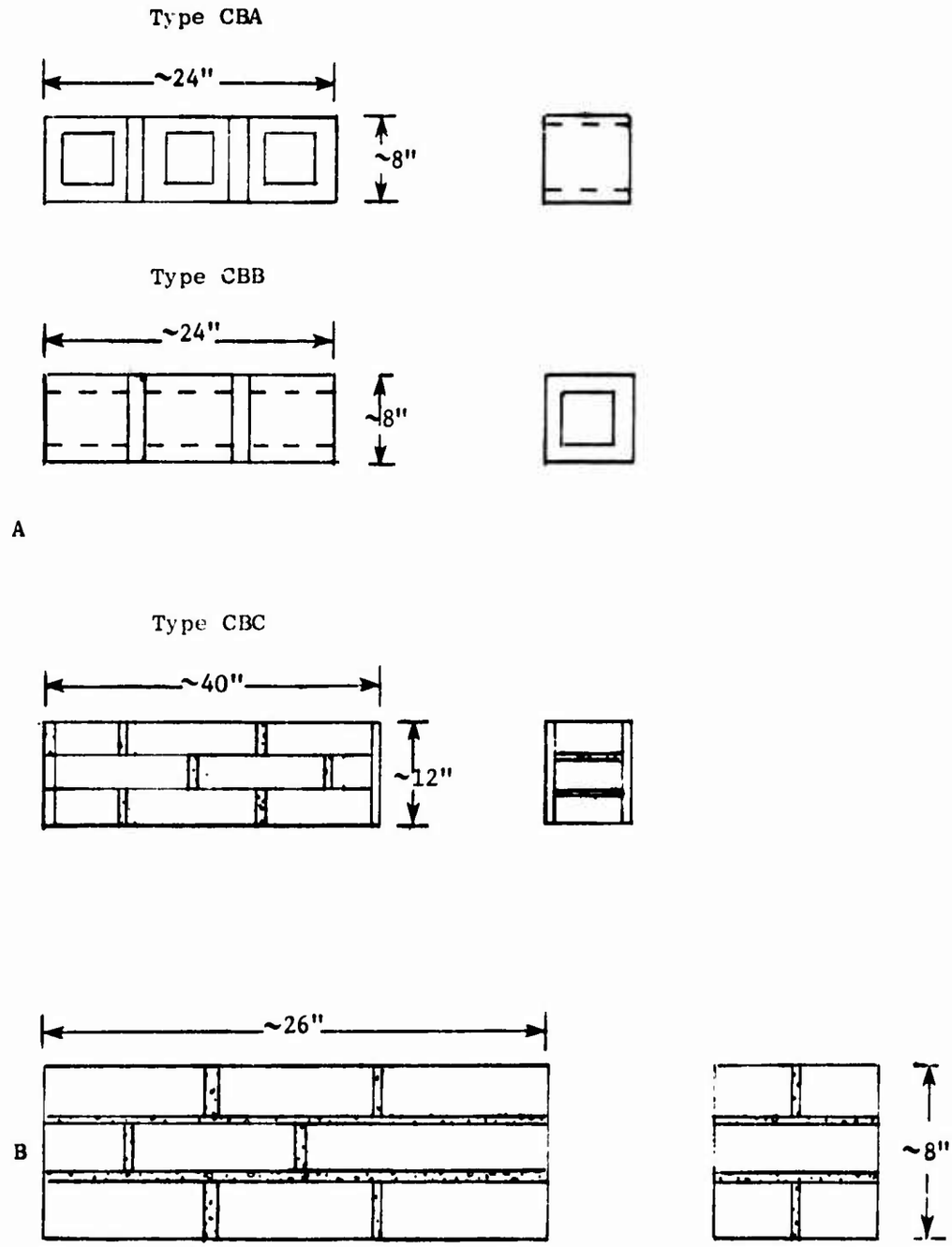

Fig. C-2. Brick and Concrete Beam Patterns.

Listed under beam properties in Tables C-1 and C-2 are the results of the brick and concrete block beam tests conducted to date.

Some static tests on 3 additional type beams (see Fig. C-3) were performed at the Shock Tunnel during this reporting period. The brick beams and the concrete block beams were built horizontally into a 4 ft wide heavy-walled passageway and mortared into the passageway so they arched under load. A portable hydraulic jack equipped with a pressure gauge was used to test 3 specimens as shown in Figs. C-4A and C-4B. Figure C-5 diagrams the methods of loading these beams and lists the loads necessary to break them. Figures C-6A and C-6B show typical failure crack patterns in the brick beams, and Figs. C-7A and C-7B show a concrete block beam after failure and at a later time when further deflection of the beam caused pieces to fall out.

The concrete block-brick composite beams were constructed in a vertical position, like the walls they accompanied. For testing the beams were laid on heavy-walled iron pipes and loaded at the third-points. A sketch of the loading method and the results of those tests are shown in Fig. C-8.

Brick and Mortar Couplets

Samples of crossed brick couplets were fabricated for each wall. These couplets were used to determine the tensile bond strength of mortar to brick and the tests were performed according to ASTM Specification C321-64. The results of these tests are given in Table C-1.

Mortar Specimens

The Type "S" mortar mixture was proportioned by volume according to the following: 1 part Portland Cement, 1/4 to 1/2 part hydrated lime, and 4 parts damp loose sand. The amount of water applied to each batch of mortar was adjusted to produce a consistency that could be conveniently handled by a mason. To obtain measurements of compressive and of splitting strengths, three 2 in. diameter by 4 in. long cardboard cylindrical molds were filled for each new batch of mortar.

Table C-1

SUMMARY OF STATIC TEST DATA

Brick									
Designation			Beam Properties		Mortar Properties (average)		Bond Properties (average)		Composite Compression Strength (psi)
Batch No.	Date	Ident. No.	Brick Pattern	Flexural Strength (psi)	Compressive Strength (psi)	Tensile Strength (psi)	Tensile Strength (psi)	Shear Strength (psi)	
11	6/71	64			1566				
		65			2046				
		66			2109				
		67							
		68-1	1/2B	208					
		68-2	1/2B	253					
		69	B	125					
12	2/72	71-1	E	172	1754	410	61	61	2203
		71-2		191					
13	4/72	74	B	273	2531	459	102	81	2133
		75		150					
		76		159					
14	6/72	80	B	208	1814	165	-	73	2237
		81		160					
		82		179					
15	12/72	83	B	181	2127	245	101	-	2638
		84		152					
		85		117					
		86		195					
		87-1		153					
		87-2		171					
		88-1		155					
		88-2		119					
16	6/73	92	B	173	1819	518	-	-	2526
		94		220					
		95		167					
8	1969	96	B	164	3162	647	87	-	2526

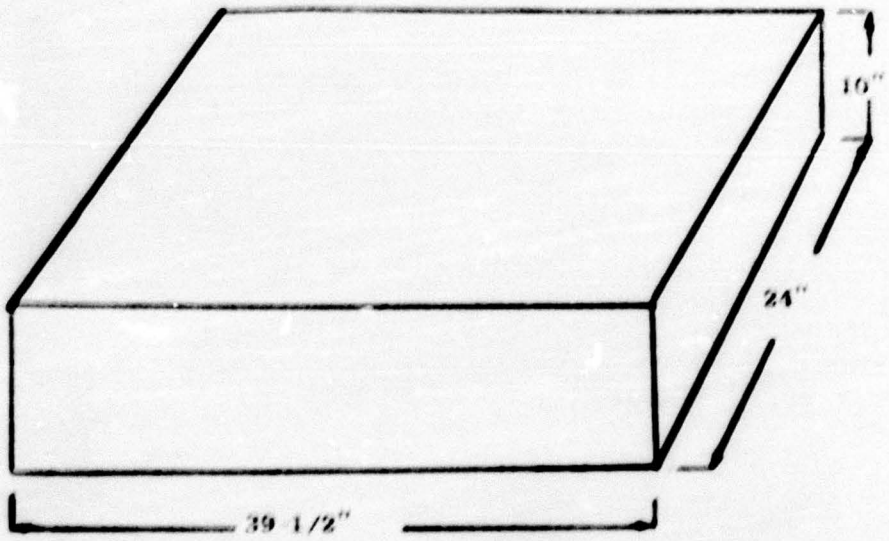

Brick and Concrete Block

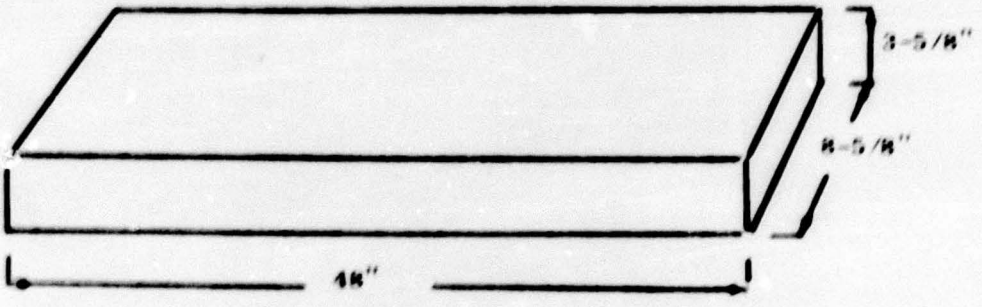

Brick

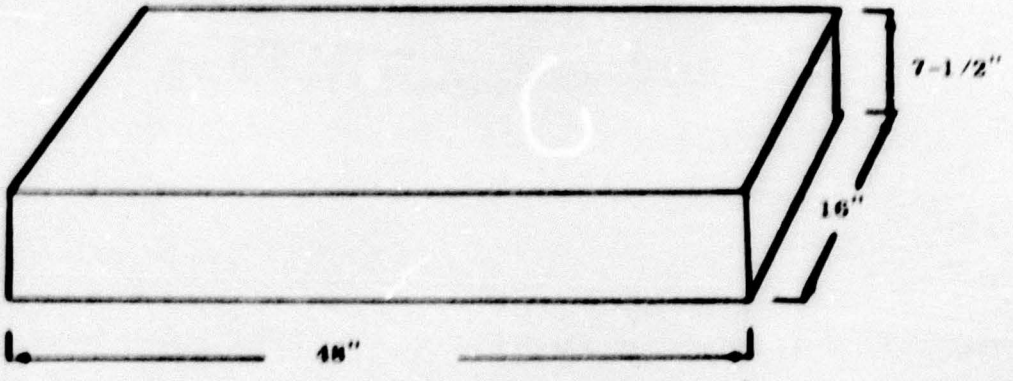

Concrete Block

Fig. C-3 Special Type Brick and Concrete Beam Patterns.

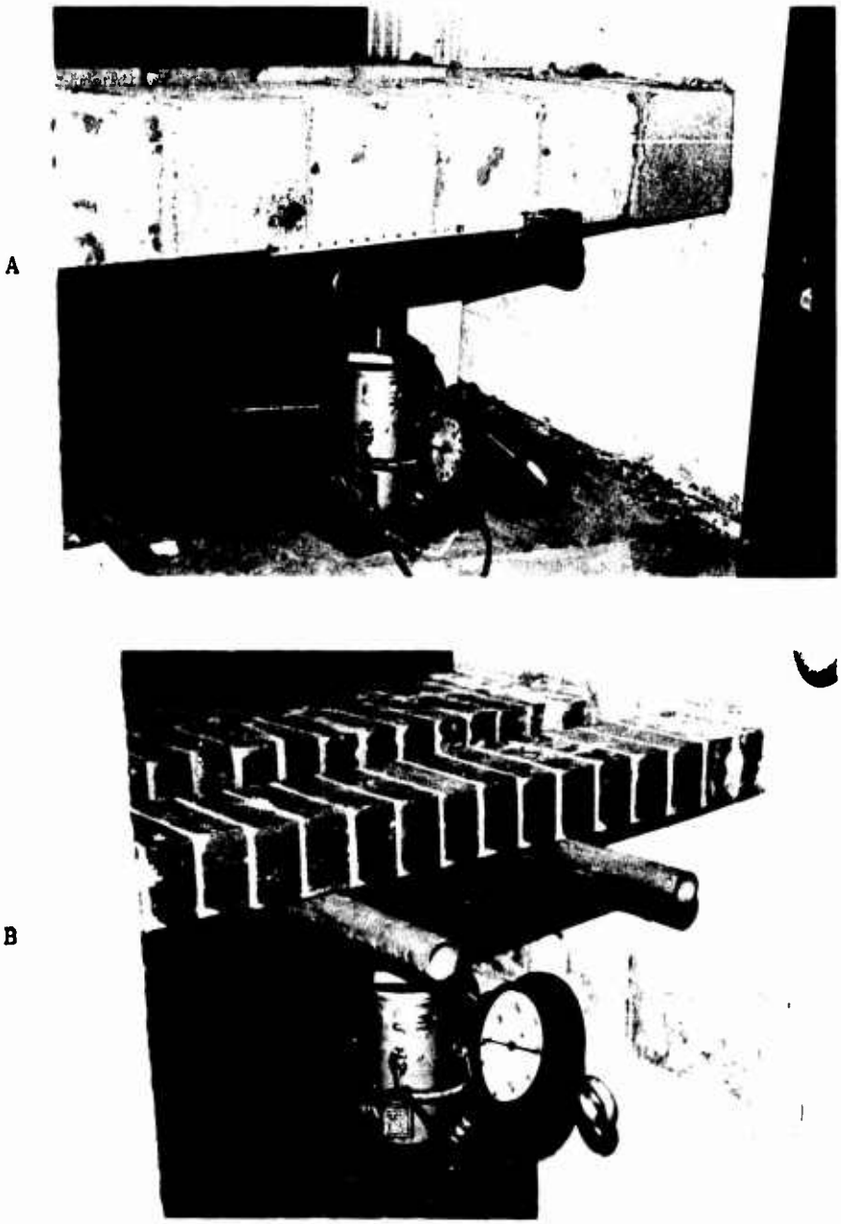

Fig. C-4. Test Method for Brick and Concrete Block Arched Beams.

Results of Tests on Brick Beams

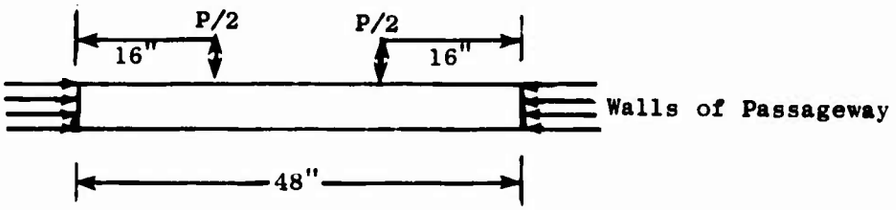

Test #1	P = 12100
2	P = 10500
3	P = 8836
avg.	P = 10479

Results of Tests on Concrete Block Beams

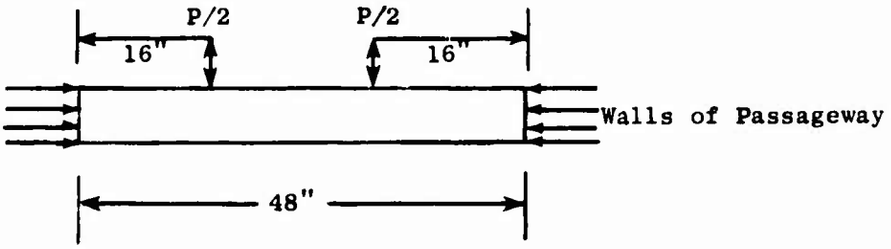

Test #1	P = 12700 lbs
2	P = 10500 lbs
avg.	P = 11600 lbs

Fig. C-5. Method of Loadi..g and Test Results for Brick and Concrete Block Arched Beams.

Fig. C-6. Typical Failure Crack Patterns Arched Brick Beams.

Fig. C-7. Typical Failure Concrete Block Arched Beam.

Results of Tests on Brick - Concrete Block Beams

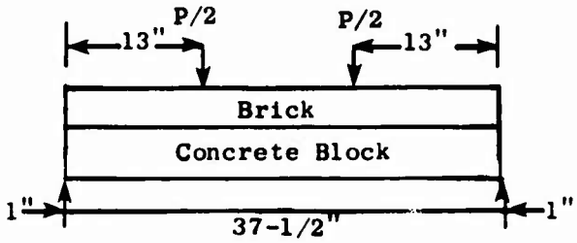

Test #1	P = 9388 lbs
2	P = 7731 lbs
3	P = 7180 lbs
avg.	P = 8100 lbs

Fig. C-8. Method of Loading and Results From Composite Brick and Concrete Block Beam Tests.

Table C-2

SUMMARY OF STATIC TEST DATA

Concrete Block							
Designation			Beam Properties		Mortar Properties (average)		Block Properties (average)
Batch No.	Date	Ident. No.	Block Pattern	Flexural Strength (psi)	Compressive Strength (psi)	Tensile Strength (psi)	Compressive Strength (psi)
2CB	2/72	72-1	CBA	73	2531	459	3484
		72-2	CBB	184			
		72-3	CBB	122			
		73-1	CBA	62			
		73-2	CBA	50			
		73-3	CBB	147			
3CB	4/72	77	CBC(1)	180	2531	459	3580
		78-1	CBC	182			
		78-2	CBC	185			
4CB	4/73	89-1	CBC	84.2	2643	406	4038
		89-2	CBC	122			
		89-3	CBC	149			
5CB	5/73	90-1	CBB	178	1886	346	3941
		90-2	CBB	117			
		90-3	CBB	128			
		91-1	CBC	109			
		91-2	CBC	167			
6CB	6/73	93-1	CBC	110	2197	518	4000

(1) Note on concrete block beams CBC center point loading was used because of limit of height on loader.

Capped mortar cylinders were tested in compression and uncapped cylinders were tested according to the splitting tensile strength test described in ASTM designation C496-64T. For this test, the load was applied along the specimens as shown in the sketch below.

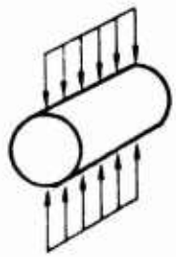

Data from these tests are shown in Tables C-1 and C-2.

Concrete Cylinders

For walls built outside the Shock Tunnel and, subsequently, (after curing) moved into the tunnel for testing in an arched mode samples of the concrete used to fix the walls in place were taken. This concrete, made with Type III (high early) cement, was used in order to achieve satisfactory support conditions in as short a time as possible. Satisfactory support was defined as achieved when the concrete compressive strength was higher than expected composite compressive strength of the wall materials; this condition was ordinarily attained in 3 days. Three samples were taken from each batch of concrete and allowed to cure next to the wall for at least one day before being brought to the laboratory for testing. Typical compressive stress levels measured in these cylinders before testing the walls were around 4500 psi, substantially higher than the composite compressive strengths measured for brick walls (see Table C-1), and higher than the compressive strengths for concrete blocks (see Table C-2).

Bricks and Concrete Blocks

Specimen bricks and concrete blocks were sampled during construction of each batch of walls.

Brick specimens were tested in flexure and in compression according to ASTM standard C67-66. Specimens which had been broken in flexure were capped with plaster of paris before being tested in compression.

Concrete block specimens were tested in compression and in "line loading." The compression loaded blocks were capped with plaster of paris on a glass plate to ensure parallelism and flatness of the bearing surfaces. Data from both the brick and concrete block tests are shown in Table C-2.

Other Masonry Assemblies

Three types of masonry assemblies were utilized for the determination of composite compressive strength, brick-mortar shear bond strength, and "line-loading" properties of brick and brick-concrete block composite assemblies. Sketches of these assemblies are shown in Fig. C-9.

Composite compressive strength and related parameters (E, modulus of elasticity; and E^*, a tentative modulus for line load)* were determined for 3 and 6 brick assemblies (see Fig. C-9A and C-9B). Loads were transmitted through and distributed evenly by steel plates at top and bottom as shown in Fig. C-10A; deflections were measured by dial gauges calibrated at .001" intervals. The composite compressive strength for 3 and 6 brick assemblies were averaged for each batch, and are tabulated in Table C-1, while corresponding E values were determined for stress and strain values averaged for each batch and for all batches for each type of assembly, and tabulated in Tables C-3 and C-4.

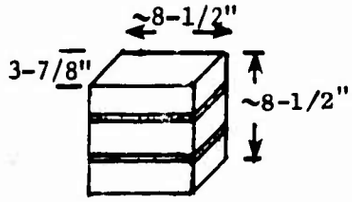

A. 3-Brick

B. 6-Brick

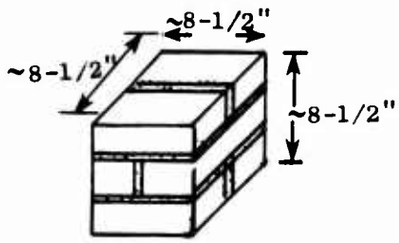

C. Brick-Concrete Block

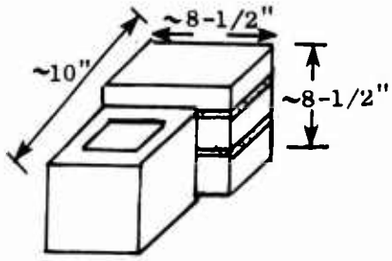

Fig. C-9. Sketches of Masonry Assemblies.

Table C-3

STATIC TEST DATA FOR 8-1/2" x 3-7/8" x 8-1/2"
BRICK ASSEMBLIES IN COMPRESSION - STANDARD TEST

Group	Specimen Number	p (lbs)	f_ℓ (lb/in.)	f_c' (psi)	E
1	1	60,000	7,100	1,800	355,000
	2	67,000	7,900	2,000	410,000
	3	71,000	8,400	2,200	435,000
	average	66,000	7,800	2,000	400,000
2	1	97,000	11,300	2,900	486,000
	2	63,000	7,500	1,900	257,000
	3	87,000	10,200	2,600	465,000
	4	99,000	11,700	3,100	597,000
	5	89,000	10,000	2,700	333,000
	6	47,000	5,500	1,400	240,000
	average	80,000	9,500	2,400	396,000
3	1	87,000	10,100	2,600	781,000
	2	93,000	10,800	2,900	548,000
	3	89,000	10,400	2,800	264,000
	4	58,000	7,000	1,800	188,000
	5	88,000	10,400	2,800	489,000
	6	73,000	8,700	2,300	304,000
	average	81,000	9,600	2,500	429,000
Grand Average		78,000	9,200	2,400	410,000

Table C-4

STATIC TEST DATA FOR 8-1/2" x 8-1/2" x 8-1/2"
BRICK ASSEMBLIES IN COMPRESSION

Group	Specimen Number	p (lbs)	f_ℓ (lb/in.)	f_c' (psi)	E
1	1	>200,000	>23,500	>2,800	>784,000
	2	140,000	16,500	1,900	370,000
	3	196,000	23,100	2,700	342,000
	average	>179,000	>21,000	>2,500	>499,000
2	1	>190,000	22,400	2,600	635,000
	2	>200,000	>22,900	>2,900	>1,013,000
	3	>200,000	>22,700	>2,900	> 777,000
	4	>200,000	>22,400	>2,900	> 724,000
	5	>200,000	>22,400	>2,900	> 608,000
	6	>200,000	>22,400	>2,900	> 555,000
	average	>198,000	>22,500	>2,800	> 719,000
3	1	167,000	19,600	2,300	442,000
Grand Average		>189,000	>21,800	>2,700	>625,000

The brick specimens that were line-loaded were treated in similar fashion, except that loading was as shown in drawings B and C of Fig. C-10. Discussion of these tests and their rationale may be found in Section 3 of this report. Early tests of this type did not include measurement of the deflection; for these tests only stress information is available. Later tests were made with dial gauges so comparison with area loaded specimens from the same batch might be made, and values of E and E^* were developed. These values were averaged in the same way that E values were averaged for the compressive strength specimens, and are tabulated in Tables C-5 and C-6.

To gain more information on the "line loading" problem, some tests were performed with the edges of the specimens loaded vertically. For these, the load was applied through steel bars on the outer 1/4 in. or 1/2 in. of one edge of the specimen. Fig. C-11 shows how the load was applied, and Table C-7 presents the results from these tests.

Masonry assemblies consisting of brick and concrete block (type C in Fig. C-9) were line loaded only. Half of the specimens were capped so as to allow loading of the brick, and half, to allow loading of the concrete blocks. Here, too, deflection readings were made and values of E and E^* developed as described above and in Section 3. The data from these tests is presented in Tables C-8 and C-9.

Additional compression and line loading tests were conducted on concrete blocks. The "line loaded" blocks were capped at a slope of 1:10, and tested like the comparably capped masonry specimens shown in Fig. C-12. Values of E and E^* obtained are in Tables C-10 and C-11.

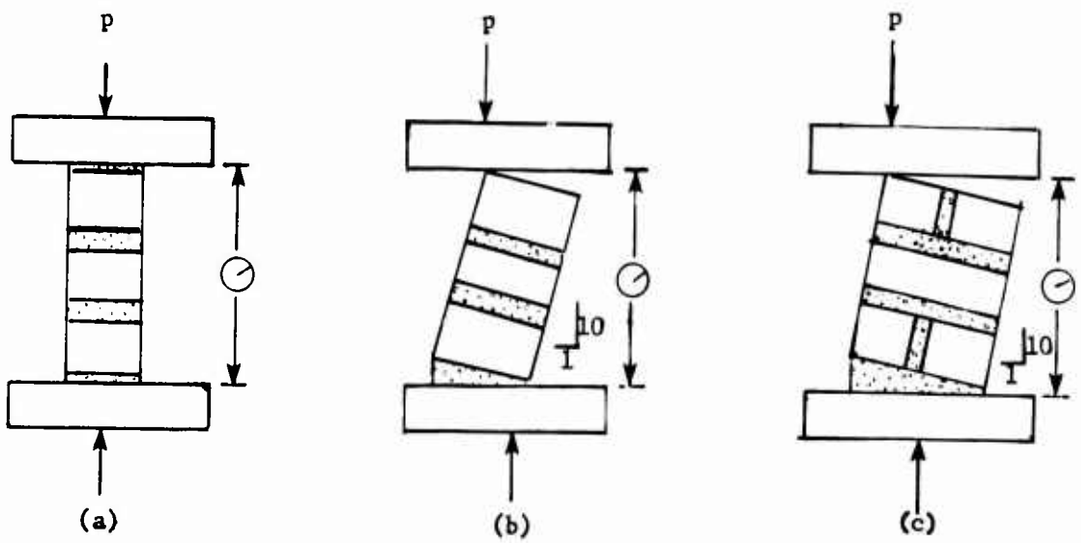

Fig. C-10. Brick Assemblies Tested in Compression.

Table C-5

STATIC TEST DATA FOR 8-1/2" x 3-7/8" x 8-1/2"
BRICK ASSEMBLIES IN "LINE LOADING"

Group	Specimen Number	p (lbs)	f_l (lb/in.)	f_c' (psi)	E	E*
1	1	27,500	3,800	1,030	83,000	307,000
	2	33,700	3,900	1,050	104,000	385,000
	average	34,000	3,800	1,040	95,000	352,000
2	1	18,000	2,000	560	69,900	250,000
	2	28,000	3,100	860	94,100	337,000
	3	23,000	2,500	710	64,100	228,000
	4	32,000	3,500	990	77,700	276,000
	5	33,500	3,700	1,010	71,100	263,000
	6	35,000	3,900	1,080	83,800	302,000
	average	28,300	3,100	870	76,800	276,000
3	1	28,000	3,100	850	67,700	248,000
	2	22,500	2,500	680	71,300	261,000
	3	20,500	2,300	620	67,700	248,000
	average	23,700	2,600	720	68,900	252,000
Grand Average		28,100	3,100	860	77,700	282,000

Table C-6

STATIC TEST DATA FOR 8-1/2" x 8-1/2" x 8-1/2"
BRICK ASSEMBLIES IN "LINE LOADING"

Group	Specimen Number	p (lbs)	f_ℓ (lb/in.)	f_c' (psi)	E	E*
1	1	51,000	5,300	710	74,700	560,000
	2	46,000	4,800	640	70,900	532,000
	3	52,000	5,400	720	59,500	446,000
	average	49,700	5,200	690	68,300	513,000
2	1	37,500	3,900	520	40,100	303,000
	2	39,500	4,100	550	70,600	534,000
	3	45,000	4,700	620	25,900	196,000
	4	35,000	3,700	480	47,300	357,000
	5	47,500	5,000	660	74,000	559,000
	average	40,900	4,300	570	51,600	390,000
3	1	48,000	5,000	660	21,100	159,000
	2	36,000	3,700	500	47,300	355,000
	3	36,500	3.800	510	29,500	221,000
	average	40,200	4,200	500	32,600	245,000
Grand Average		43,100	4,500	600	51,000	384,000

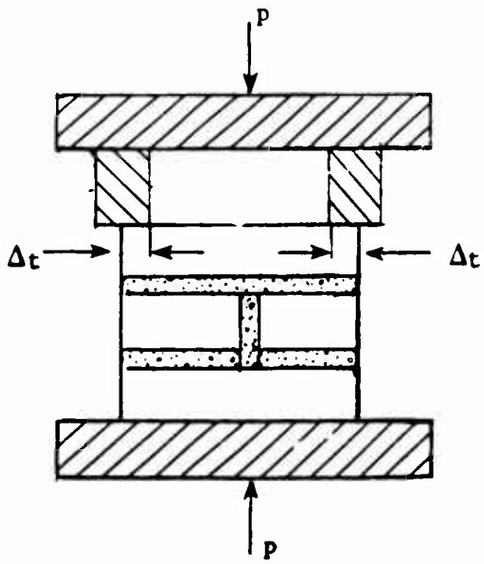

Fig. C-11. Vertical "Line Loading" of Brick Assemblies.

Table C-7

TEST DATA FOR VERTICAL "LINE LOADING"
OF BRICK/MORTAR SPECIMENS

Δ_t	p	f_c'	f_ℓ
1/4"	10,900	171	680
	13,465	211	840
	13,990	217	825
	15,200	237	950
1/2"	13,980	260	875
	33,000	515	2,070
	34,000	540	2,160
	19,000	297	1,191

Table C-8

STATIC TEST DATA FOR BRICK CONCRETE BLOCK COMPOSITE
"LINE LOAD" ON BRICK

Specimen Number	p (lbs)	f_ℓ (lb/in.)	f_c' (psi)	E	E*
1	44,000	4,800	520	67,500	620,000
2	32,000	3,500	380	44,900	413,000
3	40,000	4,300	470	45,400	417,000
Average	39,000	4,200	460	52,600	483,000

Table C-9

STATIC TEST DATA FOR BRICK CONCRETE BLOCK COMPOSITE
"LINE LOAD" ON BLOCK

Specimen Number	p (lbs)	f_ℓ (lb/in.)	f_c' (psi)	E	E^*
1	23,000	2,700	300	28,700	261,000
2	21,500	2,600	280	35,900	327,000
3	25,500	3,000	330	21,900	199,000
4	23,000	2,700	300	19,100	174,000
Average	23,200	2,800	300	26,400	240,000

Fig. C-12A. Concrete Block

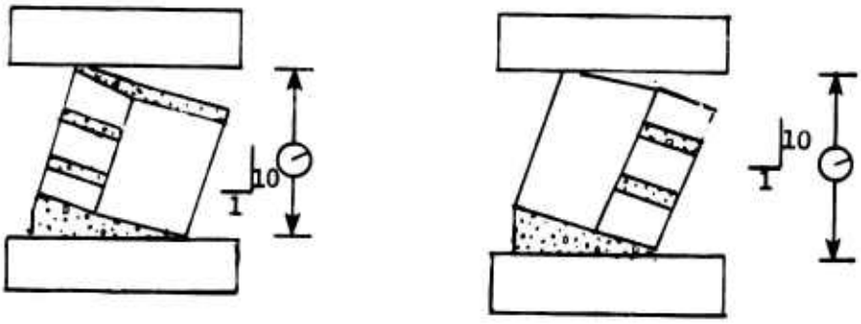

Fig. C-12B. Concrete Block Composite.

Table C-10

STATIC TEST DATA FOR CONCRETE BLOCKS
IN COMPRESSION

Specimen Number	p (lbs)	f_ℓ (lb/in.)	f_c' (psi)	E
1	116,500	13,700	3,610	635,000
2	84,300	9,900	2,610	520,000
3	63,600	7,500	1,970	592,000
4	66,200	7,800	2,050	259,000
Average	82,600	9,700	2,560	501,000

Table C-11

STATIC TEST DATA FOR CONCRETE BLOCKS
IN "LINE LOADING"

Specimen Number	p (lbs)	f (lb/in.)	f_c' (psi)	E	E^*
1	31,400	3,500	970	84,100	302,000
2	27,000	3,000	840	53,600	192,000
3	26,500	2,900	820	69,600	250,000
4	36,000	4,000	1,120	119,500	429,000
Average	30,200	3,400	940	81,700	293,000